# NASA Tech Briefs

National
Aeronautics and
Space
Administration


The 1980 Index to NASA Tech Briefs Is Now Available. [See Page A2.]

*Facilities for the ship-to-shore transfer of liquefied natural gas were designed with the help of NASA work on cryogenic flow lines for rocket engines. Several commercial installations, such as this one operating in Boston, Massachusetts, benefited substantially from the NASA technology.* [See the bottom of page A1.]

Vol. 6, No. 2

Summer 1981

# About the NASA Technology Utilization Program

The National Aeronautics and Space Act of 1958, which established NASA and the United States civilian space program, requires that "The Administration shall provide for the widest practicable and appropriate dissemination of information concerning its activities and the results thereof."

To help carry out this objective, NASA's Technology Utilization (TU) Program was established in 1962. Now, as an element of NASA's Technology Transfer Division, this program offers a variety of valuable services to help transfer aerospace technology to nonaerospace applications, thus assuring American taxpayers maximum return on their investment in space research; thousands of spinoffs of NASA research have already occurred in virtually every area of our economy.

The TU program has worked for engineers, scientists, technicians, and businessmen; and it can work for you.

## NASA Tech Briefs

*Tech Briefs* is published quarterly and is free to engineers in U.S. industry and to other domestic technology transfer agents. It is both a current-awareness medium and a problem-solving tool. Potential products . . . industrial processes . . . basic and applied research . . . shop and lab techniques . . . computer software . . . new sources of technical data . . . concepts . . . can be found here. The short section on New Product Ideas highlights a few of the potential new products contained in this issue. The remainder of the volume is organized by technical category to help you quickly review new developments in your areas of interest. Finally, a subject index makes each issue a convenient reference file.

## Further Information on Innovations

Although some new technology announcements are complete in themselves, most are backed up by Technical Support Packages (TSP's). TSP's are available without charge and may be ordered by simply completing a TSP Request Card found at the back of this volume. Further information on some innovations is available for a nominal fee from other sources, as indicated. In addition, Technology Utilization Officers at NASA Field Centers will often be able to lend necessary guidance and assistance.

## Patent Licenses

Patents have been issued to NASA on some of the inventions described, and patent applications have been submitted on others. Each announcement indicates patent status and availability of patent licenses if applicable.

## Other Technology Utilization Services

To assist engineers, industrial researchers, business executives, Government officials, and other potential users in applying space technology to their problems, NASA sponsors Industrial Applications Centers. Their services are described on page A7. In addition, an extensive library of computer programs is available through COSMIC, the Technology Utilization Program's outlet for NASA-developed software.

## Applications Program

NASA conducts applications engineering projects to help solve public-sector problems in such areas as safety, health, transportation, and environmental protection. Two applications teams, staffed by professionals from a variety of disciplines, assist in this effort by working with Federal agencies and health organizations to identify critical problems amenable to solution by the application of existing NASA technology.

## Reader Feedback

We hope you find the information in *NASA Tech Briefs* useful. A reader-feedback card has been included because we want your comments and suggestions on how we can further help you apply NASA innovations and technology to your needs. Please use it; or if you need more space, write to the Director, Technology Transfer Division, P. O. Box 8757, Baltimore/Washington International Airport, Maryland 21240.

NASA Tech Briefs

National Aeronautics and Space Administration

SUMMER 1981
Volume 6, Number 2



*COVERS: The photographs on the front and back covers illustrate developments by NASA and its contractors that have resulted in commercial and nonaerospace spinoffs. To find out more about the Cryogenic Pipeline Technology, Circle 78 on the TSP Request Card at the back of this issue. For more information on the Portable Radiometer, see "Portable Radiometer Monitors Plant Growth" (GSC-12412) on page 47 of NASA Tech Briefs, Vol. 6, No. 1.*

## About This NASA Publication

NASA Tech Briefs, a quarterly publication, is distributed free to qualified U.S. citizens to encourage commercial application of U.S. space technology. For information on publications and services available through the NASA Technology Utilization Program, write to the Director, Technology Transfer Division, P. O. Box 8757, Baltimore/Washington International Airport, Maryland 21240.

"The Administrator of National Aeronautics and Space Administration has determined that the publication of this periodical is necessary in the transaction of the public business required by law of this Agency. Use of funds for printing this periodical has been approved by the Director of the Office of Management and Budget."

## Change of Address

If you wish to have NASA Tech Briefs forwarded to your new address, use the Subscription Card enclosed at the back of this volume of NASA Tech Briefs. Be sure to check the appropriate box indicating change of address, and also fill in your identification number (T number) in the space indicated.

## Communications Concerning Editorial Matter

For editorial comments or general communications about NASA Tech Briefs, you may use the Feedback card in the back of NASA Tech Briefs, or write to: The Publications Manager, Technology Transfer Division (ETD-6), NASA Headquarters, Washington, DC 20546. Technical questions concerning specific articles should be directed to the Technology Utilization Officer of the sponsoring NASA Center (addresses listed on page A4).

## 1980 Index

To obtain a copy of the 1980 Index to NASA Tech Briefs, Circle 79 on the TSP Request Card at the back of this issue.

## Acknowledgements

NASA Tech Briefs is published quarterly by the National Aeronautics and Space Administration, Technology Transfer Division, Washington, DC: Administrator: **James E. Beggs;** Director, Technology Transfer Division: **Floyd I. Roberson;** Publications Manager: **Leonard A. Ault.** Prepared for the National Aeronautics and Space Administration by **Logical Technical Services Corp.:** Editor-in-Chief: **Jay Kirschenbaum;** Art Director: **Ernest Gillespie;** Senior Editor: **Jerome Rosen;** Chief Copy Editor: **Oden Browne;** Staff Editors: **Donald Blattner, Larry Grunberger, Ted Selinsky, George Watson;** Graphics; **Concetto Auditore, Luis Martinez, Janet McCrie;** Editorial & Production; **Richard Johnson, Jeanne Bonner, Cintra Maharaj, Barbara Mauney, Vincent Susinno, John Tucker, Ernestine Walker.**

# NASA TU SERVICES

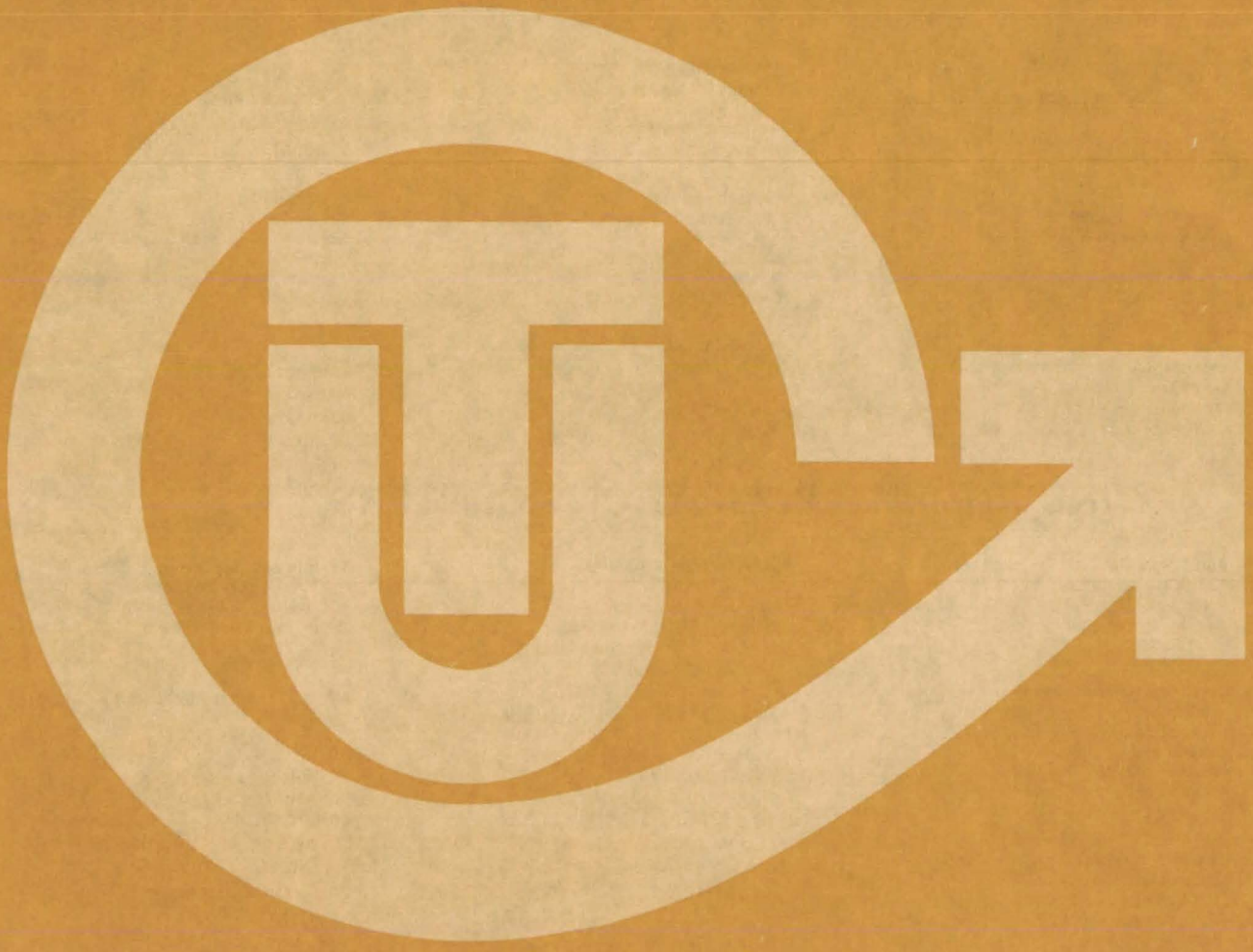

# NASA TECHNOLOGY UTILIZATION NETWORK

## ★ TECHNOLOGY UTILIZATION OFFICERS

*Stanley A. Miller*
**Ames Research Center**
Code 240-10
Moffett Field, CA 94035
(415) 965-6471

*Stanley A. Miller*
**Hugh L. Dryden Flight Research Center**
Code 240-10
Moffett Field, CA 94035
(415) 965-6471

*Donald S. Friedman*
**Goddard Space Flight Center**
Code 702.1
Greenbelt, MD 20771
(301) 344-6242

*John T. Wheeler*
**Lyndon B. Johnson Space Center**
Code AT-3
Houston, TX 77058
(713) 483-3809

*U. Reed Barnett*
**John F. Kennedy Space Center**
Code PT-SPD
Kennedy Space Center, FL 32899
(305) 867-2780

*John Samos*
**Langley Research Center**
Mail Stop 139A
Hampton, VA 23665
(804) 827-3281

*Harrison Allen, Jr.*
**Lewis Research Center**
Mail Code 7-3
21000 Brookpark Road
Cleveland, OH 44135
(216) 433-4000, Ext. 6422

*Leonard A. Ault*
**NASA Headquarters**
Code ETD-6
Washington, DC 20546
(202) 755-2244

*Aubrey Smith*
**NASA Resident Office-JPL**
4800 Oak Grove Drive
Pasadena, CA 91103
(213) 354-4849

*Gilmore H. Trafford*
**Wallops Flight Center**
Code OD
Wallops Island, VA 23337
(804) 824-3411, Ext. 201

*Ismael Akbay*
**George C. Marshall Space Flight Center**
Code AT01
Marshall Space Flight Center, AL 35812
(205) 453-2224

## ● INDUSTRIAL APPLICATIONS CENTERS

**Aerospace Research Applications Center**
1201 East 38th Street
Indianapolis, IN 46205
*John M. Ulrich, director*
(317) 264-4644

**Computer Software Management and Information Center (COSMIC)**
Suite 112, Barrow Hall
University of Georgia
Athens, GA 30602
*Robert L. Brugh, director*
(404) 542-3265

**Kerr Industrial Applications Center**
Southeastern Oklahoma State University
Durant, OK 74701
*James Harmon, director*
(405) 924-0121, Ext. 413

**NASA Industrial Applications Center**
701 LIS Building
University of Pittsburgh
Pittsburgh, PA 15260
*Paul A. McWilliams, executive director*
(412) 624-5211

**New England Research Applications Center**
Mansfield Professional Park
Storrs, CT 06268
*Daniel Wilde, director*
(203) 486-4533

**North Carolina Science and Technology Research Center**
Post Office Box 12235
Research Triangle Park, NC 27709
*James E. Vann, director*
(919) 549-0671

**Technology Applications Center**
University of New Mexico
Albuquerque, NM 87131
*Stanley Morain, director*
(505) 277-3622

**NASA Industrial Applications Center**
University of Southern California
Denny Research Building
University Park
Los Angeles, CA 90007
*Robert Mixer, acting director*
(213) 743-6132

## ■ STATE TECHNOLOGY APPLICATIONS CENTERS

**NASA/University of Florida**
**State Technology Applications Center**
500 Weil Hall
University of Florida
Gainesville, FL 32611
*J. Ronald Thornton, director*

| | |
|---|---|
| Gainesville: | (904) 392-6760 |
| Boca Raton: | (305) 395-5100, Ext. 2292 |
| Fort Lauderdale: | (305) 776-6645 |
| Jacksonville: | (904) 646-2478 |
| Orlando: | (305) 275-2706 |
| Pensacola: | (904) 476-9500, Ext. 426 |
| Tampa: | (813) 974-2499 |

**NASA/University of Kentucky**
**State Technology Applications Program**
109 Kinkead Hall
University of Kentucky
Lexington, KY 40508
*William R. Strong, manager*
(606) 258-4632

## ◆ PATENT COUNSELS

*Robert F. Kempf*
*Asst. Gen. Counsel for patent matters*
**NASA Headquarters**
Code GP-4
400 Maryland Avenue, SW.
Washington, DC 20546
(202) 755-3954

*Darrell G. Brekke*
**Ames Research Center**
Mail Code: 200-11A
Moffett Field, CA 94035
(415) 965-5104

*Paul F. McCaul*
**Hugh L. Dryden Flight Research Center**
Code OD/TU Office - Room 2015
Post Office Box 273
Edwards, CA 93523
(213) 354-2734

*John O. Tresansky*
**Goddard Space Flight Center**
Mail Code: 204
Greenbelt, MD 20771
(301) 344-7351

*Marvin F. Matthews*
**Lyndon B. Johnson Space Center**
Mail Code: AL-3
Houston, TX 77058
(713) 483-4871

*James O. Harrell*
**John F. Kennedy Space Center**
Mail Code: SA-PAT
Kennedy Space Center, FL 32899
(305) 867-2544

*Howard J. Osborn*
**Langley Research Center**
Mail Code: 279
Hampton, VA 23665
(804) 827-3725

*Norman T. Musial*
**Lewis Research Center**
Mail Code: 500-311
21000 Brookpark Road
Cleveland, OH 44135
(216) 433-4000, Ext. 346

*Leon D. Wofford, Jr.*
**George C. Marshall Space Flight Center**
Mail Code: CC01
Marshall Space Flight Center, AL 35812
(205) 453-0020

*Paul F. McCaul*
**NASA Resident Office-JPL**
Mail Code: 180-601
4800 Oak Grove Drive
Pasadena, CA 91103
(213) 354-2700

## ▲ APPLICATION TEAMS

*Doris Rouse, director*
**Research Triangle Institute**
Post Office Box 12194
Research Triangle Park, NC 27709
(919) 541-6980

*James P. Wilhelm, director*
**SRI International**
333 Ravenswood Avenue
Menlo Park, CA 94026
(415) 326-6200, Ext. 3520

# TECHNOLOGY UTILIZATION OFFICERS

Technology transfer experts can help you apply the innovations in NASA Tech Briefs.

**The Technology Utilization Officer** at each NASA Field Center is an applications engineer who can help you make use of new technology developed at his center. He brings you NASA Tech Briefs and other special publications, sponsors conferences, and arranges for expert assistance in solving technical problems.

**The Technology Utilization Officer** at each NASA Field Center is an applications engineer who can help you make use of new technology developed at his center. He brings you NASA Tech Briefs and other special publications, sponsors conferences, and arranges for expert assistance in solving technical problems.

**Technical Support Packages (TSP's)** are prepared by the center TUO's. They provide further technical details for articles in NASA Tech Briefs. This additional material can help you evaluate and use NASA technology. You may receive most TSP's free of charge by using the TSP Request Card found at the back of this issue.

***Technical questions about articles*** *in NASA Tech Briefs are answered in the TSP's. When no TSP is available, or you have further questions, contact the Technology Utilization Officer at the center that sponsored the research* [see page A4].

# NASA INVENTIONS AVAILABLE FOR LICENSING

Over 3,500 NASA inventions are available for licensing in the United States — both exclusive and nonexclusive.

**Nonexclusive licenses** for commercial use of NASA inventions are encouraged to promote competition and to achieve the widest use of inventions. They must be used by a netotiated target date.

**Exclusive licenses** may be granted to encourage early commercial development of NASA inventions, especially when considerable private investment is required. These are generally for 5 to 10 years and usually require royalties based on sales or use.

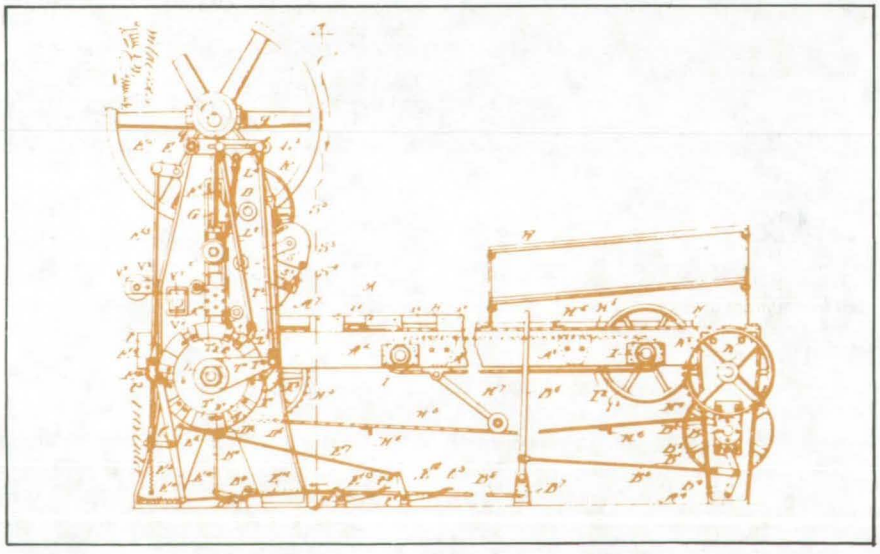

**Additional licenses available** include those of NASA-owned foreign patents. In addition to inventions described in NASA Tech Briefs, *"NASA Patent Abstract Bibliography"* (PAB), containing abstracts of all NASA inventions, can be purchased from National Technical Information Service, Springfield, VA 22161. The PAB is updated semiannually.

***Patent licenses for Tech Briefs*** *are frequently available. Many of the inventions reported in NASA Tech Briefs are patented or are under consideration for a patent at the time they are published. The current patent status is described at the end of the article; otherwise, there is no statement about patents. If you want to know more about the patent program or are interested in licensing a particular invention, contact the Patent Counsel at the NASA Field Center that sponsored the research* [see page A5]. *Be sure to refer to the NASA reference number at the end of the Tech Brief.*

# APPLICATION TEAMS

## Technology-matching and problem-solving assistance to public-sector organizations

**Application engineering projects** are conducted by NASA to help solve public-sector problems in such areas as safety, health, transportation, and environmental protection. Some application teams specialize in biomedical disciplines; others, in engineering and scientific problems. Staffed by professionals from various disciplines, these teams work with other Federal agencies and health organizations to identify critical problems amenable to solution by the application of existing NASA technology.

***Public-sector organization*** *representatives can learn more about application teams by contacting a nearby NASA Field Center Technology Utilization Office* [see page A4].

# INDUSTRIAL APPLICATIONS CENTERS

## Computerized access to over 10 million documents worldwide

**Computerized information retrieval** from one of the world's largest banks of technical data is available from NASA's network of industrial Applications Centers (IAC's). The IAC's give you access to 1,800,000 technical reports in the NASA data base and to more than 10 times that many reports and articles found in nearly 200 other computerized data bases.

**The major sources include:**

- *750,000 NASA Technical Reports*
- *Selected Water Resources Abstracts*
- *NASA Scientific and Technical Aerospace Reports*
- *Air Pollution Technical Information Center*
- *NASA International Aerospace Abstracts*
- *Chem Abstracts Condensates*
- *Engineering Index*
- *Energy Research Abstracts*
- *NASA Tech Briefs*
- *Government Reports Announcements*

and many other specialized files on food technology, textile technology, metallurgy, medicine, business, economics, social sciences, and physical science.

**The IAC services** range from tailored literature searches through expert technical assistance:

- *Retrospective Searches:* Published or unpublished literature is screened, and documents are identified according to your interest profile. IAC engineers tailor results to your specific needs and furnish abstracts considered the most pertinent. Complete reports are available upon request.
- *Current-Awareness Searches:* IAC engineers will help design a program to suit your needs. You will receive selected monthly or quarterly abstracts on new developments in your area of interest.
- *Technical Assistance:* IAC engineers will help you evaluate the results of your literature searches. They can help find answers to your technical problems and put you in touch with scientists and engineers at appropriate NASA Field Centers.

**Prospective clients** *can obtain more information about these services by contacting the nearest IAC* [see page A4]. *User fees are charged for IAC information services.*

# STATE TECHNOLOGY APPLICATIONS CENTERS

## Technical information services for industry and state and local government agencies

**Government and private industry** in Florida and Kentucky can utilize the services of NASA's State Technology Applications Centers (STAC's). The STAC's differ from the Industrial Applications Centers described on page A7, primarily in that they are integrated into existing state technical assistance programs and serve only the host state, whereas the IAC's serve multistate regions.

**Many data bases,** including the NASA base and several commercial bases, are available for automatic data retrieval through the STAC's. Other services such as document retrieval and special searches are also provided. (Like the IAC's, the STAC's normally charge a fee for their services.)

***To obtain information*** *about the services offered, write or call the STAC in your state* [*see page A4*].

# COSMIC®

## An economical source of computer programs developed by NASA and other government agencies

**A vast software library** is maintained by COSMIC — the Computer Software Management and Information Center. COSMIC gives you access to approximately 1,600 computer programs developed for NASA and the Department of Defense and selected programs for other government agencies. Programs and documentation are available at reasonable cost.

**Available programs** range from management (PERT scheduling) to information science (retrieval systems) and computer operations (hardware and software). Hundreds of engineering programs perform such tasks as structural analysis, electronic circuit design, chemical analysis, and the design of fluid systems. Others determine building energy requirements and optimize mineral exploration.

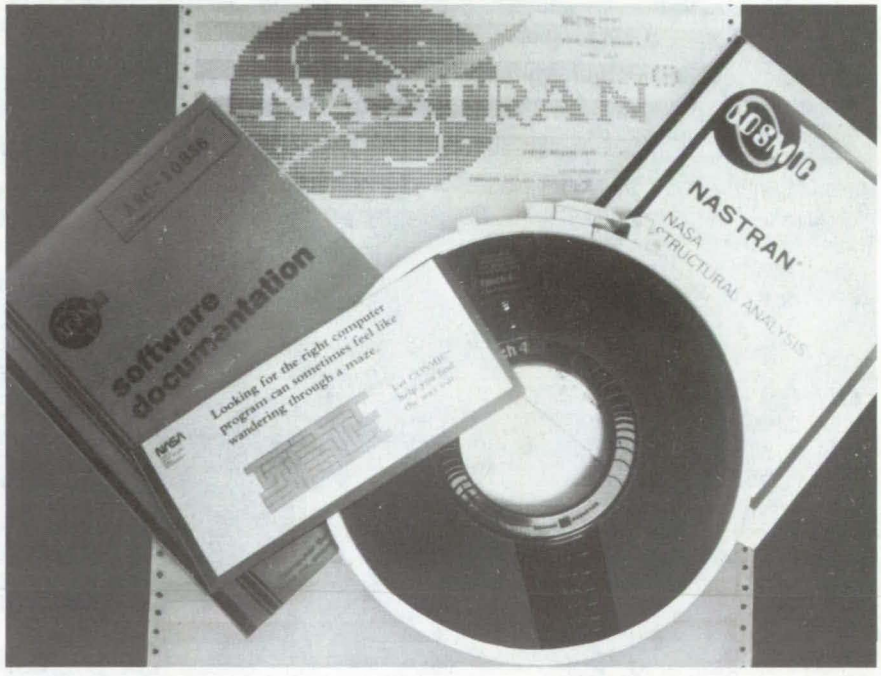


**COSMIC services** go beyond the collection and storage of software packages. Programs are checked for completeness; special announcements and an indexed software catalog are prepared; and programs are reproduced for distribution. Customers are helped to identify their software needs; and COSMIC follows up to determine the successes and problems and to provide updates and error corrections. In some cases, NASA engineers can offer guidance to users in installing or running a program.

***Information about programs*** *described in NASA Tech Briefs articles can be obtained by completing the COSMIC Request Card at the back of this issue. Just circle the letters that correspond to the programs in which you are interested.*

# NEW PRODUCT IDEAS

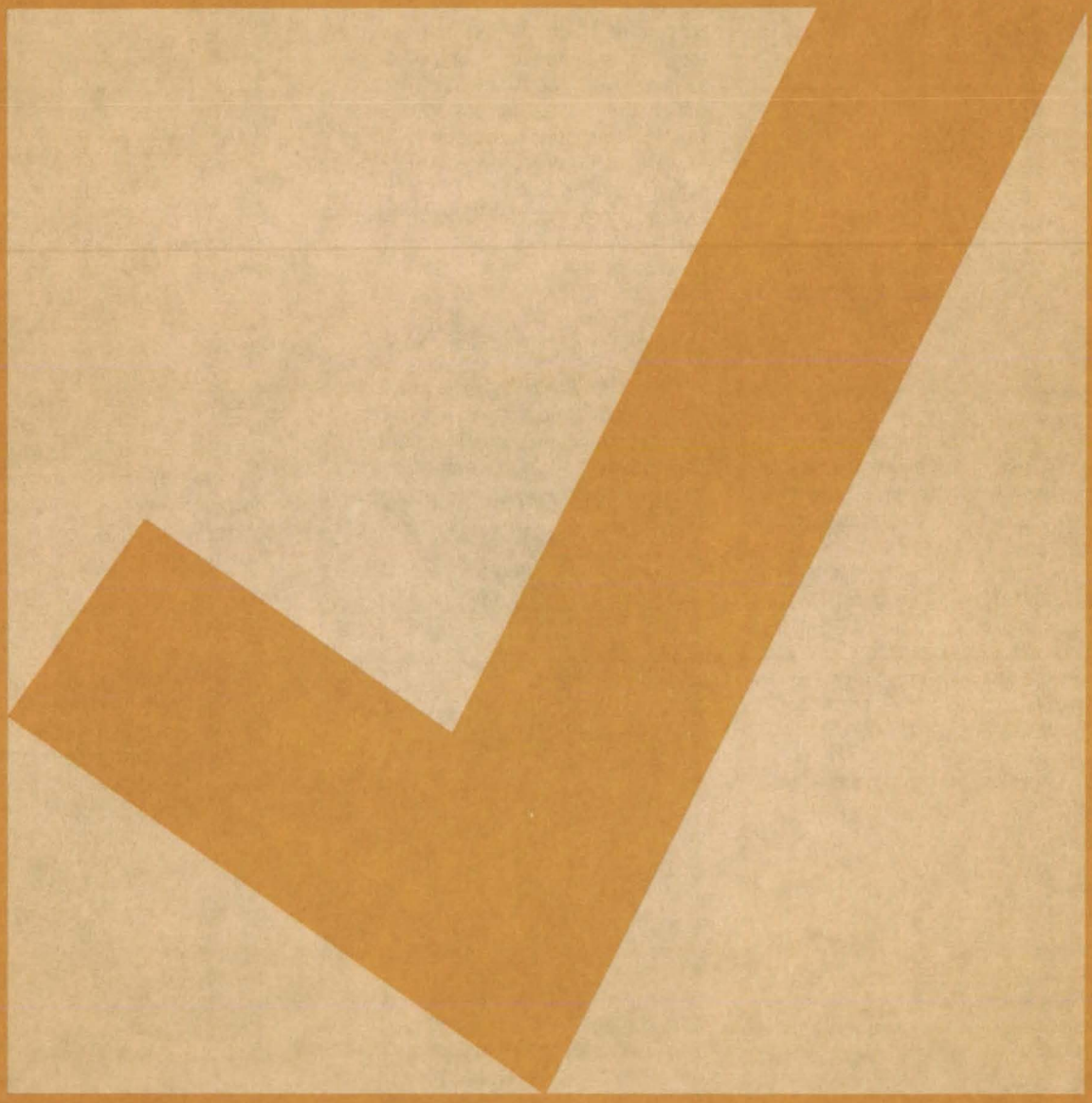

**NEW PRODUCT IDEAS** are just a few of the many innovations described in this issue of NASA Tech Briefs and having promising commercial applications. Each is discussed further on the referenced page in the appropriate section in this issue. If you are interested in developing a product from these or other NASA innovations, you can receive further technical information by requesting the TSP referenced at the end of the full-length article or by writing the Technology Utilization Office of the sponsoring NASA center (see page A4). NASA's patent-licensing program to encourage commercial development is described on page A6.

## Unidirectional Flexural Pivot

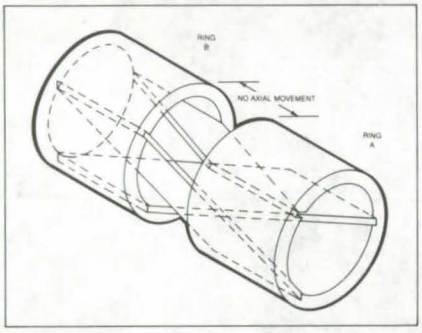


A new flexural pivot deflects in only one direction, either clockwise or counterclockwise, and has a longer operating life than many previous designs. The durable pivot is a frictionless bearing that is particularly suitable for small angular deflections. Two coaxial rings are fastened in a connection that is rigid for axial motion, is rigid for one direction of rotation, but permits flexure for the opposite direction of rotation. The two rings are interconnected by three flat metal parallelograms (the springs) welded into grooves in the rings. The springs prevent the rings from moving either toward or away from each other.
(See page 204)

## High-Efficiency dc/dc Converter

High efficiency at low power and an ability to provide an output either larger or smaller than its input voltage are the unique features of a new dc/dc converter. The circuit could possibly be packaged as an efficient power supply for CMOS logic. Consisting of a precision reference source and an error amplifier, the converter provides ±12 V from an unregulated dc source of from 14 to 40 V. When operated at 28 Vdc input, it has an efficiency of 80 percent or greater from a power level of 300 mW up to 1 watt.
(See page 124.)

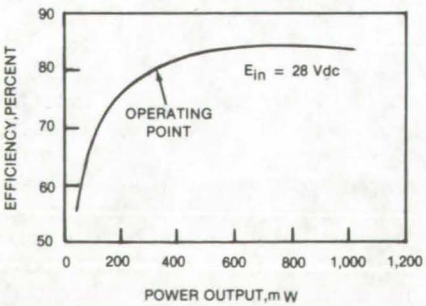


## Lightweight Face Mask

New lightweight masks protect the faces of epileptic and cerebral palsy patients during seizures. The lightest of the new masks weighs only 136 grams.

Similar masks could also protect football linesmen and riot-control police. The new masks consist of inner and outer layers of fiberglass cloth, with seven cloth layers between them; the layers are vacuum-molded together using a thermosetting epoxy resin.
(See page 220.)

## Superabsorbent Fabric

A multilayer fabric contains gel-forming polymer and copolymer containers that absorb from 70 to 200 times their weight of liquid. The superabsorbent

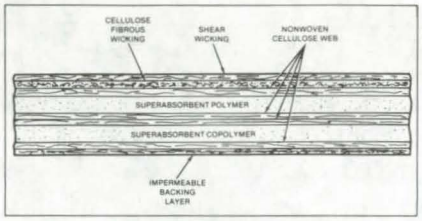


fabric can be used in baby diapers, female hygiene napkins, and hospital bedpads; because the material binds fluids in the form of a gel, the surface in contact with the skin is comfortable and dries rapidly. It might also have uses in moisture retainers for plants and in the improvement of dry soil. Until the reaction between the liquid and the absorbent gel-forming masses occurs, a backing layer retains the liquids within the fabric.
(See page 168)

## Thermal Diode

High forward-mode conductance is combined with rapid reverse-mode shutoff in a new heat pipe. The design of the pipe is simpler and more compact than other thermal-diode heat pipes and requires no special materials, forgings, or unusual construction techniques. One leg of the

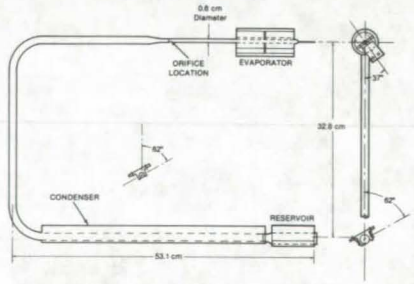


U-shaped heat pipe ends at the evaporator, which is coupled to the instrument to be cooled, and the other leg is the condenser, which terminates in a liquid reservoir. A narrow orifice within the pipe "chokes off" the evaporator when the condenser is hotter than the evaporator.
(See page 185)

## Flame-Retardant Coating

| Fire-Retardant Additive | Additive/Polymer Weight Ratio | Substrate | BOI |
|---|---|---|---|
| DBO/AO | 40/60 | Nomex* | 24 |
| DBO/AO | 60/40 | Nomex | 28 |
| DBO/AO/AP | 54/46 | Nomex | 28 |
| DBO/AO/AP | 70/30 | Nomex | 32 |
| DBO/AO/AP | 70/30 | Nylon | 23 |
| DBO/AO/AP | 70/30 | Nylon (Coated Both Sides) | 29 |
| DBO/AO | 40/60 | Neoprene-Coated Nylon | 29 |
| DBO/AO/AP | 70/30 | Neoprene-Coated Nylon | 32 |

*Heat-resistant nylon; trademark of E. I. du Pont de Nemours & Co.

A polyurethane-based coating makes fabrics flame- and abrasion-resistant, yet retains their flexibility. The coating, which is sealed to the fabric by heat, produces lightweight, impermeable fabrics that are firesafe and can withstand rough use. The coated fabrics are suitable for rainwear, clothing for hazardous environments, and leakproof containers. The coating consists of thermoplastic polyurethane combined with flame-retardant fillers in various proportions. The combination yields an elastomer that can be bonded to woven or knit fabrics and bonded webs of natural or synthetic fibers, such as cotton, rayon, nylon, polyester, and polyamide.
(See page 167)

## Indium Second-Surface Mirrors

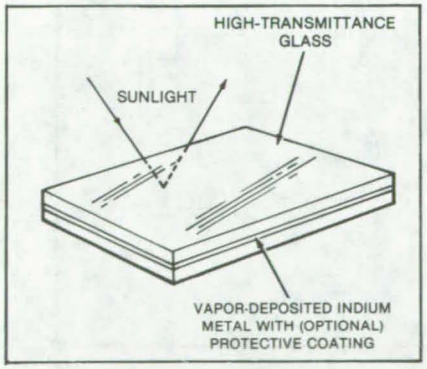


Corrosion-resistant second-surface mirrors, which may be used in solar-energy concentrators, are constructed from indium metal vapor-deposited on glass. The new mirrors are comparable in reflectance to silvered or aluminized mirrors and would resemble ordinary second-surface mirrors with metal deposited on the rear of the glass and a protective coating. Indium is well suited to vacuum deposition onto glass: It has relatively low melting and boiling points and wets smooth, clean glass. At room temperature, indium is resistant to corrosion in air; it also resists attack by organic acids and is a longer-lived reflective material than silver or aluminum.
(See page 228)

## Cam-Design Torque Wrench

A new torque wrench for electrical connectors automatically tightens its grip with increasing torque. It requires only minimal clearance between the connector and adjacent structures. The wrench is operated with one hand and can be used on connectors of various shapes. A set of such wrenches would accommodate a range of connector

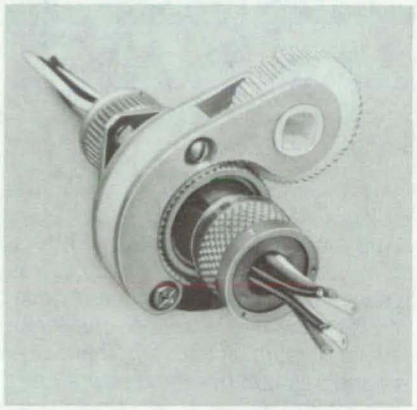

sizes. An eccentric wheel in the new wrench increases the frictional load on the connector as the torque is increased. The gripping surfaces of the tool are plastic to prevent damage to the surface finish of the connector.
(See page 203)

## Surface Seal for Carbon Parts

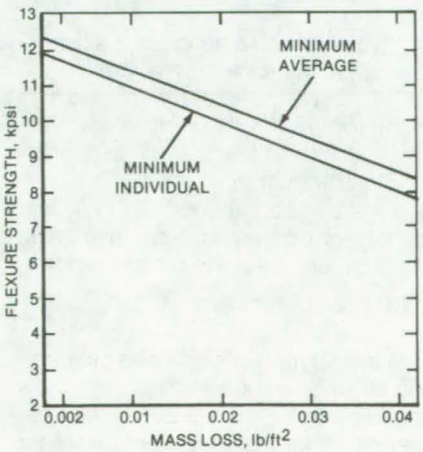


Surface pores in parts made of graphite or reinforced-carbon/carbon materials are sealed by a silicon carbide-based antioxidation coating. The coating, which could possibly be developed as a patch or sealer "kit" for carbon parts, inhibits subsurface oxidation and thus lengthens part life at high temperature. The starting material for the coating is graphite felt, which is converted to silicon carbide felt by processing it according to a prescribed time/temperature schedule. The part is prepared by rubbing with a fine abrasive paper and wiping with an alcohol-moistened cheesecloth. The sealant is applied with a brush, spatula, or blade. After a first coat is applied and cured, the coating and curing procedure is repeated.
(See page 164)

## Four-Degree-of-Freedom Platform

A new movable platform could be built at relatively low cost with readily available components. It could be useful in stabilizing shipboard equipment, material-handling machinery, and construction equipment. The platform moves in four degrees of freedom — simultaneous pitch, roll,

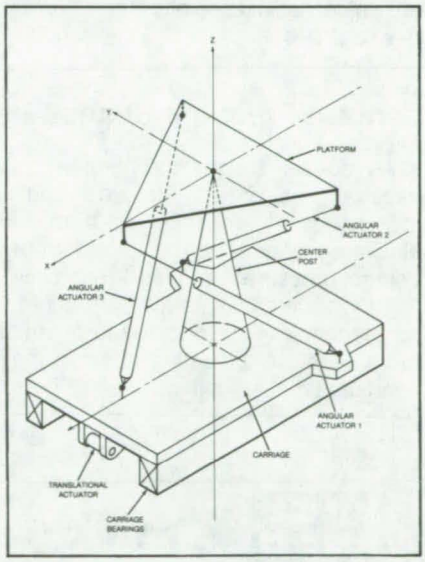


yaw, and displacement. Three canted hydraulic actuators transmit angular motion, while a carriage transmits translational motion to the supporting surface. Because the platform has less dead mass than gimbaled support surfaces, it requires less energy and can respond more rapidly. Since the three actuators produce only angular, rather than translational motion, their stroke is kept to a reasonable length. Mechanical stops prevent overtravel.
(See page 211.)

## Latch With Single-Motion Release

An improved latching and locking mechanism cannot be loosened by vibration, yet can be released by one hand turning a lever. The latch holds an object securely and allows it to be removed easily when necessary. A quick-load/quick-release mechanism allows an object such

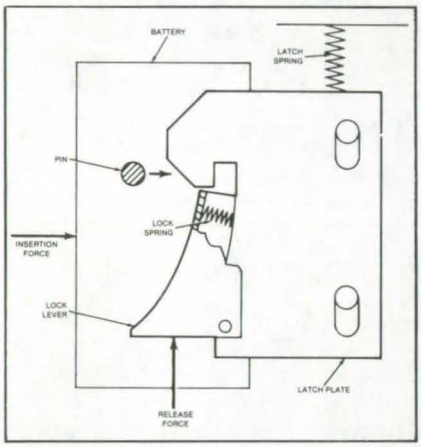


as a battery to be inserted with a single motion, locks and latches the object, and releases the object in a single motion. To release an object, the operator simply pushes on the flat edge of a lever.
(See page 214)

## Contact-Pressure Sensor

An optical sensor for mechanical hands senses contact pressure through the change in light reflected from an elastic covering. The measurement of contact pressure improves the sensitivity of robot manipulators by giving better feedback of the gripping force and more sensitive indication of when the hand contacts an object. Optical fibers

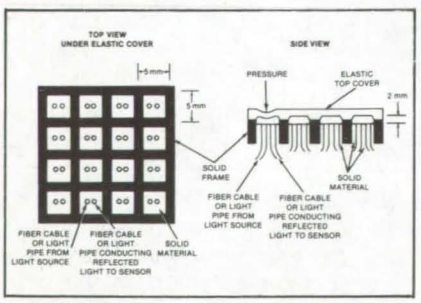


bring light into cells on the gripping surface. The light is reflected from the flexible covering into other fibers leading to detectors. Distortion of the covering due to tactile pressure changes the amount of the reflected light. If only touch indication is desired, a threshold detector can be included in the electronics.
(See page 207.)

## Simpler Variable-Speed Drive for Fan or Pump

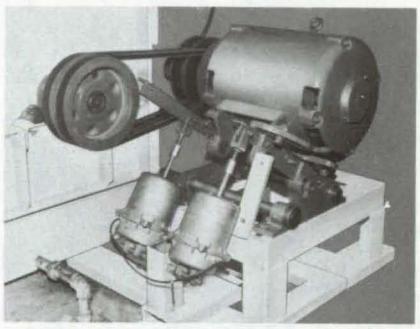

The static pressure developed by a fan or pump is used directly to control its speed in a new variable-speed drive unit. This new drive is a simple, low-cost way of varying speed automatically. Fan and pump current and power consumption are also reduced. Pneumatic motors activated by pressure pivot the main drive motor, changing belt tension and causing the effective diameter of the variable pulley to change. The pivoting occurs under low friction, so that little force is needed to open the pulleys.
(See page 199.)

## Improved Cure-in-Place Adhesives

Two improved cure-in-place silicone-elastomer-based adhesives are flexible at low temperatures and withstand high temperatures without disintegrating. They also have low thermal expansion and low thermal conductivity. Both elastomers can be extruded from conventional repair guns and should find use in applications requiring high-performance adhesives, such as sealants for solar collectors. The key feature of the compounds is the addition of hollow microsphere fillers to the elastomer resin. The microspheres keep the adhesive in place during repair and prevent it from being drawn off by capillary forces prior to cure. Phenolic microspheres increase the char yield, while silicone microspheres form a viscous protective melt.
(See page 164).

## Surface-Contamination Inspection Tool

A new inspection tool detects surface contamination by measuring photoelectron emission in air. The photoemission from metals, epoxy paint, and other materials illuminated with 2,500-Å UV light is measured under ordinary atmospheric conditions, so surfaces can be inspected in factory or in the field. The photoelectrons travel through the air between the surface under inspection and a collector that is part of the tool. Hydrocarbons or silicone contaminant are detected by a

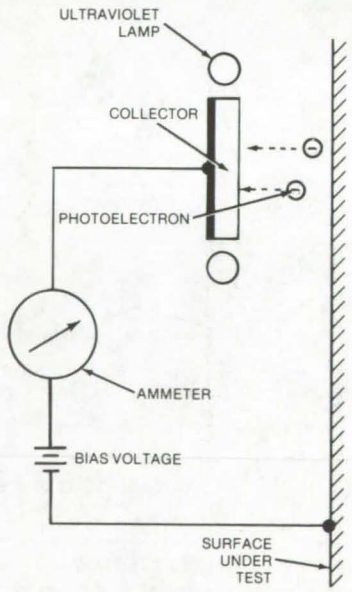


reduction of the photoemmission current below the normal clean-surface value. Other contaminants may cause an increase in current above the normal level.
(See page 190)

# Electronic Components and Circuits

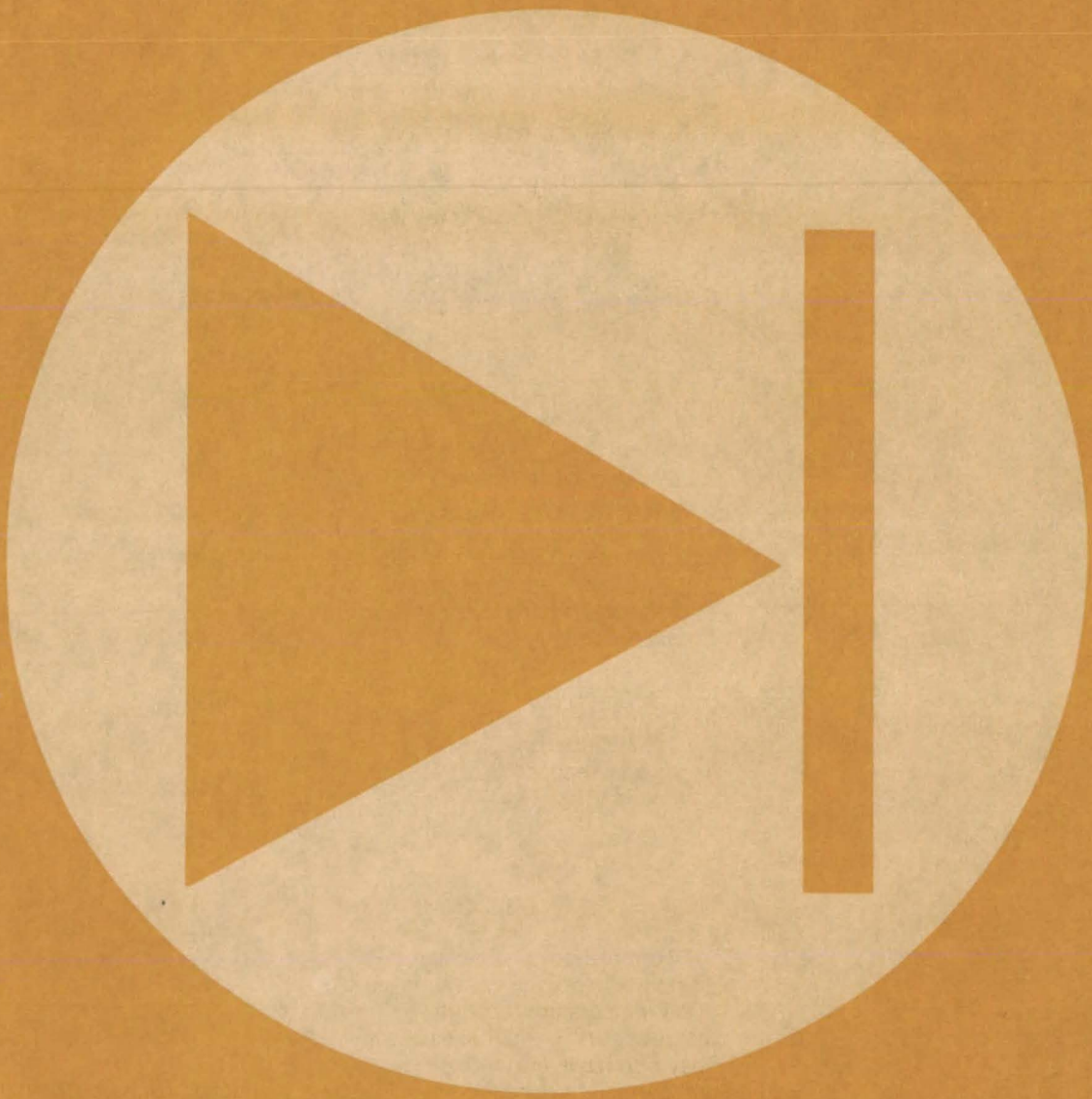

## Hardware, Techniques, and Processes



## Books and Reports

# Solar-Array Simulator

A test circuit has the V/I characteristic of a photovoltaic array.

*Lyndon B. Johnson Space Center, Houston, Texas*

For testing systems that are powered by solar cells, it is convenient to have a power source that generates the same voltage/current characteristic as a photovoltaic array. Such a solar-array simulator has been built for evaluating the power extension package in the Space Shuttle. It produces the V/I curves of photocell sources, offering a wide range of normal or degraded characteristics and even duplicating the transient behavior under partial illumination associated with morning and evening penumbra. Several units can be paralleled to supply any power level.

The relationship between output voltage and output current from a typical array is shown in the top portion of the figure. The curve has three zones. Zone 1 is an essentially-linear V/I characteristic; Zone 3 is the characteristic of a constant-current source; and zone 2 is very similar to the nonlinear turn-on characteristic of a diode.

The simulator circuit is shown at the bottom of the figure. A standard commercial laboratory power supply, with a current-limiting feature and provision for program control, is the primary power source. The current-limiting feature is utilized to duplicate zone 3 behavior. Prior to the start of a test, the limit is set at the required maximum current.

A fixed 1-ohm power resistor in series with a variable electronic load (available commercially) duplicates the zone 1 and zone 2 characteristics. The electronic-load output impedance varies in response to a control voltage $V_C$, which is derived through a feedback network from a shunt resistance.

When the control voltage is above 5 volts, the impedance of the variable load is only about 0.1 ohm or less, which is small compared to the fixed 1-ohm resistor. In this regime, the simulator duplicates zone 1 behavior. As $V_C$ decreases, the variable impedance increases, and the simulator moves into zone 2. Two manual adjustments in the feedback network are made to optimize the "knee" of the zone 2 characteristic.

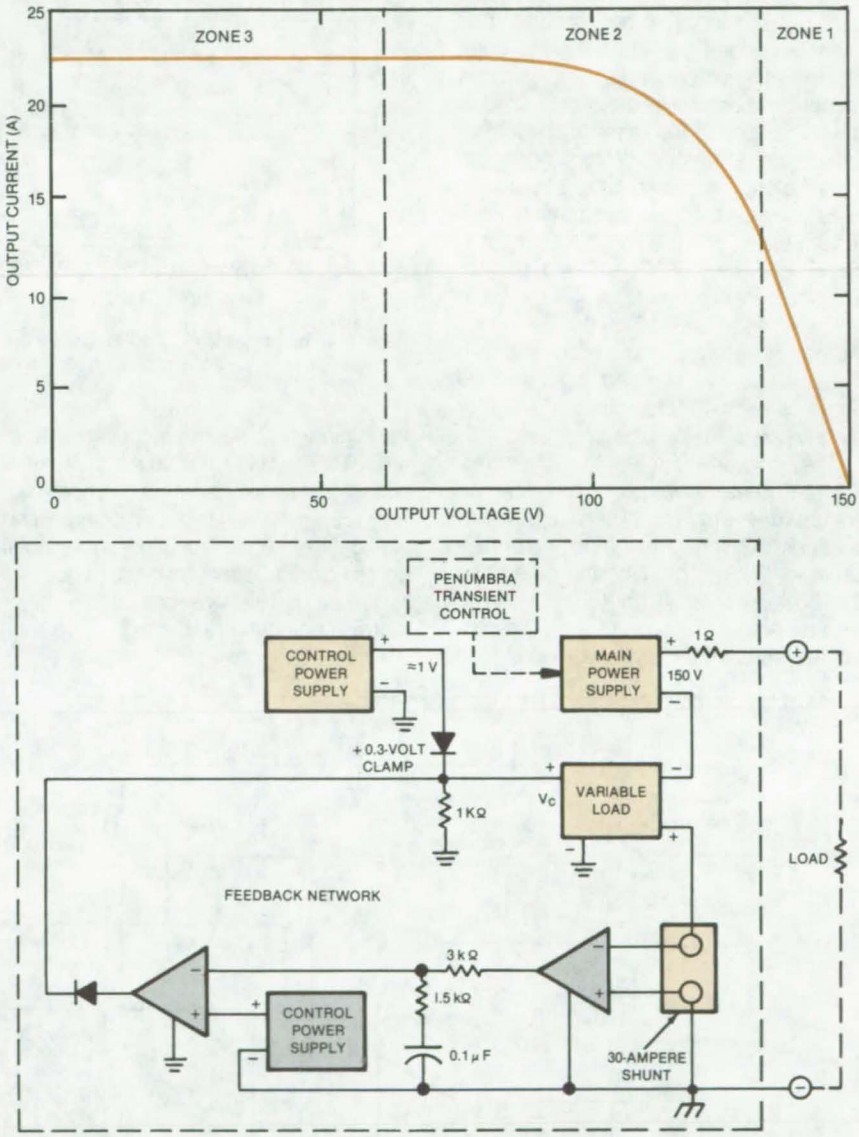


The **Solar-Array Characteristic** (top) is accurately simulated by the circuit at the bottom. Thus the circuit can be used in testing systems that are designed to be powered by photovoltaic cells.

By changing the controls on the front of the main power supply, or by using the programing capability, the simulator can be changed to approximate the characteristics of different solar arrays. The transient response to morning and evening penumbra or cloud cover can also be simulated that way.

*This work was done by Marion C. Wright of Lockheed Corp. for* **Johnson Space Center.** *For further information, Circle 1 on the TSP Request Card.*
*MSC-18864*

# High-Efficiency dc/dc Converter

Output 12 volts is derived from inputs up to 40 volts, with up to 80 percent efficiency.

*Lewis Research Center, Cleveland, Ohio*

A high-efficiency dc/dc converter has been developed that provides the commonly used voltages of ±12 V from an unregulated dc source of from 14 to 40 V. It was developed for use in a spacecraft instrument. At nominal design conditions, the efficiency achieved was 80 percent, which is twice that of any commercial unit tested. When operated at 28 Vdc input, it has an efficiency of 80 percent or greater from the design power level of 300 mW up to 1 watt, as shown in Figure 1. Efficiency increases at lower input voltages. It can deliver 300 mW over an input voltage range of 13 to 40 Vdc, making it ideal for battery-powered equipment.

The converter (refer to schematic, Figure 2) consists of a precision reference source and error amplifier ($U_1$), which pulse-width-modulates an astable oscillator ($U_2$) to produce the gate drive for power MOSFET switch ($Q_1$) in a multiple-output Cuk power stage. The control and reference circuits were designed for minimum power consumption. Use of an XR-L555 CMOS timing circuit as a voltage-controlled pulse-width modulator and the LM10 lower-power op-amp and voltage reference resulted in a total control-circuit drain of just under 1 milliampere. This was one of the major factors contributing to the high overall efficiency of the converter.

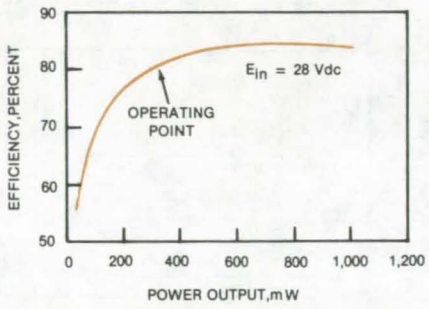


Figure 1. **Efficiency vs. Power Output** is shown for the ±12-V dc/dc converter.

Generation of the basic switching waveform is done by the XR-L555 timing circuit. A diode across pins 6 and 7 allows separate control of the charge and discharge of timing capacitor $C_6$, making possible the generation of a less-than-50-percent-duty-cycle output directly. Resistor $R_7$ controls the pulse width and therefore the switch "on" time, while $R_8$ controls the pulse spacing. With no control voltage applied, the pulse width is 10μs. It can be controlled by a voltage at pin 5, but can only be decreased because diode $D_2$ blocks an increase in control voltage that would be required to increase the pulse width. Fixing the maximum pulse width does two things. It provides a rough limit on output power and allows the circuit to start independent of the control. When power is first applied to the supply, $U_2$ starts oscillating at maximum pulse width. As the output voltage increases to 12V, which takes about 7 ms, the control loop starts to decrease the

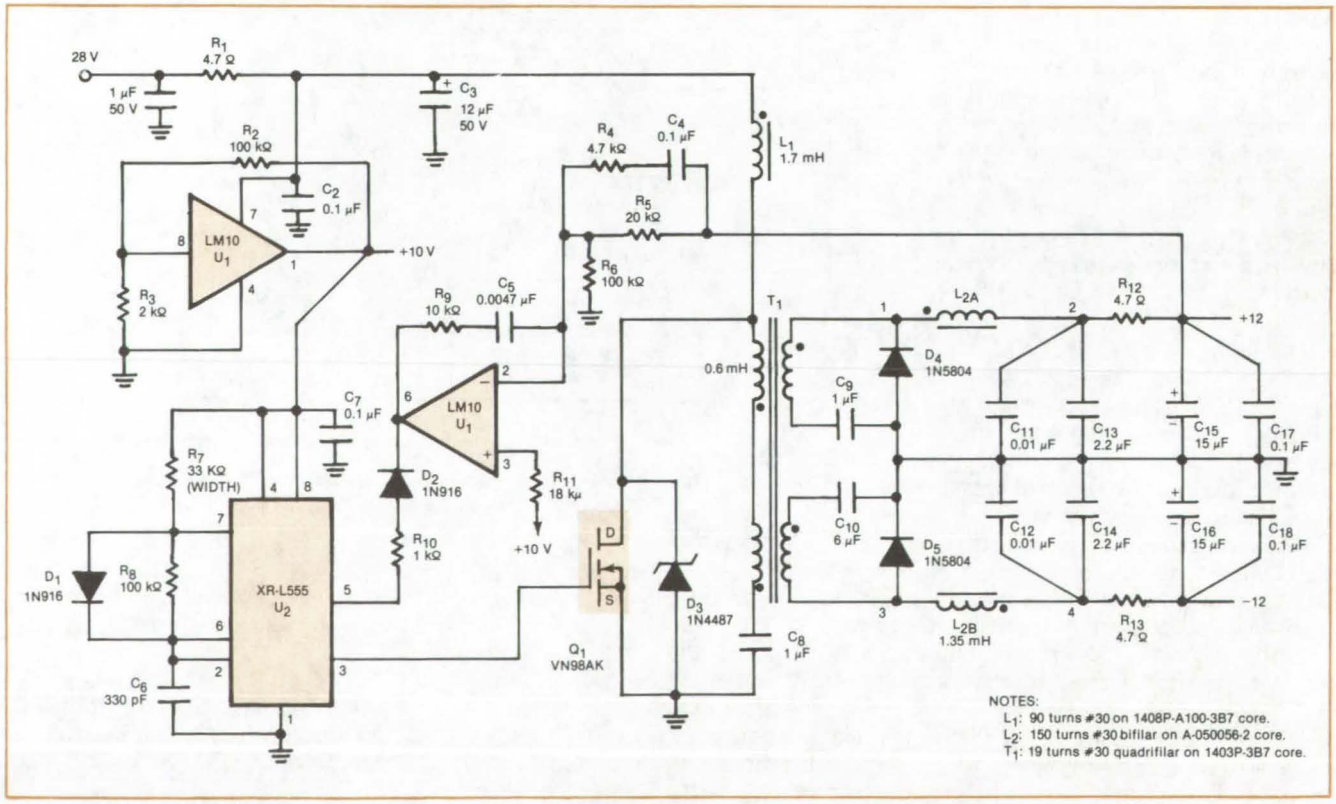


Figure 2. This **Circuit Schematic** shows the configuration of the ±12-V dc/dc converter.

pulse width to maintain regulation. Overshoot at turn-on is no more than 5 percent. Besides limiting inrush current during turn-on, this control philosophy prevents the initial error signal from forcing excess pulse widths that would saturate the input transformer and cause destructive overcurrents. When driving the design load, the on and off times are about 4 and 38 microseconds, respectively.

Power for $U_2$ and voltage reference for the error amplifier are provided by one-half of the LM10. Its internal 200-mV reference signal is amplified to 10 V for these functions. The other half of the LM10 is used as the error amplifier. It compares a portion of the +12-V output to the 10-V reference and drives the modulation input of $U_2$.

One limitation of the control as shown is that the minimum pulse width possible is 1 microsecond. This is not narrow enough to maintain output voltage regulation when the load is removed completely. A minimum load of 80 mW is required.

Since the maximum output power is 1 watt, this results in a usable range of power output of greater than 12 to 1, which is more than adequate for this essentially-fixed-load application. If desired, the uncontrolled duty cycle could be set lower, restricting the maximum power output and shifting the operating range downward. The remainder of the circuit in Figure 2 is the Cuk power converter with its input and output filters.

Limiting maximum pulse width provides a rough current limit and improves turn-on characteristics. Operating frequency is 25kHz and was chosen low to minimize losses. The circuit has been operated at above 100 kHz with somewhat reduced efficiency.

The unique features of this converter are its high efficiency at low power level and its ability to provide an output either larger or smaller than the input voltage. This high efficiency makes it an excellent supply for use with the very popular CMOS family of logic circuits.

*This work was done by John Sturman of* **Lewis Research Center.** *No further documentation is available.*
*LEW-13486*

# Wire-Wrap Chatter Detector

Detector responds to resistance changes of as little as 0.1 ohm.

*NASA's Jet Propulsion Laboratory, Pasadena, California*

A monitoring circuit responds to changes in resistance as little as 0.1 ohm. It has been used to detect defective wire-wrap connections during thermal and vibration tests.

A schematic diagram of the detector is shown in the figure. When connected to the input terminal, the wire-wrap circuit completes the voltage-divider chain of $R_1$, $R_X$, and $R_2$. Before testing, variable resistor $R_1$ is adjusted to set the voltage at point A to 2.48±0.005 V, while $R_3$ is used to set the voltage at the inverting input of the comparator to 2.50±0.005 V.

An increase in $R_X$ due to a defective wire wrap or any other reason will cause the voltage at point A to rise. If the increase in resistance exceeds 0.28 ohm, the change in voltage will exceed 0.03 volt, sufficient to trigger the comparator by overcoming the 0.02-V bias. The comparator output is fed to a one-shot multivibrator that controls a light-emitting diode. The comparator output also advances a two-digit counter.

$R_X$ must return to near its original value before the circuit can detect another increase. If the voltage at point A can be held 0.01 V below the reference voltage, then changes in $R_X$ as small as 0.092 ohm can be detected.

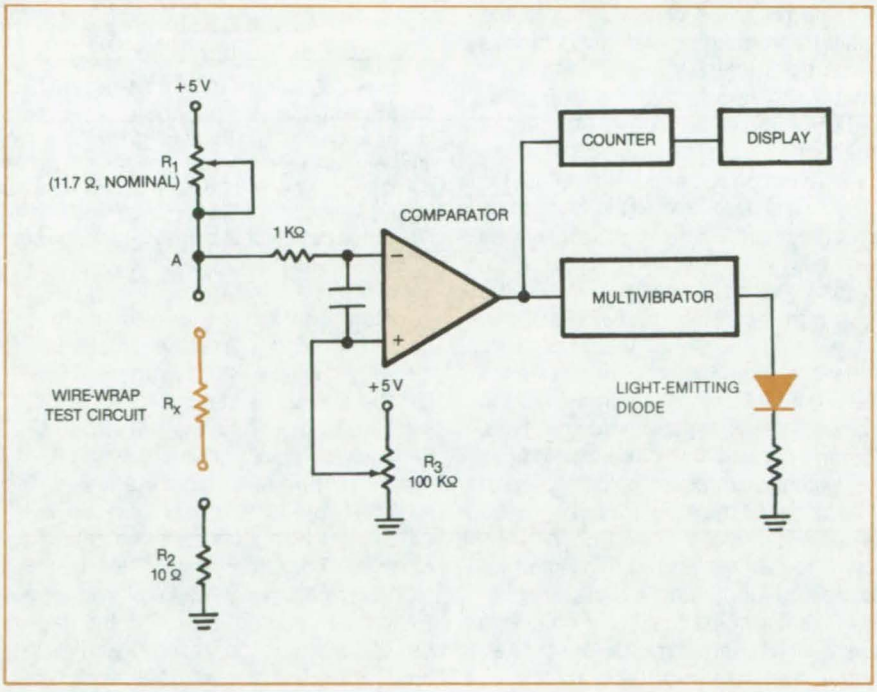


The **Wire-Wrap Chatter Detector** responds to small increases in resistance at defective contacts. A defect is indicated to the operator by a light-emitting diode and by an increase in the count on a two-digit display.

*This work was done by Gregory Z. Fisch and Thomas J. Borden of Caltech for* **NASA's Jet Propulsion Laboratory.** *For further information, Circle 2 on the TSP Request Card.*
*NPO-15290*

# Electronically Calibratable Clock

Apparent clock rate is automatically corrected when the display is reset to the correct time.

*Langley Research Center, Hampton, Virginia*

A calibration circuit corrects the apparent clock rate (ACR) of a digital clock without altering the oscillator frequency. The calibration circuit does not require iterative adjustments to a reference frequency or rate, and the correction to the ACR is controlled by pushbuttons.

Most electronic digital clocks or watches have an internal, adjustable, trimmer capacitor that alters the resonant frequency of a quartz crystal oscillator. The trimmer capacitor is initially adjusted to set the oscillator frequency equal to a standard. The accuracy can be within seconds per month, but crystal aging, temperature variations, and wearing habits alter the clock rate. Furthermore, altering the clock case configuration by opening or closing it changes the influence of the stray capacitance of the case on the oscillator frequency, and this influence varies from watch to watch. An even greater problem is that the user must turn the trimmer adjustment through a small angle, wait a week or so to observe the effect, and then readjust it. Often, a third adjustment is necessary to achieve an accuracy of 1 second per week.

Using the new circuit shown in the figure, the crystal frequency is not changed. Rather, the apparent clock rate is changed by circuitry that calculates the amount of error when the clock display is set to the correct time. The error-calculation circuitry modifies the digital-countdown reset point to slow or speed the ACR accordingly. External pushbuttons speed up or slow down the ACR, and the amount of change needed in the ACR is calculated and set automatically. Errors due to crystal aging, temperature, or other effects are precisely corrected.

The basic elements of an electronic watch are shown without color in the diagram. Elements in color make up the error-correction circuit. The difference in the new device is that when the slow-clock-gate or fast-clock-gate pushbutton is pressed, the OR gate is activated, which turns on an error counter. The output E of the error counter goes to correction-calculation circuitry, where the quantity $N + (2^{n-m} + N)E/T$ is computed. (The factor T is from a total-elapsed-time circuit, which starts counting when the reset pushbutton is depressed.)

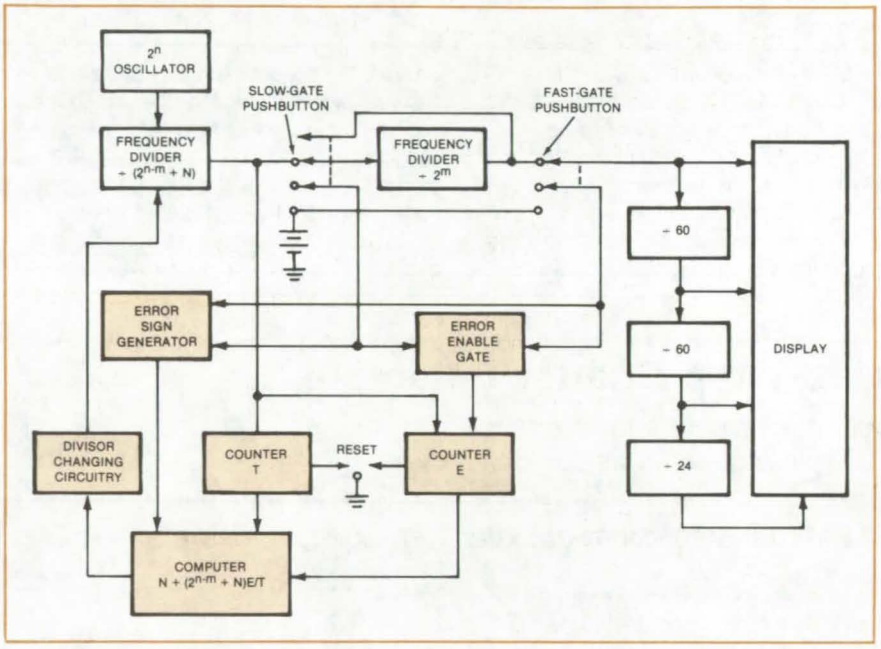


A **Clock-Calibration Circuit** (in color) is added to a conventional digital clock or watch. Rather than changing the crystal oscillator frequency, the divisor of the digital-countdown circuit is changed so that the ACR is adjusted. A calibration sequence begins some elapsed time T after the reset button is pushed. When the slow-clock pushbutton or the fast-clock pushbutton is pressed to reset the display to the correct time, the pushbutton also starts the error counter, and the quantity N is calculated (with sign). When the pushbutton is released, the current value of N adjusts the digital-countdown circuit to give the correct ACR.

When the ACR error correction is calculated, the correction-calculation circuitry sends the number, N, to the digital-countdown circuit . N is added to the countdown divisor if the fast-clock switch is depressed, and it is subtracted if the slow-clock switch is depressed. Based on N, the digital-countdown circuit changes the digital-countdown output such that it emits a pulse after $(2^n \pm N)$ oscillator cycles, rather than $2^n$ oscillator cycles. Thus, while the clock time is being properly set, its ACR is being precisely modified so that the ACR error is eliminated.

The ACR can be adjusted in two ways. In the first method, the user holds down one of the pushbuttons, stopping or speeding the clock as needed, until the displayed clock time is the same as a standard time (such as broadcast time pulses); when the button is released, the clock time and the ACR are both corrected to match the standard time signal. In the second method, the clock is set ahead to an anticipated time signal; when the button is released, the clock time and ACR again are corrected to the proper time and rate.

This technique is applicable to any timer or counter that counts up to a predetermined number and then outputs a pulse to a readout register or to control another device. The method is a simple way to alter the period between pulses. It can also be used to

design a precise, correctable frequency standard.

*This work was done by John R. Davidson and Joseph S. Heyman of* **Langley Research Center.** *For further information, Circle 3 on the TSP Request Card.*

*This invention is owned by NASA, and a patent application has been filed. Inquiries concerning nonexclusive or exclusive license for its commercial development should be addressed to the Patent Counsel, Langley Research Center [see page A5]. Refer to LAR-12654.*

## Load Pulser Is Sparkless

An SCR and timer periodically turn line current on and off.

*John F. Kennedy Space Center, Florida*

Sometimes it is necessary to find out which fuse or circuit breaker controls a particular ac line or wall outlet. One simple way is to short-circuit the line and then check for an open circuit breaker or fuse; however, this method turns off power to all receptacles on that circuit. A better technique, which is widely used, is to pulse the current — for example, by turning a lamp on and off — and then to use a "clip-on" current meter to find out which line carries the pulsating current.

The pulsating current is conventionally produced by a load pulser, which consists of a cam-operated switch that repeatedly connects and disconnects a resistor across the line or receptacle. Unfortunately, the switch generates sparks at the contacts and therefore is not safe in hazardous environments (such as areas where combustible gases or vapors may be present).

To avoid the spark danger, a new electronic load pulser uses a silicon-controlled rectifier (SCR) driven by a 555 timer to open and close the connection to a power resistor (see figure). The entire assembly of SCR, timer, dc supply for the timer, and resistor is mounted in a compact housing; it is simply plugged into the outlet for which the circuit breaker is to be identified.

The electronic load pulser can be used to verify 110/120-volt or 208-volt receptacles. If a stepdown transformer is added, 480-volt circuits may also be checked. Using the 2N685 SCR, up to 25 amperes can be pulsed. It should find applications in the chemical, petroleum, and transportation industries.

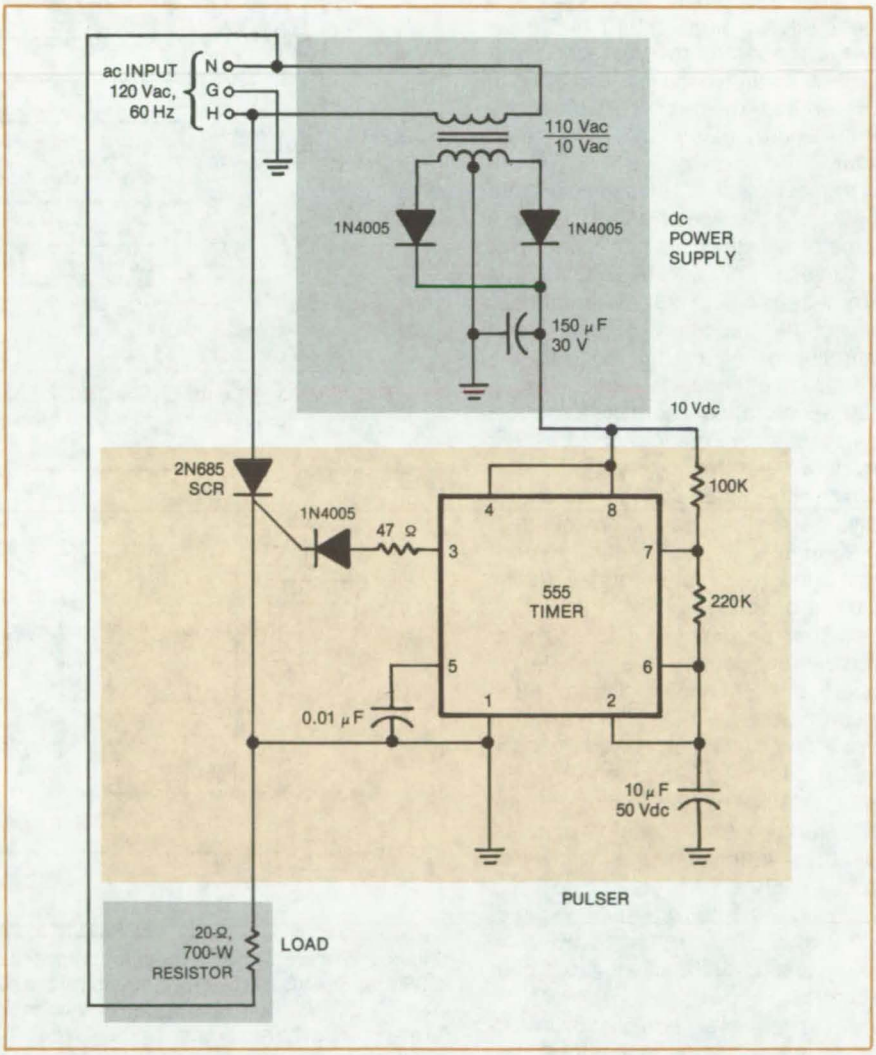


The **Electronic Load Pulser** uses a silicon-controlled rectifier (SCR) to open and close a circuit. It replaces a motor-driven mechanical switch, which causes sparks.

*This work was done by Franklin D. Washburn of Boeing Services International, Inc., for* **Kennedy Space Center.** *No further documentation is available.*

*Inquiries concerning rights for the commercial use of this invention should be addressed to the Patent Counsel, Kennedy Space Center [see page A5]. Refer to KSC-11199.*

# Alternating-Current Motor Drive for Electric Vehicles

An efficient inverter and ac motor would give electric vehicles extra miles per battery charge.

*NASA's Jet Propulsion Laboratory, Pasadena, California*

A proposed inverter circuit, when combined with a new drive circuit that has been successfully tested, could make ac motors more economical than dc motors in electric vehicles. The ac motors are preferred because they are more efficient, simpler, and more reliable than dc. Until now, however, ac motors have been impractical because conversion losses in conventional inverters more than offset the energy gained by using the ac motor.

The new electric drive (see Figure 1) controls the speed of a polyphase ac motor by varying the frequency of the inverter output. A closed-loop current-sensing circuit automatically adjusts the frequency of a voltage-controlled oscillator that controls the inverter frequency, to limit starting and accelerating surges. At low vehicle speeds, the motor turns the vehicle wheels through a gear train, shifted either manually or automatically. A reverse gear is not needed, since logic circuits in the inverter ensure that the motor rotates in the required direction.

At the beginning of the motor acceleration period, the inverter is excited at frequencies two to three times that required to drive the motor at baseline speed. This reduces the rated volts/hertz required by the motor and keeps the motor current from surging. As the motor accelerates, the inverter frequency is lowered until it reaches that required to drive the motor at its operating speed. Higher speeds are obtained by manually adjusting the oscillator to higher frequency.

In conventional polyphase inverters — which have efficiencies between 90 and 95 percent, most of the energy loss results from switching and commutation; static forward drop accounts for only 1 or 2 percent of the loss. The new inverter, shown in Figure 2, uses a combination of silicon-controlled rectifiers (SCR's) and power field-effect transistors (PFET's) to reduce switching and commutation losses, resulting in an efficiency in the 98- to 99-percent range.

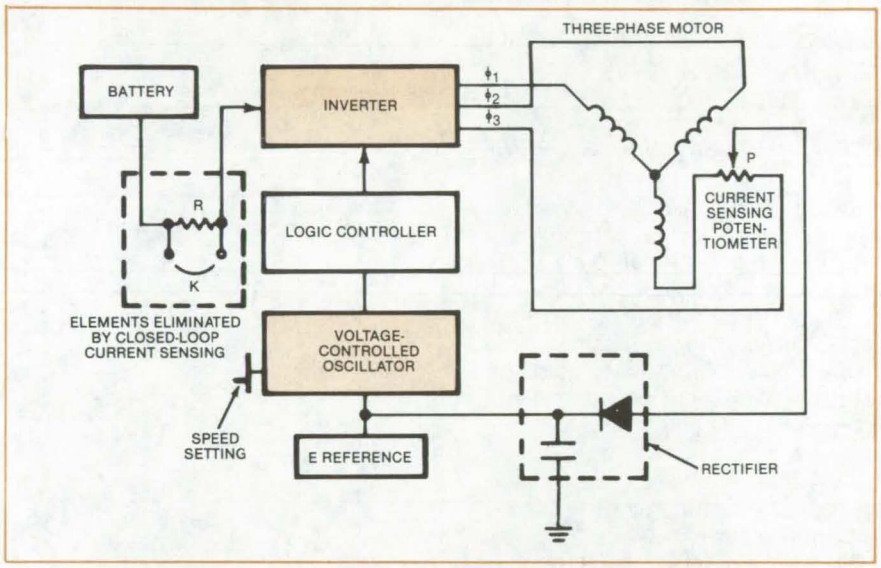


Figure 1. A **Voltage-Controlled Oscillator** adjusts the inverter frequency in response to the motor current, to limit starting and accelerating surges.

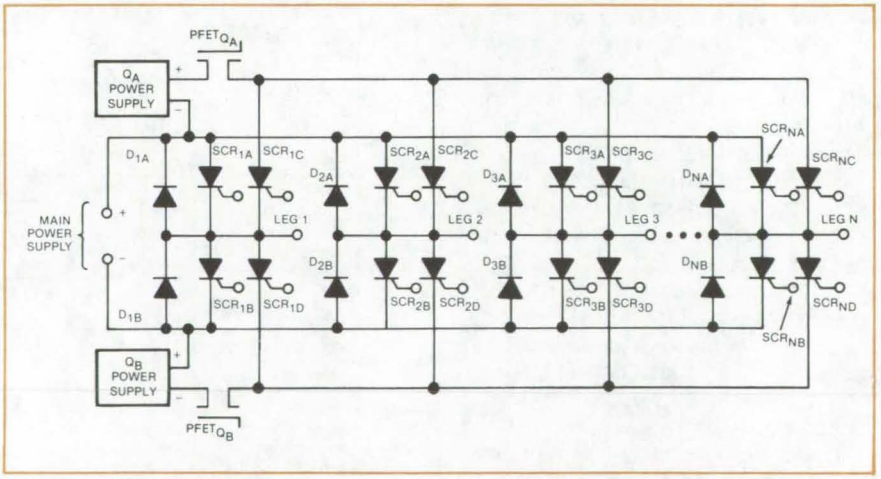


Figure 2. **Electric Vehicle Inverter** is composed of main SCR's (suffixes A and B) and steering SCR's (suffixes C and D) under the control of a pair of power field-effect transistors $Q_A$ and $Q_B$. The PFET's in turn are controlled by external logic circuitry that regulates the inverter frequency in response to the motor-speed requirements. The small power supplies for $Q_A$ and $Q_B$ supply saturation voltage to these PFET's and are responsible for no more than 0.2 percent of the total throughput power.

Since PFET's are free from second breakdown, a failing of other power transistors, turn-on and turnoff voltages can be allowed to rise or fall rapidly, independent of the load. Thus

switching losses are kept very low for all load currents, including low ones.

A pair of main SCR's and a pair of antiparallel diodes form the switching and reactive recovery elements for each of the N phases of the inverter. Each of the 2N main SCR's is positively gated during the "on" intervals and negatively gated during the "off" intervals.

Turnoff commutaton and voltage rise rate are controlled by a pair of PFET's for all main SCR's. A pair of steering SCR's for each phase directs the PFET-controlled commutation signals to the appropriate main SCR. The antiparallel diodes across the SCR's make it possible to brake the vehicle regeneratively, without cumbersome polarity-reversal circuits, so that the kinetic energy of the vehicle can be used to charge the battery.

For maxium efficiency and lowest cost, the inverter and ac motor should have four or more phases. As the number of phases is increased, the current ratings of the individual PFET's may be reduced. At the same time, inverter ripple and electromagnetic interference are reduced. The reduced current per phase allows smaller, faster SCR's to be used.

Because PFET's, when used in combination with SCR's, carry current over small duty cycles, the losses caused by PFET "on" resistance are quite small. This is in contrast to all-PFET inverters, in which the resistance losses are high.

*This work was done by Stanley Krauthamer and Wally E. Rippel of Caltech for* **NASA's Jet Propulsion Laboratory.** *For further information, Circle 4 on the TSP Request Card.*

*Inquiries concerning rights for the commercial use of this invention should be addressed to the Patent Counsel, NASA Resident Office-JPL [see page A5]. Refer to NPO-14768 and NPO-14830.*

# Two-Stage Linearization Circuit

High accuracy is obtained by combining analog and digital corrections.

*Langley Research Center, Hampton, Virginia*

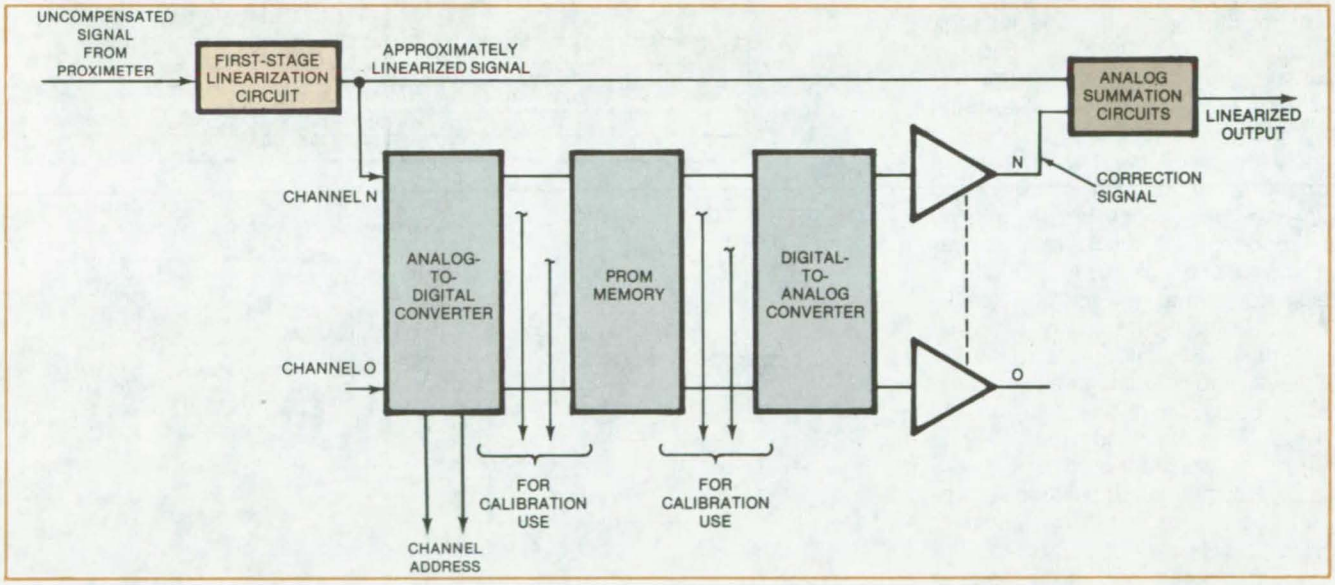


**Proximity-Sensor Linearization Circuit** has two stages. The first-stage linearization is accurate to about 3 percent; accuracy of the final output is better than 0.5 percent. By modifying the contents of the PROM, the circuit can also be used to derive a nonlinear output.

A proposed circuit for linearizing the output of a position sensor would have an absolute accuracy of better than 0.5 percent. The new circuit is also self-calibrating.

Linearization occurs in two stages: First, the sensor output is conditioned by an analog linearization circuit that has a room-temperature accuracy of about 3 percent. The first-stage output is then supplemented by a digital correction. The combined accuracy would far exceed that of either the analog or the digital circuit.

The input signal to the circuit must be monotonic. As shown in the block diagram, the first-stage output is time-sampled as one channel of a multichannel system. The signal is digitized, and the result specifies an address of the programable read-only memory (PROM). The output of the memory is the second-stage correction, which is summed with the first-stage approximation to yield the final signal.

Self-calibration is possible if a relatively-simple plug-in control unit is added. In the first step of the calibration, commands would be issued to a remote positioning table to move to the

(continued on next page)

position corresponding to the first memory address. When the table is accurately positioned, the unit automatically enters the program mode.

In the program mode, the signal is adjusted and continuously compared to the actual displacement. When the signal and displacement agree, the correction is programed into the specified memory location. The device then increments the position, and the calibration sequence is repeated until all data points have been programed.

When all positions are calibrated, the control unit advances to the check mode and resets. In the check mode, the sensors are swept back to the starting point and reset. During the sweep, the linearized signal is continuously compared with the actual position. If any point is not within the acceptance window dictated by the analog comparison, the machine halts and waits for further commands. It is estimated that the time required for calibration and test would be less than an hour.

The single-channel process is easily expanded by multiplexing, and resolving accuracy is limited only by the bit capacity of the analog-to-digital converter. Each channel would require an analog signal conditioner.

The technique can be used to derive any signal output using any monotonic input signal. Although originally developed to provide accurate linear signals, the concept could also derive accurate nonlinear outputs.

*This work was done by Gary C. Waldeck and Joe B. Dendy of Sperry Flight Systems for* **Langley Research Center.** *For further information, Circle 5 on the TSP Request Card.*
*LAR-12577*

# Lightweight, Low-Loss dc Transducer

Direct current is measured by a lightweight, magnetically coupled transducer.

*NASA's Jet Propulsion Laboratory, Pasadena, California*

A direct-current transducer that weighs only 4 grams measures dc without actually being wired into the circuit under test. The new tranducer measures currents of about 1 ampere, but it could be fabricated for currents on the order of tenths of an ampere simply by modifying the number of turns on the dc input winding. The miniature device consumes 16 mW, only one-tenth as much as a heavier (60-gram) previous model. Originally designed to reduce weight on spacecraft, the transducer may be used terrestrially to monitor motors, electric vehicles, and biomedical equipment.

The operation of the miniaturized device is similar to that of its forerunner. Constant-amplitude, fixed-frequency alternating voltage is applied to a pair of excitation windings, one on each core. The direct current to be measured is fed to another winding pair (the control windings) and creates a magnetic flux that varies with the current magnitude.

Since the effective core reactance varies with the degree of saturation of the core produced by the control current, the rectified output of the excitation windings is a direct current dependent on control current.

This output current is applied to the feedback winding in a direction to oppose the control current, thus linearizing the operation of the magnetic amplifier. The feedback current is measured by a current shunt, thus providing an output voltage that is a direct measure of the input (control) current and isolated electrically from the control-current circuit.

| WINDING No. | NUMBER OF TURNS | AMERICAN WIRE GAGE (AWG) | WOUND ON | TERMINATION (AWG) |
|---|---|---|---|---|
| 1 | 833 | 46 | CORE A | 30 |
| 2 | 833 | 46 | CORE B | 30 |
| 3 | 1,000 | 46 | BOTH CORES | 30 |
| 4 | 1 | 24 | BOTH CORES | 24 |
| 5 | 1 | 24 | BOTH CORES | 24 |

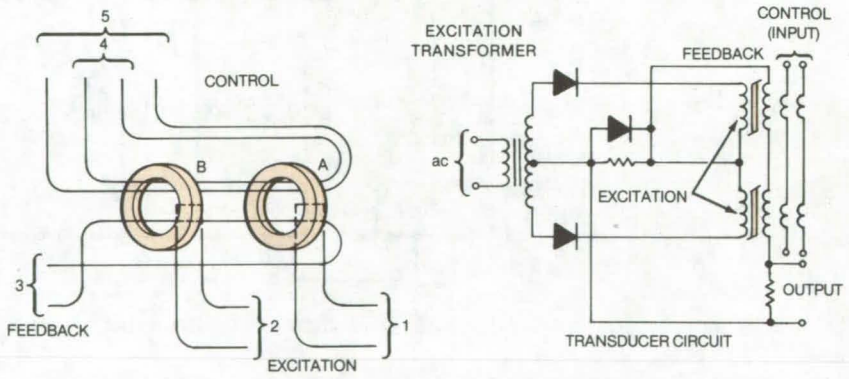


**Miniature dc Transducer** has five windings: Nos. 1 and 2 are ac excitation inputs, Nos. 4 and 5 are dc control inputs, and No. 3 is for feedback. The wire gages are selected for minimum size and weight. The size and number of turns of the dc windings are selected according to the dc current range to be measured — in this case for a current on the order of 1 ampere.

The transducer was miniaturized by careful choice of core and wire sizes. It has five windings on two cores (see figure), which are made of an iron/nickel alloy. Two windings — the excitation windings — are wound on separate cores. The

control and feedback windings are wound on both cores. Excitation and feedback windings are wrapped around the full 360° periphery of the toroidal cores. Two dc windings are provided, each with one turn (for a 1-ampere direct current). The turns ratio of the feedback coil to each of the excitation coils is 1.2 to 1, and the winding tolerance is ±0.1 percent.

The coil wires are insulated by a plastic sheath, and fiberglass tape 3 mils (0.08 mm) thick is wound around all the windings. The transducer is designed for an excitation frequency of 10 kHz and an ac drive voltage of about 10 V. When potted, the transducer weight increases to 9 grams.

*This work was done by Satoshi Nagano, Terry Koerner, Phil Brisendine, Howard Weiner, and Robert Detwiler of Caltech for* **NASA's Jet Propulsion Laboratory.** *For further information, Circle 6 on the TSP Request Card.*
*NPO-14618*

## Impact-Energized Transmitter

A mechanically-linked piezoelectric ceramic is the energy source for radio transmission.

*Marshall Space Flight Center, Alabama*

Impact-induced strain in a piezoelectric ceramic could power a short-range transmitter. The proposed impact-energized radio transmission would eliminate the need for external power sources or for batteries, which are often short lived and impractical to replace under operating conditions. The short-range transmitter was originally conceived for use in coal mining to communicate the presence of a coal/shale boundary.

When the object to which the transmitter is attached strikes something or is struck, the mechanically strained ceramic is polarized and acts as a charged capacitor. Because the ceramic is strained by the force acting on it, a voltage that is related to the magnitude of the force is generated across the electrodes of the ceramic. In the proposed transmitter, the strain-induced charge is fed to a resonant RLC circuit (see figure), which oscillates at a frequency determined by the values of its inductor and capacitor. The oscillating current then drives a simple antenna, which transmits a short pulse of electromagnetic energy at the resonant frequency to a receiver tuned to this frequency. The energy stored in the piezoelectric transducer could be released when either the strain or voltage on the ceramic exceeds the preset threshold.

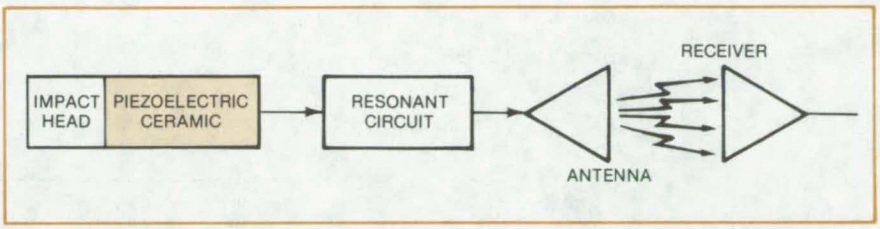


A **Piezoelectric Ceramic,** which is attached to an impact head, supplies the energy to drive a resonant circuit and antenna. A receiver tuned to the resonant frequency receives the short pulse.

The concept has been demonstrated in the laboratory. With a breadboard circuit and antenna, the deformation of a piezoelectric ceramic supplied sufficient voltage to propagate an electromagnetic pulse over a typical distance required for a coal/shale monitor.

*This work was done by Peter H. Broussard, Jr., of* **Marshall Space Flight Center.** *No further documentation is available.*

*Inquiries concerning rights for the commercial use of this invention should be addressed to the Patent Counsel, Marshall Space Flight Center [see page A5]. Refer to MFS-25379.*

# Books and Reports

These reports, studies, and handbooks are available from NASA as Technical Support Packages (TSP's) when a Request Card number is cited; otherwise they are available from the National Technical Information Service.

## Study of Two Digital Charge-Coupled Devices

Two CCD's are evaluated for long-term reliability.

A recent report describes a reliability study of two charge-coupled-device (CCD) shift registers. A major objective of the study was to establish a methodology for selecting, testing, screening, derating, and applying CCD's.

The devices studied were commercially available items selected as representative of CCD products employing the N-channel silicon-gate metal-oxide-silicon technology. One was a surface-channel device (SCCD), while the other was of the burried-channel type (BCCD). The two types were compared to determine whether

(continued on next page)

either had an inherent advantage for long-term space applications.

The report includes a discussion of CCD structures and operating principles. The characteristics of SCCD and BCCD types are compared. The physical construction is analyzed in terms of appearance, dimensions, certain physical tests, fabrication techniques, and circuit functions.

Each device is characterized by pin-to-pin electrical tests: These include both initial measurements to obtain reference data and measurements taken after environmental screening, thermal stress, temperature-cycle, overvoltage, and 4,000-hour life tests. The electrical measurements were performed at numerous times during the course of this testing and included device current, input-gate leakage, voltage offset, voltage gain, noise, bandwidth, and transfer efficiency.

All units that failed during the tests were examined and grouped by failure mode. Samples were analyzed to determine failure mechanism, probable cause, and the relationship between the failure and the operating condtions.

The specific conclusions and recommendations resulting from the study are complex and depend to an extent on numerous quantitative factors. As a general conclusion, it appears that both CCD types are reliable when operated within their ratings and exhibit stable characteristics in long-term operation. An initial electrical and environmental screening program is required to obtain reliable devices with the desired operating characteristics.

*This work was done by D. D. Wilson and V. F. Young of Martin Marietta Corp. for* **Marshall Space Flight Center.** *Further information may be found in NASA CR-161630 [N81-15193/NSP], "Study of Digital Charge Coupled Devices" [$21.50]. A paper copy may be purchased [prepayment required] from the National Technical Information Service, Springfield, Virginia 22161. The report is also available on microfiche at no charge. To obtain a microfiche copy, Circle 7 on the TSP Request Card.*

*MFS-25606*

# Electronic Systems

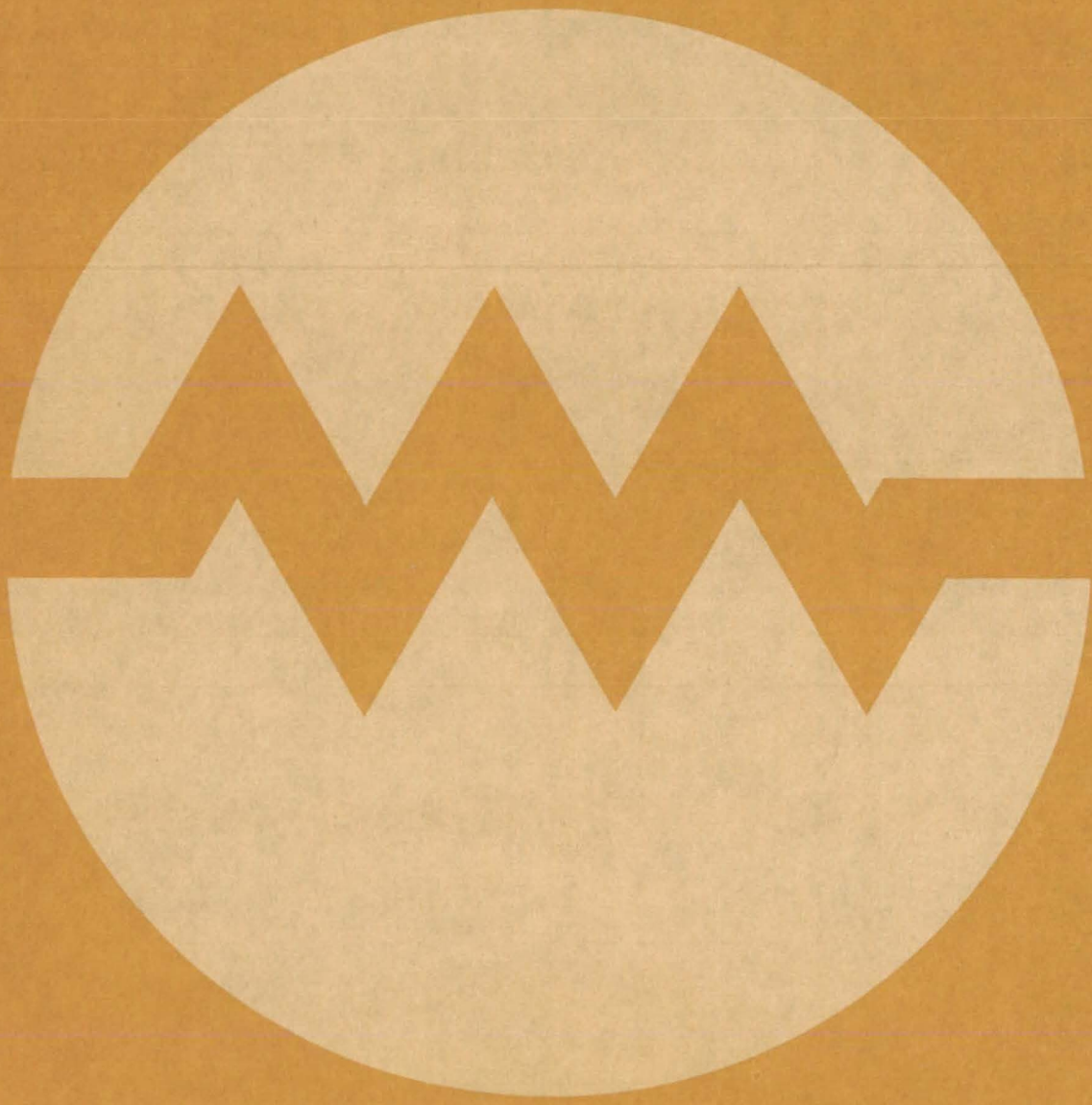

## Hardware, Techniques, and Processes

# Testing Patchboard Connections Automatically

Computer-controlled verifier reduces test time and improves reliability and accuracy.

*John F. Kennedy Space Center, Florida*

The maze of interconnections in Space Shuttle telemetry patchboards are rapidly checked by an automated test system. Verification procedures that take several days to complete when done manually are completed in only a few minutes by the new computer-controlled system. Up to 1,632 interconnections are tested by the present configuration. It can be adapted easily to other computer and communications networks.

The figure illustrates the block diagram of the 1,632-pin patchboard verifier. Under control of the computer, the register and the decoders direct signals in sequence to each of the 1,632 points. While a signal is being sent to 1 point, each of the remaining 1,631 points is scanned in sequence by the data selectors, also under computer control. The receipt of a signal at one of the scanned points indicates a connection, and this information is stored in the computer memory.

The verifier back plane contains plugs that mate with corresponding pins of the patchboard. At first, a patchboard known to be wired correctly is placed in the patchboard-verifier fixture. The connections are traced and recorded for use in the verification of other boards.

When another board is placed in the fixture, its signals are compared with those recorded from the standard board. If an error is found, the computer prints out proper patching instructions. The test operator can also command the computer to wait while a correction is made, checking the change and continuing the test if the change is correct.

The patchboard verifier, computer, and software performed satisfactorily in acceptance tests. The system is now used in quality performance checks on telemetry patchboards and will be used for testing before and during Space Shuttle launches.

*This work was done by John W. Brunson of IN-TEL-12 for* **Kennedy Space Center.** *For further information, Circle 8 on the TSP Request Card.*

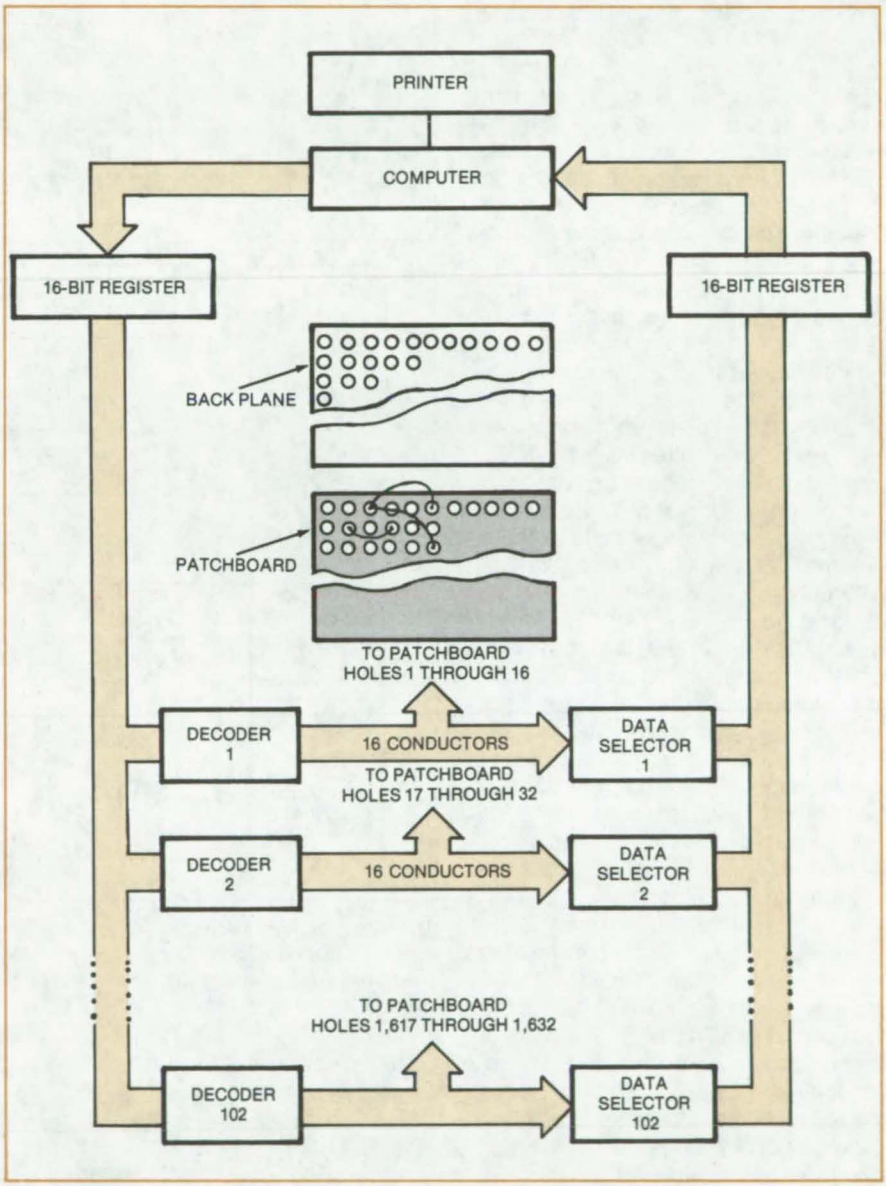


The **Patchboard Verifier** sequentially scans each pin on the patchboard and notes its connection, if any, to all of the other pins. The connection pattern is automatically compared with one known to be correct. An entire patchboard of 1,632 connections can be verified in about a minute.

*This invention has been patented by NASA [U.S. Patent No. 4,267,594]. Inquiries concerning nonexclusive or exclusive license for its commercial development should be addressed to the Patent Counsel, Kennedy Space Center [see page A5]. Refer to KSC-11065.*

# Array Processor Has Power and Flexibility

A proposed architecture combines the best features of lockstep and multiprocessor arrays.

*Ames Research Center, Moffett Field, California*

A proposed processor architecture would have the flexibility of a multi processor and the computational power of a lockstep array. Using an efficient interconnection network, it accommodates a large number of individual processors and memory modules. The present design, suitable for very large scientific simulation problems at sustained computational rates up to $10^9$ floating-point operations per second and other applications, has 512 processors and 521 memory modules.

Multiprocessor arrays, in which individual machines execute code independently but share a common memory, are usually limited to a relatively small number of processors. This is in contrast to the lockstep array, where many processors cooperate to execute synchronously a complex operation. With only a few exceptions, however, the lockstep array is limited to processing data that are in "vector" form; that is, the same operation is applied to each data element in a "vector," which is uniformly spaced within memory (or which has been gathered into a uniformly spaced area in memory). Those lockstep machines that allow computations on data outside of the simple vector form nonetheless fall far short of the flexibility offered by the multiprocessor.

In the new architecture, shown in the figure, each of the 512 processors has its own memory, which holds its own program and data; there is also a shared memory, consisting of 521 individual memory modules. Each processor independently and asynchronously sends requests for data to the shared memory.

Two functions are performed in nonreplicated hardware:

1. The issuing of lockstep commands, when all processors have arrived at predetermined points in their own programs and are in "wait" states: The estimated elapsed time between when the last processor arrives in its wait state and the issuance of the lockstep command is about 160 ns, or roughly the round-trip delay from the processor to a central point and back.
2. The processing of operations that are the same for all machines in the array: This includes the management of the data flow in and out of shared memory, communication with the external environment, the control of diagnostics, and other system software.

The first function is contained within a hardware item called the "coordinator"; whereas the second function is distributed among the coordinator, the controller for a staging memory (data-base memory), and a diagnostic controller.

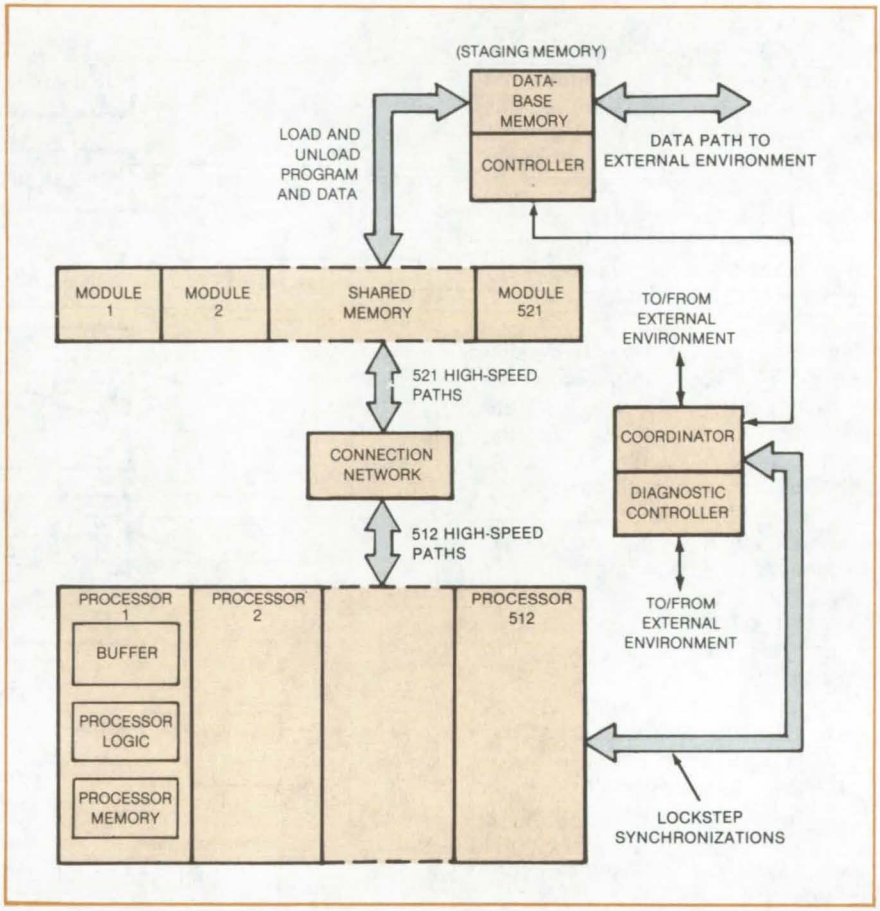


This **Array Architecture** would be suitable for very large scientific simulation problems and other applications. The amount of hardware required to perform the interconnections between the processor and memories grows as N log N (where N is the number of interconnected devices), rather than as $N^2$.

*This work was done by George H. Barnes, Stephen F. Lundstrom, and Phillip E. Shafer of Burroughs Corp. for* **Ames Research Center.** *For further information, Circle 9 on the TSP Request Card.*

*Inquiries concerning rights for the commercial use of this invention should be addressed to the Patent Counsel, Ames Research Center [see page A5]. Refer to ARC-11292.*

# Automatically Reconfigurable Computer

Modular system changes its architecture to maximize either reliability or capacity.

*Marshall Space Flight Center, Alabama*

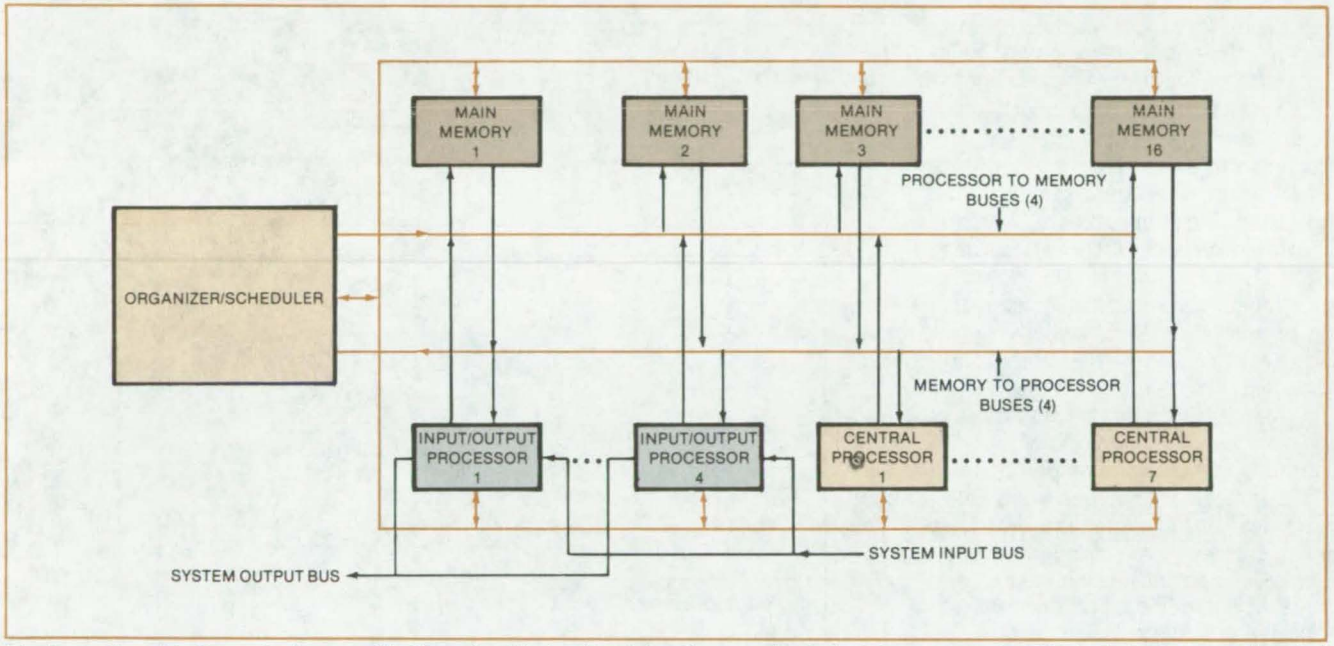


The **Reconfigurable Computer** is assembled from four kinds of modules: the organizer/scheduler, memory, input/output processor, and central processor.

A modular computer originally developed for spacecraft automatically reconfigures its architecture in response to changing operational needs. When high reliability is necessary, circuit modules involved in computation are switched into a redundant role to be available immediately if an operating module fails. During periods of extensive computation, the redundant modules are switched over to handle the heavy data load.

The computer consists of a group of central processors, input/output processors, memory modules, and an organizer/scheduler that coordinates the reconfiguraions of these elements (see figure). A reconfiguration is initiated by a signal from a control panel or by a fault interrupt from one of the modules.

A unique intermodule interface logic makes possible rapid and reliable reconfigurations at reasonable costs in power, volume, and complexity. The various modules and the organizer/scheduler communicate through redundant signal buses. Access to the buses and communication paths between the elements are determined by a system of priority requests, memory allocation, and fault detection. For example, the highest hardware priority goes to the organizer/scheduler, since the operation of the rest of the system depends on the successful completion of the organizer/scheduler tasks. Input/output elements and central processors have an ordered sequence of lower priorities.

A simplified version of the organizer/scheduler was breadboarded in transistor-transistor logic using small-scale integrated circuits. For maximum reliability it would ultimately be implemented with CMOS LSI (complementary-metal-oxide semiconductor large-scale-integration) technology. The circuit required the equivalent of 1,174 logic gates. It is simple enough to be implemented on two or three LSI circuits.

*This work was done by Hughes Aircraft Co. for* **Marshall Space Flight Center.** *For further information, including circuit details, Circle 10 on the TSP Request Card.*
*MFS-25455*

# Fast Holographic Comparator

Holographic subtraction enables rapid preprocessing of multiple channels of analog data.

*Langley Research Center, Hampton, Virginia*

An integrated optical-data preprocessor now under development is intended to operate on a set of analog voltages that are the outputs of a set of remote sensors — for example, the multichannel spectral signature of seawater as observed by a satellite orbiting Earth. The preprocessor, which is integrated on an $LiNbO_3$ crystal, uses holographic subtraction to compare simultaneously an optical phase analog of a number, N, of signal voltages with N predetermined reference voltages.

Three operating modes are possible: a "screening" mode in which the incoming data are compared to a single, holographically-recorded reference set; an "identification" mode in which incoming data are compared to a large number of reference sets, and a best fit is identified; and a novel "self-subtraction" mode in which the preprocessor automatically adjusts to slowly-changing input signals, exhibiting only the rapidly varying signals as outputs.

A schematic of the preprocessor, shown in the figure, illustrates its use as a high-speed multichannel data comparator. The signal beam is modulated by the electro-optic effect occurring under the data-input electrodes, to which the reference (comparison) data voltages are applied. A hologram is thus made at the intersection between the signal and reference beams, with the set of signal voltages serving as the phase object.

Next, an appropriate phase shift is introduced into the reference beam while voltages representative of the unknown set are impressed upon the data-input electrodes. If they are identical to the reference set, then the holographic process insures that no light reaches the detector. If they do not match the reference set, light arrives at the detector in proportion to the mismatch. Thus, a simple discriminator at the detector output can be set to flag data that exceed a predetermined degree of mismatch so that the data can be transmitted or

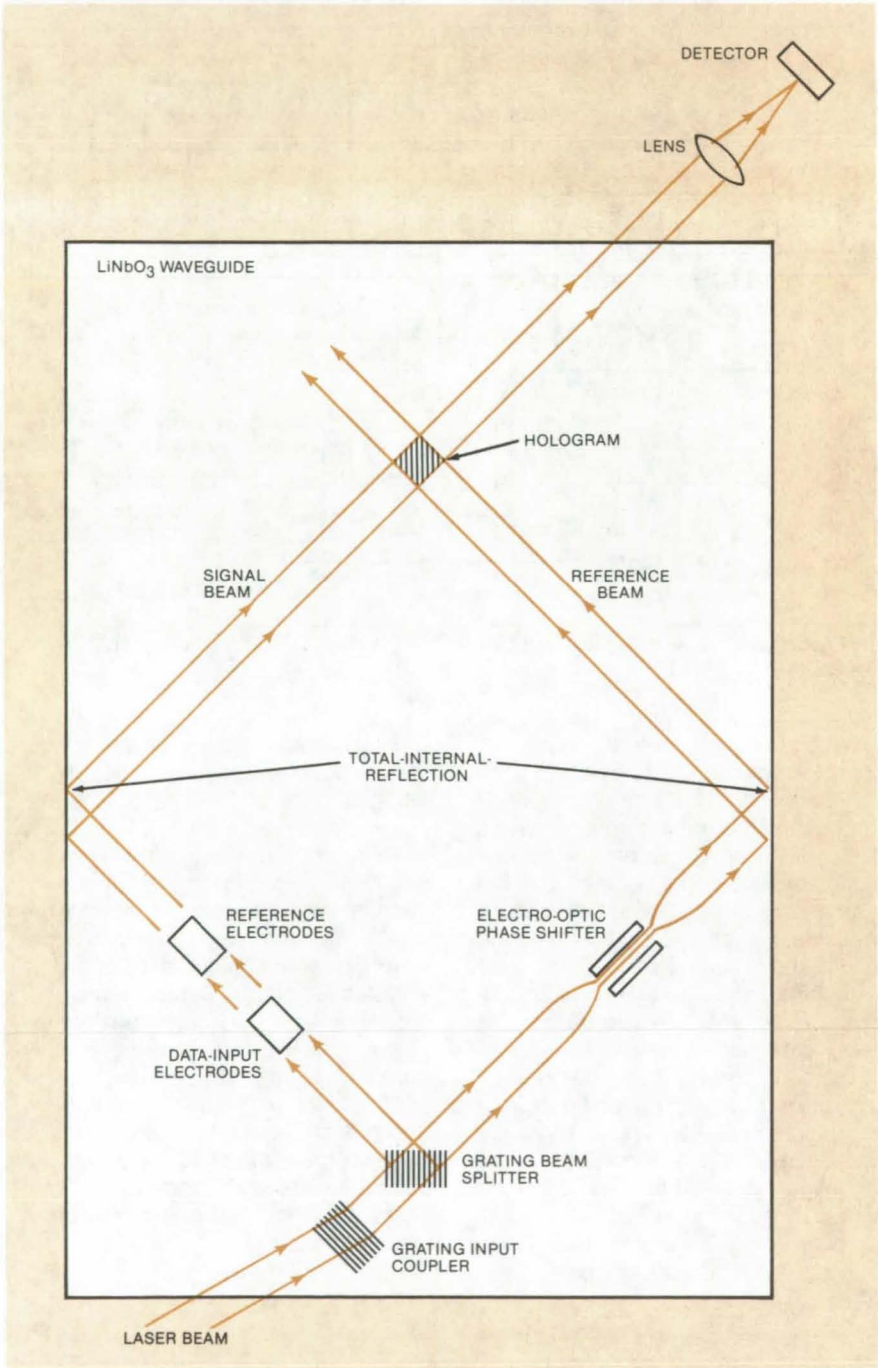


The **Fast Holographic Comparator** is an integrated-optical system constructed on an $LiNbO_3$ waveguide chip. Only the laser, lens, and detector are external to the chip. Aluminized surface gratings with periods ranging from 0.55 to 1.7 $\mu$m serve as the input coupler and beam splitter. The light beams striking the edges are returned by ordinary total internal reflection.

stored for further analysis. This mode of operation is called the "screening" mode.

In the "identification" mode, reference voltages of negative polarity are applied to the reference electrodes while the unknown data signals (of positive polarity) are applied to the data-input electrodes. If the two sets are equal (but opposite in sign), their effects cancel. If a library of reference voltages exists, it should be possible to cycle through the entire library of, say, $10^4$ reference sets in $10^{-3}$ seconds to find a best fit to the unknown set.

The unique electro-optic and photorefractive properties of $LiNbO_3$ are responsible for the success of the system. Holograms are formed in crystalline $LiNbO_3$ through the photoexcitation of electrons trapped at impurity sites, which electrons then migrate toward dark regions and are retrapped. The associated space-charge field gradient produces local changes in the index of refraction, yielding a phase-shift hologram. The space-charge fields decay by electrical conduction, with lifetimes from seconds to months depending on crystal purity and exposure to light. Holograms may be fixed by heating, which allows the migration of positive ions to the vicinity of the trapped electrons.

In the "self-subtraction" mode, the set of unknown data voltages serves as the reference set for the next set of unknown data voltages. Signal changes that are slow compared with the rate of hologram formation do not disturb the null condition, while rapid signal changes generate a difference pattern at the detector. If the new signal persists, it becomes a new baseline, with null output. The device may be viewed as a differentiator or edge detector.

The "self-subtraction" hologram can be part of a "smart" preprocessor, able to discriminate between rapid and gradual signal changes, obviating the need to pass along baseline data to downstream processing devices. In satellite remote-sensing, for example, the preprocessor could detect the multichannel spectral signature of contaminated water while ignoring baseline ocean spectra, including such slowly varying changes as those due to solar elevation. Baseline data would be neither stored nor transmitted (but can be recovered by inputting a null signal to the comparator), thereby conserving data-processing capacity.

Applications require the optimization of hologram equilibration time with respect to the rate-of-change of effects to be discriminated; this depends on dopant concentration and valence state as well as the wavelength and intensity of the laser light. Equilibration times as short as a few seconds have been obtained. A prototype 3-channel preprocessor has been built but not optimized for self-subtraction, and a 16-channel preprocessor has been designed.

*This work was done by David W. Vahey of Batelle Columbus Laboratories for* **Langley Research Center**. *Further information may be found in NASA CR-3151 [N79-30010/NSP], "An Investigation for the Development of an Integrated Optical Data Processor" [$14]. A copy may be purchased [prepayment required] from the National Technical Information Service, Springfield, Virginia 22161.*

*LAR-12509*

# Controller Regulates Auxiliary Source for Solar Power

## Solar-powered system exchages power with utility line, depending on load and insolation.

*Marshall Space Flight Center, Alabama*

A novel application of the power-factor controller would regulate the input of auxiliary energy to a solar-powered system in response to the availability of Sunlight. The scheme does not use a Sun sensor, and it eliminates frequent on/off switching of the auxiliary power source. If a power-factor controller with regenerative braking is used, collected solar energy not needed to operate the machine would be converted to electricity and transferred to the utility powerline. While the system was conceived for use with a compressor as the load and a solar battery as the varying power source, it could be applied to other power-source and power-utilization schemes.

As shown in the figure, two induction motors turn the shaft of the compressor. One of the motors is

(continued on next page)

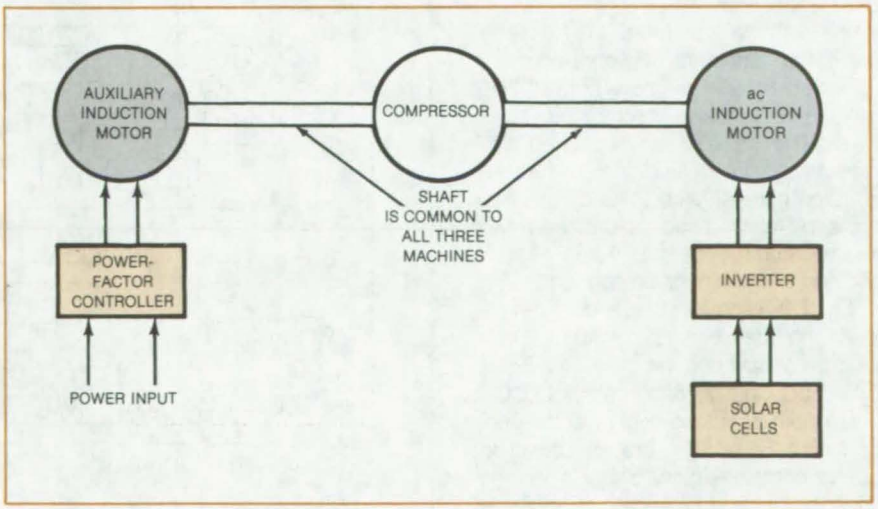


A **Load Driven by Two Motors** continuously draws power from a varying source (solar cells) and a steady auxiliary source (utility company). The power-factor controller apportions the electrical load between the two sources to maintain motor speed.

powered by a solar array through an inverter. The auxiliary motor is powered by the utility line through a power-factor controller. [See, for example, "Three-Phase Power-Factor Controller" (MFS-25560), *NASA Tech Briefs*, Vol. 6, No. 1, p. 3.]

In previous systems, a Sun sensor detects if the available Sunlight is not sufficient to run the compressor. The solar array is then switched off, and the auxiliary motor takes over. On partly cloudy days, however, the switching is frequent, and the power transfer is very inefficient.

In the new system, the power-factor controller automatically adjusts the auxiliary-power input to maintain the auxiliary motor at synchronous speed as the load varies. Ignoring friction and motor losses, the net mechanical load presented to the auxiliary motor equals the total shaft load less the portion of the shaft load supplied by the solar-powered motor. The auxiliary motor carries the full load in the absence of solar power.

If a power-factor controller with regenerative braking is used, then any excess solar-cell capacity can be used to advantage. When the solar-powered motor supplies shaft power in excess of the load, the controller automatically switches the auxiliary motor into a generating mode, thus supplying power to the utility line.

For economy, both motors could share a common housing or even a common magnetic core (but with isolated windings). The principle is also applicable to systems in which the primary motor is not electrically powered (for example, a steam-driven turbine).

*This work was done by Frank, J. Nola of* **Marshall Space Flight Center.** *No further documentation is available.*

*Inquiries concerning rights for the commercial use of this invention should be addressed to the Patent Counsel, Marshall Space Flight Center [see page A5]. Refer to MFS-25637.*

# Improved Parallel-Access Alinement Network

A relatively-simple digital logic circuit channels data signals in a parallel data-processing system.

*Ames Research Center, Moffett Field, California*

A new alinement network uses a control word to direct data stored in the parallel memory modules to appropriate parallel processor modules. The data may be directed back to the memory modules in the same manner. The arrangement is not as costly as the complex crossbar network, is easier to control than the 2 N-$\log_2$-N-element (N being the number of ports on one side) alinement network, and is faster than a network using a single alinement layer.

An example illustrated in Figure 1 shows the alinement networks connecting seven parallel memory ports (MP's) with seven parallel processing ports (PP's). The network is partitioned into three levels. Each level includes seven selection gates (Figure 2). Each has two inputs (A and B), an output, and two selection-control inputs, $E_0$ and $E_S$.

When a logic one is present on the $E_0$ (or $E'_0$ or $E''_0$) control input, a data path is established between input A and the output; with a logic one, on the $E_S$ (or $E'_S$ or $E''_S$) control input, a path is established between input B and the output. All the control inputs $E_0$ and $E_S$ are structured to receive complementary binary levels, so that a logic one at $E_0$ implies a logic zero at $E_S$ and vice versa.

All the selection gates in a given level may have their control inputs $E_0$ and $E_S$ connected in parallel. Thus, 3 bits of a

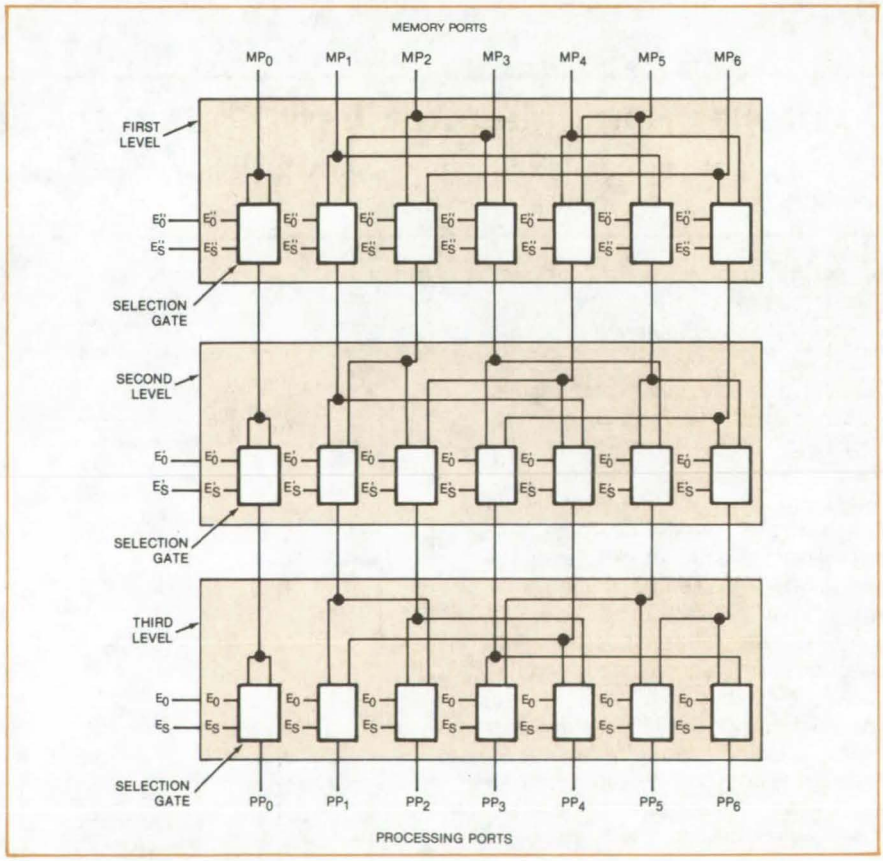


Figure 1. **Parallel-Access Alinement Network** channels elements of a data array from memory ports to processor ports using a hardware-generated binary control word. Depending on the control word selected, the data may be shifted in increments or transposed in each of the three levels to reach the appropriate processing ports. A similar arrangement (not shown) with reversed wiring is used to return the data from the processing ports to the respective memory modules.

control word m determine the data flow or shifting between the memory ports $MP_0$-$MP_6$ and the processing ports $PP_0$-$PP_6$. The most significant bit of m controls the third level, the second most significant bit the second level, and the least significant bit the first level. In essence, the word m controls the $E_S$ input of the selection gates while a binary complement of m feeds the $E_0$ input of the gates.

A control word m of 000 would introduce no shifting, and thus the data would flow directly between the memory ports $MP_0$-$MP_6$ and the processing ports $PP_0$-$PP_6$. For a control word m of 100, a shift of 4 (modulo 7) would occur in the third level with no shift in the other two levels. Likewise, a control word m of 010 would introduce a shift of 2 (modulo 7) in the second level, and a control word m of 001 would introduce a shift of 3 (modulo 7) in the first level. Of course, such shifts may occur simultaneously in more than one level.

The selection gate is unidirectional, and a second set is necessary to permit reverse data flow from the processing ports to the memory ports. A reverse wiring arrangement of Figure 1 is set up to feed the data back to the memory ports through another set of third, second, and first levels in the same manner in which the data were transferred to the processing ports. The entire operation controlled by the word m can channel the data from

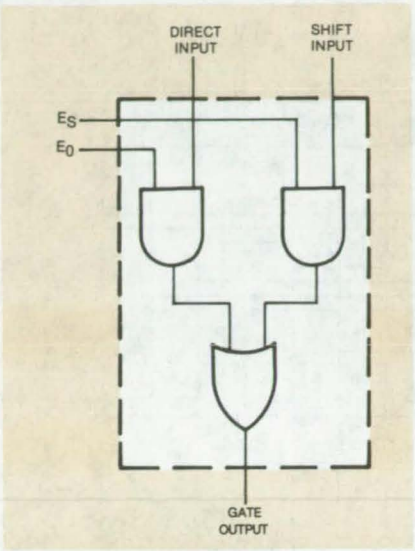


Figure 2. A **Selection Gate** used in this network incorporates two AND gates feeding an OR gate. In some logic families the OR gate may be fabricated as a "wired OR."

the memory ports to the desired processing ports and return the data back to the same memory ports.

The alinement network may be extended to N memory ports and N processing ports. The number of levels in this case is equal to $\log_2(N)$ rounded up to the nearest integer. In the illustrated example, where N = 7, $\log_2$ (N) rounded up to the nearest integer. equals 3. the total number of gates required for a general case is then multiplied rounded up to the nearest integer.

The value of m is computed by a programed read-only memory (ROM). An input parameter d defining the distance between the data elements that are to be accessed determines m from the relationship $d = k^m$ modulo N, where k is relatively prime to N and is a primitive root of N. The value of k determines the specific wiring patterns shown in Figure 1. For example, to access elements $a_{11}$, $a_{12}$, $a_{13}$, $a_{14}$, and $a_{15}$ in parallel from a 5-by-5 array, the distance d is unity and no shifting is needed. However, to access the data elements $a_{11}$, $a_{21}$, $a_{31}$, $a_{41}$, and $a_{51}$, the distance d = 5, and m is computed accordingly to produce the necessary shift.

[Also see the following related article "Parallel-Access Alinement Network Using Barrel Switches" (ARC-11162).]

*This work was done by George H. Barnes of Burroughs Corp. for* **Ames Research Center.** *For further information, Circle 11 on the TSP Request Card.*

*Title to this invention, covered by U.S. Patent No. 4,162,534, has been waived under the provisions of the National Aeronautics and Space Act [42 U.S.C. 2457(f)] to Burroughs Corp., P.O. Box 517, Paoli, Pennsylvania 19301.*
*ARC-11155*

# Parallel-Access Alinement Network Using Barrel Switches

Two barrel switches direct data flow in a parallel processing system.

*Ames Research Center, Moffett Field, California*

One practical version of the parallel-access alinement network described in the preceding article ["Improved Parallel-Access Alinement Network"(ARC-11155)] utilizes two barrel switches for interfacing N parallel memory modules with N parallel processing elements. This approach offers the same relative advantages described in the preceding article.

Switches are interconnected as shown in the illustrated example, where 17 memory ports (MP's) are connected to 17 processor ports (PP's).

The first barrel switch shifts, when required, the stored d-vectors to the leftmost starting position for processing through the second barrel switch. The ordered output-data paths of the first barrel switch are connected to the ordered input-data paths of the second barrel switch, in sequence according to $d = k^m$ modulo N, where d represents the ordering of the output-data paths of the first barrel switch and m represents the ordering of the input-data paths of the second barrel switch. The symbol N is the number of memory ports (17 in this example) and k is a primitive root of N that equals 3 in this case. The zero-ordered output-data path of the first barrel switch connects directly to the zero-ordered processor port.

Data paths 0 through 15 of the second barrel switch are connected to the processor ports $PP_1$ through $PP_{16}$ in a sequence opposite that connecting the first to the second barrel switch.

The switch-control operations are relatively simple. An S control input causes the first barrel switch to shift the starting

(continued on next page)

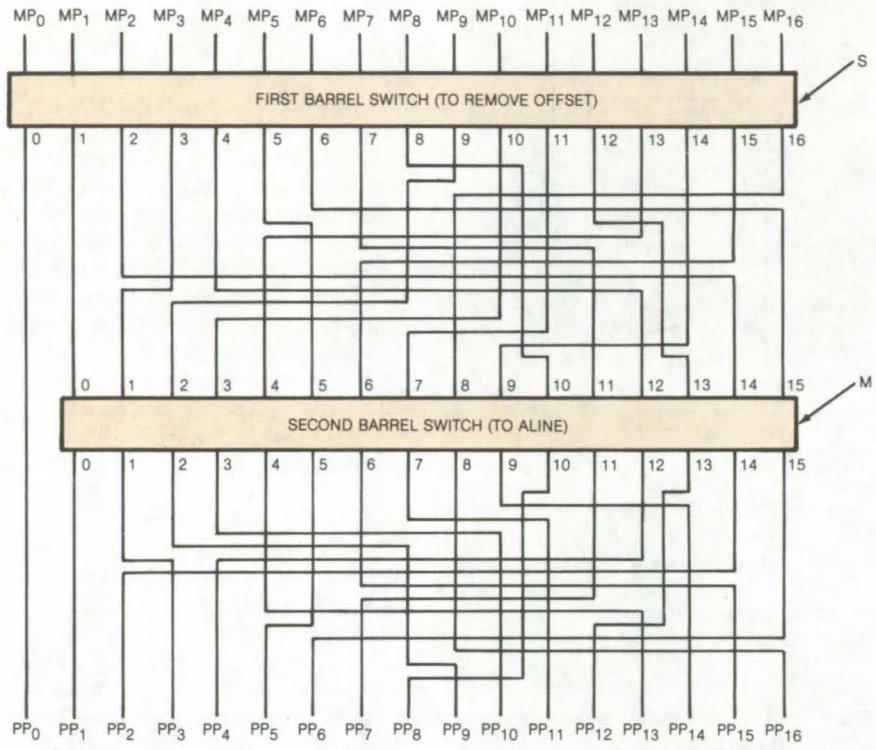


This **Alinement Network** uses two electronic barrel switches to direct data flow in a parallel data-processing system. Each switch can shift a multibit parallel input a predetermined number of places to the left or right, end off, or end around in one clock-pulse.

data element of a stored d-vector to the leftmost (0) output-data path of the first barrel switch. An m control input causes the second barrel switch to produce the desired shift increment. The increment is equal to the distance d (which is the distance between the data elements sought to be accessed).

The value of m is derived from $d = k^m$ modulo N. The value d is used to address a ROM (read-only memory) that has been programed to produce the value m at address d. Although m could be generated by software, hardware is usually preferred because it is faster.

In applications where d vectors are stored having starting data elements all available at memory port $MP_0$, the first barrel switch is not required. Also, this alinement network could be positioned between other similar sets of parallel ports requiring the alinement.

*This work was done by George H. Barnes of Burroughs Corp. for* **Ames Research Center.** *For further information, Circle 12 on the TSP Request Card.*

*Title to this invention, covered by U.S. Patent No. 4,223,391, has been waived under the provisions of the National Aeronautics and Space Act [42 U.S.C. 2457(f)], to Burroughs Corp., P.O. Box 517 Paoli, Pennsylvania 19301.*
*ARC-11162*

# Physical Sciences

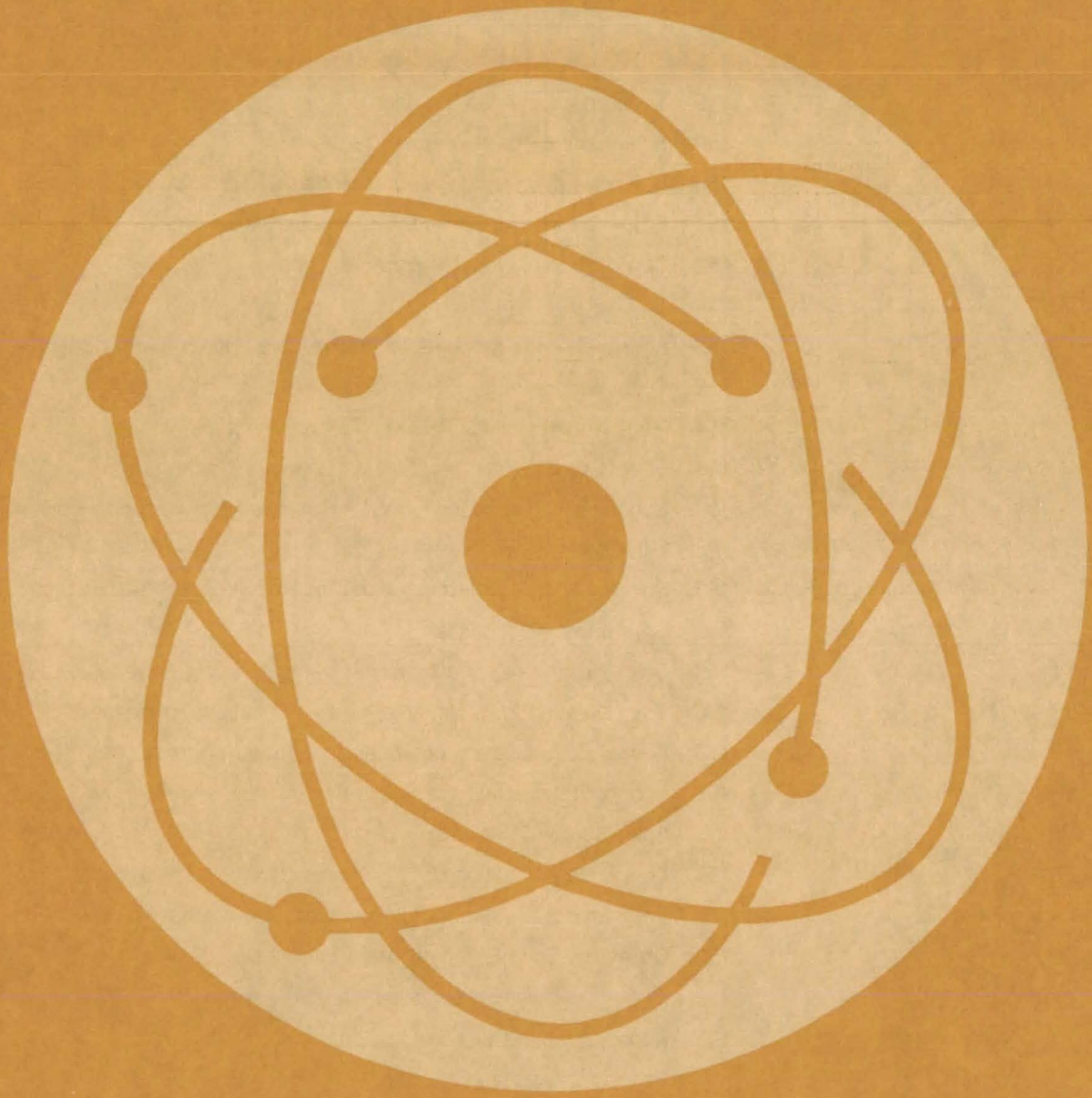

## Hardware, Techniques, and Processes



## Books and Reports

# Compact Ion Source for Mass Spectrometers

Cyclotron-resonance device uses miniature components and a permanent magnet for small size, low weight, and low cost.

*NASA's Jet Propulsion Laboratory, Pasadena, California*

A miniature cyclotron-resonance ion source furnishes ions of a gas sample to a mass spectrometer. In the past, ion-cyclotron-resonance mass spectrometers were large, heavy, and expensive. One used in previous NASA experiment fit in a magnet gap of about 2 inches (5 cm), so a large power-consuming electromagnet was necessary to supply the required magnetic field. The new device, in contrast, is miniaturized to fit in a gap on only 0.5 inch (1.2 cm); therefore, a small permanent magnet is sufficient to furnish the required field.

A production prototype of the miniaturized ion source is shown in Figure 1, and a schematic diagram illustrating its functional operation is shown in Figure 2. Gas molecules are ionized by the impact of electrons from the hot filament. The magnetic field, in conjunction with the electrostatic drift field, causes the ions to move in circles with a superimposed drift toward the spectrometer.

The compact ion source can be used for studying ion-molecule reactions by ion cyclotron-resonance methods in a conventional mass spectrometer with either a magnetic sector or a quadrupole sector. This feature also allows the device to be used as a chemical ionization source at pressures as low as $10^{-7}$ torr ($1.3 \times 10^{5}$ N/m$^2$). It can also be used as a stand-alone ion cyclotron-resonance spectrometer.

*This work was done by Vincent G. Anicich and Wesley T. Huntress, Jr., of Caltech for* **NASA's Jet Propulsion Laboratory.** *For further information, Circle 13 on the TSP Request Card.*

*This invention has been patented by NASA [U.S. Patent No. 4,206,383]. Inquiries concerning nonexclusive or exclusive license for its commercial development should be addressed to the Patent Counsel, NASA Resident Office-JPL [see page A5]. Refer to NPO-14324.*

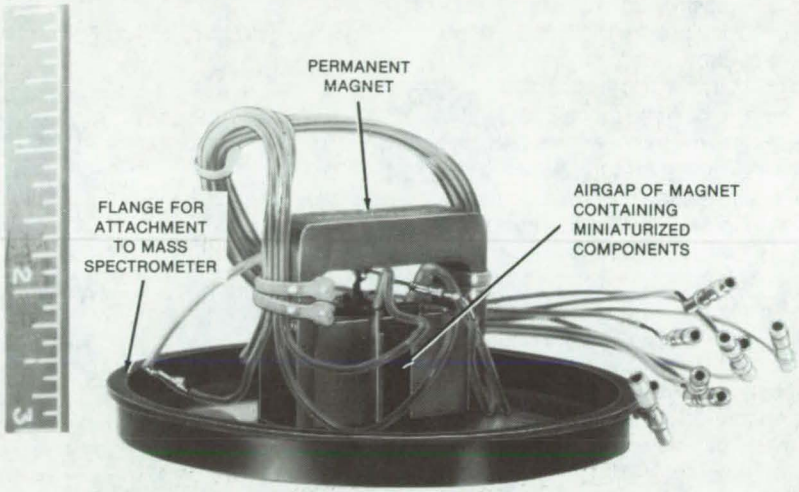


Figure 1. A **Production Prototype** of the ion source fits in the narrow gap of a permanent magnet.

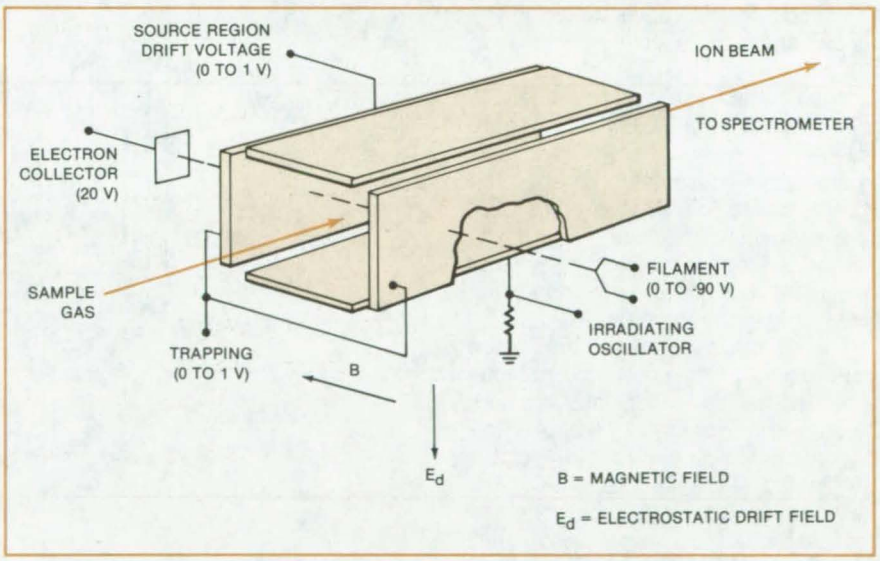


Figure 2. **Gas Molecules Are Ionized** by electrons from the hot filament. The magnetic field, acting with the electrostatic drift field, causes the ions to move in circles with a superimposed drift perpendicular to both fields; that is, toward the exit.

# 3-D Manipulator for Mass Spectrometer

Dual bellows move a specimen in three mutually perpendicular directions.

*Ames Research Center, Moffett Field, California*

Small mass-spectrometer specimens are positioned in three dimensions by a manipulator that employs two bellows to provide a vacuum seal and accommodate movement of the specimen holder. The manipulator inner bellows (see figure) allows vertical (z-axis) movement through 300 mm. The outer bellows allows horizontal movement (along x- and y-axes) through 25 mm, as well as fine vertical adjustments. An operator moves the specimen to place part of it at the focal point of a laser-beam vaporizer. The manipulator is similar to one used previously to position samples in an electron microscope.

Previously, O-rings sealed the specimen-holder column; but the sliding of the column over the rings caused wear, aggravated by the inevitable small scratches in the column metal. The rings leaked and had to be replaced often. Moreover, they allowed movement of the specimen only along the z-axis.

When the sample chamber is pumped down sufficiently, the gate valve to the mass spectrometer is opened, and the operator pushes the sample column upward by hand so that the specimen is close to the ion source. A stop on the specimen-holder alinement rods prevents the specimen from striking the ion source.

The operator selects the area to be vaporized with the aid of a microscope attached to the laser lens system. Then, still looking through the microscope, the operator manipulates the fine-adjustment knobs to bring the selected area of the specimen into focus. Finally, the laser is fired. A small amount of the specimen is vaporized and is analyzed by the mass spectrometer in the usual way.

*This work was done by James C. Cirner, Ingeborg Harding-Barlow, and Kenneth G. Snetsinger of* **Ames Research Center.** *For further information, Circle 14 on the TSP Request Card.*

*ARC-11323*

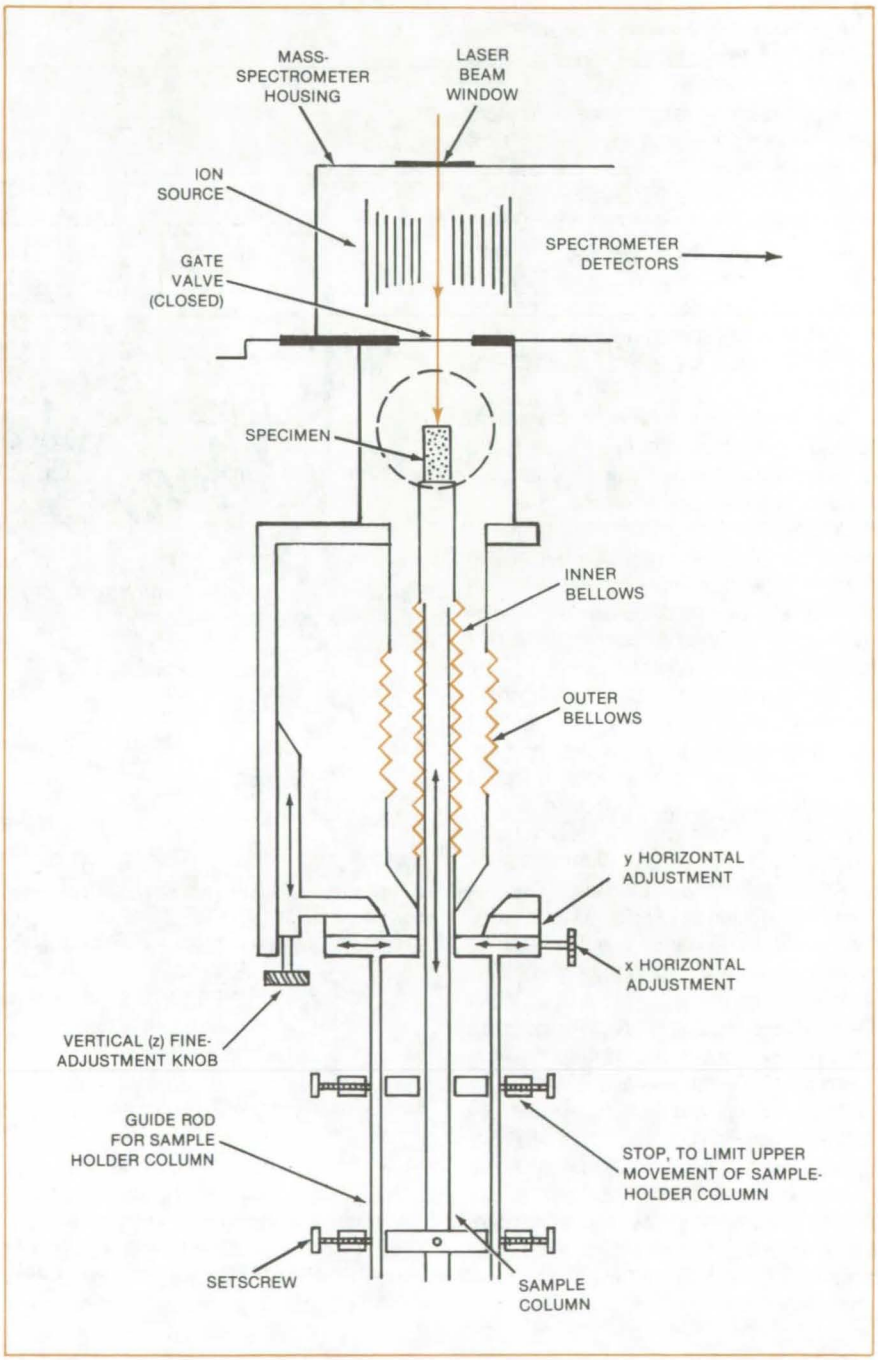


**Inner Bellows and Outer Bellows** accommodate vertical and horizontal motion, respectively, of the specimen holder. The y-axis movement is in and out of the plane of the page. The specimen-holder column is hollow so that electrical wires can pass through it to the specimen.

# Efficient Energy-Storage Concept

Masses supported by flexible cable would be used for energy storage and attitude stabilization in space platforms.

*Marshall Space Flight Center, Alabama*

A system proposed for spacecraft energy storage and attitude stabilization may be more efficient than batteries or fuel cells. When fully developed, the concept could be part of an orbiting solar-energy collection system. Solar energy would be temporarily stored in the system and then transmitted to Earth by microwaves or other method.

The new proposal combines two previously tested concepts: gravity-gradient pumping and the variable-moment-of-inertia flywheel. Gravity-gradient pumping is the extraction of energy from a spatially nonconstant gravitational field by synchronizing changes in the moment of inertia of a system with its rotation in the field. A variable-moment-of-inertia flywheel can be increased or decreased in energy without applying a torque (so that the angular momentum remains constant). In an orbiting energy-storage system, the combination would store considerable energy for a given weight.

The system, shown in the figure, consists of a reel with a cable wound around it, two masses attached to the ends of the cable, a motor/generator, and a gearhead, all mounted on a platform through a rotating joint. The platform is to be stabilized with the spin axis perpendicular to the orbital plane.

The system is started by spinning it about its axis while the cables are completely retracted. As the angular velocity is increased, the cables are gradually extended. In orbit, gravity-gradient pumping would be used to increase the angular velocity; i.e., the cables would be retracted when they lie along or nearly along the orbital radius and would be extended when they lie perpendicular or nearly perpendicular to it.

Energy is stored in the system by driving the motor/generator as a motor to retract the cables; energy is extracted by allowing the cables to extend and using the motor/generator as a generator.

By using gravity-gradient pumping to bring the masses up to operating speed and by using the variable moment of inertia to change the stored energy, no torques need to be applied to the system. All applied forces are one-dimensional, along the line joining the two masses. Thus, a lightweight cable made of a strong synthetic material is all that is needed to support the masses. Previous flywheels required heavier rigid structural elements to absorb the necessary two-dimensional forces.

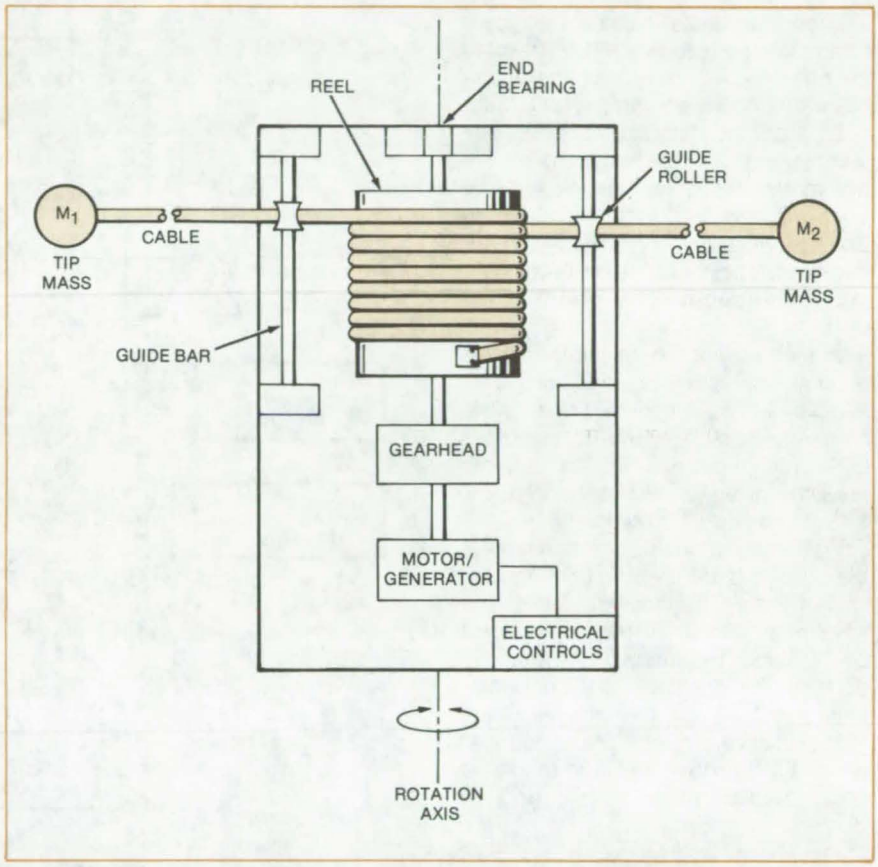


The **Space-Platform Energy-Storage and Attitude-Stabilization System** utilizes the variable moment of inertia of two masses attached to the ends of a retractable cable. It would be brought to its initial operating speed by gravity-gradient pumping.

*This work was done by Lott W. Brantley, Jr., and Charles Rupp of* **Marshall Space Flight Center.** *For further information, Circle 15 on the TSP Request Card.*

*Inquiries concerning rights for the commercial use of this invention should be addressed to the Patent Counsel, Marshall Space Flight Center [see page A5]. Refer to MFS-25331.*

# EMR Gage Would Measure Coal Thickness Accurately

Electron magnetic resonance shows potential for automatic machine control in coal mines

*Marshall Space Flight Center, Alabama*

Laboratory tests indicate that electron magnetic resonance (EMR) would be effective in measuring the thickness of coal overlying a rock substrate. When fully developed, the technique might be adapted to an automatic thickness gage for the control of mining machinery. Three EMR techniques have been studied: two-frequency, transient-response, and balanced-bridge continuous-wave.

In the first approach, two radio-frequency signals are applied to a coal sample in a magnetic field. The magnetic-field intensity is adjusted until free electrons in the sample resonate at one of the radio frequencies. Under this condition, the RF signals mix, producing sidebands at the sum and difference frequencies. One of the sidebands is detected, and its strength indicates the presence of coal. Since the resonant frequency depends on position in the inhomogeneous field of the magnet, the frequency is a measure of the depth at which EMR is observed. The magnetic field is varied to scan over a range of depths.

In a laboratory model of the EMR probe (see figure), signals at 400 MHz and 5 MHz are directed at the sample. The upper sideband (at 405 MHz) is detected by a crystal-controlled frequency converter tuned to 405 MHz connected to a communications receiver. The EMR probe is noncontacting and potentially has a measurement range of more than 6 inches (15 cm) and an accuracy within one-half inch (1.3 cm). In addition, it responds quickly enough to be used on moving equipment.

The transient-response approach potentially offers a sensitive, noncritical means for detecting coal. However, the short decay time (a few nanoseconds) of the EMR response from coal imposes serious recovery-time problems, which may be difficult to overcome without going to upper microwave frequencies where the magnetic-field intensity required for resonance would be impractical.

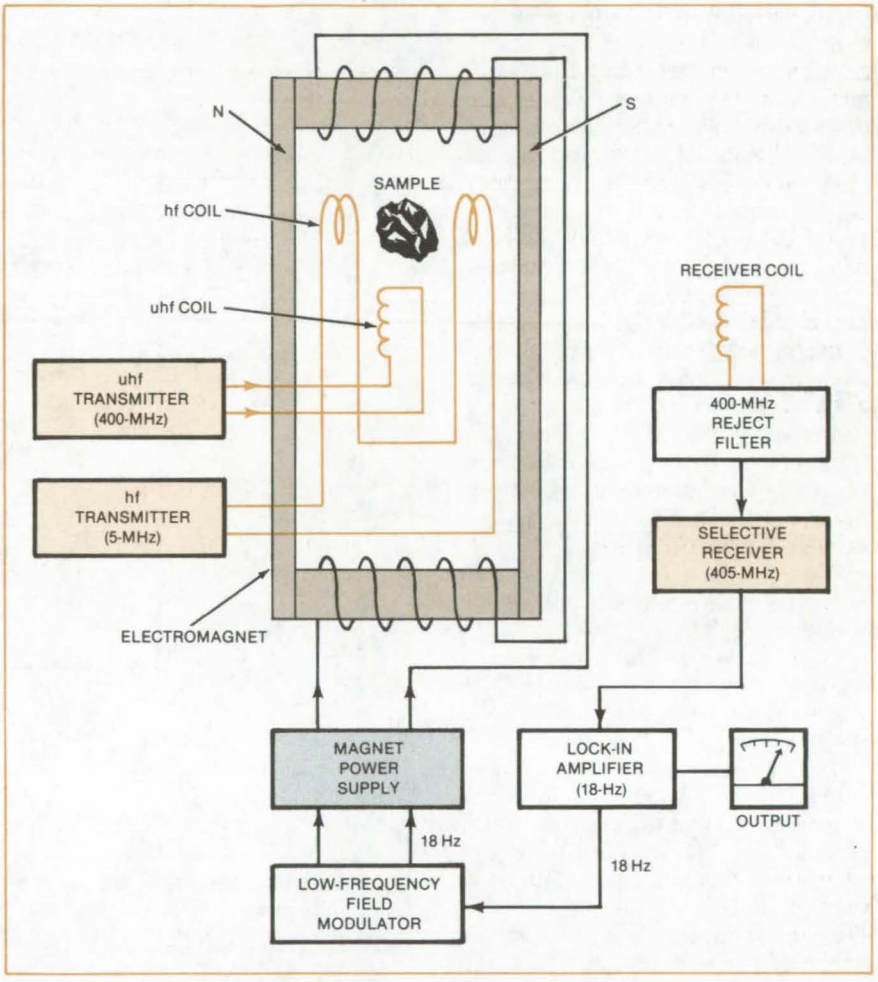


In this **Prototype Dual-Frequency EMR System,** the sample is irradiated by two radio frequencies. The signals are mixed, producing sum and difference output frequencies that are detected by the receiver. The magnetic field is varied to scan the resonant spot through the sample. In a system designed for field use, the electromagnet is U-shaped, so that the sample can be adjacent to, rather than inside, the probe. Also, the same coil is used for transmitting and for receiving.

Although a single-frequency signal can stimulate an EMR response from coal, the response is at the same frequency as the stimulus (but much weaker). It is therefore necessary to discriminate against the stimulus at the receiving coil. A balanced-bridge circuit that nulls any stimulus signal at the receiver can be used for this purpose. However, such a circuit requires adjustments that may be too critical for the use in a coal mine. The dual-frequency approach eliminates this problem.

*This work was done by J. Derwin King and W. L. Rollwitz of the Southwest Research Institute for* **Marshall Space Flight Center.** *For further information, Circle 16 on the TSP Request Card.*
*MFS-25555*

# Sensors for Precise Tracking

One sensor tracks the Sun; the other follows the motion of a flat panel.

*Marshall Space Flight Center, Alabama*

Two sensors proposed for checking the orientation of a spacecraft instrument package could find uses in systems requiring precise position control. Among suggested applications are controllers for solar concentrators, optical and electron-beam lithography, and telescope mounts. One sensor tracks the Sun by imaging four symmetrically located points at the edge of the solar disk. The other monitors the pitch, roll, and yaw of a flat panel known as an "occulter," used in the X-ray coronagraph instrument package.

The Sun sensor views the Sun through a small hole as shown in Figure 1. Four sectors of the solar limb are viewed through four pairs of pentaprisms (two pairs are shown). The constant-deviation characteristic of a pentaprism minimizes problems of alinement and stability.

The four sectors are imaged onto the field stop by the objective lens. Shown in the inset of Figure 1, the field stop contains four cross-shaped windows, each with a separate detector behind it. When the sensor is pointed directly at the Sun, each image is centered over a detector window. When the system is centered on the Sun, a change of 0.3 second in angular orientation produces a signal change of 1.1 percent.

The band-pass filters over the entrance aperture and the objective lens tune the Sun sensor to a particular band of frequencies, reducing the effects of stray light. The coarse Sun sensors are used for initial acquisition of the Sun and to increase the angular range of the system.

Two cube corner reflectors, seen in Figure 2, are used in the sensor that tracks the occulter position. A cube corner reflector forms a virtual image of a point source. Each reflector is illuminated by a separate source and tracked by a telescope. As the occulter moves in pitch and yaw, the images shift together; but in a roll about the occulter center, the images move in opposite directions. Relative motion of the images from the two cube corner reflectors distinguishes different kinds of motion and can be used to control the occulter orientation.

*This work was done by T. F. Zehnpfenning of Visidyne for* **Marshall Space Flight Center.** *For further information, Circle 17 on the TSP Request Card.*
*MFS-25579*

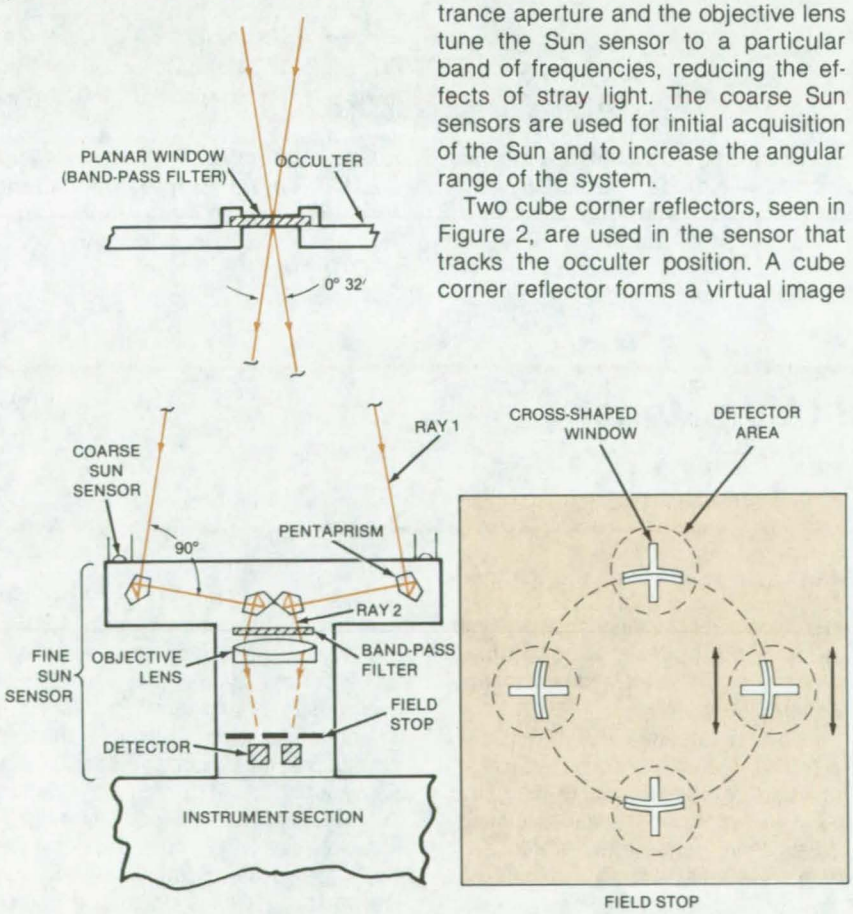


Figure 1. The **Sun-Sensor Optical System** uses four pairs of pentaprisms to simplify alinement and reduce mechanical-stability requirements. (Two pairs are shown here.) The cross-shaped windows in the field stop enhance the sensitivity of the signal detectors to changes in angular position.

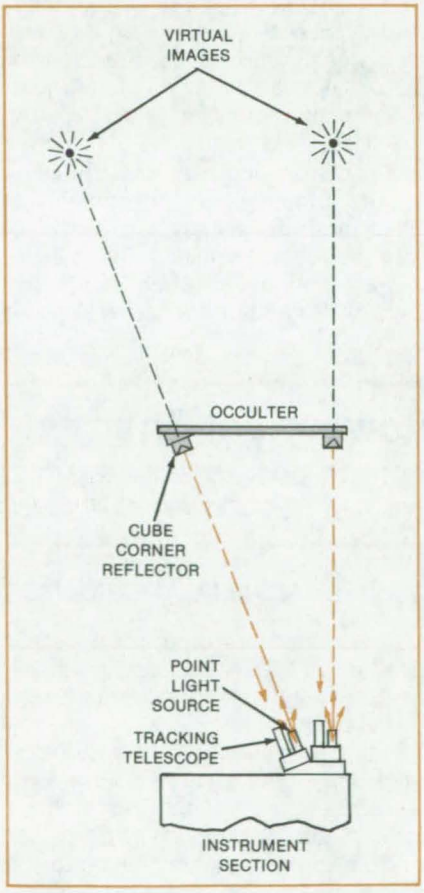


Figure 2. **Two Virtual Images** viewed by telescopes mark the position and orientation of the occulter panel. The reflector vertex, point source, and corresponding virtual image are all equally spaced along a straight line.

# Solar Concentrator is Gas-Filled

Gas-filled reflector has a clear front film and a metalized back film.

*NASA's Jet Propulsion Laboratory, Pasadena, California*

A proposed reflector for concentrating solar rays to a point focus would be rugged, lightweight, inexpensive, and easy to transport. It is made of two flexible polymer films with pressurized gas between them. The first film is clear, serving as a protective cover and pressure envelope; the second film is metalized to serve as a concentrating mirror. The focal length of the mirror is adjusted by changing the gas pressure.

As can be seen from the figure, the metalized reflecting surface is protected by the front film and by the pressurizing gas, which may be an inert or reducing atmosphere. The front film is easily replaced and cleaned. Since it is not in a region of high solar flux during operation, it would not be melted or burned. Emergency defocusing is possible by quick depressurization.

The focal length of the concentrator is monitored and controlled by a position sensor on the back surface of the mirror film. This surface may be screened from wind by a perforated guard, if necessary.

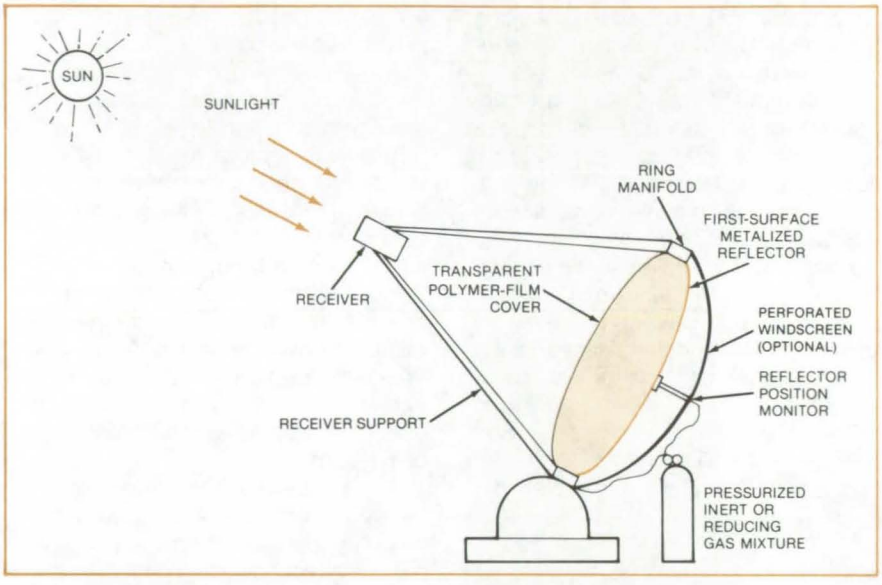


A proposed **Solar Concentrator** uses a flexible pressure-focused first-surface metalized polymer film.

Other features shown in the figure, such as the pressurization system and receiver support structure, would be conventional.

*This work was done by Peter O. Frickland, Frank Bouquet, Marc A. Adams, and Robert R. Hale of Caltech for* **NASA's Jet Propulsion Laboratory.** *For further information, Circle 18 on the TSP Request Card.*
*NPO-15416*

# Powerplant Thermal-Pollution Models

Three models predict the nature of thermal plumes from powerplant discharge into water.

*John F. Kennedy Space Center, Florida*

Three mathematical models developed under NASA sponsorship accurately predict powerplant thermal pollution of bodies of water.

A three-dimensional model for estuaries and other coastal regions where wave height is significant was evaluated by aerial infrared photography at Anclote Anchorage on the northern Florida coast. The model predictions match the infrared data within 1° C on the average. This "free-surface" model computes the water velocity, temperature, and surface-height variations with time, given a set of initial conditions and time-varying boundary conditions, which are available from local tidal and discharge data.

A second three-dimensional model, intended for lakes where waves are insignificant, was evaluated in the same way. This "rigid-lid" model is as accurate as the free-surface version and, like it, is readily adapted to different sites. The rigid-lid model was evaluated at Lake Keowee (see figure) in South Carolina.

Although three-dimensional models are ideal for predicting detailed behavior of thermal plumes, they are prohibitively costly for long-term simulations. A one-dimensional model more suitable for that purpose was evaluated at Lake Keowee and found to simulate satisfactorily the 1971–79 period. The evaluation was based on environmental records as well as on aerial photography. The model assumes horizontal homogeneity, but includes the effects of area change with depth, radiative penetra-

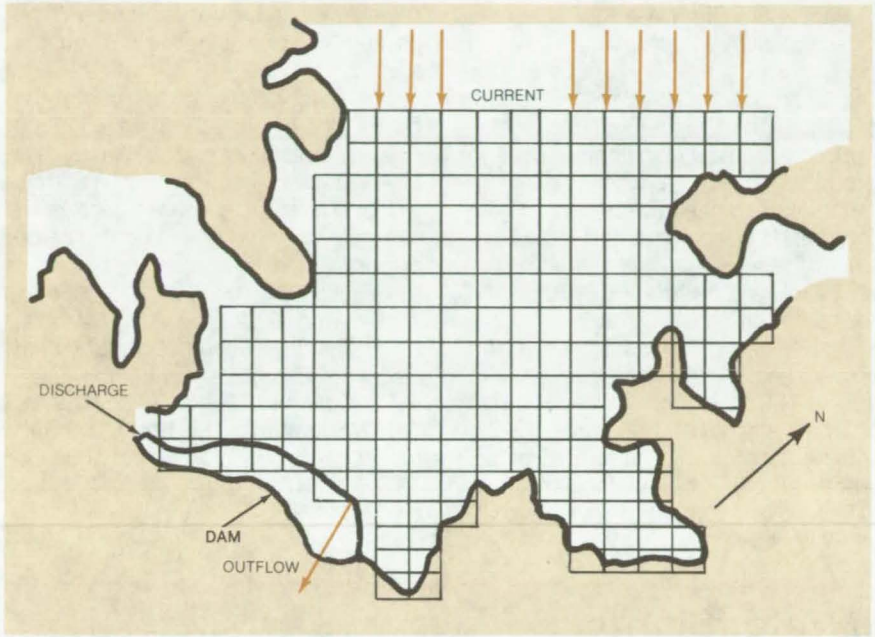


**Key Section of Three-Dimensional Model Simulation** of Lake Keowee is a section of the lake adjacent to the Oconee nuclear station. Discharge to the lake is from the station, and the outflow from the lake passes over Keowee Dam. The grid used in the rigid-lid model is shown.

tion through the water surface, interaction between wind and buoyancy gradients, and heat transfer by convection from the surface.

The free-surface model accommodates major changes in ocean currents. It performs equally well for summer and winter conditions and widely-different atmospheric conditions.

The rigid-lid model accurately predicts changes in a thermal plume caused by other inputs and outputs, such as pumped-water storage and hydroelectric-plant discharges. The one-dimensional model predicts the approximate stratification in a lake with such inputs and outputs over a long period.

*This work was done by Samuel S. Lee and Subrata Sengupta of the University of Miami for* **Kennedy Space Center.** *For further information, Circle 19 on the TSP Request Card.*
*KSC-11210*

# Proposed Integrated Radio-Telescope Network

## An extensive technical and economic analysis reveals significant research advantages for a 10-site network.

*NASA's Jet Propulsion Laboratory, Pasadena, California*

According to a comprehensive study, a proposed network of radio telescopes, controlled by a central computer and managed by a single organization, offers the potential for research on a scale that could not be matched by present privately- and publicly-owned radio telescopes. With 10 antenna sites in the contiguous United States, Alaska, and Hawaii, the network would establish base lines thousands of miles long (see figure). It will then be feasible to conduct experiments on such diverse research subjects as:

- The structure of the energy sources in quasars and galactic nuclei and the nature of the processes involved in the enormous energy releases in these objects,
- The structure of compact radio sources,
- Distance measurements within the galaxy and to other galaxies,
- Stellar evolution,

(continued on next page)

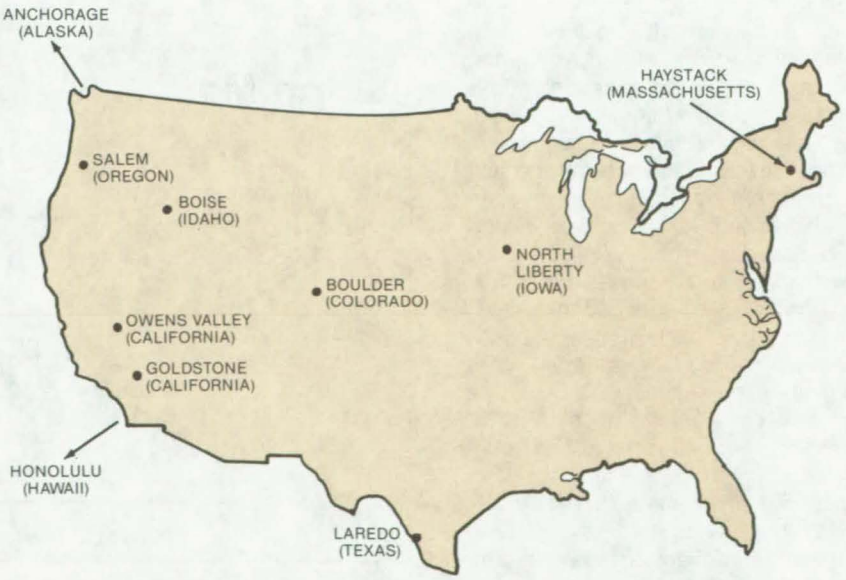


**Sites for a Representative 10-Antenna Array** will be scattered around the United States. The sites shown here have been recommended because they have good communications facilities and because they would perform well in combination.

- The testing of theories of gravitation by observing the bending of radio waves by the Sun and by distant galaxies,
- The motion of Earth's pole in space, and
- The determination of continental drift and other deformations in Earth's crust.

The antennas will be linked to the computer center by telephone circuits. At the center, an operator will receive frequent reports on an antenna performance and will respond quickly to problems at any site. The central computer will control computers at the sites; these computers in turn will control antenna pointing, tape-recorder operation, data logging and other functions.

Each site will have a fully-steerable Cassegrainian antenna, about 25 m in diameter, with a feed for each of four reception bands: 1.3-, 2.8-, 6-, and 18- to 21-cm. The 1.3-cm band has recently become a band of major interest and promises to be especially revealing. Feeds and front-end receivers for the four bands will be mounted in one turret at the vertex of the antenna dish, and each will be rotated into position for reception on command.

The received signals will be mixed down to an intermediate frequency of 100 to 500 MHz and will be recorded on magnetic tape. The tapes will be transported to the controll center, where all pair combinations of tapes will be cross-correlated. Forty-five independent cross correlations will be carried out for the full 10-antenna system.

Postobservation data analysis at the center will convert the magnetic-tape data into maps, displays, or other useful presentations. A map-processing system with both color and gray-scale displays will allow interactive viewing and modification of maps.

*This work was done by M. H. Cohen, M. S. Ewing, G. S. Levy, R. K. Mallis, A. C. S. Readhead, and J. R. Smith of Caltech and D. C. Backer of the University of California, Berkeley, for* **NASA's Jet Propulsion Laboratory.** *For further information, Circle 20 on the TSP Request Card.*
*NPO-15417*

# Combustion of Coal/Oil/Water Slurries

Proposed test setup would measure the combustion performance of new fuels.

*NASA's Jet Propulsion Laboratory, Pasadena, California*

A bench-scale laboratory setup is proposed to test the combustion performance of coal/oil/water formulations. Such mixtures are being considered as petroleum substitutes in oil-fired furnaces.

Tests by others of the combustion of coal/oil slurries in oil burners show mixed results. Problems with smoke, excessive emission, and lower flame intensity are encountered as the coal loading is increased to beyond 40 percent, because it is difficult to mix a solid fuel such as coal with its gaseous air oxidizer. However, intimate mixing must occur if combustion is to be complete.

When water is added to the slurry and the mixture is burned, microexplosions occur because the emulsified water superheats and then vaporizes explosively. This process blasts the oil from the surface of coal, which then starts burning nearly as rapidly as the oil itself. A microexplosion distributes the burning droplet mass into smaller droplets. It appears most beneficial to promote intense microexplosions, because they must be sufficient to project coal particles free from the emulsion.

The bench-scale apparatus pro-

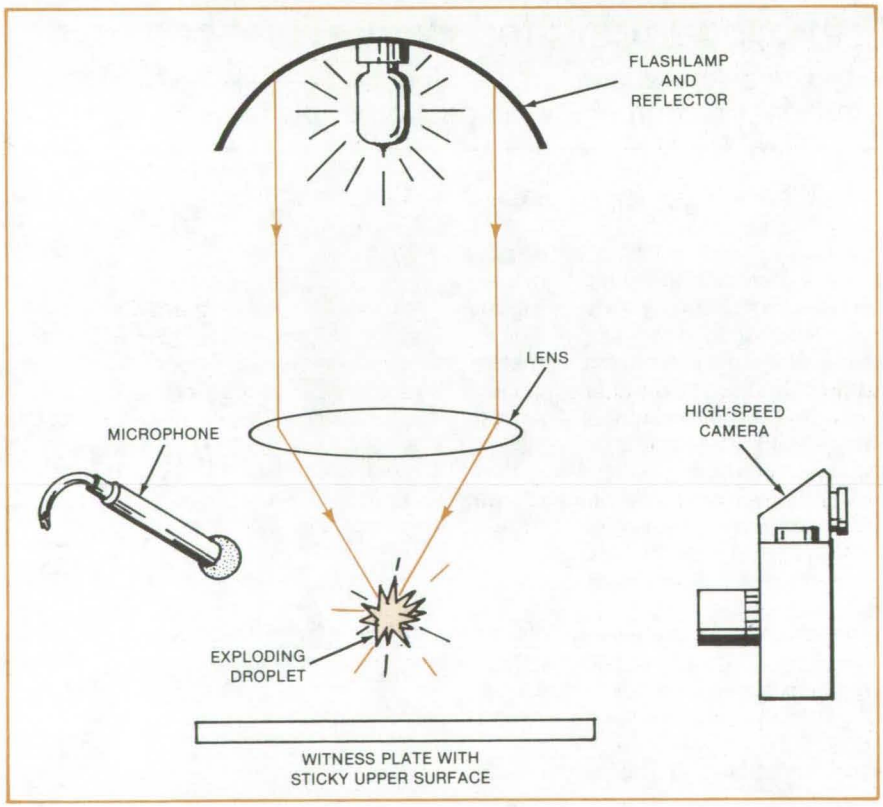


**Combustion-Test Setup** rapidly heats a droplet of coal/oil/water mixture and records the resulting explosion.

posed to measure the intensity and energy release due to the microexplosions is shown in the figure. Radiation from a flashlamp would be focused to heat a droplet of the mixture to be tested. The intensity of the resulting microexplosion and the effectiveness of the separation of coal particles from the emulsion would be inferred from high-speed photographs, acoustic-signature recordings, and the dispersion pattern left on the witness plate.

*This work was done by Raymond O. Kushida of Caltech for* **NASA's Jet Propulsion Laboratory.** *For further information, Circle 21 on the TSP Request Card.*
*NPO-15462*

# Books and Reports

These reports, studies, and handbooks are available from NASA as Technical Support Packages (TSP's) when a Request Card number is cited; otherwise they are available from the National Technical Information Service.

## Energy-Storage Modules for Active Solar Heating and Cooling

A melting salt hydrate stores 12 times as much heat as rocks and other heavy materials.

Commercial energy-storage modules that use a material that melts to store heat are the subject of a new 34-page report. The phase change from solid to liquid enables more heat to be stored than is possible with an inert material, such as rock, masonry, concrete, and other heavy materials. The energy is stored mostly as latent heat; that is, heat that can be stored and recovered without any significant change in temperature. The phase-change material, which melts at about 90° F (32° C), is a salt hydrate mixture based on ordinary glauber salt. Also, the mixture has additives that insure nucleation and prevent segregation.

The salt hydrate mixture is permanently sealed in specially designed containers molded of high-density polyethylene. Each container has ribs and air passages for maximum heat transfer to and from the air flowing through them. The containers have a specific storage capacity of about 70 Btu/lb vs. 6 Btu/lb (163 J/kg vs. 14 J/kg) for rock and similar materials. Thus for the same storage capacity, only one-twelfth as much material is needed, resulting in reduced space, a big factor in building costs. A typical storage capacity of $3.0 \times 10^5$ Btu ($3.2 \times 10^8$ J) can fit in a closet space.

Each container is supported by a steel frame. The frame units are joined by vertical connecting rods to make a module 2 ft (0.6 m) high. The standard module 2 by 2 by 2 ft consists of eight frame units and containers. The containers can be removed and reinstalled by disassembling the module. In any suitable insulated enclosure connected to a horizontal air-circulating system, the 2-$ft^3$ module can be assembled in parallel to increase storage capacity and/or in tandem to increase heat-transfer efficiency.

The report describes the development, evaluation, and testing of the modules. Illustrations and descriptions of the module, installation and operating instructions, and performance test results are also included.

*This work was done by John C. Parker of* **Marshall Space Flight Center.** *Further information may be found in DOE/NASA TM-82415 [N81-23604/NSP], "Development and Testing of Thermal Energy Storage Modules for Use in Active Solar Heating and Cooling Systems — Final Report" [$6.50]. A paper copy may be purchased [prepayment required] from the National Technical Information Service, Springfield, Virginia 22161. The report is also available on microfiche at no charge. To obtain a microfiche copy, Circle 22 on the TSP Request Card.*
*MFS-25681*

## Solar Water-Heater Design and Installation

In one application, it should reduce oil use by 40 percent.

A design with installation sketches and instructions along with purchase specifications for components of a solar water-heating system is available. Although the system has not yet been built, it is designed to preheat well water to be used in a camp shower and washhouse at a Young Men's Christian Association (YMCA) camp in Aurora, Ohio. The heating system is designed to raise the temperature of 2,000 gallons (7,600 liters) of water 20° F (11° C), on a bright, sunny day.

Engineers at the NASA Lewis Research Center performed this civic-service project to provide this water heating system for the YMCA of Cleveland. The YMCA requested a solar heating project both as a public demonstration, and a teaching aid to encourage the use of solar energy, and also to reduce the amount of heating oil used to heat water at the camp. The system uses 16 air-type solar collectors, each 4 by 8 feet (1.2 by 2.4 meters). Heat storage is provided in a rock bin. Both the rock bin and the room that contains the air handling equipment and controls are housed underground in a precast concrete tank with necessary special openings cast in during fabrication. Components specified are commercially available, and cost estimates are given.

In general, the system works as follows: Solar-heated air is pumped from the collectors through the rock bin from the top to the bottom. An air handler circulates the heated air through an air-to-water heat exchanger, which transfers the heat to the incoming well water. It is estimated that the solar water heater will reduce the amount of heating oil required to heat water at the camp by about 40 percent over a year's period.

*This work was done by Paul Harlamert, Jarman Kennard, and Julius Ciriunas of* **Lewis Research Center.** *To obtain a copy of the design, Circle 23 on the TSP Request Card.*
*LEW-13665*

## Heat-Transfer Fluids for Solar-Energy Systems

Test results are reported for noncorrosive fluids for solar-heating and cooling systems.

Noncorrosive heat-transport fluids that would be compatible with both metallic and nonmetallic solar collectors and plumbing systems, or combinations of them, were tested to demonstrate their corrosion and freeze protection. The investigation of these fluids for active, closed-loop solar-heating and cooling systems is the subject of a 43-page report.

To test the fluids, a stand was equipped with aluminum, copper, steel, and nonmetallic solar collectors, associated components, and copper plumbing to circulate the transport fluids. All systems were charged with fluids and sampled monthly. Deionized water, hard water, monoethylene glycol, glycerin, propylene glycol, and triethylene glycol were the fluids tested in the metallic collectors An ethylene glycol with inhibitors and 50 percent deionized water was used as the solar heat-transport fluid with nonmetallic collectors.

The tests showed that most aqueous glycol mixtures with proper corrosion inhibitors can give adequate corrosion and freeze protection and an extended boiling point in closed-loop systems using either copper, aluminum, steel, or plastic collector plates and copper plumbing. Of the materials tested, copper is the preferred material to resist corrosion. Steel also gives long life against corrosion.

Among the fluid properties tested, and tabulated in the report, are color, specific gravity, freeze point, pH, ash content, equilibrium boiling point, reserve alkalinity, and viscosities. The report also includes tables and figures of X-ray inspections for corrosion, and there are schematics of solar-heat transport systems and heat rejection systems.

*This work was done by John C. Parker of* **Marshall Space Flight Center.** *Further information may be found in DOE/NASA TM-82395 [N81-16584/NSP], "Development and Testing of Heat Transport Fluids for Use in Active Solar Heating and Cooling Systems" [$6.50]. A paper copy may be purchased [prepayment required] from the National Technical Information Service, Springfield, Virginia 22161. The report is also available on microfiche at no charge. To obtain a microfiche copy, Circle 24 on the TSP Request Card.*
*MFS-25629*

## Effects of High Temperature on Collector Coatings

Heat-resistance tests reveal variations among common coating materials

According to a new report, electroplated black chrome is a good coating for concentrating collectors in which temperatures are in the 650° to 800° F (340° to 430° C) range. Black-chrome thermal emittance is low, and its solar-absorption properties are not seriously degraded at these temperatures. Other common coatings — chemically-blackened stainless steel and electroplated black-chrome/vanadium alloy — seem suited for flat-plate collectors, which operate at lower temperatures. The blackening on stainless steel deteriorates significantly when it is exposed to temperatures above 800° F (430° C), and the thermal emittance of black chrome/vanadium is excessive at high temperatures.

The black coatings are used to increase the absorption of solar energy by the base metal while decreasing the emission of infrared energy. They are intended to improve the efficiency of solar collectors.

Test panels containing the coatings were heated in a furnace at varying temperatures up to 1,200° F (650° C). Optical properties were measured before and after exposure to the heat. Coatings known to have good optical properties but low resistance to heat were not included in the evaluation.

The coatings were produced by either electroplating or chemical treatment of metal substrates (low-carbon steel for the black chrome and black chrome/vanadium, stainless steel for the blackened stainless steel). The process parameters were adjusted to produce coatings with optimum solar-absorption properties.

All three coatings were subjected to salt-spray. All were corrosion resistant.

*This work was done by James R. Lowery of* **Marshall Space Flight Center.** *To obtain a copy of the report, Circle 25 on the TSP Request Card.*
*MFS-25651*

## Solar Heating and Cooling for a Controls Manufacturing Plant – Lumberton, New Jersey

Comprehensive report documents computer-controlled system.

A system description, test data, major problems and their resolution, performance, operation and maintenance, manufacturer's literature, and drawings are all part of a 257-page report on the solar heating and cooling of a 40,000-ft$^2$ (3,700-m$^2$) manufacturing building. The Lumberton, New Jersey, installation, which has separate solar-collector and cooling-tower areas located away from the building, is completely computer controlled. It supplies about 50 percent of the heating load and 40 percent of the air-conditioning load for the facility. The system has 6,000 ft$^2$ (560 m$^2$) of double-glazed flat-plate collectors, external above-ground storage tanks, controls, an absorption chiller, heat recovery, and a cooling tower.

The solar collectors are located within an earth berm that surrounds them and protects them from high winds. The collectors consist of 12 arrays located in two rows of 6 each. Each array is individually controlled so that it can be tilted in an east/west axis from upside down in bad weather to the correct angle for optimum collection on a given day or a given hour that day. The solar-collector loop between the building and the berm is supported by a bridge.

The solar storage consists of six steel tanks insulated with urethane and painted white. The tanks, which have a 50,000-gallon (190,000 l) total capacity, are located outside the building above ground and adjacent to the mechanical

room. All piping is made of glass-reinforced high-temperature modified epoxy to reduce pipe weight and for fabrication ease.

The building is of conventional steel-post-within-wall construction, with the outside walls and roof insulated with sprayed urethane foam. Sales offices near the south wall of the building contain the only windows — 6-ft by 6-in. (1.8 m by 15 cm) doubled-glazed slit windows for low energy loss and burglary protection.

Within the building are four large air-handling units with large built-in copper fin-tube heat exchangers. The units have dual-speed fan motors and four sets of four coils. This allows preheating with low-quality solar-heated water and final heating with high-quality solar- or electrically-heated hot water to make the maximum use of solar-energy storage. The air- handling unit in conjunction with 12 overhead fans maintain a 2° F (1° C) differential between the floor and the slightly-sloping 18- to 20-foot (5.5- to 6-m) ceiling.

*This work was done by RKL Controls Co. for* **Marshall Space Flight Center.** *Further information may be found in DOE/NASA CR-161679 [N81-23597/NSP], "Solar Heating and Cooling System Installed at RKL Controls Company, Lumberton, New Jersey — Final Report" [$20]. A paper copy may be purchased [prepayment required] from the National Technical Information Service, Springfield, Virginia 22161. The report is also available on microfiche at no charge. To obtain a microfiche copy, Circle 26 on the TSP Request Card.*
*MFS-25665*

## Solar Space and Water Heating for Hospital — Charlottesville, Virginia

Most of the heating needs are supplied for a 50-bed hospital.

The solar installation at a 50-bed Charlottesville, Virginia, hospital is designed to supply 67 percent of the space heating and 71 percent of the hot water for the facility. The system, which is described in an 86-page report, consists of 88 single-glazed selectively-coated baseplate collector modules, hot-water coils in the air ducts, a domestic-hot-water preheat tank, a 3,000-gallon (11,350-l) concrete urethane-insulated storage tank, and other components.

Elevated above the storage tank, the collectors are mounted on the roof in a sawtooth arrangement of 12 rows facing south, inclined at an angle of 53° from the horizontal. There are eight collectors in eight rows and six collectors in four rows. Circuit setters control the flow. All the rows are sloped to the centerline of the roof so that they drain back to the storage tank when the circulating pump stops, eliminating any need for freeze protection. The drain-back feature of the system is accomplished in part by a combination air-vent/vacuum-breaker assembly. The connectors in the individual rows are connected with copper pipe couplings; this arrangement is referred to as "internally-manifolded" solar collectors.

The 7,000-ft$^2$ (650-m$^2$) hospital, which provides around-the-clock patient care, had to replace the existing roof completely to accommodate the solar array. Since the system became operational in December 1979, no major problems have been encountered with either the roof or the system. However, in all probability, the system will have to be dismantled partially or totally when the useful life of the roof expires in 15 to 20 years.

Included in the report are extracts from site files, descriptions of component systems, specifications, and design drawings. The report also contains information on installation, maintenance and operation instructions, acceptance test reports, and manufacturer's product literature.

*This work was done by the David C. Wilson Neuropsychiatric Hospital for* **Marshall Space Flight Center.** *Further information may be found in DOE/NASA CR-161675 [N81-22471/NSP], "Solar Space and Water Heating System Installed at Charlottesville, Virginia" [$9.50]. A paper copy may be purchased [prepayment required] from the National Technical Information Service, Springfield, Virginia 22161. The report is also available on microfiche at no charge. To obtain a microfiche copy, Circle 27 on the TSP Request Card.*
*MFS-25666*

## Solar Hot Water for a Motor Inn — Las Vegas, Nevada

Collectors supply almost three-quarters of inn needs.

A solar hot-water installation at a motor inn in Las Vegas, Nevada, is described in a new report. The report contains descriptions of the design philosophy, the operation of the system, and problems and solutions. It provides drawings of the solar roof plan, operator's instructions, manufacturers' brochures, and a copy of the acceptance report.

The system supplies 74 percent of the hot-water load of the 96-unit motor inn. It employs seven banks of eight collectors each on the roof of the inn. Total area of the flat-plate, liquid-medium collectors is approximately 1,200 ft$^2$ (110 m$^2$). Two bundles of heat-exchanger tubes transfer solar heat to the domestic hot-water system in a 2,500-gallon (9,500-liter) tank.

The system was put into operation in the summer of 1979. During initial tests, 18 collectors developed leaks at solder joints between the waterway and the internal header. The absorbers were replaced, and since then the system has operated satisfactorily.

The report offers suggestions for improvements in the system. For example, insulation on the heat-exchanger piping in the mechanical room would reduce heat loss, and a greater distance between the inlet and outlet pipes in the domestic hot-water tank would prevent hot water from being returned to the solar storage tank.

*This work was done by LaQuinta Motor Inns, Inc., for* **Marshall Space Flight Center.** *Further information may be found in DOE/NASA CR-161642 [N81-21535/NSP], "Solar Hot Water System Installed at Las Vegas, Nevada — Final Report" [$6.50]. A paper copy may be purchased [prepayment required] from the National Technical Information Service, Springfield, Virginia 22161. The report is also available on microfiche at no charge. To obtain a microfiche copy, Circle 28 on the TSP Request Card.*
*MFS-25646*

## Solar Heating for a Bottling Plant — Jackson, Tennessee

Tubular solar-energy collectors are expected to supply 55 percent of the total thermal load.

A new report describes a retrofit solar-heating system designed for and installed in a bottle works in Jackson, Tennessee. The system consists of 9,480 square feet (880 square meters) of evacuated-tube solar collectors with attached specular cylindrical reflectors. An estimated 55 percent of the winter space-heating load for the large production building and the hot-water load for bottle-washing equipment during the remainder of the year will be supplied by the solar-heating system.

Evacuated tubular solar collection was chosen over the flat-tube collectors originally planned because it offered greater potential for refrigeration and air-conditioning. The roof-mounted solar-collector array is tilted 50° from the horizontal. This steep tilt angle biases the year-round system toward winter space-heating demand, which far exceeds the hot-water load for the remainder of the year. A superstructure tied to the vertical columns of the building and installed above the roof helps to support the collector array.

Storage is provided by two steel hot-water tanks located within the plant production building. High-volume storage is used because the 4-day workweek at the plant causes heavy draining, which must be made up in storage on nonworking days.

Four shell-and-tube heat exchangers transfer stored heat from the tanks to the bottle washer. Space heating from storage utilizes 16 hydronic unit heaters located throughout the building. The collector pumps are activated to store energy whenever insolation surpasses a certain threshold value.

*This work was done by Energy Solutions, Inc., for* **Marshall Space Flight Center.** *Further information may be found in DOE/NASA CR-161586 [N81-73511/NSP], "Solar Heating System Installed at Jackson, Tennessee — Final Report" [$14]. A paper copy may be purchased [prepayment required] from the National Technical Information Service, Springfield, Virginia 22161. The report is also available on microfiche at no charge. To obtain a microfiche copy, Circle 29 on the TSP Request Card.*
*MFS-25595*

## Economic Evaluation of Observatory Solar-Energy System

The long-term performance at the site is used to analyze other sites.

The long-term economic performance of a commercial solar-energy system was analyzed and used to predict its economic performance at four additional sites. Described in a report that is now available, the analysis was done to demonstrate the viability of the design over a broad range of environmental and economic conditions. Reports on other commercial systems analyzed in much the same way are described in the articles that follow.

The site analyzed is the 50-seat Memorial Observatory in Lincoln, Nebraska; the other cities included in the study are: Albuquerque, New Mexico, Fort Worth, Texas, Madison, Wisconsin, and Washington, D.C. These cities were chosen for the availability of long-term weather data, heating degree days, cold-water-supply temperature, solar insolation, utility rates, market potentials, and type of solar system.

The observatory energy collection and storage system consists of nine collectors having an area of 481 $ft^2$ (45 $m^2$) with air as the transport medium and 347 $ft^3$ (10 $m^3$) of rock storage. Solar-heated air is supplied directly to the heated space or to rock storage. When solar energy is not adequate to meet the space-heating demand, an auxiliary natural-gas furnace supplies the additional energy.

The report concludes that solar energy is not economically beneficial under the assumed economic conditions for any of the five cities. The analysis takes account of the long-term average environmental conditions, loads, fuel costs, and other economic factors that are applicable to each of the five cities.

The analysis method selected, which requires a common basis for evaluation, optimizes the collector size through the f-chart design procedure. The procedure uses a set of design charts that estimate the thermal performance of the solar-energy system based on collector characteristics, storage, energy demands, and regional long-term weather. Using the resulting analysis, an iterative procedure selects the collector area that minimizes life-cycle cost — the cost of acquiring, operating, and maintaining the solar installation. Once the optimal collector size is determined, the resulting thermal and economic performance can be obtained.

The topics covered by the report are system description, study approach, economic analysis and system optimization, analysis results, and economic uncertainty analysis. The report also includes tables and graphical presentations of life-cycle costs for the five cities and appendixes covering the f-chart procedure, uncertainty analysis equations, energy costs for the analysis sites, and the computation of UA values.

*This work was done by the Federal Systems Division of IBM Corp. for* **Marshall Space Flight Center.** *Further information may be found in DOE/NASA CR-161724 [N81-25510/NSP], "Solar Energy System Economic Evaluation — Final Report for Seeco Lincoln, Lincoln, Nebraska" [$9.50]. A paper copy may be purchased [prepayment required] from the National Technical Information Service, Springfield, Virginia 22161. The report is also available on microfiche at no charge. To obtain a microfiche copy, Circle 30 on the TSP Request Card.*
*MFS-25682*

## Economic Evaluation of Single-Family-Residence Solar-Energy Installation

Space and hot-water preheating system is evaluated for five cities.

Using the same analytic approach as in the preceding article, an economic evaluation of a solar-energy installation in Tunkhannock, Pennsylvania, was performed. Like the preceding report, the 100-page report on this installation includes the predicted economic perform-

ance for the same four additional cities that typify a broad range of environmental and economic conditions.

The solar-energy system was designed for both space heating and domestic hot-water preheating for a 1,000-ft$^2$ (93-m$^2$) single-family residence in Tunkhannock. Flatplate collectors that use air as the transport fluid form a 208.5-ft$^2$ (19.4-m$^2$) collector array. Energy is transferred to and from storage by a liquid-to-air heat exchanger. In the two main tanks, the storage capacity is 240 gallons (900 l) of water. Auxiliary energy for the hot-water system is supplied by electricity and for space heating by fuel oil.

The report concludes that solar-energy systems of the type installed at the Tunkhannock site are not economically beneficial under the assumed conditions at Tunkhannock and two other cities — Fort Worth, Texas, and Madison, Wisconsin. Only in Albuquerque, New Mexico, and Washington, D.C. — as a result of the insolation and cost of electricity in these two cities — was the solar-energy system found to be profitable.

The report contains graphs and tables that present the evaluation procedure and its results. It also contains appendixes that aid in understanding the methods used.

*This work was done by the Federal Systems Division of IBM Corp. for* **Marshall Space Flight Center.** *Further information may be found in DOE/NASA CR-161723 [N81-24532/NSP], "Solar Energy System Eonomic Evaluation — Final Report for Fern Tunkhannock, Tunkhannock, Pennsylvania" [$9.50]. A paper copy may be purchased [prepayment required] from the National Technical Information Service, Springfield, Virginia 22161. The report is also availble on microfiche at no charge. To obtain a microfiche copy, Circle 31 on the TSP Request Card.*
*MFS-25683*

## Economic Evaluation of Townhouse Solar-Energy System

### System is designed to supply 65 percent of heating and 75 percent of hot water.

A solar-energy site in Columbia, South Carolina, is comprised of four townhouse apartments. As in the two preceding articles, an economic evaluation of this solar-energy system and the projected performance of similar systems in four other selected cities are summarized in a 103-page report.

The solar-collection system consists of 24 flat-plate liquid collectors connected in parallel and augmented by pyramidal reflectors that collect and store energy in a 2,500-gallon (9,500-l) tank. The transport fluid is water. The collector array, the area of which is 1,152 ft$^2$ (107 m$^2$), is located behind the window in the attic of two of the townhouses.

The solar-energy system is designed to supply 65 percent of the heating load of $2.1 \times 10^7$ Btu/month ($8.5 \times 10^3$ watts) and 75 percent of the domestic hot water load based on an average hot-water load of $3.02 \times 10^6$ Btu/month ($1.2 \times 10^3$ watts). Solar-heated water is pumped in a loop between an internal heat exchanger within the 2,500-gallon storage tank and the heat exchangers within four 120-gallon (450-l) hot-water heaters that supply individual apartments with hot water. An electric element in each tank supplies the necessary auxiliary energy to meet the hot-water demand. Solar-heated water is also supplied to a direct solar-to-air heat exchanger or to a multifunctional heat pump that supplies space-heating energy to each apartment.

The study concludes that solar energy is not economically beneficial under the assumed economic conditions at any of the sites considered in this study. Over a 20-year period, the study estimates that for the initial investment of $22,173 (adjusted for Federal tax credits) at the site, the backup fuel costs would be $43,751, and the life-cycle savings would be $25,090. Of the five cities considered in the study, the least expensive place to operate this solar-energy system is Fort Worth, Texas; the most expensive is Washington, D.C.

Characteristics of the analysis sites are shown in graphs — of solar fraction vs. collector area, of thermal performance of solar-energy system with optimized collector area, of optimization of collector area, of annual expenses for solar-energy system and conventional system, and of payback — for the solar-energy system for each of the five cities. The costs and savings for each city over a 20-year analysis period are summarized in a table.

*This work was done by the Federal Systems Division of IBM Corp. for* **Marshall Space Flight Center.** *Further information may be found in DOE/NASA CR-161722 [N81-23605/NSP], "Solar Energy System Economic Evaluation — Final Report for Wormser, Columbia, South Carolina" [$11]. A paper copy may be purchased [prepayment required] from the National Technical Information Service, Springfield, Virginia 22161. The report is also available on microfiche at no charge. To obtain a microfiche copy, Circle 32 on the TSP Request Card.*
*MFS-25684*

## Economic Evaluation of Office Solar-Heating System

### The long-term economic performance of the system is analyzed

The solar-energy system at the U.S. Department of Transportation Test Center at Pueblo, Colorado, was designed to provide 34 percent of the combined space heating and hot-water preheating to an office area located in the corner of a warehouse. An economic evaluation of the installation and five other similar installations around the country is the subject of a 109-page report. The objective of the analysis is to report the long-term economic performance of this system at its installation site and to extrapolate the results to four other locations and an alternate site. The format and analysis in this report are the same as in the preceding three reports, except that Yosemite, California, was added to the cities being analyzed.

The Pueblo solar-energy system is located at a warehouse used to test trains. The energy collection and storage consist of 583 ft$^2$ (54 m$^2$) of flat-plate collectors, a petroleum-based thermal-energy transport fluid, and a 1,100-gallon (4,160-l) water-filled storage tank. If solar energy is not sufficient to meet the space-heating demand, an auxiliary propane-gas furnace supplies the additional energy. An air-circulation fan and motor-driven dampers distribute the energy to the office area. The hot-water auxiliary is a standard electric-resistance, immersion heater in a 30-gallon (115-l) domestic hot-water tank.

(continued on next page)

The study estimates that the Pueblo installation would cost more in backup fuel than its initial investment and concludes that under the assumed economic conditions, the installation is not economically beneficial. For other reasons, the five additional sites were also evaluated as being uneconomical. However, if 1985 escalated values for fuel, costs, mass production, and improved design and installation techniques were applied, a significantly higher degree of savings could be realized — as would be true of the results for all the systems reported on in this series.

*This work was done by the Federal Systems Division of IBM Corp. for* **Marshall Space Flight Center.** *Further information may be found in DOE/NASA CR-161725 [N81-23607/NSP], "Solar Energy Economic Evaluation — Final Report for Colt Pueblo, Pueblo, Colorado" [$11]. A paper copy may be purchased [prepayment required] from the National Technical Information Service, Springfield, Virginia 22161. The report is also available on microfiche at no charge. To obtain a microfiche copy, Circle 33 on the TSP Request Card.*
*MFS-25685*

## Dormitory Solar-Energy-System Economics

Report analyzes a prepackaged unit for a single-family residence.

A prepackaged solar-energy assembly was evaluated as part of the Solar-Heating and Cooling Development Program. A 102-page report analyzes the long-term economic performance of the system at a dormitory installation and extrapolates to four additional locations about the United States. The evaluation, like others in the program series (see preceding articles), is based on life-cycle costs versus energy savings. The method of evaluation is the f-chart procedure for solar-heating and domestic hot-water systems.

The solar-energy system is integrated into the dormitory heating and hot-water system at the Mississippi Power and Light training center in Clinton, Mississippi. Generally, it was designed for single-family residences in the United States, with the exception of the extreme north and regions with low heating degree days.

The dormitory solar-energy unit includes flat-plate collectors, with a collector area of 259 $ft^2$ (24 $m^2$), using air as the transport fluid. Air is circulated by two blowers: One blower circulates air from the array to storage, and the other circulates air from the collector array or rock storage to the building. In the heat exchanger, solar-heated water circulates by thermosiphoning to a 52-gallon (200-l) preheat tank, and supply water for two 30-gallon (110-l) hot-water tanks is drawn from the preheat tank. An electric heater supplies the auxiliary energy.

Energy savings result from the replacement of conventional energy forms by solar energy after the costs of producing the solar energy are deducted. With this criterion and others, the report concludes that the system would be unprofitable at all sites; that is, over a 20-year life cycle, the system would not pay for itself.

*This work was done by the Federal Systems Division of IBM Corp. for* **Marshall Space Flight Center.** *Further information may be found in DOE/NASA CR-161726 [N81-24531/NSP], "Solar Energy System Economic Evaluation — Final Report for IBM System 4, Clinton, Mississippi" [$11]. A paper copy may be purchased [prepayment required] from the National Technical Information Service, Springfield, Virginia 22161. The report is also available on microfiche at no charge. To obtain a microfiche copy, Circle 34 on the TSP Request Card.*
*MFS-25693*

## Two-Story-Dwelling Solar Installation

Roof-mounted solar-energy system in Georgia is evaluated.

Life-cycle costs of conventional energy systems are compared with those of solar-energy systems in an economic evaluation of a two-story Georgia dwelling. The savings are expressed as the difference between the total fuel savings that result from operation of the solar-energy system and the increased costs that result from the investment in, operation of, and maintenance of the solar-energy system. Of the five sites considered in the report — Newnan, Georgia, Albuquerque, New Mexico, Fort Worth, Texas, Madison, Wisconsin, and Washington, D.C. — only Albuquerque, where the average solar insolation is about 1,800 Btu/$ft^2$/day (0.07 W/m2), is this solar-energy system marginally profitable. All other sites were analyzed as being unprofitable.

The solar-energy system is installed in a two-story dwelling located in Newnan, Georgia. It heats the space and preheats the hot water for the residence. Fourteen single-glazed flat-plate collectors with a total area of 392 $ft^2$ (36.4 $m^2$) are mounted on the roof. Heat is transferred by air and stored by a horizontal rock bin.

A central air handler with integral blower and damper controls distributes the solar-heated air to the heated space or to and from the rock-storage bin. Auxilliary heating is supplied by an electric heat pump and supplemented by electric heaters when outdoor temperatures drop below 15° F (-9° C). A heat exchanger for hot-water preheating transfers heat to an 80-gallon (300-l) preheat tank.

The 103-page report of the economic analysis covers the system description, the study approach, the economic analysis, the results of the analysis, and the economic uncertainty analysis. An elaboration on some of the equations, procedures, and parameters used in the analysis is found in the report appendixes.

*This work was done by the Federal Systems Division of IBM Corp. for* **Marshall Space Flight Center.** *Further information may be found in DOE/NASA CR-161727 [N81-24585/NSP], "Solar Energy System Economic Evaluation — Final Report for Contemporary Newnan, Newnan, Georgia" [$11.00]. A paper copy may be purchased [prepayment required] from the National Technical Information Service, Springfield, Virginia 22161. The report is also available on microfiche at no charge. To obtain a microfiche copy, Circle 35 on the TSP Request Card.*
*MFS-25697*

## Ranger Station Solar-Energy System Receives Economic Evaluation

A Glendo, Wyoming, installation shows potential for savings.

The economic performance of the Glendo Reservoir Ranger Station solar-energy system in Wyoming and its extrapolated performance in four other

locations around the United States is reviewed in a new report. The data used in the analysis were generated from measurements obtained at the ranger station and from economic and environmental information that are available to anyone interested in evaluating a potential solar-energy installation. The format and analysis in the report are the same as in the preceding evaluations, which are all part of the Solar-Heating and Cooling Development Program.

The installation for the 1,078-ft$^2$ (100-m$^2$) Wyoming ranger station was retrofitted with 294 ft$^2$ (27 m$^2$) of flat-plate collectors, a 1,000-gallon (3,784-l) hot-water storage tank, and a 65-gallon (250-l) hot-water tank, together with pumps and heat exchangers, to transfer solar energy on command from a controller. It is a passive drain-down system that uses water as the heat-transfer medium for space and hot-water heating.

For the Glendo ranger station, the evaluation showed a cumulative loss of $1,775 for a 20-year projected life of the solar installation. With a reasonable and favorable change in the economic variables considered, there is a possibility of a savings with the Glendo solar-energy system. Of the four extrapolated sites,only Albuquerque showed the same possibility.In general, the report concluded that the solar-energy system of the type installed at Glendo would not be economically beneficial under the assumed economic conditions for the five sites considered.

*This work was done by the Federal Systems Division of IBM Corp. for* **Marshall Space Flight Center**. *Further information may be found in DOE/NASA CR-161728 [N81-24541/NSP], "Solar Energy System Economic Evaluation — Final Report for IBM System 3, Glendo, Wyoming" [$11.00]. A paper copy may be purchased [prepayment required] from the National Technical Information Service, Springfield, Virginia 22161. The report is also available on microfiche at no charge. To obtain a microfiche copy, Circle 36 on the TSP Request Card.*
*MFS-25699*

## Economic Evaluation of Dual-Level-Residence Solar-Energy System

Thermal and economic performance is based on an optimal collector area that minimizes life-cycle costs.

In the Operational Test Site Development Program, many solar-energy systems, designed by different contractors, are analyzed for their economic profitability. A 105-page report, one in a series of economic evaluations of the different installations, analyzes a system installed in an Akron, Ohio, residence.

To establish a common basis of evaluating all the systems, the method optimizes the collector size through the f-chart design procedure. The procedure uses a set of design charts, developed by detailed simulations, that estimate the thermal performance of a solar-energy system based on collector characteristics, storage, energy demands, and regional long-term weather data. Using these results, an optimal collector area is chosen that minimizes life-cycle costs. From this optimal size the thermal and economic performance is evaluated.

The Akron solar-energy system supplies both space heating and hot-water preheating for a 1,840-ft$^2$ (170-m$^2$) dual-level single-family residence. Using a 546-ft$^2$ (51-m$^2$) flat-plate collector array, energy is absorbed and transferred to 270 ft$^3$ (7.6 m$^3$) of rock storage located on the lower level of the house. Air is the transport fluid.

An air-to-liquid heat pump coupled to a 1,000-gallon (3,780-l) water-storage tank supplies the auxiliary space heating and cooling, and energy stored in the tank is used for space heating. Electricity is the auxiliary energy source for water and space heating. The system is fitted with sensors, as are all the systems in the evaluation program, to monitor flow rate, temperature, electric power, and insolation.

Under the assumed economic conditions at four of the cities considered in the evaluation — Akron, Ohio, Fort Worth, Texas, Madison, Wisconsin, and Washington, D.C. — this type of energy system was found unprofitable. Only in Albuquerque, New Mexico, where the solar insolation is about 1,800 Btu/ft$^2$/day (240 W/m$^2$) and electricity cost is high ($0.070/kWh), is this energy system marginally profitable.

*This work was done by the Federal Systems Division of IBM Corp. for* **Marshall Space Flight Center**. *Further information may be found in DOE/NASA CR-161729 [N81-25541/NSP], "Solar Energy System Economic Evaluation — Final Report for Solaron Akron, Akron, Ohio" [$11]. A paper copy may be purchased [prepayment required] from the National Technical Information Service, Springfield, Virginia 22161. The report is also available on microfiche at no charge. To obtain a microfiche copy, Circle 37 on the TSP Request Card*
*MFS-25700*

## Economic Evaluation of Single-Family-Residence Solar-Energy System

The cost of the system overshadows the fuel savings.

Optimizing the design of a solar-energy system to minimize its cost is the basis of an economic evaluation of a Carlsbad, New Mexico, installation. To achieve a broader range of environmental and economic parameters, four other locations — Albuquerque, New Mexico, Fort Worth, Texas, Madison, Wisconsin, and Washington, D.C. — plus the actual installation were evaluated, using data extrapolated from the Carlsbad system. The report of the evaluation is part of a series that evaluates a number of different solar installations.

The installation is located in a single-family residence at Carlsbad Caverns National Park. Its collector array consists of 408 ft$^2$ (38 m$^2$) of flat-plate air collectors. Solar energy is stored in a bin containing

(continued on next page)

about 24,000 lb (10,900 kg) of rocks. When solar energy is insufficient to supply space heating, an oil furnace makes up the difference.

The optimal solar-energy systems range in size from 336 $ft^2$ (31 $m^2$) of collector area at Albuquerque to 192 $ft^2$ (18 $m^2$) at Fort Worth. With optimal collector areas defined, the report shows that solar energy can supply a significant portion of the total load at Carlsbad, Albuquerque, Fort Worth, and Washington. This is not true at Madison because there is no optimal system of the type evaluated that can be defined there. The reasons for this are the low insolation available, the relatively low cost of conventional energy, and the cost of the system.

A comparison of the fuel costs with and without a solar-energy system demonstrates that Carlsbad and Albuquerque are the only analysis sites that offer significant fuel savings. However, the other solar costs are significant enough to overshadow the fuel savings; and in the final analysis, at no site will the solar-energy system pay for itself. The major problem is the system cost, which ranges from $25,941 at Albuquerque to $22,862 at Fort Worth. These costs include the system hardware and installation but not the effective discount of the Federal tax credit, which reduces the cost to $21,428 and $18,862, respectively. The cost of conventional energy would have to increase more than anticipated while the cost of the system remained the same or decreased for the system to be economically feasible at any site.

The report concludes that where solar-energy system investment costs are presently high (as is the case for this system), the future promise of savings due to increased conventional energy costs is not optimistic. This is because the cost of the system tends to increase at a rate not significantly less than the cost of conventional energy.

*This work was done by the Federal Systems Division of IBM Corp. for* **Marshall Space Flight Center**. *Further information may be found in DOE/NASA CR-161730 [N81-25542/NSP], "Solar Energy System Economic Evaluation — Final Report for IBM System 1B, Carlsbad, New Mexico" [$9.50]. A paper copy may be purchased [prepayment required] from the National Technical Information Service, Springfield, Virginia 22161. The report is also available on microfiche at no charge. To obtain a microfiche copy, Circle 38 on the TSP Request Card.*
*MFS25701*

# Materials

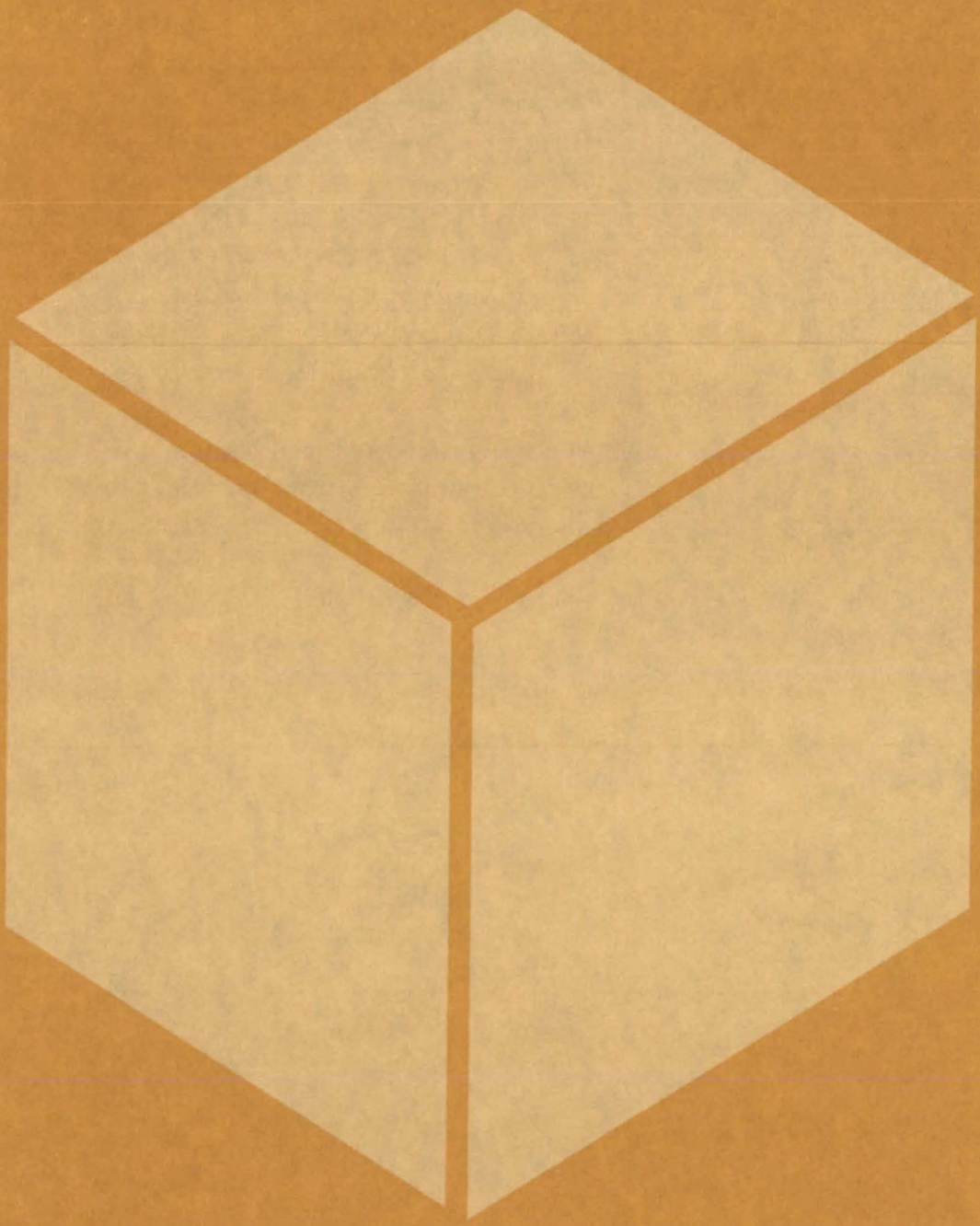

## Hardware, Techniques, and Processes



## Books and Reports

# System Controls and Measures Oxygen Fugacity

Ceramic-electrolyte cell monitors the oxygen fugacity in high-temperature reactions.

*Lyndon B. Johnson Space Center, Houston, Texas*

A system developed at Johnson Space Center controls and measures oxygen fugacity in high-temperature chemical research. A ceramic-electrolyte cell is the sensing element. All the hardware needed to control the gas flow and temperature and to measure the cell electromotive force is included. An analytic balance allows in situ thermogravimetric sample analysis.

The oxygen fugacity, a measure of effective partial oxygen pressure in a nonideal multicomponent chemical system, is of interest to geologists, chemists, and metallurgists in research on the valence states of elements. At atmospheric pressures and high temperatures, gas mixing is often used to control the oxygen fugacity: Two gases that react to produce oxygen are accurately mixed and allowed to flow over a sample in the furnace. Typical gases include carbon dioxide and carbon monoxide or hydrogen and carbon dioxide.

Oxygen fugacity is measured directly in terms of the voltage across a calcia-stabilized zirconia ceramic-electrolyte cell. The cell is mounted in the furnace near the sample (see figure). In the temperature range of interest (600° to 1,500° C), the cell voltage is given by the equation:

$$E = \frac{RT}{4F} \ln \frac{f_x}{f_r}$$

where E is the cell voltage, R the ideal gas constant, F the Faraday constant, and $f_x$ and $f_r$ the fugacities of the unknown and reference oxygen, respectively.

Gas mixing is controlled by low-pressure regulators and metering valves. The temperature is monitored by thermocouples. Thermocouple voltages control the current through the heating coils. Programable electronics allow the furnace to remain at any temperature for up to 79 hours and then to follow a prescribed temperature variation with time. The analytical balance is integrated with the gas-mixing system to enable controlled-atmosphere thermogravimetric analysis of the sample.

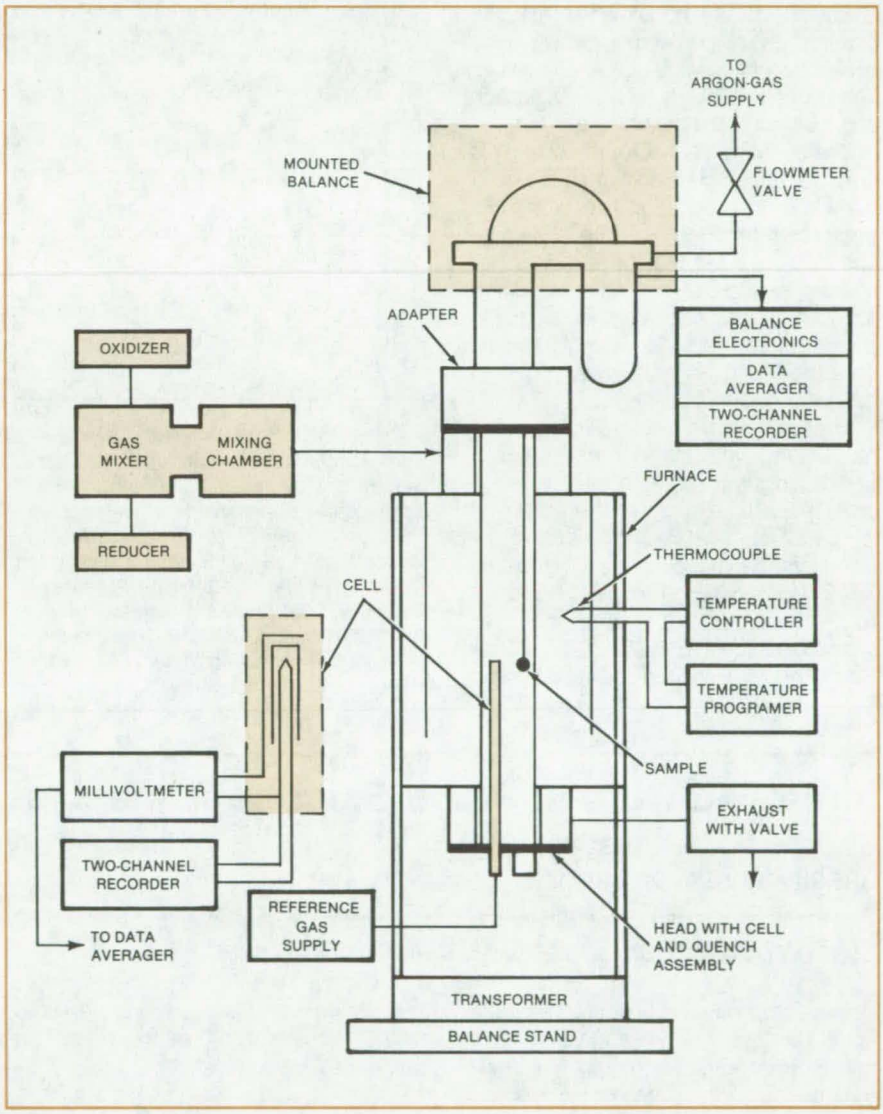


The **Oxygen-Fugacity Apparatus** includes the furnace containing the sample and the oxygen-fugacity cell, the gas-mixing system, a balance for thermogravimetric analysis, and the various control and monitoring systems. The cell voltage is related to the ratios of fugacities of the sample and reference gases.

*This work was done by Richard J. Williams of* **Johnson Space Center** *and Oscar Mullins of Lockheed Electronics Corp. Further information, including system design and operating details, may be found in NASA TM-58234 [N81-17188/NSP], "JSC Systems Using Solid Ceramic Oxygen Electrolyte Cells To Measure Oxygen Fugacities in Gas-Mixing Systems" [$6.50]. A copy may be purchased [prepayment required] from the National Technical Information Service, Springfield, Virginia 22161.*
*MSC-20096*

# Surface Seal for Carbon Parts

An antioxidation coating extends part life at high temperature.

*Lyndon B. Johnson Space Center, Houston, Texas*

Surface pores in parts made of graphite or reinforced-carbon/carbon materials are sealed by a silicon carbide-based coating. The coating inhibits subsurface oxidation and thus lengthens the part life.

The starting material for the coating is graphite felt, which is converted to silicon carbide felt by processing it according to a prescribed time/temperature schedule. The converted felt is pulverized in a ball mill, and the resulting powder is mixed with an equal weight of black silicon carbide powder. Finally, the powder mixture is combined with an equal weight of an adhesive to form a paste.

The part to be sealed is prepared by rubbing with fine abrasive paper and wiping with an alcohol-moistened cheesecloth. The sealant is applied with a brush, spatula, or blade.

After the part has dried in air, the coating is ready to be cured. The part is placed in a furnace, where it is subjected to temperatures up to 600° F (315° C) for several hours. A second coating is applied to the part after it has cooled, and the curing procedure is repeated.

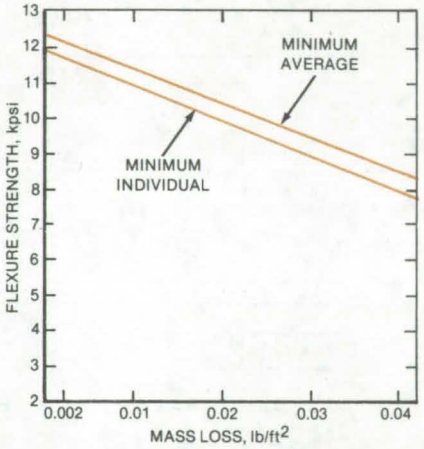


The **Acceptability of an Antioxidation Seal** is determined by flexural strength tests on specimen bars that have been heated at high temperatures for prolonged periods. Strengths of specimens should exceed the minimum values defined by the straight lines. The lines represent data for coatings 0.029 to 0.031 inch (0.74 to 0.79 millimeter) in thickness; a correction factor is applied for thinner or thicker coatings.

The coated parts are expected to pass difficult tests of their oxidation resistance. Specimens are exposed to high temperatures for prolonged periods, and their before-and-after weights are compared. The maximum mass loss per unit of surface area after exposure at 1,000° F (540° C) for 18 hours must not exceed 0.05 lb/ft2 (0.24 kg/m2). After exposure at 2,300° F (1,260° C) for 18 hours, mass loss must not exceed 0.03 lb/ft2 (0.15 kg/m2). After these heat treatments, the parts are tested for flexual strength (see figure).

*This work was done by David M. Shuford and John P. Spruiell of Vought Corp. for* **Johnson Space Center.** *For further information, including a detailed process specification, Circle 39 on the TSP Request Card.*
*MSC-18898*

# Improved Cure-in-Place Silicone Adhesives

Silicone elastomers have low density and high viscosity

*Lyndon B. Johnson Space Center, Houston, Texas*

Two improved cure-in-place silicone-elastomer-based adhesives have low thermal expansion and low thermal conductivity. The adhesives are flexible at low temperatures and can withstand high temperatures without disintegrating. Termed "RTV 560-55" and "RTV 560-32," the new ablative compounds were initially developed for in-flight repair of insulating tile on the Space Shuttle orbiter. They could find use in other applications requiring high-performance adhesives, such as sealants for solar collectors.

The key feature of the compounds is the addition of hollow microsphere fillers to the elastomer resin. The microspheres decrease the adhesive density and thermal conductivity while increasing its viscosity to between 100,000 and 600,000 centipoises. The increased viscosity keeps the adhesive in place during repair and prevents it from being drawn off by capillary forces prior to cure. Phenolic microspheres increase the char yield when the adhesive is burned, while silicone microspheres form a viscous protective melt. Ceramic fibers improve the char retention.

It is necessary to match the viscosities of the resin and catalyst to facilitate mixing. The RTV 560-32 resin is mixed with a silicone fluid that initially decreases the viscosity, allowing large quantities of the hollow microspheres (which increase viscosity) to be added. The result is a strong, light product. Both elastomers can be extruded from conventional repair guns.

The ingredients of the new formulations include:

- Methyl-phenyl silicone-elastomer resin with high-temperature filler,
- Mixture of rapid- and moderate-cure catalysts,
- Hollow microspheres,
- Low-viscosity silicone fluid, and
- Ceramic fibers as needed.

The adhesives cure within 18 hours in vacuum ($10^{-5}$ torr) at temperatures between 40° and 125° F (4° and 52° C) with very little marbling. The cure rate is varied either by changing the ratio of rapid/moderate-cure catalyst or by varying the percentage of

catalyst. Adhesion to silicone-based substrates, such as RTV 560, exceeds 50 psi (345 kN/m$^2$) for both RTV 560-55 and RTV 560-32. The shelf life of the unmixed components is at least 6 months at 80° F (27° C).

*This work was done by Creed E. Blevins, Jack Sweet, and Rudy Gonzalez of McDonnell Douglas Corp. for* **Johnson Space Center.** *No further documentation is available.*
*MSC-18782*

# Measuring Interdiffusion in Binary Liquids

Convection is suppressed by enclosing the liquids in a capillary tube.

*Marshall Space Flight Center, Alabama*

The composition, microstructure, and interdiffusion coefficients in binary alloys are determined with a new experimental technique. It is an extension of a method previously used to study interdiffusion in solids.

In the method used for solids, bars of two different metals are joined at polished faces, then heated to a temperature at which the metals diffuse into each other. This technique cannot be directly applied to liquid systems because convection would contribute to the transport of material across the interface.

The new method reduces convection by enclosing the liquids in a capillary tube. The system is further stabilized by orienting the tube so that the denser liquid lies at the bottom.

The sample is prepared by placing wires of the two metals (typically 3 centimeters long) in a capillary tube (typically 1 millimeter in diameter). In the example shown in the figure, an aluminum wire is at the top, and an indium wire (the denser one) is below.

In the experiment, the sample is heated in a wire-wound furnace and is held at a temperature above the miscibility gap, allowing diffusion to occur. At the end of the diffusion period, the sample is quenched in oil at a cooling rate of about 1,000° C/s. The result of this treatment is a specimen containing a concentration gradient that depends on the interdiffusion characteristics at the elevated temperature.

After treatment, the sample is metallographically polished to expose a longitudinal central section. Composition as a function of position along the column is determined by an electron microbeam probe. Microstructures at various positions are characterized and correlated with the composition determinations to yield relationships between microstructure and composition. Furthermore, the composition/position data are analyzed with the help of a computer to obtain the interdiffusion coefficients for the experimental temperature.

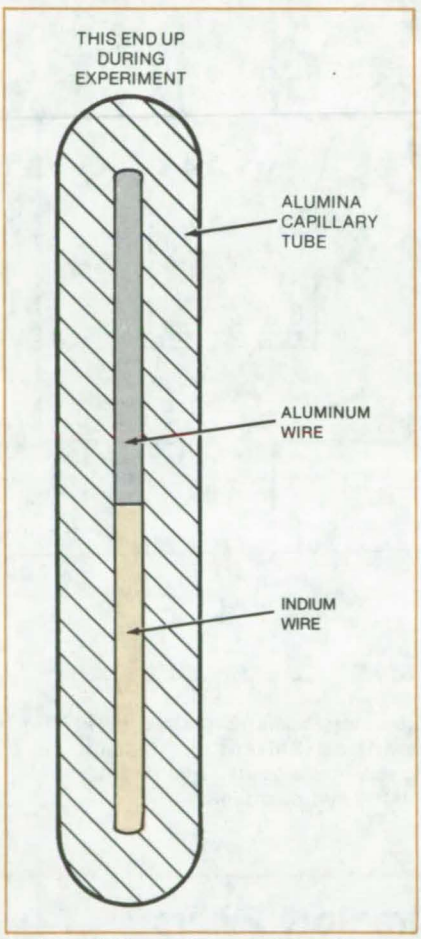


A **Liquid-Phase Binary Interdiffusion Sample** is prepared by enclosing wires of the two metals in a capillary tube with their ends touching. While the sample is at elevated temperature, the tube is kept oriented with the lighter metal at the top to prevent convection.

Some questions remain. The tube walls may affect the diffusion rates, giving rise to two-dimensional concentration profiles that are not accounted for in the method. While a capillary tube reduces convection currents, thermal gradients may still cause mixing near the interface.

The new method is a potential research tool in such areas as the zone refining of metals, the recycling of spent fuel rods, and improving the removal of slag and inclusions from steel castings. The binary systems Cu/Pb, Bi/Ga, and Te/Tl are also being studied.

*This work was done by S. H. Gelles and A. J. Markworth of Battelle Columbus Laboratories for* **Marshall Space Flight Center.** *For further information, Circle 40 on the TSP Request Cards.*

*Inquiries concerning rights for the commercial use of this invention should be addressed to the Patent Counsel, Marshall Space Flight Center [see page A5]. Refer to MFS-25576.*

# Supercritical-Fluid Extraction of Oil From Tar Sands

Low-temperature supercritical solvents reduce energy consumption and waste-disposal problems.

*NASA's Jet Propulsion Laboratory, Pasadena, California*

New supercritical solvent mixtures have been laboratory-tested for the extraction of oil from tar sands. A mixture is circulated through the sand at high pressure and at a temperature above the critical point, dissolving the organic matter into the compressed gas. The extract is recovered from the gas by depressurization. At no point in the process do liquids have to be separated from sand residues.

The Canadian method for processing tar sands from the Athabasca region begins with any of several hot-water treatments. However, this method is unsuitable for tar sands found in arid regions of the Western United States because it requires 3 to 12 parts (by volume) of water for each part of bitumen extract, and the large volume of wastewater presents a disposal problem. In addition, some U.S. tar sands are not susceptible to hot-water processing. Supercritical extraction fills the need for a more-effective solvent process without the problems associated with water consumption and disposal, high energy consumption, and the loss of solvent by absorption into the sand.

The solvent mixture has two or more components. One has low volatility and a high critical temperature and is a good solvent for the organic material in the sand. The other component has high volatility and a low critical temperature, serving mainly to lower the critical temperature of the mixture. Many combinations of common organic and inorganic liquids and gases satisfy these requirements, some with critical temperatures at or near ambient.

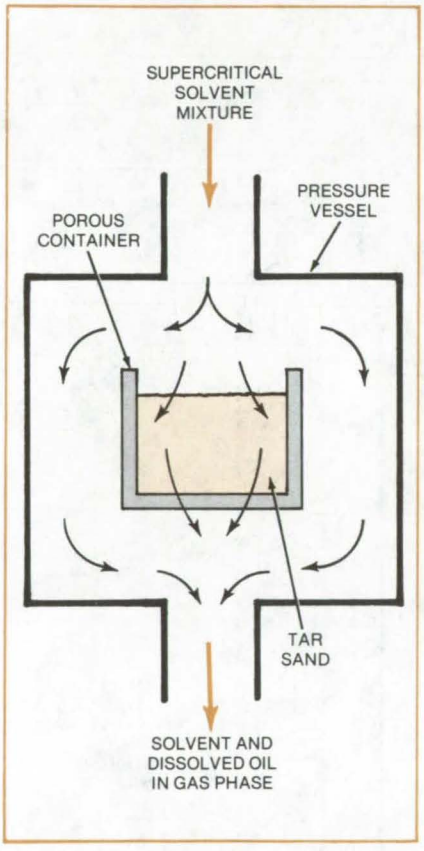


**Laboratory-Scale Experiments in Supercritical-Solvent Extraction** employed mixtures of toluene and more-volatile hydrocarbons.

Extraction occurs at or near the critical temperature. The lower operating temperatures of the mixtures result in more economical operation and in energy savings as compared to methods using one solvent and requiring higher temperatures. Because tar sands usually contain less than 10 percent of organic extract, considerable energy savings are realized if large volumes of rock do not have to be heated.

The method was tested in the laboratory with Utah tar sands. In one experiment, a solvent mixture of 75 percent by weight toluene and 25 percent methane was passed through the sand at 300°F (149° C) and 2,500 psi (1.7×107 N/m2). After 4 hours, 95 percent of the organic matter was extracted.

*This work was done by Leslie E. Compton of Caltech for* **NASA's Jet Propulsion Laboratory.** *For further information, Circle 41 on the TSP Request Card.*
*NPO-15476*

# Prolonging the Life of Refractory Fillers

A silicon carbide coating prevents embrittlement at high temperatures.

*Lyndon B. Johnson Space Center, Houston, Texas*

The useful life of a refractory glass-cloth gap filler is increased by coating it with a suspension of silicon carbide in butanol and polyethylene. The silicon carbide increases the emittance of the cloth from the 0.3-to-0.4 range to the 0.7-to-0.8 range. The coated material thus maintains a much lower temperature. For example, a cloth filler that normally operates at 2,300° F (1,260° C) operates at only 1,900° F (1,030° C) after it has been coated.

The coating is applied to the refractory-fiber cloth filler that seals the gaps between insulating tiles on the Space Shuttle orbiter. Tests showed that the cloth fibers would be embrittled by the extreme temperatures encountered on reentry into Earth's atmosphere and that only 25 percent of the thousands of fillers would be reusable after a mission. With the coating, however, 85 percent of the fillers would be reusable.

The silicon carbide/butanol/polyethylene suspension is sprayed or brushed on. The polyethylene in the butanol carrier gives the suspension sufficiently

low viscosity that the silicon carbide can penetrate the cloth fibers. The butanol evaporates after it is applied, and the polyethylene burns off when its temperature reaches approximately 1,000° F (538° C).

Many emittance-control agents and suspension agents were tried. However, only the combination of silicon carbide, butanol, and polyethylene has the required temperature resistance and flexibility.

*This work was done by Calvin Schomburg and Robert L. Dotts of* **Johnson Space Center.** *No further documentation is available.*

*Inquiries concerning rights for the commercial use of this invention should be addressed to the Patent Counsel, Johnson Space Center [see page A5]. Refer to MSC-18832.*

# Flame-Retardant Coating Is Heat-Sealed

A polyurethane-based coating makes fabrics firesafe, yet retains their flexibility.

*Lyndon B. Johnson Space Center, Houston, Texas*

A plastic coating that makes fabrics flame- and abrasion-resistant is sealed to the fabric by heat. The coating produces flexible, lightweight, impermeable fabrics that are firesafe and can withstand rough use. The coated fabric was developed for use in garments and containers for space exploration, but would also be suitable for rainwear, clothing for hazardous environments, and leakproof containers.

The coating consists of thermoplastic polyurethane combined with flame-retardant fillers: decabromodiphenyl oxide (DBO), antimony oxide (AO), and ammonium polyphosphate (AP) in various proportions (see table). Since polyurethanes are generally flammable, substantial amounts of flame-retardant additives must be blended. Weight ratios up to 70 parts retardant/30 parts polyurethane produce an ideal combination of properties. At weight ratios below 50/50, the flame resistance may be poor. At weight ratios above 70/30, the coating loses its abrasion resistance and its heat-sealing properties.

The combination of flame retardant and polyurethane yields an elastomer that can be bonded to woven or knit fabrics and bonded webs of natural or synthetic fibers, such as cotton, rayon, nylon, polyester, and polyamide. A solution of the elastomer composition is applied to a release substrate — such as silicone release paper — in an amount that yields a thin, uniform film weighing from 1 to 4 oz/yd$^2$ (34 to 135 g/m$^2$). The film is removed from the release substrate and placed on the fabric. Heat and pressure are applied to bond the film to the fabric. A bonding time of 10 seconds at 400° F and 30 lb/in.$^2$ (204° C and 207 kN/m$^2$) is sufficient to ensure a strong bond without stiffening the fabric.

| Fire-Retardant Additive | Additive/Polymer Weight Ratio | Substrate | BOI |
|---|---|---|---|
| DBO/AO | 40/60 | Nomex* | 24 |
| DBO/AO | 60/40 | Nomex | 28 |
| DBO/AO/AP | 54/46 | Nomex | 28 |
| DBO/AO/AP | 70/30 | Nomex | 32 |
| DBO/AO/AP | 70/30 | Nylon | 23 |
| DBO/AO/AP | 70/30 | Nylon (Coated Both Sides) | 29 |
| DBO/AO | 40/60 | Neoprene-Coated Nylon | 29 |
| DBO/AO/AP | 70/30 | Neoprene-Coated Nylon | 32 |

*Heat-resistant nylon; trademark of E. I. du Pont de Nemours & Co.

**The Bottom Oxygen Index (BOI) Value,** a measure of flame retardance, is high for most formulations of the new coating. The filler materials added to the polyurethane are in the ratios 3:1 for DBO/AO and 3:1:3 for DBO/AO/AP, by weight.

*This work was done by Richard P. Tschirch and Kenneth R. Sidman of Arthur D. Little, Inc., for* **Johnson Space Center.** *For further information, Circle 42 on the TSP Request Card.*

*This invention is owned by NASA, and a patent application has been filed. Inquiries concerning nonexclusive or exclusive license for its commerical development should be addressed to the Patent Counsel, Johnson Space Center [see page A5]. Refer to MSC-18382.*

# Superabsorbent Multilayer Fabric

Material contains gel-forming polymer and copolymer that absorb from 70 to 200 times their weight of liquid.

*Lyndon B. Johnson Space Center, Houston, Texas*

Solving the problem of waste disposal for astronauts has led to work on a superabsorbent multilayer fabric. The fabric contains gel-forming materials that absorb many times their weight of liquid.

The multilayer fabric can be used to make a "diaperlike" urine collection garment or a pair of shorts in which the composite is sewn into an outer layer of stretch material. Possible applications include baby diapers, female hygiene napkins, and hospital bedpads. The superabsorbent material might also have uses in moisture retainers for plants and in the improvement of dry soil.

The fabric (see figure) consists of two gel containers with sheer wicking and fibrous wicking on the side closest to the body and a liquid-impermeable, gas-permeable layer on the outside. The sheer wicking is comfortable, retains the inner layers, and permits the free flow of fluid to the interior; it can be made of natural, synthetic, or mixed fabrics. The nonwoven, cellulose fibrous wicking helps to keep the skin dry and further increases comfort.

An acrylic polymer is used in the gel container closest to the body, and a starch/acrylonitrile copolymer is used in the other. These materials absorb from 70 to 200 times their weight of liquid by trapping it in the form of a gel. A sheer web of nonwoven cellulose covers both sides of each gel container. The inner and outer cellulose layers of each container section can be bonded together to form a pouch.

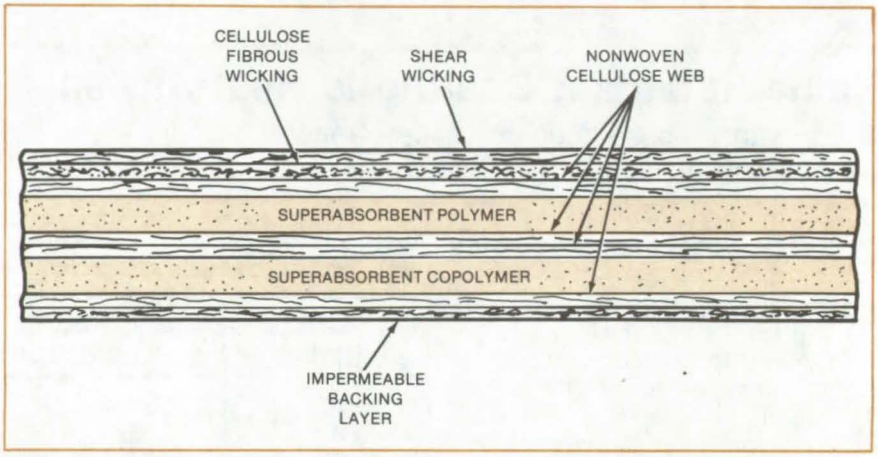


**Superabsorbent Polymer and Copolymer** form gels to bind and retain liquid in a multiply fabric. Until the reaction between the liquid and the absorbent masses forms a gel, the backing layer retains the liquids within the fabric; it also allows the material to "breathe."

Depending on the degree of absorbency desired, the amounts of polymer and copolymer can be varied. Of the two containers, the polymer container gels slower and absorbs more fluid than does the copolymer container, which gels faster to block the fluid flow rapidly and to prevent leakage.

Because the multilayer fabric mechanically and chemically binds fluids in the form of a gel, the surface in contact with the skin is comfortable and dries rapidly. Moreover, the ingredients of the fabric are nontoxic, chemically safe, and nonirritating. A fabric sample that is sized to be worn inside a space suit by female astronauts would be capable of collecting more than 1,000 $cm^3$ of fluid.

*This work was done by James V. Correale and Frederic S. Dawn of* **Johnson Space Center.** *For further information-Circle 43 on the TSP Request Card.*

*This invention is owned by NASA, and a patent application has been filed. Inquiries concerning nonexclusive or exclusive license for its commercial development should be addressed to the Patent Counsel, Johnson Space Center* [see page A5]. *Refer to MSC-18223.*

# Factors Affecting Liquid-Metal Embrittlement in C-103

New studies tie crack growth in columbium to contaminants, grain size, and stress.

*Lyndon B. Johnson Space Center, Houston, Texas*

New results of a study of weld cracks on the Space Shuttle control thrustors point toward better understanding of the cracking problem in columbium metal, which has also plagued nonaerospace users. Although liquid-metal embrittlement is known to be the cause of the problem, factors affecting the growth and severity of cracks are not well understood. the new results tie crack growth to the type of contaminants present, to grain size, and to the level of stress present while welding is done. Designers considering columbium C-103 for various critical applications would benefit by taking the new results into account.

The occurrence of liquid-metal embrittlement requires the presence of stress and liquid metal, which wets the surface of the base metal. One method for obtaining these conditions is to weld a plated, restrained sample. The

plating supplies the contaminating metal, which is liquefied by the welding heat while the weld shrinkage supplies the stress.

In the first series of tests, unconstrained samples were plated with metals commonly in contact with columbium: lead, zinc, nickel, silver, and copper. The second series tested samples of the same metals on a fixture called a "hot tear fixture," which causes a very high stress in the heat-affected zone. From the restrained tests it was found that cracking occured only when there were certain wetting metals present.

The amount of embrittlement varied among the various metals tested. The worst case was copper. The test data support the hypothesis that the embrittling metal can be deposited by vapor transport even at temperatures well below the melting point of the embrittling metal. The amount of the wetting metal can be extremely small and still cause embrittlement.

Cracking due to liquid-metal embrittlement is intergranular in most cases although portions of the cracks may be transgranular. The grain size of a single-phase material exerts a marked influence on the fracture stress during liquid-metal embrittlement. Coarser grain sizes lower the fracture strengths as do notches in the specimens.

Liquid-metal embrittlement results in either a decrease in tensile elongation prior to failure or fracture without plastic deformation at stress levels below the normal yield strength of the material. The initiation of embrittlement may be instantaneous on contact of the solid by the liquid metal, or it may be delayed until wetting of the solid material. Normally ductile materials, such as columbium, subject to tension while in contact with a liquid metal, may fracture at an abnormally low stress with little or no ductility. Unlike the initiation of fracture by corrosion, the initiation of fracture by liquid-metal embrittlement is not time dependent, and the crack continues to grow as long as the liquid is sufficient to cover part of the fracture surface and some vapor reaches the crack tip.

Three conditions were confirmed as prerequisites for the occurrence of liquid-metal embrittlement:

1. The metals do not form stable high-melting-point intermetallic compounds;
2. The metals have no significant mutual solubility; and
3. The surface of the solid metal must be wettable by the liquid metal.

This study shows that although columbium C-103 may have desirable properties from a design and performance standpoint, it is difficult to fabricate and process where a combination of high temperatures and contaminating metals is found.

*This work was done by Robert McLemore and Francis K. Lampson of The Marquardt Co. for* **Johnson Space Center.** *No further documentation is available.*
*MSC-18865*

# Books and Reports

These reports, studies, and handbooks are available from NASA as Technical Support Packages (TSP's) when a Request Card number is cited; otherwise they are available from the National Technical Information Service.

## Ultraviolet-Induced Mirror Degradation

Ultraviolet radiation attacks the backing paint and sealant.

Recent tests of second-surface mirrors show that ultraviolet radiation penetrates the glass and metalized zone and impinges upon the backing paint. According to a recent report, many of the backing materials are degraded by ultraviolet radiation. Mirror corrosion is a serious problem in solar-energy collection systems. However, because glass is an absorber of ultraviolet (UV) radiation, the role of UV in back-surface corrosion of mirrors was not previously considered to be important.

Samples of second-surface glass mirrors without any backing paint were obtained from several industrial sources. The silver metalization on these mirrors ranged from 70 to 120 mg/ft$^2$ (750 to 1,300 mg/m$^2$), and the copper overlay varied from 15 to 30 mg/ft$^2$ (160 to 320 mg/m$^2$). The near-ultraviolet transmission was measured as a function of wavelength through parts of the mirrors.

The tests showed that the UV penetrates the glass, silver, and copper, with transmission peaks at wavelengths between 326 and 340 nanometers. Thus the UV reaches the backing paint.

The effects of UV on polymeric materials have been studied, and in general all are degraded by UV. The fluorocarbons, polycarbonates, and polyesters are very sensitive. Decomposition products from organic polymers emit corrosive elements that attack silver. Gaseous chlorine is an especially aggressive corrosion agent for silver. The polymers most resistant to ultraviolet radiation are the polyimides.

*This work was done by Frank L. Bouquet, Takashi T. Hasegawa, and Edward L. Cleland of Caltech for* **NASA's Jet Propulsion Laboratory.** *To obtain a copy of the report, Circle 44 on the TSP Request Card.*
*NPO-15520*

## Low-Gravity Investigations in Cast-Iron Processing

Proposed experiments would examine the effects of processing materials in space.

A report on the state of the art in cast-iron processing identifies possible improvements that might result from processing in the absence of gravity. The report suggests areas in which the knowledge of gravitational effects could eventually lead to practical improvements in material performance.

Cast irons have great commercial appeal: They can be readily cast into intricate shapes, are relatively inexpensive, and are usually made from scrap. If certain physical properties, particularly

(continued on next page)

ductility and tensile strength, could be improved, usage could be expanded.

Cast irons are especially suited for investigations of melting behavior and solidification mechanisms in a low-gravity environment because they are complex alloys with melt constituents that have widely varying densities. These constituents are therefore susceptible to gravitationally induced segregation, thermal effects, and specific solidification mechanisms. Thus, iron castings normally have heterogeneities in chemical composition and phase constituents that contribute to nonuniformities in mechanical properties and to low property values.

Low-gravity processing offers an opportunity for better understanding of solidification behavior by eliminating gravitationally-caused material gradients in the melt. Also, containerless processing becomes possible, thus facilitating observation of the process and eliminating the influences of the container walls on nucleation and growth during solidification.

Other problem areas that would benefit from low-gravity studies include:

- The formation of chemical phase constituents that are not adequately described by simple phase diagrams;
- The formation of the stable graphite phase and the influence of composition thereon;
- Chemical heterogeneities within individual phase constituents and in interdistribution of the constituents;
- The effects of cooling rates, chemical and density differences, and externally applied influences upon nucleation and growth mechanisms in solidification; and
- The effects of gravity and container surfaces on macrochemical heterogeneity and upon sizes and distribution of the microphases.

Applications to commercial processing are not expected to result immediately from low-gravity experiments. The major immediate benefit would be a better understanding of the effects of processing variations upon final material properties. Once the effects of gravity are isolated, process improvements in both gravitational and nongravitational environments would be expected to follow.

*This work was done by William L. Frankhouser of System Planning Corp. for* **Marshall Space Flight Center.** *To obtain a copy of the report, Circle 45 on the TSP Request Card.*
*MFS-25491*

## "SiAlON" Materials for Advanced Structural Applications

New ceramics for gas turbines and other applications are strong, oxidation resistant, and chemically stable.

One group of advanced ceramic materials that are of interest for a variety of high-temperature structural applications is silicon compounds, such as silicon nitride ($Si_3N_4$) and silicon carbide (SiC). SiAlON is a new group of silicon compounds containing the elements Si, Al, O, and N as major constituents in the form of a solid solution. Most frequently, the term SiAlON refers to the $\beta$-$Si_3N_4$ solid solution called $\beta$-SiAlON. $\beta$-SiAlON has been of great interest because of its low thermal expansion, good high-temperature molulus of rupture, and good oxidation resistance. Furthermore, SiAlON materials can be fabricated by pressureless sintering to high density and thereby have the potential for providing low-cost net-shape components of intricate geometry without expensive machining.

$Si_3N_4$ and SiC ceramics have potential for use in aircraft and automobile engines and in electric-power generating systems. These ceramics combine high thermal conductivity and low coefficients of thermal expansion and consequently have high thermal-shock resistance. They also have low densities and possess excellent mechanical strength at room and high temperatures. Concurrent with the recent efforts in developing $Si_3N_4$ and SiC for structural components of high-temperature heat engines, SiAlon ceramics have become candidates for consideration.

A state-of-the-art report on SiAlON materials has recently been prepared. The report includes work on phase relations, crystal structure, synthesis, fabrication, microstructure, and properties of various SiAlON's. The essential features of compositions, fabrication methods, and microstructure are reviewed. High-temperature flexure strength, creep, fracture toughness, oxidation, and thermal-shock resistance are discussed. These data are compared to those of some currently-produced silicon nitride ceramics. This report describes key advances made in the past several years and lists 41 references published from 1971 to 1979.

*This work was done by Sunil Dutta of* **Lewis Research Center.** *Further information may be found in NASA TM-79207 [N79-30378/NSP], "State-of-the-Art of SiAlON Materials" [$5]. A copy may be purchased [prepayment required] from the National Technical Information Service, Springfield, Virginia 22161.*
*LEW-13671*

# Life Sciences

# Improved Electrophoresis Cell

Several modifications would increase resolution and throughput.

*Marshall Space Flight Center, Alabama*

Several proposed modifications are expected to improve the performance of a continuous-flow electrophoresis cell. The changes would allow better control of buffer flow and would increase resolution by suppressing thermal gradients.

The improved cell is shown in the figure. The buffer inflow is straightened and smoothed by an array of small-bore flow-conditioner tubes. Convection currents caused by joule heating in the separation chamber are suppressed by circulating a cooling fluid through passages in the casing.

The sample (usually a mixture of biological cells in a weak electrolyte or buffer) is introduced through a narrow quartz tube that extends below the flow-conditioner array, so as to disturb minimally the buffer flow. Under the action of the electric field in the separation chamber, the sample is fractionated into separate streams of particles. Upon reaching the collection chamber, each fraction ideally enters two separate partitions in the partition array. The buffer flow rate in the collection chamber is much less than that in the separation chamber, thus allowing time for the particles to sediment out of the flow and onto the bottom of the collection tray, while the buffer flows out through the exit port.

The electric field is provided by four electrodes, each of which is surrounded by a membrane that permits electrical current, but not fluid, to flow across it. Rinse buffer flows through the electrode chamber to remove gas bubbles and electrolysis products. Current flows from the electrode, through the membrane, into the interconnecting channel, and then into the separation chamber. The isolation of the electrode chambers from the buffer curtain reduces convection caused by variable flow properties near the electrodes.

The resolution of the separation depends directly on the width of the sample. Hollow quartz optical fibers with bores as small as 0.05 mm serve as insertion tubes. The quartz also permits ultraviolet radiation to be used in counting the cells.

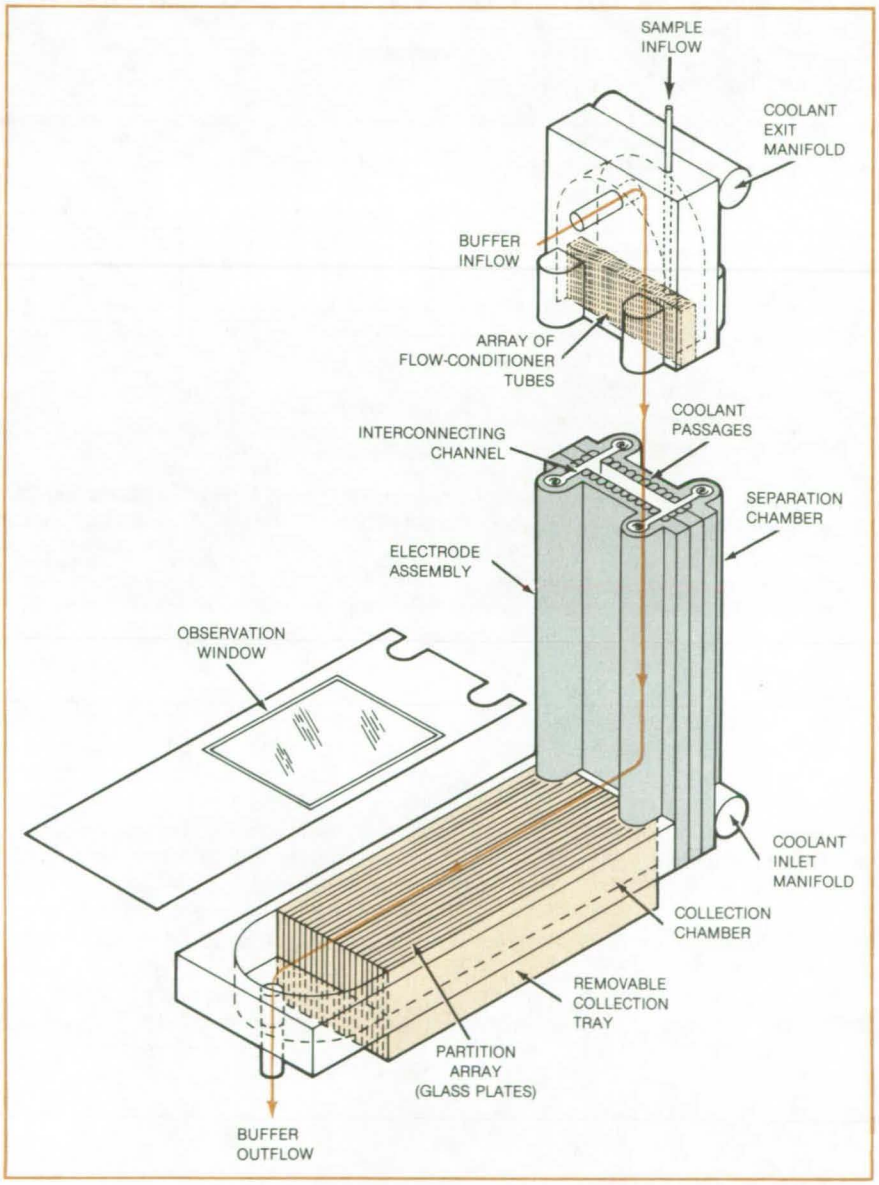


This **Improved Electrophoresis Device** would have high resolution and be easy to operate. The improvements would allow better flow control and heat dissipation.

Other advantages of the proposed system are:

- The use of cooling permits higher power levels than are possible in conventional systems;
- High-thermal-conductivity walls permit manipulation of the axial thermal gradient through external cooling;
- The fractionation of the sample can be observed through the collection-chamber window;
- Separation is not degraded because large pressure drops do not occur in the partition array;
- The collection of sample sediment only reduces the quantity of buffer needed and makes buffer recycling possible; and

(continued on next page)

• With proper selection of materials for construction, the entire assembly can be conveniently sterilized with high-pressure steam.

*This work was done by Percy H. Rhodes and Robert S. Snyder of* **Marshall Space Flight Center.** *For further information, Circle 46 on the TSP Request Card.*

*This invention is owned by NASA, and a patent application has been filed. Inquiries concerning nonexclusive or exclusive license for its commercial development should be addressed to the Patent Counsel, Marshall Space Flight Center [see page A5]. Refer to MFS-25426.*

# Speedy Acquisition of Surface-Contamination Samples

## Fast, accurate, wipe-and-rinse method uses a polyester bonded cloth.

*NASA's Jet Propulsion Laboratory, Pasadena, California*

Biological contamination of large-area surfaces can be determined quickly, inexpensively, and accurately with the aid of a polyester bonded cloth (Texwipe PBC TX409, or equivalent). The cloth is highly effective in removing microbes from a surface and releasing them for biological assay.

In comparisons with cotton swabs, a standard medium for sample collection, polyester bonded cloth was found to remove more than 97 percent of surface contamination and to release more than 90 percent of the contamination collected (see table). In contrast, cotton swabs removed slightly more than 89 percent of the contamination and released only about 75 percent.

| Contamination Collector | Total No. of Samples | Removal (%) | Recovery (%) | Coefficient[a] of Variation (%) |
|---|---|---|---|---|
| Polyester Bonded Cloth | 12 | 97.2 | 90.4 | 15.9 |
| Cellulose Cloth | 12 | 97.5 | 72.0 | 47.6 |
| Cotton Swab | 64 | 89.6 | 75.2 | 12.3 |

[a]For Recovery

**A Comparison of Removal and Recovery Values** for three types of contamination collectors shows the higher efficiency of the polyester bonded cloth.

Moreover, polyester bonded cloth can sample a far greater area than a cotton swab in far less time. For example, a bioassay of a 1,000-in.$^2$ (6,450 cm2) area requires 250 cotton swabs. The same area can be assayed with a single polyester bonded cloth. An experienced bioassay team requires 2 minutes per cotton swab to collect a sample from an area of only 4 in.2 (26 cm2). During the same time, the team can sample an area of at least 1,147 in.2 (0.74 m2) with a polyester bonded cloth.

The cloth, which measures 23 by 23 cm, is prepared by sterilizing it in an autoclave. Then, folded in quarters, it is moistened with 5 ml of sterile water. To collect a microbe sample, the user wipes the entire surface, using a reciprocal motion and constant, steady pressure. The cloth is then refolded so that the contaminated part is inside, and the surface is wiped again, in a direction perpendicular to the first wipe. After one more folding and perpendicular wipe, the user puts the cloth in a dry, sterile glass container.

The cloth should be moved to the laboratory and processed within an hour. A buffered rinse solution is added to the container, and it is placed in an ultrasonic bath at 25 kHz for 2 minutes. The cloth is stirred briefly and removed. The buffered solution is plated with the appropriate bacteriological medium on agar culture plates, which are incubated at 32° C aerobically. After 72 hours, a colony count is made of the culture plates.

In releasing contaminants, the polyester bonded cloth was found to be superior to other commercial clean-room cloths, including spun-bound polyamid cloths and cellulose cloths. Although the cloth-wiping method was originally developed for the Space Shuttle and other spacecraft, its speed and efficiency make it suitable for other applications of environmental microbiology.

*This work was done by John R. Puleo and Larry E. Kirschner of Caltech for* **NASA's Jet Propulsion Laboratory.** *For further information, Circle 47 on the TSP Request Card.*
*NPO-14934*

### *Laser/Heterodyne Measurement of Temperature and Salinity*

A proposed visible-light laser/heterodyne receiver would remotely measure the temperature and salinity of subsurface water. Since these qualities greatly affect aquatic life, the receiver would be useful in environmental monitoring. Its operation is based on acoustic/optical scattering of light.
(See page 181.)

### *Lightweight Face Mask*

New face masks protect epileptic and cerebral palsy patients during seizures. The lightweight masks, which weigh as little as 136 grams, are fabricated of fiberglass, a fiber, and thermosetting epoxy resin. Configurations could be designed for other applications.
(See page 220.)

### *Superabsorbent Multilayer Fabric*

High moisture retention is the key quality in a multilayer fabric that can be used in baby diapers, feminine hygiene napkins, and hospital bedpads, as well as in moisture retainers for plants. The fabric includes two gel containers, one holding a polymer and the other a copolymer, that can absorb 70 to 200 times their weight of liquid.
(See page 168.)

# Retractor Tool for Brain Surgery

Concentric sleeves are successively inserted into an expandable tube.

*Marshall Space Flight Center, Alabama*

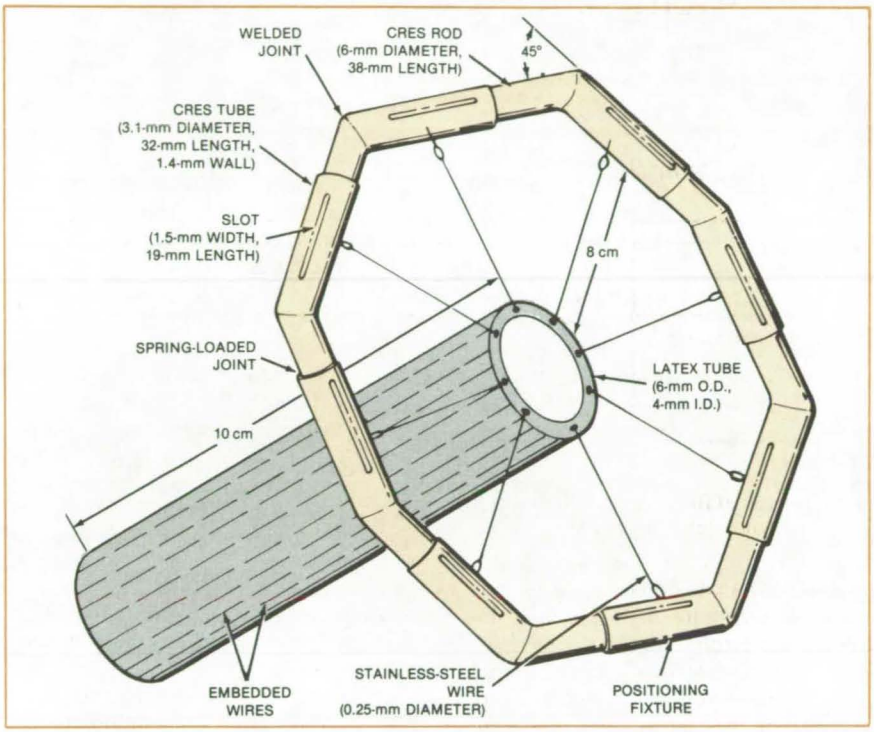


Figure 1. The **Proposed Brain-Surgery Tool** has an octagonal fixture for positioning a latex tube over an incision. Eight stainless-steel wires embedded in the latex extend to hold the positioning fixture. Another eight are also embedded in the latex.

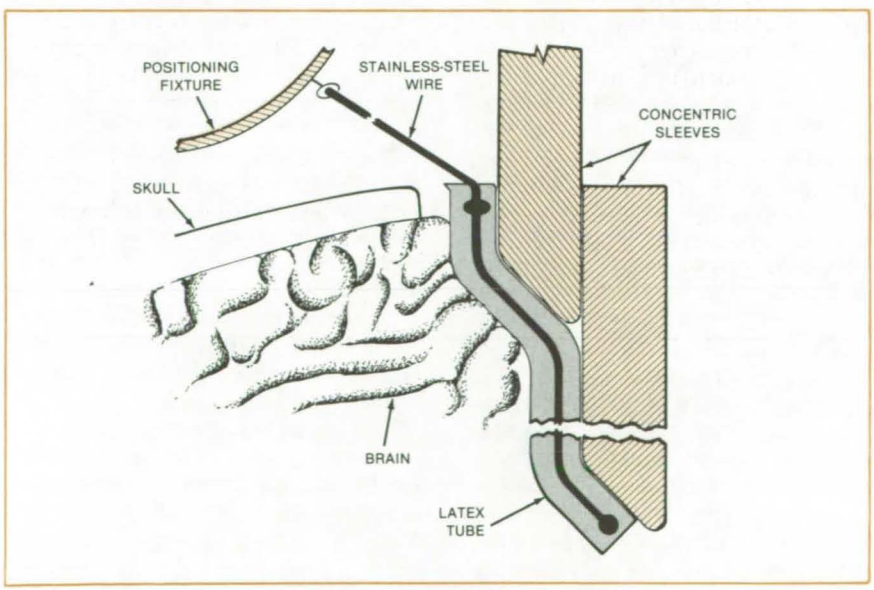


Figure 2. **Concentric Sleeves** are successively inserted into the expandable latex tube. The first sleeve is placed over a solid rod (not shown). The last sleeve is a stainless-steel tube 1 inch in diameter. It is overcoated with Teflon (or equivalent) material.

The proposed tool shown here would make a temporary opening, or tunnel, through the brain. Successive concentric sleeves are inserted to create the tunnel through which surgery is performed.

As seen in Figure 1, an octagonal positioning fixture is attached to a latex tube by stainless-steel wires. Natural latex is used because it expands up to 700 percent. For this application, the latex is made unidirectional by embedded longitudinal stainless-steel wires. The wires also help the successive sleeves (made of Teflon, or equivalent, material) slide into the latex tube.

To use the tool, a solid rod is first inserted into the latex tube. The rod, tube, and positioning fixture are then placed over an incision in the region in which surgery is to be performed. The first sleeve is then inserted around the rod, and the rod is removed. Then the next larger sleeve is inserted around the first one, which is also removed. This step is repeated for the remaining, successively larger sleeves, as shown in Figure 2. The largest sleeve, through which the surgery will be performed, is a stainless-steel tube 25 millimeters (1 inch) in diameter with a 0.5-millimeter wall. Its outer surface is coated with Teflon material.

The removal sequence is the reverse of the installation sequence. The expansion of the latex tube is stepped down, removing the pressure on the brain before the tube is slid over brain tissue. The rod is also removed before the latex tube is removed.

*This work was done by Ray Helms and Terry Hayes of* **Marshall Space Flight Center.** *No further documentation is available.*

*Inquiries concerning rights for the commercial use of this invention should be addressed to the Patent Counsel, Marshall Space Flight Center [see page A5]. Refer to MFS-25380.*

# Improved Method for Culturing Guinea-Pig Macrophage Cells

Proper nutrients and periodic changes in the culture medium maintain cell viability for a longer period.

*Marshall Space Flight Center, Alabama*

By adding proper nutrients and by changing the cultivation medium periodically, the viability of guinea-pig macrophage cells being cultivated can be maintained at almost 100 percent for over 2 weeks. The new method uses a thioglycolate solution, instead of mineral oil, to induce the macrophage cells in guinea pigs and also uses an increased percent of fetal-calf bovine serum in the cultivation medium. Previously, the best cell viability that could be obtained by other methods was 30 to 40 percent.

Macrophage cells play significant roles in the body's healing and defense systems. The electrophoretic mobility of macrophage cells obtained from human subjects containing tumors is slower than that of normal human macrophage cells. Though originally investigated for use in electrophoretic experiments in space, where macrophage cells would need to be kept viable for a month, the new cultivation method may increase the utility of the cells for indicating cancer.

Normally, an injection of 20 ml of sterile, warm, light, mineral oil, or 20 ml of a 4-percent thioglycolate solution, in the peritoneal tissue of guinea pigs induces the production of macrophage cells. Mineral oil, however, is slightly toxic on macrophage cells, which engulf it, and inhibits their development. By using thioglycolate instead of mineral oil, these cells can metabolize the thioglycolate and utilize it as a carbon and sulfur source. Also, thioglycolate lowers the redox potential in the medium so that it is more favorable for the growth of the cells.

The culture, in the new method, contains 20 percent fetal-calf serum instead of the conventionally-recommended 7 percent; and fresh medium is added every 12 hours. The increase in cell viability attributable to the increase in fetal-calf serum content to 20 percent may be due to the increase in the binding of cell surfaces, and an increase in phagocytosis. Also, periodically changing the cultivation medium keeps its pH relatively constant at about 7.2 by removing accumulated organic acids and other toxic cellular products. In a batch culture process, the pH changes from 7.2 to 6.2 in 3 days, and the cell viability is reduced 94 percent.

The cell viabilities are determined by adding 1 ml of cell suspension to 0.1 ml of trypan blue dye. Viable cells exclude the dye, and a percentage of viable cells is obtained from the ratio of nonstained cells to total cells.

*This work was done by Jacob Savage of Alabama A&M University for* **Marshall Space Flight Center.** *Further information may be found in NASA CR-158777 [N79-27814/NSP], "Preparation of Guinea Pig Macrophage for Electrophoretic Experiments in Space, Final Report" [$6.50]. A paper copy may be purchased [prepayment required] from the National Technical Information Service, Springfield, Virginia 22161. The report is also available on microfiche at no charge. To obtain a microfiche copy, Circle 48 on the TSP Request Card.*
*MFS-25307*

# Books and Reports

These reports, studies, and handbooks are available from NASA as Technical Support Packages (TSP's) when a Request Card number is cited; otherwise they are available from the National Technical Information Service.

## Aerial Infrared Photos for Citrus Growers

Handbook advises on benefits and methods.

Managers, owners, and caretakers of citrus groves can obtain important benefits from aerial photography with color infrared film, according to a recently issued handbook. The colors and patterns in IR photographs of groves furnish an accurate record of the numbers of trees in production, trees of different sizes, healthy trees, replacement trees needed for next year, replacement trees needed 2 years from date of photograph, missing trees, and dead trees. In addition, the photographs help growers to locate such problems as wet and dry areas, weeds, grassy areas, noxious trees, nematode-damaged areas, malfunctioning sprinklers, and broken irrigation ditches and pipes.

Addressed primarily to commercial growers of citrus fruits in Florida and oriented to the climate, soil, geography, and practices in that state, the handbook is illustrated with many sample color infrared photographs. It tells how to plan a photographic mission, covering such topics as flight route, the overlap of successive frames, estimating the number of frames, light limitations, and the scale of photography.

The interpretation of photographs is discussed in detail. The necessary equipment for interpretation is described — light table, magnifying lenses, and microfiche viewers, for example. Advice is given on rating tree condition; identifying the effects of diseases, insects, and nematodes; and evaluating the effects of soil, water, and weather.

An appendix gives information on the history, theory, and practice of aerial color infrared photography. A glossary defines technical terms.

*This work was done by Carlos H. Blazquez and Frank W. Horn, Jr., of* **Kennedy Space Center.** *Further information may be found in NASA RP-1067 [N81-21437/NSP], "Aerial Color Infrared Photography: Applications in Citriculture" [$9.50]. A copy may be purchased [prepayment required] from the National Technical Information Service, Springfield, Virginia 22161.*
*KSC-11209*

# Mechanics

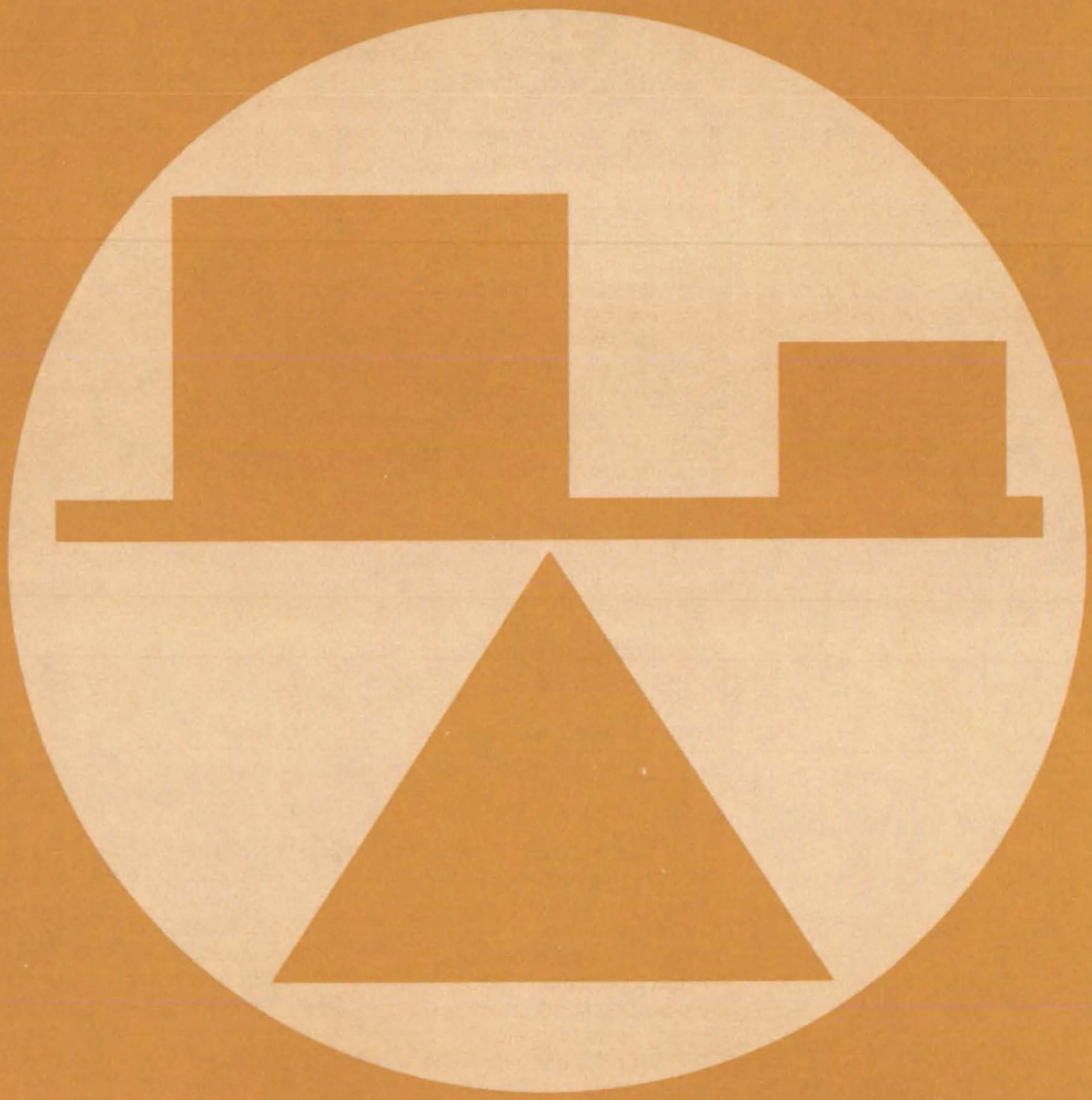

## Hardware, Techniques, and Processes



## Books and Reports



## Computer Programs

# Flight-Management Algorithm for Fuel-Conservative Descents

Increased fuel savings result from improved accuracy in profile descent.

*Langley Research Center, Hampton, Virginia*

Rising fuel costs combined with other economic pressures require more-efficient air traffic control and aircraft operations. The Federal Aviation Administration has developed an automated time-based metering form of air traffic control for arrivals into the terminal area called local flow management/profile descent (LFM/PD). LFM/PD saves fuel by matching the airplane arrival flow to the airport acceptance rate through time-control computations and by allowing the pilot to descend at his discretion from cruise altitude to the metering fix in an idle-thrust, clean configuration (landing gear up, flaps zero, speed brakes retracted).

Substantial fuel savings have resulted from LFM/PD, but air traffic control workload is high since the radar controller maintains time management for each airplane through either speed control or path stretching with radar vectors. Pilot workload is also high since the pilot must plan for an idle-thrust descent to the metering fix using various "rules of thumb".

NASA has flight-tested in its Terminal Configured Vehicle Boeing 737 research airplane a new flight-management descent algorithm designed to increase fuel savings. The algorithm reduces the time dispersion of airplanes crossing the metering fix at the time designated by Air Traffic Control by transferring the responsibility of time navigation from the radar controller to the flightcrew. A three-dimensional path with terminal time constraints (four-dimensional) is determined by the algorithm for an airplane to make an idle-thrust, clean-configured descent to arrive at the metering fix at a predetermined time, altitude, and airspeed. The descent path is calculated using linear approximations of airplane performance accounting for gross weight, wind, and nonstandard pressure and temperature effects. The algorithm is applicable to both an integrated flight-management system with continuous flight guidance and to a hand-held calculator using conventional cockpit instrumentation.

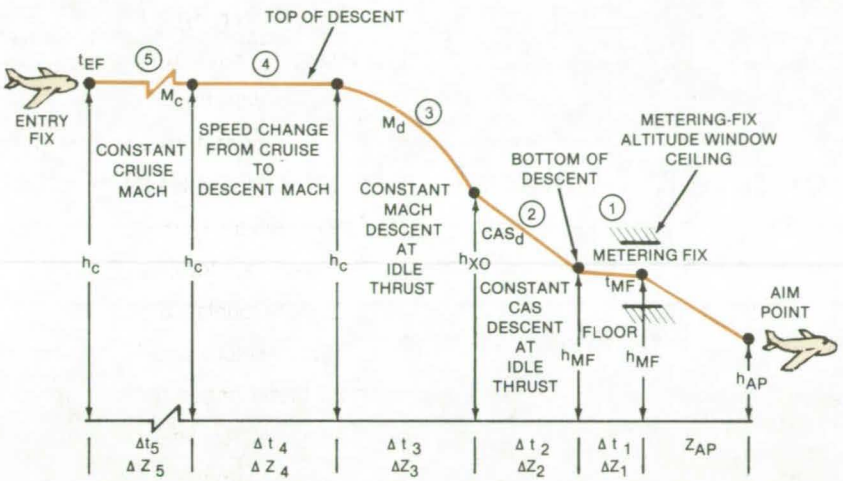


CAS = calibrated airspeed, kn

$CAS_d$ = calibrated descent airspeed, kn

$h_{AP}$ = altitude at aim point, m

$h_c$ = altitude at cruise, m

$h_{MF}$ = altitude at metering fix, m

$h_{XO}$ = altitude at transition from constant mach descent to constant airspeed descent, m

$Z_{AP}$ = distance between metering fix and aim point, nmi

$M_c$ = mach number at cruise

$M_d$ = mach number in descent

t = time, s

$t_{EF}$ = time assigned to cross entry fix, h:min:s

$t_{MF}$ = time assigned to cross metering fix, h:min:s

**LFM/PD Vertical Plane Geometry** is shown for path between entry fix and aim point.

As shown in the diagram, each path segment from the entry fix to the metering fix is numbered according to the order in which it is calculated by the algorithm. To ensure compatibility with standard airline operating practices, the path is calculated based on the descent being flown at a constant mach number with transition to a constant calibrated airspeed and with speed changes being flown at constant altitude

Segment 5 begins at the entry fix and is flown at a constant cruise altitude and a constant cruise mach number. Segment 4 is a relatively short path segment in which the speed of the airplane may be changed from the cruise mach number $M_c$ to the descent mach number $M_d$. Segment 4 is eliminated if the descent and cruise mach numbers are the same.

The descent to the metering-fix altitude is accomplished along the next two path segments, segments 3 and 2. Segment 3 is flown at a constant mach number. As altitude is decreased along this path segment, the calibrated airspeed increases. The desired descent calibrated airspeed is obtained at the beginning of segment 2. The descent is continued along this path segment at a constant calibrated airspeed.

When the metering-fix altitude is obtained, the airplane is flown at a constant altitude along segment 1 and slowed from descent airspeed to the designated metering-fix calibrated airspeed. This path segment is eliminated if the descent and metering-

(continued on next page)

fix airspeeds are the same. After passing the metering fix, the airplane is flown directly to the aim point.

Flight test data were obtained on 19 flight test runs to the metering fix. The standard deviation of metering-fix arrival-time error was 12 seconds with no arrival-time error greater than 29 seconds. Comparable statistics for time error accumulated between the top of descent and the metering fix, a distance of approximately 40 nautical miles (75 kilometers), are a standard deviation of 6.9 seconds with no error greater than 15 seconds. The calibrated airspeed and altitude errors at the metering fix indicated standard deviations of 6.5 knots and 23.7 meters (77.8 feet), respectively, and the maximum errors were less than 12.9 knots (6.6 m/s) and 51.5 meters (169 feet).

*This work was done by Charles E. Knox of* **Langley Research Center** *and Dennis G. Cannon of Boeing Commercial Airplane Co. Further information may be found in NASA TP-1717 [N80-33404/NSP], "Development and Test Results of a Flight Management Algorithm for Fuel-Conservative Descents in a Time-Based Metered Traffic Environment" [$6.50].A copy may be purchased [prepayment required] from the National Technical Information Service, Springfield, Virginia 22161.*

*LAR-12814*

# Moisture in Composites Is Measured by Positron Lifetime

## Moisture content and depth distribution would be measured simultaneously.

*Langley Research Center, Hampton, Virginia*

A new technique is expected to measure the moisture content and moisture depth distribution in fiber-reinforced polymeric composites. The technique is based on the dependence of positron lifetime on the moisture content of the composite specimen.

Previous techniques for nondestructive measurement of moisture degradation in composites include ultrasonic methods, nuclear-magnetic-resonance pulse-relaxation spectroscopy, and microwave techniques. However, none of these techniques measures moisture content and depth distribution simultaneously.

The low density and high strength of fiber-reinforced polymeric composites make them attractive for lightweight structures in aerospace and nonaerospace applications. However, the composites pick up moisture when exposed to hot, moist environments for extended periods. The moisture degrades the mechanical properties of the materials. Water vapor migrates along the fiber/matrix interface, weakening the fiber/matrix bond. Water also diffuses through the polymeric matrix and degrades the matrix-dominated properties of the composite materials. Furthermore, the daily absorption/desorption cycles experienced by the polymeric composites in service cause cyclic stresses in the outer layers and produce fatigue damage.

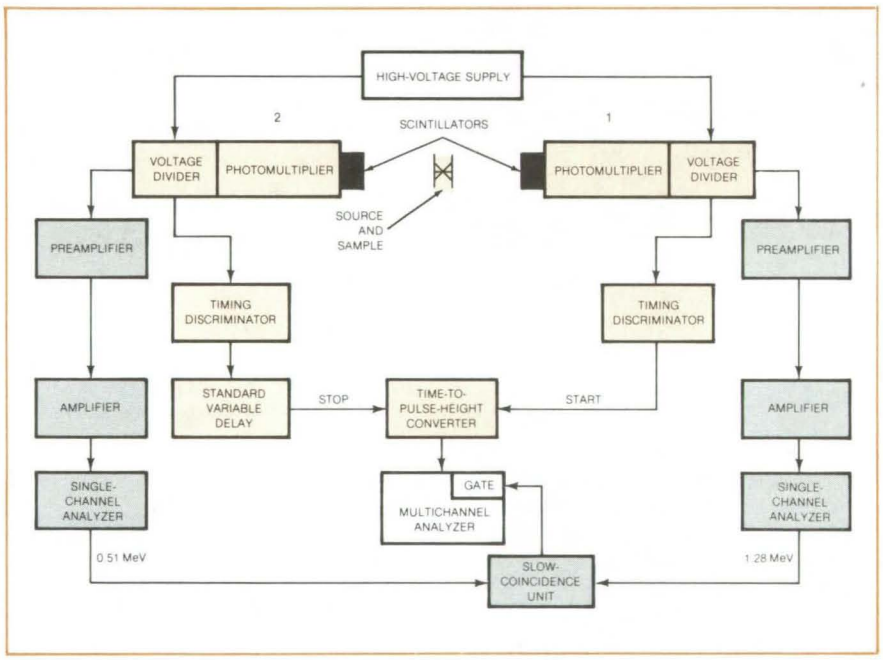


Figure 1. **Fast/Slow-Coincidence Circuit** is used in positron lifetime measurement of moisture in composite materials.

Most positron lifetime studies make use of positron radioactive sources, which emit a gamma ray when the positron is produced. The instant of gamma-ray emission provides a "reference" time for the positron lifetime measurement. The time delay between the detection of the reference gamma ray in detector 1 at time $t_1$ and the positron-annihilation photon in detector 2 at time $t_2$ is a measure of the positron lifetime in the medium where the positrons annihilate.

Figure 1 is a schematic diagram of the fast/slow-coincidence system for positron lifetime measurement. The fast "timing" channels include timing discriminators and a time-to-pulse-height converter that produces signals with an amplitude proportional to the time interval $(t_2 - t_1)$ between the detection of the two events in detectors 1 and 2. The

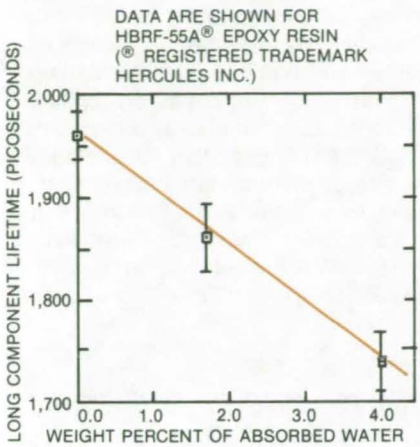


Figure 2. The **Effect of Moisture on Positron Lifetime** is shown for one composite-material epoxy resin.

slow "energy" discriminating channels provide further identification of the pair of events between which the time interval is being measured. The lifetime spectrum consists of the number of events as a function of the time delay between their arrival at the respective detectors.

A typical positron lifetime experiment with a 10-$\mu$Ci $Na^{22}$ source required about 24 hours for a lifetime-measurement statistical accuracy of $\leq$1.5 percent. Lifetime measurements were made on dry, partially-saturated (approximately-uniform), and fully-saturated test specimens.

The results of moisture-induced reduction in long component lifetime for a typical sample are shown in Figure 2. They indicate that positron lifetime in resins and fiber-reinforced resin-matrix composites is a linearly decreasing function of the moisture content of the specimen, being minimum at the saturation moisture level. Thus, for uniformly distributed moisture in the specimen, radioactive-source-derived continuous-energy positrons can measure the fractional moisture content nondestructively.

For specimens having nonuniform moisture distribution, it would be necessary to use magnetically-analyzed positron beams to define the location where the positrons come to rest in order to measure the fractional moisture content there. By using continuously-tunable-energy monoenergetic positron beams, it should be possible to map the moisture depth distribution in the test specimen. Thus, the positron lifetime technique appears to be a viable method for nondestructively measuring the moisture content and, potentially, for measuring the moisture depth distribution in polymeric substances.

*This work was done by Jag J. Singh of* **Langley Research Center** *and William H. Holt and Willis Mock, Jr., of the Naval Surface Weapons Center. Further information may be found in NASA TP-1681 [N80-27428/NSP], "Moisture Determination in Composite Materials Using Positron Lifetime Technique" [$5]. A copy may be purchased [prepayment required] from the National Technical Information Service, Springfield, Virginia 22161.*

*LAR-12776*

# Laser/Heterodyne Measurement of Temperature and Salinity

Remote-sensing technique separates the effects of water temperature and salinity.

*Langley Research Center, Hampton, Virginia*

A proposed visible-light laser/heterodyne receiver would remotely measure the temperature and salinity of subsurface water. Its operation is based on the acoustic/optical scattering of light by sound waves.

The thermal motion of water molecules gives rise to high-frequency sound waves, which interact with light through the mechanism of Brillouin scattering. Monochromatic laser light scattered by the water undergoes a frequency shift proportional to the temperature and salinity of the scattering volume. The frequency shifts are in the megahertz-to-gigahertz range and fall within the response bandwidth of heterodyne receivers.

As shown in the figure, light scattered by the water is combined with the incident laser light through beam-splitting optics, and the combination is

(continued on next page)

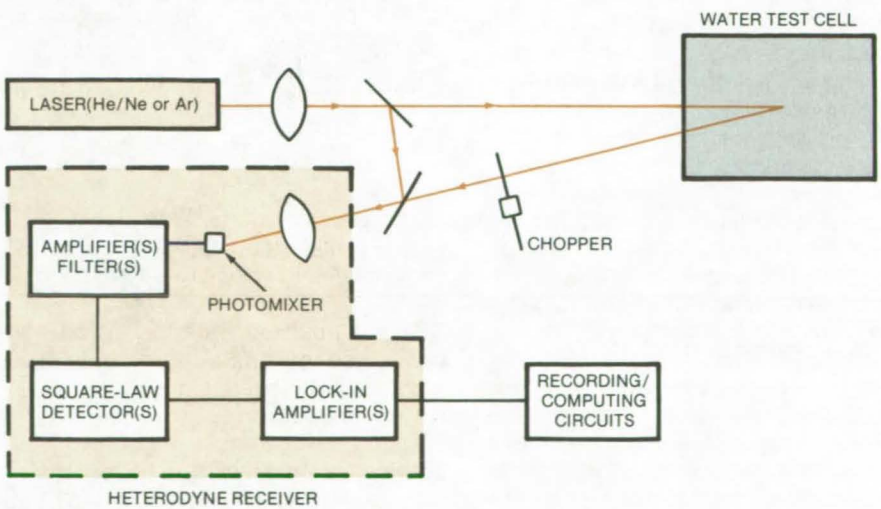


The **Laser/Heterodyne Experimental Setup** would measure the frequency shift and spectral line width of light scattered from the test volume. Water salinity and temperature are determined from these parameters.

incident on a photomixer. The photomixer signals are processed through amplifier/filter/square-law detector circuitry and fed to a recorder that displays an intensity-vs.-frequency graph. This graph is the spectrum of the Brillouin scattering. The frequency shift and spectral line width indicate the temperature and salinity of the water.

The new technique departs from earlier techniques in that it is based on Brillouin scattering alone and uses a measurement of the line width of the Brillouin line in addition to the amount of frequency shift of the Brillouin line unambiguously to separate temperature and salinity effects. The high spectral resolution required for the frequency shift and line width measurements is best obtained by using heterodyne technology. The spatial resolution and depth information on salinity and temperature obtained by optical heterodyne detection are potentially superior to those obtained by current remote-sensing techniques. These improvements are inherent to the wavelength of visible light and the heterodyne measurement process, where angular fields of view are set by the coherence property of light.

Application of this concept is foreseen in current research on energy conversion from ocean currents produced by thermal gradients and on future marine remote-sensing programs. The concept is also applicable to environmental monitoring systems, since water temperature and salinity greatly affect aquatic life.

*This work was done by Daniel J. Jobson, Carl L. Fales, and Stephen J. Katzberg of* **Langley Research Center.** *For further information, Circle 49 on the TSP Request Card.*

*Inquiries concerning rights for the commercial use of this invention should be addressed to the Patent Counsel, Langley Research Center [see page A5]. Refer to LAR-12766.*

# Wingtip-Vortex Turbine Lowers Aircraft Drag

A turbine captures some of the energy lost in aircraft wingtip vortexes.

*Langley Research Center, Hampton, Virginia*

The wingtip vortex causes roughly 40 percent of aircraft drag at cruise speed. A byproduct of lift, vortex flow influences the downwash field of the wing, resulting in substantial energy losses.

Previous attempts to recover energy from the vortex and to reduce drag include the wingtip end plate, wingtip-mounted fan-jet engines, and the winglet. To this list is now added a new device, the wingtip-vortex turbine, which is expected to be even more effective in minimizing vortex-induced energy losses.

The wingtip-vortex turbine (see figure) operates in the crossflow of the lift-induced vortex; i.e., flow not parallel to the flightpath. Each turbine blade generates a force as a result of the angle of attack between the blade and nonstreamwise local flow. Due to the unique crossflow of the vortex, each blade remains at a constant angle of attack, assuring a constant loading. The lift force produced by the turbine blades is converted to rotational energy, which can relieve the main propulsion system of such tasks as lighting and air-conditioning. The turbine could power boundary-layer control systems or the proposed all-electric aircraft control system. Also, in the process of extracting energy from the vortex, there is a reduction in induced drag of the aircraft because of the degradation of the vortex by the vortex turbine.

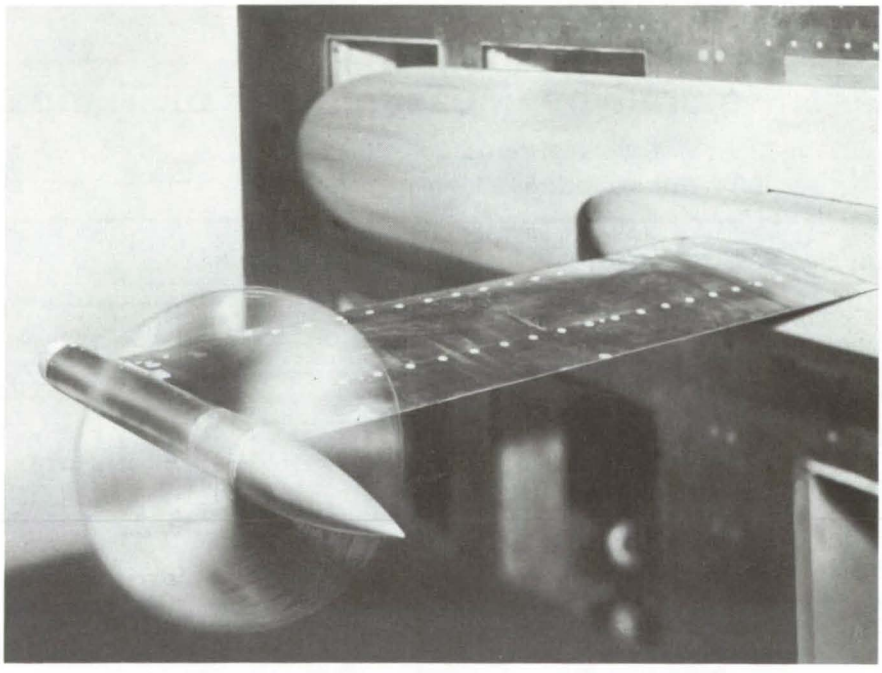

**Wingtip-Vortex Turbine** converts lost vortex energy to rotational energy and reduces induced drag.

The turbine has symmetrical blades that are alined with the flightpath such that no energy is extracted from the engine other than the frictional drag due to the added wetted area of the turbine plus a small additional form drag. The vortex flow direction is approximately perpendicular to the stream direction, with the maximum tangential vortex-core velocity approx-

imately 30 percent of the velocity of the aircraft. The flow angle relative to the turbine blades is therefore approximately 16°. The vortex turbine in this environment rotates as a result of lift force generated by each turbine blade and its position relative to the turbine axis.

The ability of the turbine to recover energy from the vortex may be increased by cambering the airfoil section of the turbine blades. The classical vortex cross-sectional velocity distribution indicates that the greatest vortex velocity occurs tangent to the vortex core and diminishes radially from that point. Therefore, further improvement may be gained by tapering the turbine blades such that the tip chord is smaller than the root, exposing the largest blade area to the highest energy portion of the vortex while the blade area and associated blade drag are reduced in the low-energy region of the vortex.

Tests conducted at a lift coefficient of 0.4 and a mach number of 0.70 indicate that the total drag of the wing with the vortex turbine installed is less than that for the wing alone. This "end-plate" effect is lessened as the turbine changes from a static to a rotational mode. The maximum reduction in induced drag would occur at zero turbine rotation, and as the turbine rotational speed is increased, the reduction in induced drag is decreased. Wind-tunnel tests indicate, however, that by properly designing the turbine blades, blade airfoil camber, and blade taper, the energy recovered by the vortex turbine exceeds the energy loss associated with the decrease in induced-drag reduction.

*This work was done by James C. Patterson, Jr., of* **Langley Research Center.** *No further documentation is available.*

*This invention is owned by NASA, and a patent application has been filed. Inquiries concerning nonexclusive or exclusive license for its commercial development should be addressed to the Patent Counsel, Langley Research Center [see page A5]. Refer to LAR-12544.*

# Engine-Vibration Analyzer

## A proposed vibration monitor would indicate out-of-limits conditions.

*Marshall Space Flight Center, Alabama*

A proposed circuit would monitor the vibration spectrum of engines under test or in service. It could detect subtle out-of-specification conditions and could be programed to shut down the engine if an out-of-limits condition develops. Possible uses of the monitor are in bench testing automobiles and outboard motors and as a safety device in very critical engine applications.

A block diagram of the concept is shown in the figure. The voltage output from a vibration transducer mounted on the engine block is filtered to extract all frequencies except those in a selected range of interest. The signal then passes through a circuit block that forms the root-mean-square integrated over a given time interval. This function is proportional to the vibration-energy content in the specified frequency band during the time interval.

A comparator checks whether the energy exceeds a preset limit. If so, it trips an indicator. The comparator output can also be connected to a latching relay to shut down the engine.

The circuit could be tuned for different frequency bands of interest and for different time intervals. If the vibration energy in a particular band or interval exceeds the specification, the corresponding indicator would be turned on.

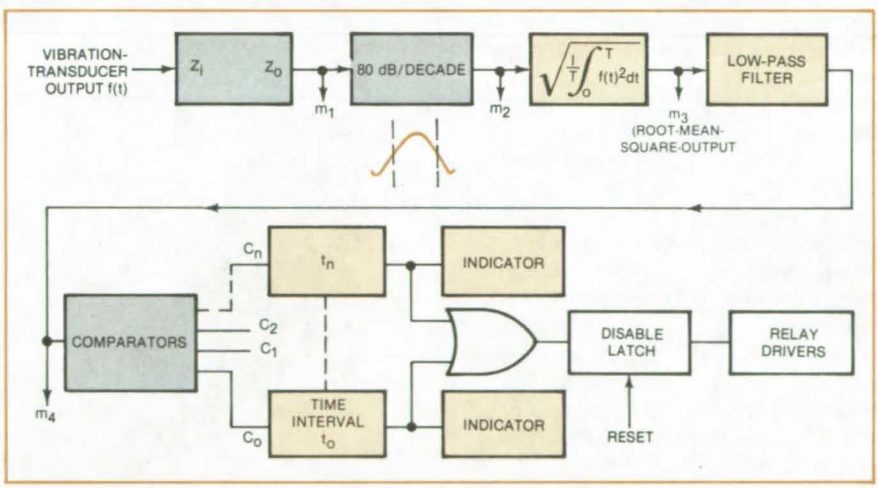


The **Engine-Vibration Analyzer** would monitor vibration-frequency components in selected bands. Test points are designated as $m_1$, $m_2$, $m_3$, and $m_4$.

*This work was done by Vincent R. Tolmei of Rockwell International Corp. for* **Marshall Space Flight Center.** *No further documentation is available.*
*MFS-19320*

# Tire Temperature and Pressure Monitor

A wheel-mounted miniature transmitter would signal dangerous conditions to the driver or pilot.

*Langley Research Center, Hampton, Virginia*

A proposed system would warn drivers or pilots when tire temperature or pressure falls outside of safe limits. An outgrowth of minaturized electronics for measuring lunar-soil bearing strength from spacecraft, the concept could improve safety and reduce operating costs for aircraft, automobiles, trucks, and other vehicles. It also has possibilities as a research tool for experiements on vehicle safety.

In one configuration of the device, illustrated in Figure 1, a bimetallic sensor moves in response to temperature changes on the wheel to which it is attached. The sensor closes a primary circuit and a secondary circuit, which energize a radio transmitter (see Figure 2). The type of signal depends on whether just the primary circuit or both circuits are closed. The primary circuit energizes a transmitter that emits a signal of predetermined frequency. Excessive temperatures cause the secondary circuit to energize a subcarrier oscillator, which modulates the signal.

A receiver at a remote location, such as the cabin or cockpit, picks up the signals and displays a warning light when temperatures are moderately high. When excessive temperatures are encountered and the secondary circuit is closed, the receiver activates a warning speaker. As an alternate to the bimetallic strip, thermistors and small transducers can be used for determining temperature and pressure.

Several applications of the tire monitor have been considered. For example, the wheels of modern aircraft may be subjected to abnormally high temperatures, particularly during taxi if brakes are used excessively, resulting in wheel or tire failure without the pilot's knowledge. For land vehicles, abnormal tire pressures can lead to excessive fuel consumption, excessive tire wear, tire failure, and (on rare occasions) a vehicle fire. On double-bogie wheels, one tire of a pair could lose pressure, but this may not be evident to the driver. A single tire failure could overload the adjacent tire and cause it to fail also.

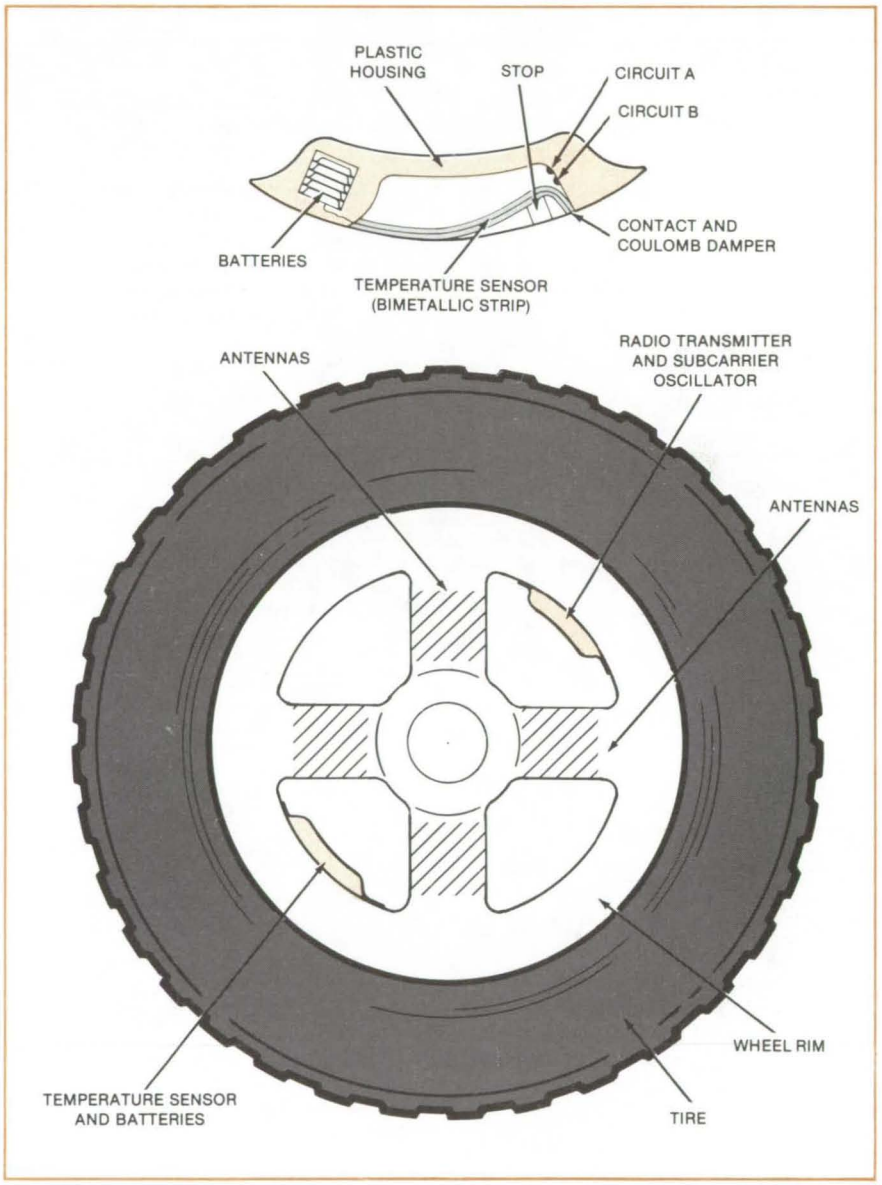


Figure 1. The **Tire Monitor** would include a sensor and a radio transmitter mounted so as not to imbalance the wheel. The sensor and batteries are enclosed in a plastic housing on the rim.

In the past, various devices have been utilized to signal tire pressure or temperature. Examples are a whistle attached to a valve stem to signal excessive tire pressure or a flag that extends from the wheel when a critical pressure or temperature is approached. In other systems, sliprings transmit information across rotating components. These devices are either incapable of continuously monitoring

the wheel temperatures and pressures or are mechanically complex, expensive, or inaccurate. The new sensor promises to have none of these shortcomings.

*This work was done by Ian O. MacConochie and Alfred G. Beswick of* **Langley Research Center.** *No further documentation is available.*

*Inquiries concerning rights for the commercial use of this invention should be addressed to the Patent Counsel, Langley Research Center [see page A5]. Refer to LAR-19262.*

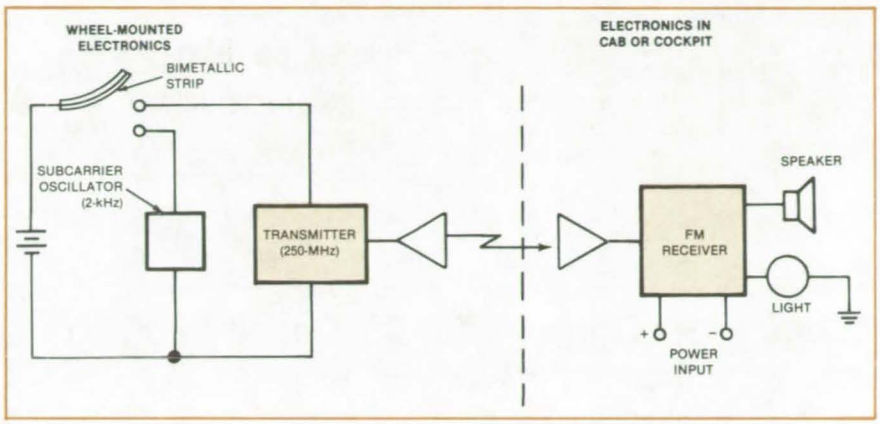


Figure 2. The **Transmitter and Receiver** would be assembled from miniature components. Lightweight electronics able to withstand high g-forces were developed by NASA for monitoring soil strength on the Moon from an orbiting spacecraft. Approximate weights are: eight batteries, 4 oz (0.1 g); speaker, 2 oz (0.05 g); switch, 1 oz (0.03 g); light, 0.5 oz (0.01 g); subcarrier oscillator, 1 oz (0.03 g); transmitter, 3 oz (0.08 g); and receiver, 16 oz (0.4 g).

# Orifice Blocks Heat Pipe in Reverse Mode

## Thermal diode shuts down rapidly if sink temperature exceeds source.

*Ames Research Center, Moffett Field, California*

High forward-mode conductance is combined with rapid reverse-mode shutoff in a heat pipe originally developed to cool spacecraft payloads. A narrow orifice within the pipe "chokes off" the evaporator if the heat sink becomes warmer than the source. During normal operation, with the source warmer than the sink, the orifice has little effect. The design is simpler and more compact than other thermal-diode heat pipes and requires no special materials, forgings, or unusual construction techniques.

As shown in the figure, the heat pipe is U-shaped. One leg ends at the evaporator, which is coupled to the instruments that are to be cooled. The other leg is the condenser, which terminates in a liquid reservoir. An aluminum saddle brazed to the reservoir attaches to a radiator. A solid plate with a small orifice adjacent to the wall is located inside the heat pipe near the entrance to the evaporator.

In the conducting mode, vapor is transported from the evaporator

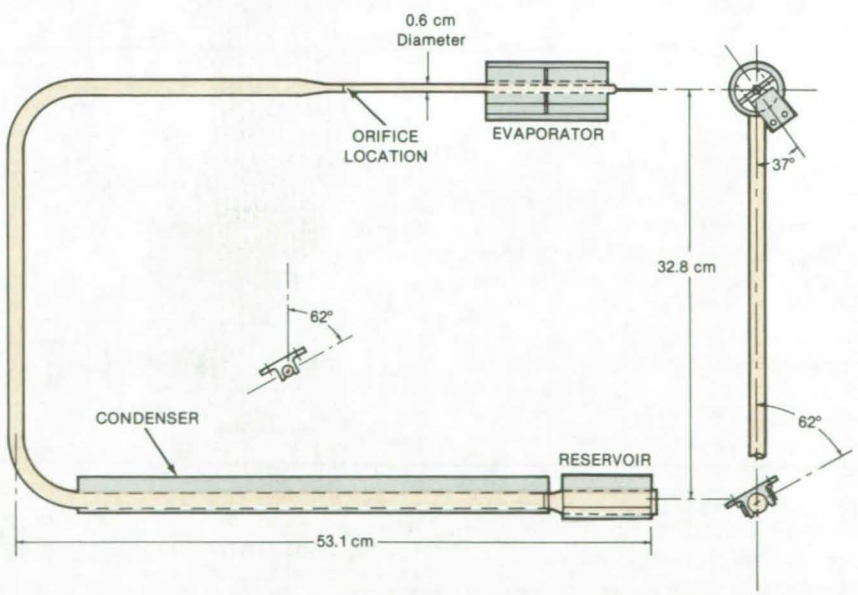


In the **Diode Heat Pipe,** liquid blockage at the orifice restricts the reverse flow of heat when the condenser is hotter than the evaporator. In a design developed to cool spacecraft payloads, forward conductance is 7.4 W/°C at 200 K. Reverse-mode shutdown occurs about 7 minutes after the sink temperature rises above that of the source.

through the orifice to the condenser. In this normal operating mode, the reservoir completely fills with excess liquid. The only effect of the plate is to create a small pressure drop at the orifice.

If the reservoir is exposed to heat that raises it to a higher temperature than the evaporator, excess fluid condenses in the vapor space of the evaporator. Heat-pipe action rapidly ceases when a liquid meniscus forms across the orifice, retaining the excess liquid in the evaporator.

*This work was done by Joseph P. Alario of Grumman Aerospace Corp. for* **Ames Research Center.** *For further information, Circle 50 on the TSP Request Card.*

*Inquiries concerning rights for the commercial use of this invention should be addressed to the Patent Counsel, Ames Research Center (see page A5). Refer to ARC-11341.*

# Rangefinder Corrects for Air Density and Moisture

Phase-locked pulses carry information about air density and moisture content.

*Goddard Space Flight Center, Greenbelt, Maryland*

A proposed distance-measuring instrument compensates for variations in both dry atmospheric density and water-vapor content. The instrument would be expected to be more accurate than previous laser-ranging instruments.

The new rangefinder sends three signal trains to the target: Two trains are at optical frequencies, and one is at a microwave frequency. All three signals are phase-locked. At the target, the three signals are reflected back to the instrument. The primary advantage of the new technique is the use of a single laser to generate both optical signals and the phase reference for the microwave signal.

In making the round trip, the two optical-frequency signals travel at slightly different speeds because of the wavelength dependence of the speed of light in dry air. The microwave signal travels at a speed that depends on both the water-vapor and the dry-air density. The speed differences would be observed as

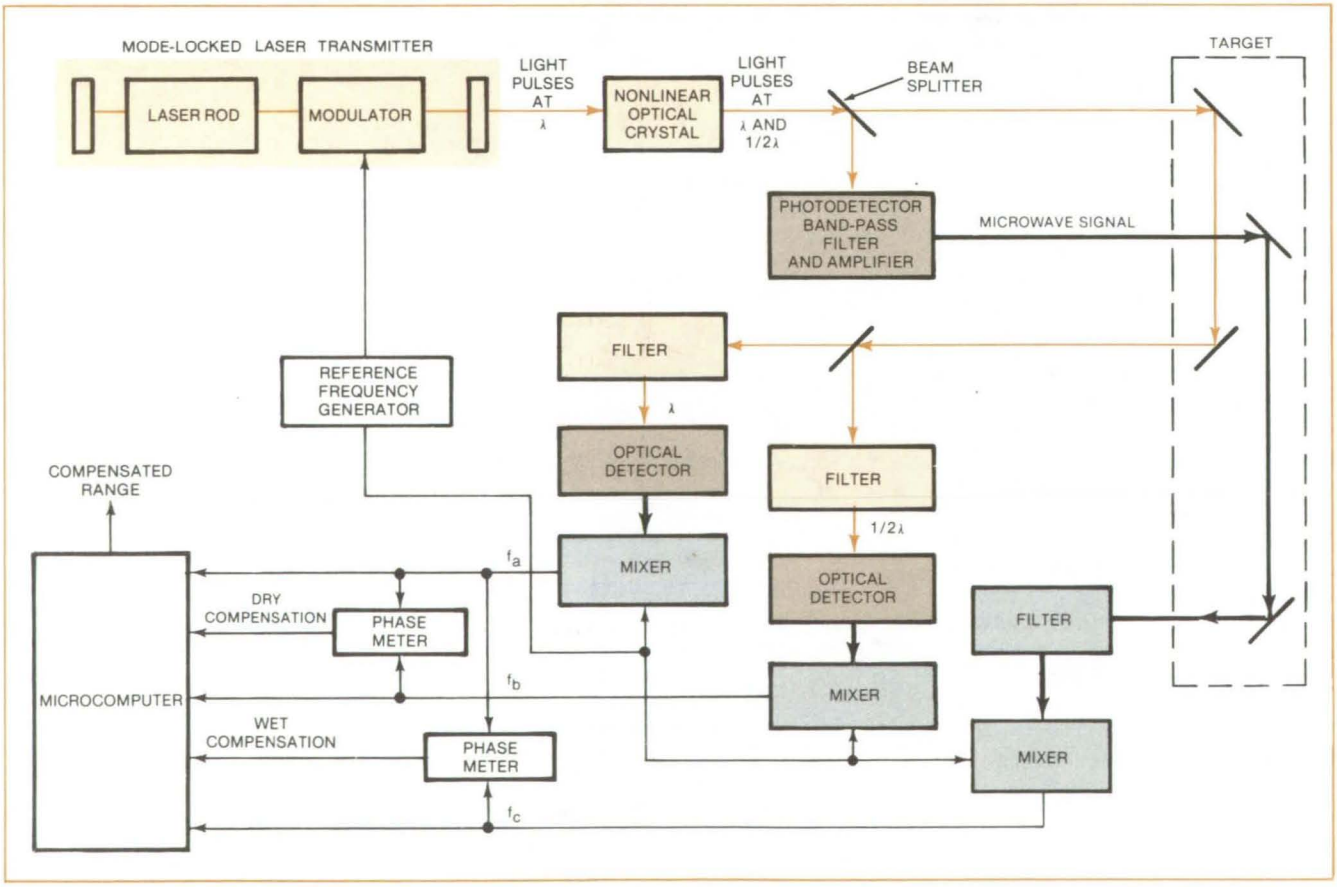


The **Phase Differences Between Signals** at optical and microwave frequencies are used to determine the range to a target and to compensate the range measurements for the density and moisture content of the air.

phase differences between signals and would be used to calculate the distance to the target, corrected for the effects of the wet- and dry-air densities.

As shown in the figure, an intracavity modulator mode-locks the laser output into pulses at a repetition frequency in the range of 200 to 500 MHz and a pulse width of about 100 ps. The pulsed beam passes through a nonlinear optical crystal, which converts part of the energy to light at one-half the wavelength of the source beam, so that there are two pulse trains — one at wavelength $\lambda$ and the other at $1/2\lambda$ — both locked precisely in phase.

The laser output contains strong frequency components that are harmonics of the fundamental pulse rate. These frequency components extend well into the microwave frequency range.

One of the harmonics, in the range from 2 to 10 GHz, is extracted by a photodetector and band-pass filter. This microwave energy is locked in phase with the optical signals, since it is derived from the same source, and is also directed at the target.

When the two optical pulse trains are reflected by the target and collected by the instrument, each is demodulated to extract the same microwave frequency as the microwave portion of the transmitted beam. The reflected microwave signal is also collected. All three signals thus have the same microwave frequency, but they differ in phase according to the effects of the atmosphere and distance to the target. The three signals are mixed with a local oscillator signal to produce three signals at a lower frequency (for convenience in processing) but with the same phase difference as before.

The signals ($f_a$ and $f_b$) derived from the two reflected optical pulse trains are fed to a phase meter that determines the dry-air component of phase delay. The signals ($f_c$ and $f_a$) derived from the reflected microwave frequency and one reflected optical pulse train are fed to a phase meter that determines the wet-air component. The dry and wet components and all three signals are processed by a small computer or microprocessor, which calculates the range of the target, compensated for both the wet and dry density of the atmosphere.

*This work was done by James B. Abshire of* **Goddard Space Flight Center.** *For further information, Circle 51 on the TSP Request Card.*

*This invention is owned by NASA, and a patent application has been filed. Inquiries concerning nonexclusive or exclusive license for its commercial development should be addressed to the Patent Counsel, Goddard Space Flight Center* [see page A5]. *Refer to GSC-12609.*

# Faster Test for Cable Seals

## A simple vacuum technique speeds immersion tests.

*Marshall Space Flight Center, Alabama*

Applying a vacuum shortens the time it takes to immersion-test electrical cable. The vacuum encourages rapid displacement of trapped air by the electrically conductive saltwater used in the tests. Control of the partial vacuum also enables control of the severity of water exposure.

To test a cable seal, the sealed or spliced area is immersed in an NaCl solution [typically, 5 percent by weight NaCl at 60° to 100° F (16° to 38° C)]. The solution with the submerged splice is placed in a vacuum chamber (see figure), which is then pumped down to the desired partial vacuum [typically, 9.5 psia ($6.6 \times 10^4$ N/m$^2$ absolute)]. Bubbles will be observed at a leaking seal.

The system is then returned to atmospheric pressure and the cable tested for insulation resistance: A bare wire is inserted in the solution to serve as the return path to electrical ground, and the resistance is measured between the cable conductor, cable shield, and ground. Samples not meeting the minimum-resistance specifications are rejected.

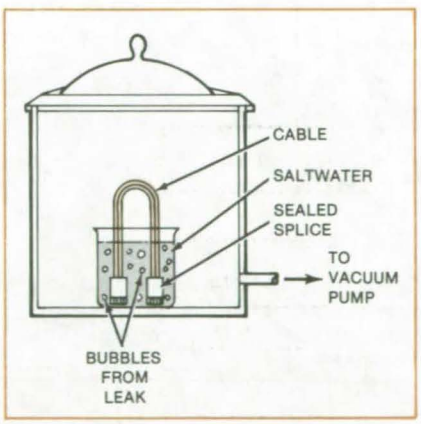


The **Vacuum-Assisted Immersion Test** is much faster than conventional atmospheric immersion tests of cable seals. The vacuum speeds the removal of air, allowing its replacement by the conductive salt solution in leaking specimens.

Previously, a 24-hour immersion was necessary to assure the displacement of trapped air. The improved method takes only 10 minutes. It should also be applicable to the testing of potted connectors and of cable insulation for sealing.

*This work was done by A. T. Sheppard of Martin Marietta Corp. for* **Marshall Space Flight Center.** *No further documentation is available.*
*MFS-25618*

# Circuit Counts Carbon Fibers

Monitor counts potentially-damaging fiber fragments.

*NASA's Jet Propulsion Laboratory, Pasadena, California*

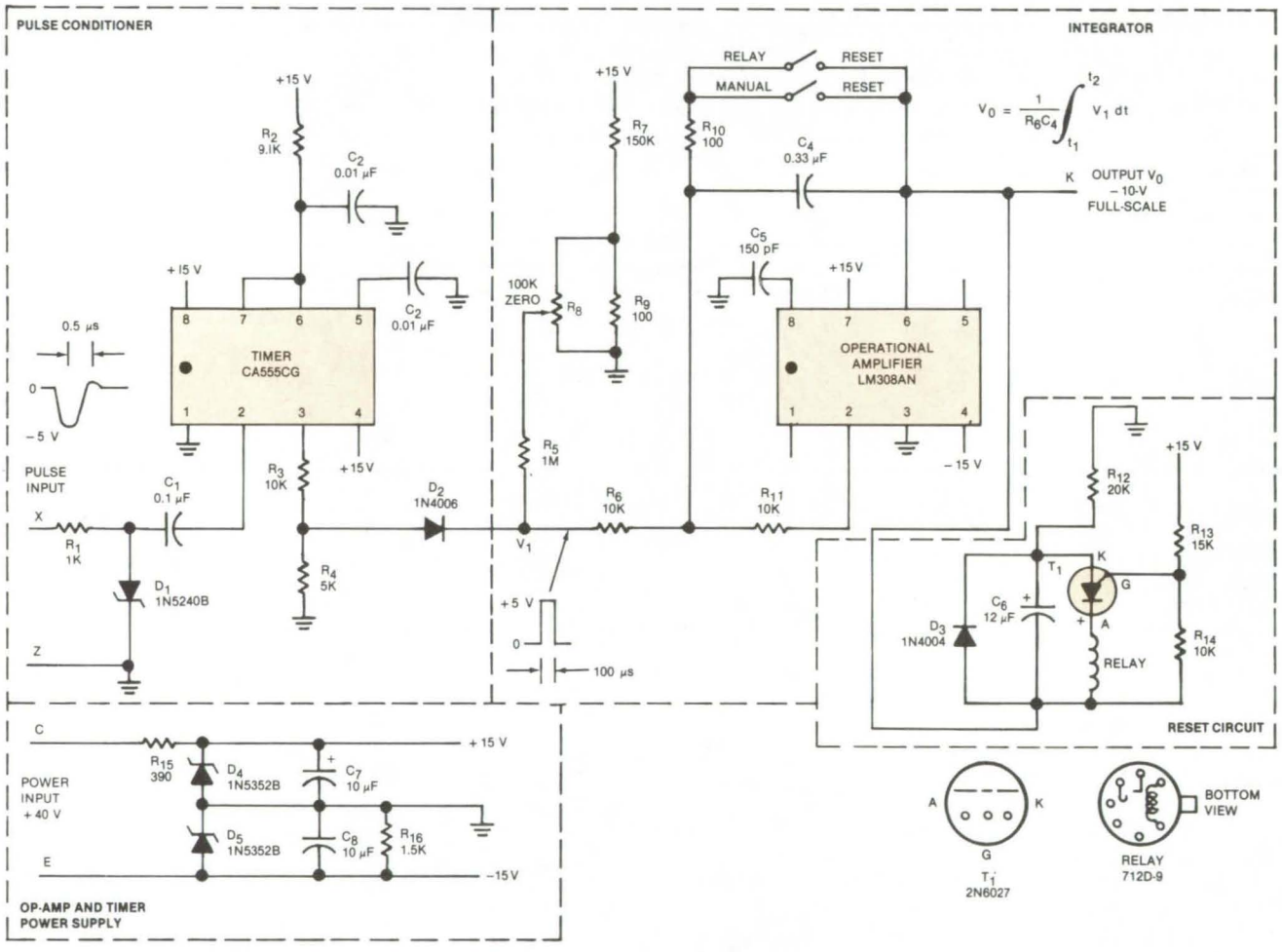


**Carbon Fibers Are Counted** when they fall on the high-voltage grid. An arc discharge vaporizes the fiber and triggers the timer. The equal-duration pulses from the timer are integrated by the operational amplifier, giving an output voltage that is proportional to the number of fibers incident after the reset switch was opened. If two or more fibers arrive at the grid simultaneously, they are vaporized one at a time; thus all of them are counted.

Airborne carbon fibers are collected and counted by a comblike high-voltage grid connected to an electronic pulse counter. Even if several fibers reach the detector simultaneously, they are counted individually.

Epoxy resins reinforced by fine carbon fibers are used in automobiles, airplanes, and other structural applications. Typically several millimeters long, the fine fibers are electrically conductive and are not oxidized, vaporized, or otherwise affected by fires in which the resin binder is consumed. Once expelled from the composite, the fibers can settle in unprotected electronic equipment and, being conductive, can cause shorting and power failure.

Recently, NASA has carried out an extensive program to assess the risk to the public from carbon fibers released in civil-aircraft accidents. During this study, various instrumentations were used to measure carbon-fiber concentration and deposition in various tests. A real-time high-voltage grid detector and counting circuit were developed (see figure).

The comb grid structure was chosen because it intercepts the airborne fibers while allowing combustion products to pass through and because it is immune to spurious short circuits caused by soot and moisture. High-voltage/high-current operation eliminates problems caused by contact resistance and fiber bounce.

Experiments show the optimum sensing voltage to be between 500 and

1,500 volts. The voltage depends on the spacing of the grid elements; higher voltages are required for larger spacings. The sensing grids initially were gold-plated brass rods of various diameters, but more-recent constructions utilize square-edge stock. Typical spacing of the grid elements ranged from 1 to 5 millimeters.

A power supply maintains the optimized high voltage across the grid sensor rods. Transient high currents occur as each fiber fragment contacting the grid elements shorts the circuit to discharge a capacitor. The discharge current is measured to give an indication of the resistance across the discharge, which is related to the fiber length, and the integrator counts the fibers.

It has been found that only one discharge occurs at any instant even when many fragments are incident on the same sensing elements at the same time. It is believed on a statistical basis that it is highly unlikely that more than one conducting path would have exactly the same resistance as any other at the same instant. Thus arcing would proceed sequentially starting with the path of least resistance. Because of this, it is believed that the current flow is only for a single fiber and does not result from the combined effect of several fibers.

The high-voltage grid detector has also proved useful for counting fiber segments collected on sticky tapes in field tests. The tape holding the captured fibers is brought into contact with the grid elements. For this application, a fast high-voltage pulser circuit is utilized. Automatic counting up to $10^3$ counts per second is possible, eliminating the need for laborious visual counting under a microscope.

*This work was done by Lien C. Yang of Caltech for* **NASA's Jet Propulsion Laboratory.** *For further information, Circle 52 on theTSP Request Card.*

*This invention is owned by NASA, and a patent application has been filed. Inquiries concerning nonexclusive or exclusive license for its commercial development should be addressed to the Patent Counsel, NASA Resident Office-JPL [see page A5]. Refer to NPO-14940.*

# Multipressure and Temperature Probe

## Single aerodynamic-flow probe measures six parameters simultaneously.

*Ames Research Center, Moffett Field, California*

A new aerodynamic probe consists of a small cylinder surrounding two commercially-available differential-pressure sensors and a network of tiny tubes leading to various ports. The probe can measure six aerodynamic parameters simultaneously; i.e., the steady and fluctuating components of total temperature, total pressure, and static pressure. Effectively, it replaces six conventional probes, eliminating unnecessary obstructions and distortions of aerodynamic flow patterns in wind tunnels.

All the probe components (see figure) are housed in 5-mm-diameter Lexan plastic, or equivalent, cylindrical tube. Because the tube is small, its resistance to flow patterns is minimal. The cylinder includes six grooves cut on the inside wall: three along the entire cylinder length and three to nearly half its length. Three long and two short 0.5-mm-diameter steel tubes are epoxied into the grooves. One short groove is used for electrical wiring that supplies power and recording data to and from the two pressure sensors.

(continued on next page)

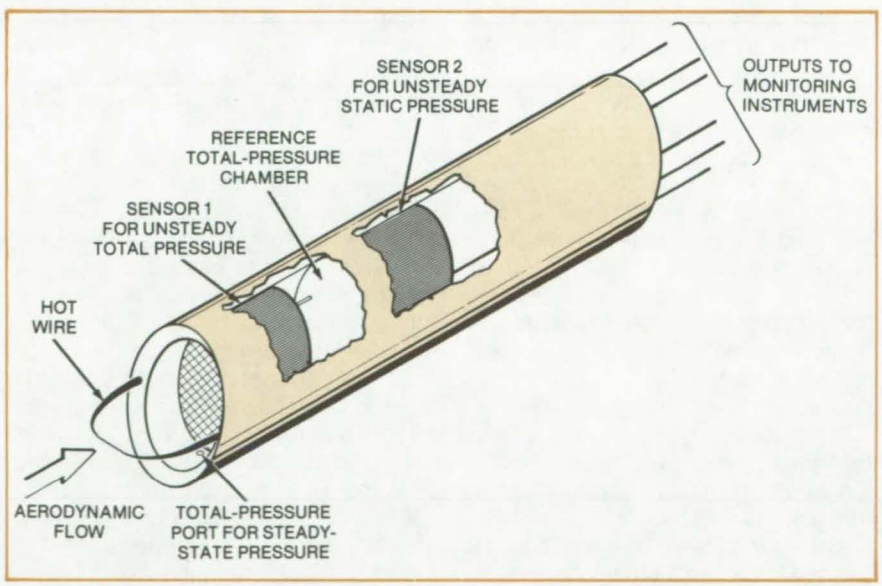


An **Aerodynamic Probe** is a small cylinder tube holding a network of tiny tubes leading to various ports. Six parameters are recorded simultaneously with little interference with the aerodynamic flow. Two tubes connected by a hot-wire tungsten probe sense steady and fluctuating components of aerodynamic flow temperatures. Another set of two tubes measures steady components of total and static pressures; the feedbacks from these tubes are input into differential-pressure sensors 1 and 2 to measure the fluctuating components of the above pressures. The data are recorded by instruments at the back end (right side) of the probe.

One pair of full-length tubes is joined by a hot-wire, 5-μm-diameter tungsten element positioned into the flow path. This element, is used to measure the steady and unsteady temperatures of the aerodynamic flow.

The steady components of total and static pressures are recorded via two tubes. The back end of each tube is connected to a 0.5-mm-diameter coiled tube 3-m long. Both coiled tubes end in a T-connection. One branch of a T-connector used to measure the total pressure is fed to a steady-state total-pressure recorder; the other branch acts as a feedback to the reference-pressure port of sensor 1. The fluctuating total-pressure component is obtained electrically from sensor 1.

A similar arrangement is made for static-pressure measurements. The steady component is recorded via one branch of the T-connector feeding the input from the static-pressure recorder. The fluctuating component is obtained electrically via sensor 2. The sensor 2 has two inputs: one a reference orifice extending radially to the cylinder wall and the other constituting feedback from the T-connector branch of the static pressure tube.

The entire probe can be easily adapted for quick disconnection at the downstream end so that it can be replaced easily in case of failure. The probe diameter can be further reduced by using a 3-mm-diameter cylinder available from the same material stock.

*This work was done by Kizhanatham R. Raman of Raman Aeronautics Research for* **Ames Research Center.** *For further information, Circle 53 on the TSP Request Card.*
*ARC-11166*

# Surface-Contamination Inspection Tool for Field Use

Photoelectron emission is measured in air to determine surface cleanliness.

*Marshall Space Flight Center, Alabama*

An inspection tool developed for Marshall Space Flight Center detects surface contamination by measuring photoelectron emission. No vacuum chamber or controlled environment is used. The photoemission is measured under ordinary atmospheric conditions, so surfaces may easily be inspected in factories or in the field.

Most metals, epoxy paint, and many other materials emit electrons when illuminated with 2,500 Å ultraviolet light; and the emission is attenuated by thin layers (even monolayers) of ordinary hydrocarbons or silicones. The photoelectrons travel through the air between the surface under inspection and a collector that is part of the tool.

The tool is shown schematically in the figure. The ultraviolet (UV) radiation ejects electrons, which are then attracted to the collector by the electric field between the test surface and the collector. (The collector is biased positive with respect to the sample.) The electrons have insufficient energy to ionize air molecules, so the current is due to diffusing electrons rather than ions.

The closer the UV lamp is to the surface, the greater the current; but the magnitude of the current is not important as long as the ammeter signal-to-noise ratio is high. The collector must be positioned within a few millimeters of the surface for high electric field, but must not shadow the light. Therefore the collector is positioned to the side of the lamp, as shown, so that maximum UV flux hits the sample surface beneath the collector.

Photoemission from epoxy paint decays during exposure to the ultraviolet light. (Emission from surface-treated aluminum does not.) Therefore if the detector is passed over unexposed paint, the current depends on the scanning rate: If the scanning is too fast, the current may be limited by the time constant of the ammeter; and if the scanning rate is too slow, the current will drop to a very low level because of the decay process. Hence the tool is calibrated for a specified scan rate. The current remains essentially constant for rates between 0.1 and 0.4 ft/s (3 to 12 cm/s).

*This work was done by Tennyson Smith of Rockwell International Corp. for* **Marshall Space Flight Center.** *For further information, Circle 54 on the TSP Request Card.*

*Inquiries concerning rights for the commercial use of this invention should be addressed to the Patent Counsel, Marshall Space Flight Center [see page A5]. Refer to MFS-25581.*

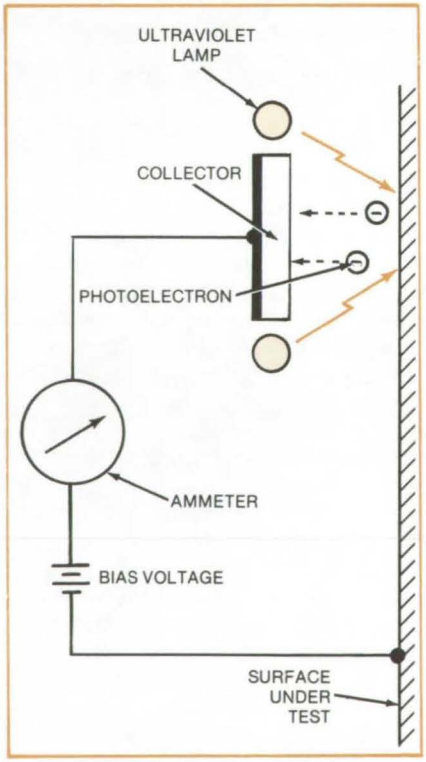


**Photoelectrons** emitted from the metal or epoxy-painted surface diffuse to the collector: Hydrocarbons or silicone contaminants are detected by a reduction of the photoemission current below the normal clean-surface value. Other contaminants may cause an increase in current above the normal level.

# Pressure Transducer Has Long Service Life

An LVDT is the sensing element in a reliable differential-pressure transducer.

*Lyndon B. Johnson Space Center, Houston, Texas*

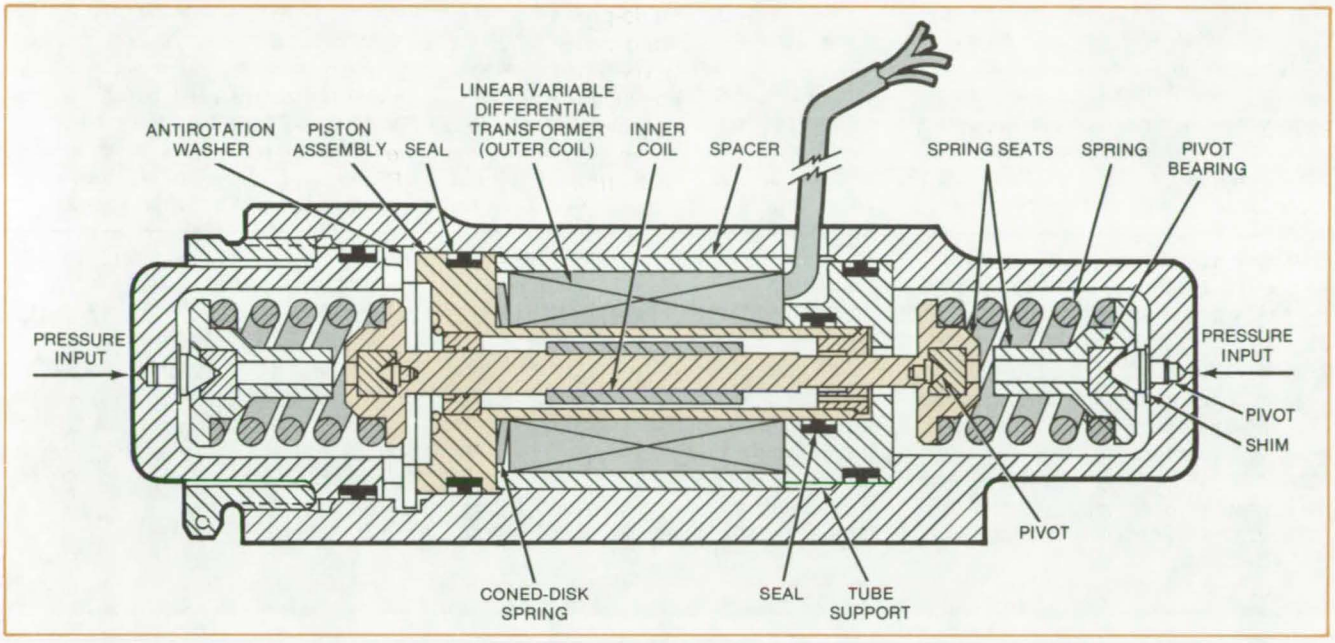


The **Differential-Pressure Transducer** includes a piston, helical springs, and a linear variable-differential transformer concentric with the piston. The transducer senses the motion of the piston in response to changes in pressure differential.

A problem with conventional Bourdon-tube or diaphragm differential-pressure transducers is that the fluids in the two pressure lines mix if the gage ruptures. This failure mode is virtually eliminated in a new transducer originally used in the elevon control lines on the Space Shuttle orbiter. The reliability and operating life of the new unit are superior to many conventional transducers.

As shown in the figure, the essential elements of the transducer are a linear variable-differential transformer, a piston coaxial with the transformer, and helical springs that bias the piston so that it is centered in the transformer when the pressures at both inputs are equal. The movable coil of the transformer is wound on the piston and moves with it. Piston motion is thus converted to an electrical signal at the transformer output.

Eight seals within the transducer prevent fluid leakage from one pressure line to the other. Even if one or both of the springs should break after many cycles, the fluids would not mix. Another advantage is that the symmetrical design is relatively insensitive to temperature shifts. The case can be made of any material compatible with the hydraulic fluids and surrounding environment.

*This work was done by Richard E. Prout of Rockwell International Corp. and Aurelius Chaves, Jr., of Moog Inc. for* **Johnson Space Center.** *No further documentation is available.*
*MSC-18904*

### *"Bottle-Brush" Heat Exchanger*

Instead of merely heating fluid at its wall, fluid is heated throughout the cross section of a new "bottle-brush" heat exchanger. The improved heat exchanger is a metal tube with heat-conducting wires extending radially inward from the wall. Heat is transferred throughout the enclosed volume.
(See page 202.)

### *System Controls and Measures Oxygen Fugacity*

A ceramic-electrolyte cell monitors the oxygen fugacity in a new research apparatus. The cell voltage is related to the ratios of fugacities of a sample and of reference gases. The apparatus includes a balance for carrying out in situ thermogravimetric sample analysis.
(See page 163.)

### *Weld-Wire Monitor*

An impedance bridge determines whether weld-wire composition and diameter are within specifications. As wire is fed to a weld joint, it passes through a sensing coil. The bridge becomes unbalanced if the wire composition or diameter changes significantly.
(See page 221.)

# Heater Composite Measures Heat Transfer

Low-cost device aids in visualizing and measuring heat-transfer properties of materials.

*Lewis Research Center, Cleveland, Ohio*

A composite consisting of commercially available elements, including a transparent plastic sheet coated with liquid-crystal material, another heater sheet with a thin layer of conducting material such as gold or carbon, and copper bus-bar strips, has been developed to measure heat transfer. This composite provides a simple, convenient, low-cost device for use in heat-transfer work for rapid evaluation of the thermal performance of both flat and simply curved objects. The objects may be either convection, conduction, or radiation heated or cooled. The composite utilizes available off-the-shelf materials and provides a convenient method, with good resolution of local temperatures and heat transfer, with measurement accuracy at near-normal room conditions.

Prior to assembly of the composite, the liquid-crystal sheet is calibrated for color change with temperature, while the heater sheet is calibrated for uniformity of heat flux. The two sheets are then bonded together to make the composite, using a thin paperlike material with double-adhesive backing. The same double-adhesive material is used to attach the composite to the object to be tested, with the heater sheet being placed next to the surface of the test object. The liquid crystal, by virtue of its color-changing properties, provides measurements of the local temperatures of the object plus a visualization of the thermal patterns developed. A heat balance and measurements of the electrical input into the conducting layer, less any heat losses, are used along with the air temperature above the layered composite and the temperature pattern indicated by the liquid-crystal sheet to provide a measure of the local heat-transfer coefficients.

*This work was done by S. A. Hippensteele, L. M. Russel, and F. S. Stepka of* **Lewis Research Center** *and R. J. Moffat of Stanford University. Further information may be found in NASA TM-81639 [N81-21313/NSP], "Evaluation of a Method for Heat Transfer Measurements and Thermal Visualization Using a Composite of Heater Element and Liquid Crystals" [$5]. A copy may be purchased [prepayment required] from the National Technical Information Service, Springfield, Virginia 22161.*

*LEW-13731*

# Books and Reports

These reports, studies, and handbooks are available from NASA as Technical Support Packages (TSP's) when a Request Card number is cited; otherwise they are available from the National Technical Information Service.

## Survey of Facilities for Testing Photovoltaics

Resources for testing systems, subsystems, and components are cataloged.

Facilities capable of testing complete photovoltaic systems, subsystems, or components are described in a 42-page report that is now available. The compilation includes the facilities and capabilities of five field centers of the national photovoltaics program, two state-operated agencies, and five private testing laboratories.

The development of photovoltaics technology for power generation has advanced from low-cost manufacture of photovoltaic cells to the systems applications of the cells. Testing is required to evaluate the system designs; therefore this compilation of system test facilities catalogs present and planned resources for such testing. The purpose of the compilation is to disseminate information on the capabilities of test facilities that will be needed by the photovoltaics program and by industry.

The results of the surveys encompass the following areas:

1. All application sectors — residential, intermediate, central-station, and remote;
2. Grid-connected and stand-alone systems;
3. Test level — total system, subsystem, or component;
4. Facility ratings — maximum power-handling capability, thermal capacity, and storage; and
5. Measurement capability as to type and accuracy, when applicable.

In addition to listing facilities for the testing of complete systems, the compilation lists facilities for testing subsystems and for environmental, product-approval, and accelerated-life testing of components. These facilities are included, even though not a part of system testing, because they are important elements of system development.

*This work was done by Robert W. Weaver of Caltech for* **NASA's Jet Propulsion Laboratory.** *To obtain a copy of the report, "System Test Facilities Existing Capabilities Compilation," Circle 55 on the TSP Request Card.*

*NPO-15361*

# Computer Programs

These programs may be obtained at very reasonable cost from COSMIC, a facility sponsored by NASA to make new programs available to the public. For information on program price, size, and availability, circle the reference letter on the COSMIC Request Card in this issue.

## Graphics for Finite-Element Analysis

Models are projected, re-oriented, and sectioned for visual analysis of responses.

One of the many advantages of finite-element analysis in structural, thermal, and fluid mechanics problems is that the model and its responses are readily displayed utilizing computer graphics. The ELPLOT program is a passive computer graphics system that could be utilized for the display of models and responses of general finite-element analyses.

Features that make ELPLOT a very general and very useful program include: a wide range of view-orientation selections, a number of alternative data-input formats, an extensive family of finite-element types, and capabilities for both static- and dynamic-response displays. ELPLOT could be incorporated as an important part of the model development and results analysis of any finite-element system.

Oblique othographic projections are employed in ELPLOT to allow the analytical model to be viewed from any orientation. In this oblique-orthographic-projection approach, Euler-angle transformations specify the orientation of the model relative to a projections (viewing) plane. Thus, the user can obtain various views of the model simply by specifying the Euler angles and the viewing plane. Portions of the model may be isolated for closer examination by either sectioning (cutting) of planes parallel to the viewing planes or by the specification of a range of element or node numbers to be included in the plot. Also, exploded views may be plotted in which the individual elements are separated to aid in detecting the presence or absence of specific elements. A symmetry capability is available to generate full model plots for situations where only portions of a structure are actually modeled due to symmetry considerations.

One-, two-, and three-dimensional finite-element families with an arbitrary number of nodes can be plotted with ELPLOT. A certain node-numbering scheme is required; however, alternate numbering schemes from other sources are easily accommodated by a built-in renumbering capability.

ELPLOT is compatible with most finite-element analysis programs due to the availablity of multiple methods of entering node and element data. Model data may be input either by reading card image records of a user-specified format, by reading a binary file of ELPLOT specifications, or by user-supplied subroutines. Plots may be generated of the undeformed model, model static response, and dynamic responses. Plots of the undeformed model may be annotated with node or element numbers. In the static-response plots, such nodal-dependent variables as displacements or temperatures may be superimposed on the model nodes. For dynamic responses, X-Y plots of the displacement or temperature-versus-time type may be generated for any number of user-specified nodes.

ELPLOT is written in FORTRAN IV for batch execution and has been implemented on a CDC 6000-series computer with a central memory requirement of approximately 55K (octal) of 60-bit words. Plotter interface is through the NASA Langley plot library, which may be adapted to virtually any X-Y-type plotter. ELPLOT was developed in 1978.

*This program was written by Earl A. Thornton and Lynn M. Sawyer of Old Dominion University Research Foundation for* **Langley Research Center.** *For further information, Circle A on the COSMIC Request Card.*
*LAR-12793*

## Finite-Element Analysis of Forced Convection and Conduction

Program simplifies computations when structural and thermal analyses are both required.

The TAP2 thermal-analysis program was developed as part of research on finite-element methodology for the thermal analysis of convectively cooled structures, such as scramjet engines and hypersonic aircraft. It is also suited for the thermal analysis of nuclear reactors, solar-panel heating systems, and other environmental applications.

In the past, the thermal analysis of convectively cooled structures with unknown fluid temperatures was performed using a lumped-parameter finite-difference approach, while structural analysis required a finite-element approach. Thus, two models of a structure had to be prepared for a complete analysis. TAP2, in contrast, uses finite-element models for the steady-state and transient thermal analysis of a structure with conductive and convective heat transfer. Therefore, TAP2 greatly simplifies data preparation when structural and thermal analyses are both required. It is also a more-efficient interface between independent thermal and structural analyses and could be used in the development of an integrated analysis system.

TAP2 uses a finite-element model to perform steady-state and transient analyses of structures. The program includes a finite-element library of six elements: two conduction/convection elements to model heat transfer in a solid, two convection elements to model heat transfer in a fluid, and two integrated conduction/convection elements to represent combined heat transfer in tubular and plate/fin fluid passages.

(continued on next page)

The finite-element formulation results in a set of nonlinear algebraic equations expressed in matrix form in terms of the temperature-dependent system conductance matrix, the unknown nodal temperature vector, and the system nodal head-load vector. Nonlinear thermal analysis due to temperature-dependent thermal parameters is performed using a Newton-Raphson iteration. Transient analyses are performed using an implicit Crank-Nicolson time-integration scheme with consistent or lumped-capacitance matrices as an option. Program outputs include nodal temperatures and element heat fluxes. Pressure drops in fluid passages may also be computed.

TAP2 is written in FORTRAN IV for batch processing and has been implemented on a CDC 6000-series computer with a central memory requirement of approximately 75K (octal) of 60-bit words. The program was developed in 1980.

*This program was written by Allan R. Wieting of* **Langley Research Center** *and Earl A. Thornton of Old Dominion University. For further information, Circle B on the COSMIC Request Card.*
*LAR-12794*

## Model Verification of Mixed Dynamic Systems

### Program compares analytical transfer functions with experiment.

MOVER uses experimental data to verify mathematical models of "mixed" dynamic systems. The term "mixed" refers to interactive mechanical, hydraulic, electrical, and other components.

For the steady-state response of a linear dynamic system, a transfer function can be defined that relates the steady-state output to a steady-state input. The transfer function can be determined experimentally by measuring input forces and output responses in a steady-state test.

When the engineer develops a mathematical model of the dynamic system, that model determines an analytical transfer function. At some stage during the design, the analytical model is compared with available experimental results to determine the validity of the math model. In a sense, the experimentally-derived transfer function and the analytically-derived transfer function are compared. If there are significant discrepancies, either the experimental data were improperly obtained or the math model is in error, usually the latter.

MOVER uses parameter-estimation techniques to verify the mathematical models. The math models of the dynamic system may be constructed from a library of simple network elements, from direct matrix input, or from a combination of both. The equations of motion for the system are computed, and the appropriate constraint relations are applied. A QR algorithm is used to obtain the characteristic eigenvalues and eigenvectors of the math model. The steady-state system response to user-specified harmonic input and the sensitivity of that response to desired model parameters are calculated.

Comparisons with experimentally obtained responses are used to obtain a revised set of model parameters. MOVER then uses the revised parameters in a new cycle of response calculations and parameter estimation. The process is continued until an acceptable tolerance is achieved between the calculated response and the measured response. The result is a revised math model that should better represent the "real" system.

MOVER is written in FORTRAN V for batch execution and has been implemented on a UNIVAC 1100-series computer with an overlaid central memory requirement of approximately 58K of 36-bit words. The program was developed in 1977.

*This program was written by D. A. Evensen, Jon D. Chrostowski, and T. K. Hasselman of J. W. Wiggins Co. for* **Marshall Space Flight Center.** *For further information, Circle C on the COSMIC Request Card.*
*MFS-23806*

## Improved Numerical Differencing Analyzer

### A system for solving differential and algebraic equations representing physical systems

SINDA, the Systems Improved Numerical Differencing Analyzer, solves physical problems governed by diffusion-type equations and that can be modeled by lumped-parameter representation. The system is most widely used as a general thermal analyzer with resistor/capacitor network representations, but it may be adapted to a wide range of problems represented by differential equations, such as Fourier, Poisson, or LaPlace equations.

SINDA solves numerically almost any set of ordinary differential equations that represent the transient behavior of a lumped-parameter system or any set of nonlinear algebraic equations that represents the steady-state conditions of a physical system. For user decision flexibility, SINDA offers several numerical solution techniques. These include such finite-difference formulations of the explicit method as: forward-difference explicit approximation, DuFort-Frankel approximation, exponential approximation, and alternating-direction approximation; also included are such formulations of the implicit method as: backward-difference implicit approximation and Crank-Nicolson approximation. The practical analysis of many physical problems, particularly thermal analyses, is readily achieved with the SINDA system.

SINDA consists mainly of a preprocessor and a subroutine library. The preprocessor accepts programs written in the SINDA language and converts them to standard FORTRAN programs. The SINDA language works with lumped-parameter representations and finite-difference solution techniques. The SINDA library consists of prewritten FORTRAN subroutines that perform common actions. The users may call these subroutines from their SINDA language programs, thus greatly reducing the programing effort required to solve many problems.

Most of the subroutines in the SINDA library were developed for solving thermal-analysis problems. As a thermal analyzer, SINDA handles such interrelated complex phenomena as sublimation, diffuse radiation within enclosures, transport-delay effects, sensitivity analysis, and thermal-network error correction.

Special subroutines, the SINFLO group, are included in the SINDA library to facilitate the thermal analyses of systems incorporating fluid-flow networks. SINDA easily accounts for pumps, valves, and heat exchangers

during a thermal analysis. The user-written SINDA language program determines the input data required and the information that is produced as output by the program.

This VAX version of SINDA is written in FORTRAN IV and MACRO for batch execution and has been implemented on a DEC VAX-11/780 computer. SINDA was adapted to the VAX in 1980.

*This program was submitted by Joseph T. Skladany of* **Goddard Space Flight Center.** *For further information, Circle D on the COSMIC Request Card.*
*GSC-12671*

## Simplified Thermal Analyzer — VAX Version

### An easy-to-use program for analyzing instrument temperature distribution and power balance

The DEC VAX 11/780 version of the Simplified Shuttle Payload Thermal Analyzer (SSPTA) aids in evaluating the thermal design of instruments to be flown in the Space Shuttle cargo bay. [The IBM 370 version of SSPTA is described in "Simplified Thermal Analyzer" (GSC-12638) on page 360 of *NASA Tech Briefs*, Vol. 5, No. 3.]

SSPTA is a collection of programs that are currently used in the thermal analysis of spacecraft, modified for quick, preliminary analysis of payloads. Although designed primarily to analyze Shuttle payloads, it can easily be used for thermal analysis in other situations.

SSPTA includes a reduced math model of the Shuttle cargo bay. One of the prime objectives in developing SSPTA was to create an easily used program. With it, the user-required input is simple, and the user is free from many of the concerns of computer usage, such as disk-space handling, tape usage, and complicated program control.

SSPTA is comprised of a system of data files called "bins," a master program, and a set of thermal subprograms. The bin system is a collection of disk files that contain data required by or computed by the thermal subprograms. SSPTA currently handles 50 bins.

The master program serves primarily as a manager for the bins and their interaction with the thermal subprograms. Inputs to the master program are simple user commands that direct the data manipulation procedures, prepare the data for these procedures, and call the appropriate thermal subprograms. The subprograms of SSPTA are all based on programs that have been used extensively in the analysis of orbiting spacecraft and space hardware.

Subprogram CONSHAD uses the user-supplied geometric radiation model to compute blackbody view factors, shadow factors, and a description of the surface model. The subprogram WORKSHEET uses the surface-model description, optical-property data, and node-assignment data to prepare input for SCRIPTF, which computes the inverses of the infrared (IR) and ultraviolet (UV) radiation transfer equations. SCRIPTF also computes the radiation coupling between nodes in the thermal model.

Subprogram ORBITAL uses the shadow tables to compute incident flux intensities on each surface in the geometric model. In subprogram ABSORB, these flux intensities are combined with the IR and UV inverses to compute the IR and UV fluxes absorbed by each surface. The radiation couplings from SCRIPTF and the absorbed fluxes from ABSORB are used by subprogram TTA to compute the temperature and power balance for each node in the thermal model.

Outputs consist of tabulated data from each of the subprograms executed during an analysis. Because SSPTA is modular, analyses may be run in whole or in part, and new subprograms may be added.

This VAX version of SSPTA is written in FORTRAN IV for batch execution and has been implemented on the DEC VAX 11/780 computer. This adaptation of SSPTA to the VAX was performed in 1980.

*This program was submitted by Joseph T. Skladany of* **Goddard Space Flight Center.** *For further information Circle E on the COSMIC Request Card.*
*GSC-12698*

## Aerodynamics of Supersonic Aircraft

### An integrated system for the analysis of supersonic configurations

A system for the design and analysis of supersonic aircraft consists of an executive driver and eight basic computer programs that build up the force coefficients of a selected configuration. The system employs modified linearized theory for the calculation of surface pressures and employs supersonic--area-rule concepts in combination with linearized theory for the calculation of aerodynamic force coefficients. The objective of the integrated system is easy-to-use supersonic design and analysis capability, with recognition of the need for constraints on linear theory to provide physical realism and with allowance for design control over the optimization cycles.

Within the system, the executive driver invokes individual modules to provide the data and computations required for configuration design or analysis. In one module, skin friction drag is computed using turbulent flat-plate theory. Wave drag is calculated in either the far-field (supersonic-area-rule) module or the near-field (surface-pressure-integration) module. The far-field module is used for wave-drag-coefficient calculations and for fuselage optimization according to area-rule concepts. The near-field module is used primarily as an analysis tool, where detailed pressure distributions are of interest.

Lifting pressures, drag due to lift, pitching moment, and trim drag are computed by the lift-analysis module, which divides the components of the configuration into a mosaic of "mach-box" rectilinear elements that are employed in obtaining linear-theory solutions. A complementary wing-desgn and optimization module computes the wing shape required to suport an optimized pressure distribution at a specified flight condition.

A geometry module handles configuration geometry. The user prepares only "drawing-type" geometry data; all "paneling" of the configuration for the-

(continued on next page)

oretical analyses is handled by the system, which requires a minimum of user-prepared input data.

The wing-pressure module summarizes and tabulates for output the wing surface-pressure data for user-specified conditions. A plot module draws configuration pictures according to user-specified size and view parameters.

The system is written in FORTRAN IV for batch execution and has been implemented on a CDC CYBER 175 with an overlaid central-memory requirement of approximately 135K (octal) of 60-bit words. Plotted output is generated for a CALCOMP plotting system. The system was developed in 1980.

*This program was written by W. D. Middleton, J. L. Lundry, and R. G. Coleman of The Boeing Co. for* **Langley Research Center.** *For further information, Circle F on the COSMIC Request Card.*
*LAR-12857*

## Dynamic-Loads Analysis of Flexible Aircraft With Active Controls

A versatile program system calculates aeroelastic effects due to turbulence and control inputs.

An integrated system of stand-alone computer programs, DYLOFLEX, analyzes dynamic loads on flexible aircraft with active controls. Large, flexible-flight vehicles and control-configured vehicles necessitate advanced analytic techniques to determine aeroelastic effects on stability and control, gust design loads, and ride qualities. DYLOFLEX capabilities include calculating dynamic loads due to continuous atmospheric turbulence, discrete gusts, and discrete control inputs. Its output includes statistical quantities and time histories describing the dynamic loads.

The individual programs in DYLOFLEX communicate with each other via externally stored files. Generally, separate execution of the individual programs is preferred so that intermediate results may be inspected. However, it is possible to execute several DYLOFLEX programs in a single sequential run.

The DYLOFLEX design philosophy is to provide for maximum versatility in the types of structural and aerodynamic models that may be used as inputs and in the types of analyses that may be performed. DYLOFLEX accepts externally-generated structural data (mode shapes, generalized mass and stiffness matrices, and lumped masses at structural nodes) from either a finite-element or a lumped-mass-beam analysis. Free-free or cantilever modes are accepted; either may be appended with rigid-body or cantiliver control-surface modes . DYLOFLEX processes up to 70 modes.

The aerodynamics generated within DYLOFLEX may represent either subsonic or supersonic flow. The degree of unsteadiness may range from quasi-steady (steady flow modified with indicial-lift-growth function) to fully unsteady (available for subsonic flow only). The analysis of the aerodynamics due to gusts includes the effects of gradual gust penetration. DYLOFLEX permits a maximum of 400 aerodynamic singularities, which may be distributed over lifting surfaces, slender bodies, and interference surfaces.

The equations of motion used in the DYLOFLEX analyses are linearized small-perturbation equations, which describe the aircraft motions and active-control-system perturbations about a trimmed, straight-and-level, 1-g flight condition. In these equations of motion, the longitudinal and lateral equations are decoupled. Within DYLOFLEX, the equations of motion may be written for a maximum of 70 degrees of freedom (including flexible, rigid-body, control-surface, and active-control-system degrees of freedom in any combination). The loads equations are written using the method of summation of forces and may be calculated at any location on the aircraft and about any arbitrary axis on the vehicle.

The results of a DYLOFLEX analysis consist of statistical measures of the dynamic loads calculated using random harmonic-analysis techniques and time histories of the dynamic loads obtained by Fourier-transform techniques. DYLOFLEX is ideal for performing parametric analyses. Once the equations of motion and the loads equations have been obtained, modifying these equations and then solving them with the solution programs involves a fraction of the computational effort that would be required to generate the new equations from scratch and then solve them.

There are eight individual programs in DYLOFLEX. Each may be used alone or in conjunction with other DYLOFLEX programs. The programs are:

1. The Modal Interpolation Program (INTERP),
2. The Doublet-Lattice Unsteady Aerodynamic Program (DUBFLX),
3. The Equations-of-Motion Program (EOM),
4. The loads Equation Program (LOADS),
5. The Equation-modifying Program (EQMOD),
6. The Linear-System Analysis Program (QR),
7. The Random Harmonic-Analysis Program (TEV156), and
8. The Time-History Solution Program (TEV126).

DYLOFLEX is written in FORTRAN IV and COMPASS for batch execution and has been implemented on a CDC 6600 computer using the NOS 1.2 operating system. The programs in DYLOFLEX have central memory requirements of approximately 200K (octal) of 60-bit words. The DYLOFLEX system was developed in 1979.

*This program was written by Boyd Perry III and Barbara J. Durling of* **Langley Research Center** *and Richard I. Kroll, Ronald D. Miller, Mack Y. Hirayama, and Richard E. Clemmons of The Boeing Co. For further information, Circle G on the COSMIC Request Card.*
*LAR-12747*

# Machinery

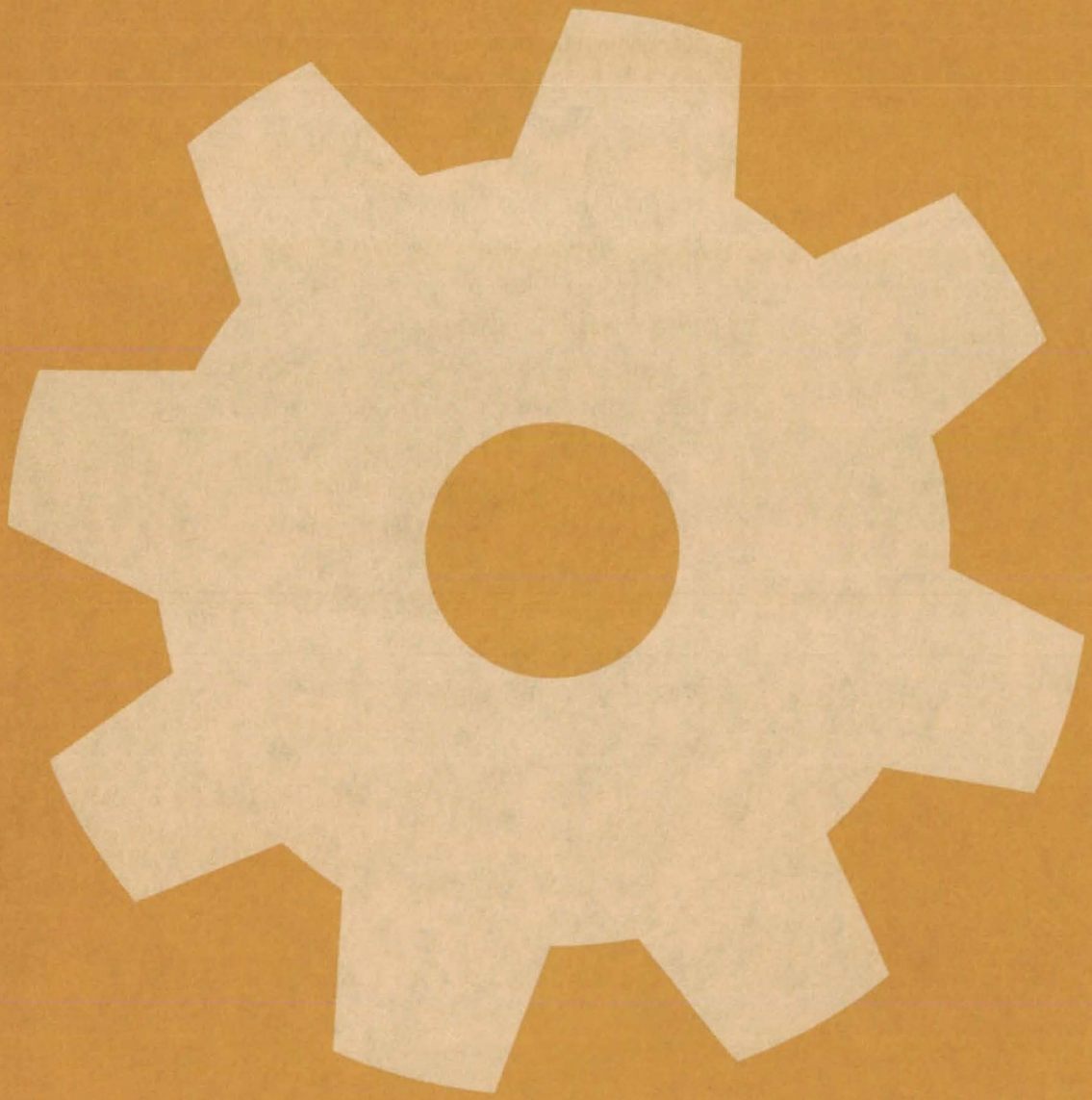

## Hardware, Techniques, and Processes

# Simpler Variable-Speed Drive for Fan or Pump

Static pressure is used directly to control speed.

*Goddard Space Flight Center, Greenbelt, Maryland*

The static pressure developed by a fan or pump is used directly to control its speed in a new drive unit. The system is simpler and more economical than many other speed controllers, although it is less accurate and has a narrower speed range. However, since very accurate control is not usually required for fans and pumps, the unit would work well in many applications.

In the new system, shown in the photographs, the main drive motor turns a spring-biased variable-sheave pulley. Pivoting the motor changes the belt tension, causing the variable pulley to change its pitch diameter and varying the speed of the fan or pump attached to the output pulley.

The motor is made to pivot by using fan or pump pressure directly to drive hydraulic or pneumatic damper motors, which extend or retract pistons connected by pivots to the main motor. An increase in pressure pivots the motor in the direction that increases belt tension. This decreases the pulley diameter and slows the speed of the driven fan or pump. If the pressure decreases, the motor is pivoted to increase the fan or pump speed.

The same principle can be applied in other geometries. For example, the motor need not be pivoted. Instead, the damper motor can drive an idler pulley to change the belt tension. The ratio of maximum to minimum speed can be increased by using two variable-speed pulleys on one shaft in an idler arrangement with two V-belts. A belt from the main motor drives one of the variable pulleys. A second belt drives the fan or pump from the second variable pulley on the shaft. By using the damper motors to swing the shaft with the variable pulleys closer to or farther from the main motor, the speed of the fan or pump may be decreased or increased, respectively. The effective diameters of both variable pulleys change, one getting larger as the other gets smaller.

*This work was done by Henry D. Obler of* **Goddard Space Flight Center.** *For further information, Circle 57 on the TSP Request Card.*

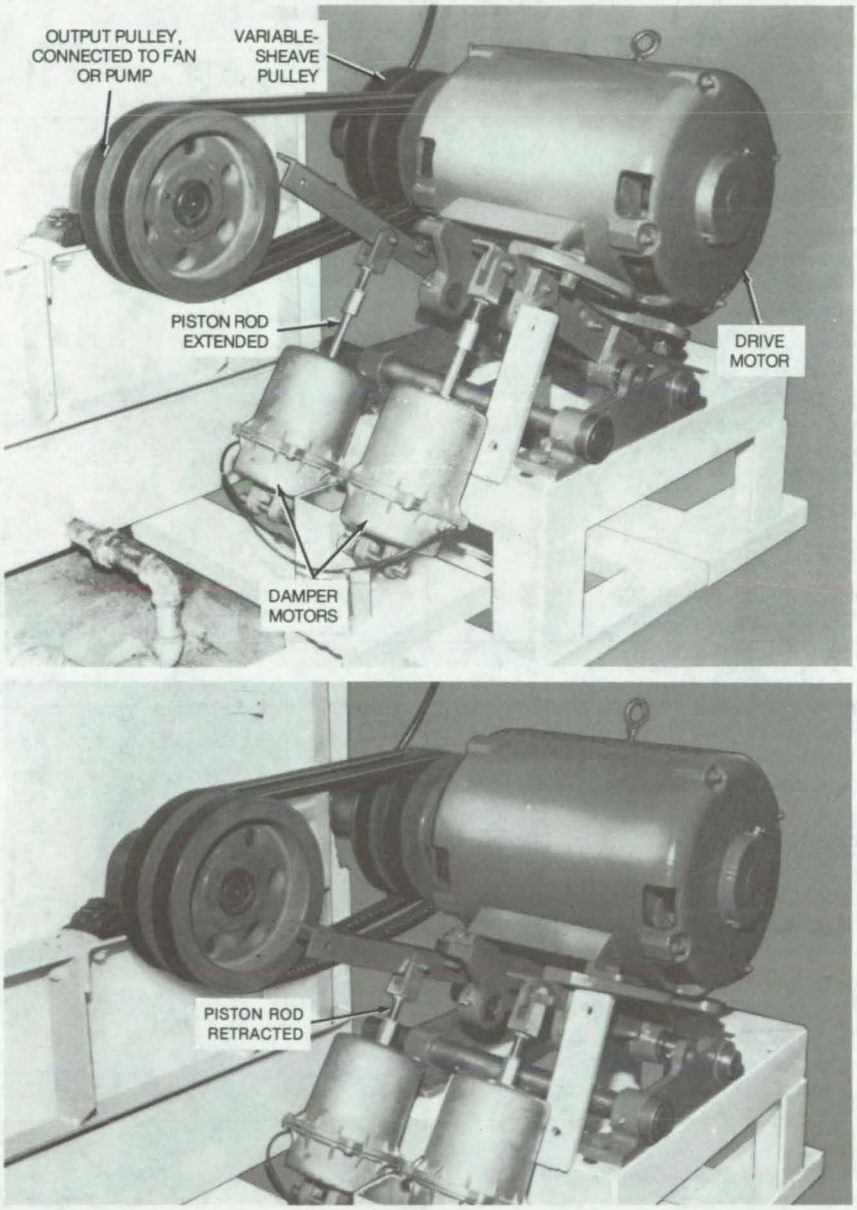


**The Variable-Speed Drive** is controlled by negative feedback of pump or fan pressure. Pneumatic motors activated by the pressure signal pivot the main drive motor, changing belt tension and causing the effective diameter of the variable pulley to change. An increase in pressure extends the piston rods (top), increasing the belt tension and slowing the belt; a decrease in pressure retracts the piston rods (bottom), increasing the belt speed.

*This invention is owned by NASA, and a patent application has been filed. Inquiries concerning nonexclusive or exclusive license for its commercial development should be addressed to the Patent Counsel, Goddard Space Flight Center [see page A5]. Refer to GSC-12643.*

# Magnetic Bearing Consumes Low Power

Linear noncontacting bearing operates in environments where lubricants cannot be used.

*Goddard Space Flight Center, Greenbelt, Maryland*

An energy-efficient linear magnetic bearing maintains a precise small separation between its moving and stationary parts. Originally designed for a cryogenic compressor on a spacecraft, the proposed magnetic bearing offers an alternative to roller or gas bearings in linear motion systems.

One form of the proposed bearing consists of a permanent magnet/electromagnet stator within the bore of a movable tubular element (see figure). The permanent magnet provides a high dc magnetic flux in the airgaps; modulation of these flux levels by the control coil current centers the longitudinal axis of the tube surrounding the stator.

At the ends of the permanent magnet are armatures wound with coils. These electromagnets provide a "vernier" magnetic flux so that the moving element is suspended precisely equidistant from the surfaces of the stator. The currents through the windings are continuously adjusted by external automatic control circuitry to maintain a constant gap.

The permanent magnet supplies most of the total flux at no expenditure of power. The electromagnets can therefore apply a high control force with little current, since the force is determined by the product of the flux of the electromagnets and the flux from the permanent magnet. Moreover, the control flux approaches zero as the movable element is centered, for further savings in power and reduced heat dissipation.

The permanent-magnet flux extends longitudinally from the magnet to the armature, then radially through the gap. The permanent-magnet flux continues along the tube wall, through the gap once more, and back to the magnet. Flux from the electromagnet coils also jumps the gap, but returns circumferentially — not longitudinally — through the tube.

Coils on diametrically opposed arms (for example, coils 1 and 2 in the figure) are connected in series, and their current is controlled by an error signal that corrects differences in the gaps on opposite sides. The error signal can be generated by position sensors mounted at each end of the armatures facing the inner wall of the tube.

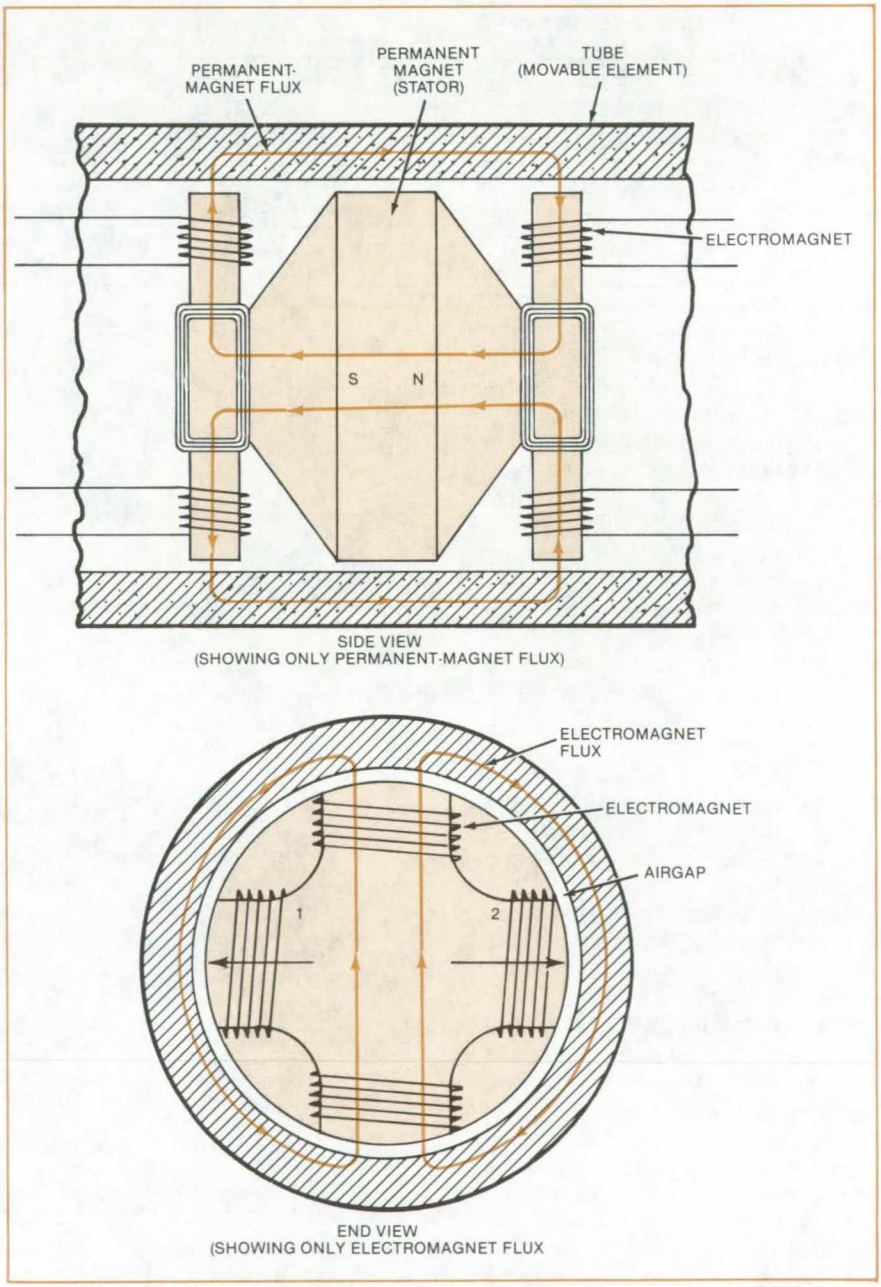


**Flux Lines From Permanent Magnet and Electromagnets** follow separate paths. Flux from the permanent magnet travels longitudinally through the tube wall, as shown in the side view of the magnetic bearing. Flux from the electromagnets travels circumferentially through the tube wall as shown in the end view.

*This work was done by Philip A. Studer of* **Goddard Space Flight Center.** *For further information, Circle 57 on the TSP Request Card.*

*This invention is owned by NASA, and a patent application has been filed. Inquiries concerning nonexclusive or exclusive license for its commercial development should be addressed to the Patent Counsel, Goddard Space Flight Center [see page A5]. Refer to GSC-12517.*

# Magnetic Bearing With Active Control

Self-regulating bearing includes velocity and position control.

*Goddard Space Flight Center, Greenbelt, Maryland*

A new magnetic shaft bearing employs electromagnets energized by signals related to shaft position and velocity. The electromagnets are arranged in orthogonal pairs. Axial and rotational shaft motions are accommodated, and lateral motions are restrained. Axial motion can also be restrained.

The figure shows a shaft with a bearing on each end. Each bearing includes four electromagnets. Magnetic flux passes from each magnet core through the gap and into the shaft, axially along the shaft, and then back through the gap into the core. The shaft, or at least the portion in the region of the bearings, is made from cold-rolled steel or other ferromagnetic material.

Power to each pair of magnets (consisting of the two on opposite sides of the shaft) is supplied by a feedback-control amplifier circuit. Eddy-current or capacitive probes sense the lateral shaft displacement along the two orthogonal axes corresponding to the magnet pairs. Each probe signal is compared with a reference voltage that corresponds to the central shaft position, and an error signal is developed. The shaft-position signal is also fed to a differentiator to obtain a velocity signal.

The position-error and velocity signals are summed and processed in a phase-shifting amplifier, which corrects for phase errors arising from eddy currents and inductances of the magnets. The amplified phase-corrected signals are fed to the pair of electromagnet coils through steering diodes. Thus, for example, a high shaft position or an upward velocity will cause the bottom coil to be energized to pull the shaft downward. The stiffness and damping of the bearing are determined, respectively, by the gains in the position and velocity portions of the circuit.

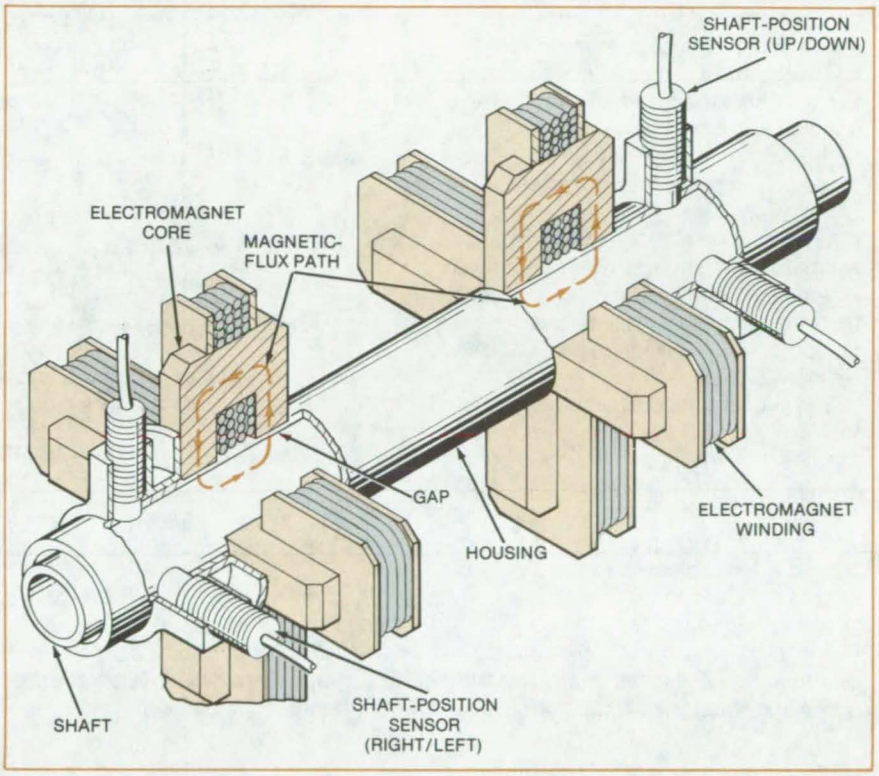


**Self-Regulating Magnetic Bearings** employ position sensors and electromagnets to restrain lateral motions of the shaft. If desired, axial motion of the shaft can also be restrained by magnets at the end of the shaft.

Axial shaft motion can be restrained by opposing permanent magnets at one end of the shaft. If an oscillatory axial motion is desired, then a signal of the appropriate frequency is applied to an axial electromagnet to modulate the permanent-magnet field.

While the lateral shaft motion could be controlled by three electromagnets at each bearing, interactions among the electromagnets would require more complex circuitry. The orthogonal arrangement eliminates interactions between the magnet pairs and between lateral motions along the two axes.

*This work was done by M. Goldowsky of North American Philips Corp. for* **Goddard Space Flight Center.** *For further information, Circle 58 on the TSP Request Card.*

*This invention is owned by NASA, and a patent application has been filed. Inquiries concerning nonexclusive or exclusive license for its commercial development should be addressed to the Patent Counsel, Goddard Space Flight Center [see page A5]. Refer to GSC-12582.*

# Spring Support for Turbopump Rotor Bearing

Bearing support is compatible with liquid oxygen.

*Marshall Space Flight Center, Alabama*

A novel bearing support for liquid-oxygen turbopumps protects against impact loads while avoiding a major disadvantage of earlier flexible supports. It allows the controlled axial movement necessary for proper operation of the pressure-operated pump impeller. While spring-loading the rotor to the midpoint of the axial movement to avoid impact-load damage to the turbopump components.

Previously, the inner part of a two-piece bearing support with interlocking antirotation lugs would be sprung by two opposing Belleville-spring washers. This support was dangerous when used with liquid oxygen because fretting friction generated local hotspots that could reach ignition temperatures.

The present support also comprises two pieces, but the inner part incorporates a beam-type cylindrical spring. As shown in the figure, alternating slots are machined into the cylindrical part. This results in a series of interconnected curved beams that can deflect in an axial direction.

Antirotation lugs are not required in this design. There are no spots concentrated loading in which fretting friction can generate high temperatures.

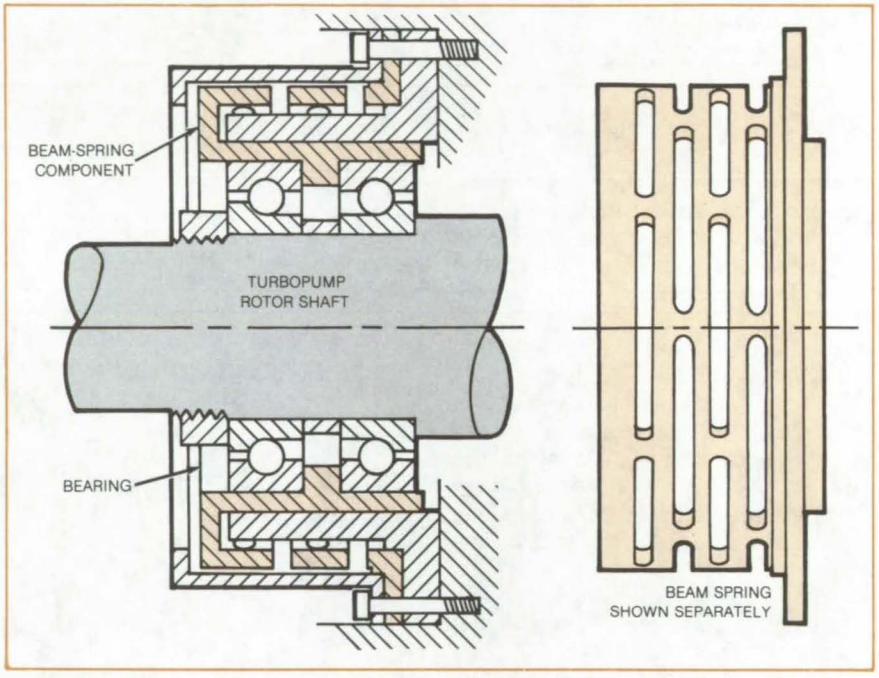


**The Spring Bearing Support** is made by machining azimuthal slots in the cylindrical portion. The resulting structure permits controlled axial deformations.

*This work was done by M. L. Stangeland and C. T. Ellingboe of Rockwell International Corp. for* **Marshall Space Flight Center.** *No further documentation is available.*

*Inquiries concerning rights for the commercial use of this invention should be addressed to the Patent Counsel, Marshall Space Flight Center [see page A5]. Refer to MFS-19624.*

# "Bottle-Brush" Heat Exchanger

Fluid is heated throughout the cross section of the tube.

*NASA's Jet Propulsion Laboratory, Pasadena, California*

An improvement in the simple tubular heat exchanger increases its effectiveness by transferring heat throughout the volume instead of merely at the wall. The modified structure (see figure) consists of a metal tube with metal wires extending radially inward.

If the outside of the tube is heated (for example, by a surrounding heating coil), heat conduction through the wall of the tube and through the radial conductors uniformly heats the cross section of the tube. If necessary, a hollow stem, as shown in the lower part of the figure, can carry a fluid in the opposite direction.

To fabricate the heat exchanger, a cylindrical brush is constructed, consisting of a solid or hollow stem and evenly-spaced radial wires of equal length. The wires are typically of copper or another good heat conductor. Orienting the wires radially minimizes the length of the conducting path, thus minimizing the thermal resistance.

The outside diameter of the brush is slightly greater than the inside diameter of the heat-exchanger tube, so that the wires are forced into contact with the wall upon insertion. The wall is pretinned, and the

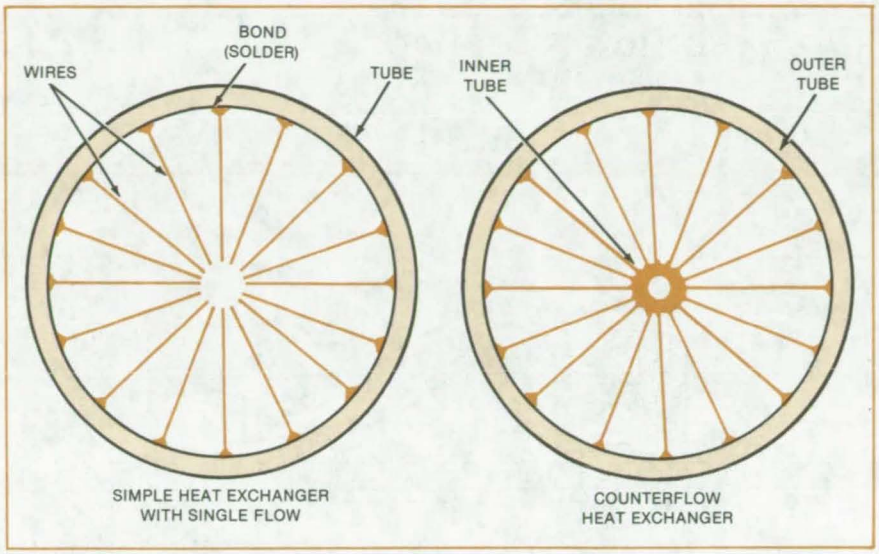


The **"Bottle-Brush" Heat Exchanger** consists of a metal tube with wires extending inward from the wall. The conduction of heat along the wires improves heat transfer to the gas or other filling.

assembly is heated after insertion to solder the wires to the wall. If desired, the stem may be removed after soldering (for example, by electric-discharge machining).

The new heat exchanger is intended for heat transfer to a powdered absorber in an adsorption compressor used as a gas source for a cryogenic refrigerator. It can be used in other systems requiring that heat exchange between particles and a tube. Suggested applications include other kinds of refrigerators, heat engines, thermal instrumentation, and heat switches.

*This work was done by Emanuel Tward and John R. Gatewood of Caltech for* **NASA's Jet Propulsion Laboratory.** *For further information, Circle 59 on the TSP Request Card.*
*NPO-15479*

## Cam-Design Torque Wrench

An eccentric wrench increases its grip as more torque is applied.

*Marshall Space Flight Center, Alabama*

A new torque wrench for electrical connectors automatically tightens its grip with increasing torque to insure against slippage. It requires only minimal clearance between the connector and adjacent structures or components. The wrench is operated with one hand and can be used on connectors of various shapes. A set of such wrenches would accommodate a range of connector sizes.

Strict requirements on torque are imposed on many critical electrical connectors. For those that require low torques, a tool must be used that firmly grasps the connector shell without slippage so that the torque can be measured accurately.

The new wrench (see figure) with an eccentric wheel acting as a cam provides higher frictional loads on the connector as the torque is increased. This eliminates slippage between the wrench and the connector. The gripping surfaces of the tool are plastic to prevent damage to the surface finish of the connector.

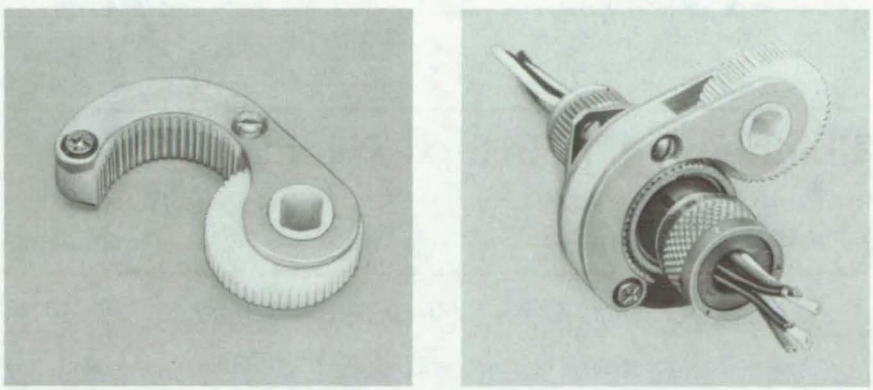

**Cam-Design Torque Wrench** is shown open (left) and applied to an electrical connector (right).

*This work was done by Paul H. Schick, Jr., and S. A. Gattuso of Rockwell International Corp. for* **Marshall Space Flight Center.** *No further documentation is available.*

*Inquiries concerning rights for the commercial use of this invention should be addressed to the Patent Counsel, Marshall Space Flight Center* [see page A5]. *Refer to MFS-19586.*

# Clamp Restrains Pressure Line

A safety restraint protects people and property if a high-pressure fitting fails.

*John F. Kennedy Space Center, Florida*

A safety restraint proposed for high-pressure hoses would protect nearby workers if a hose fitting fails. Originally suggested as a way of restraining flexible gas-transmission hose at Kennedy Space Center, the clamp could be added to existing hoses in other applications; or it can be included in new hose installations.

Shown in the figure, the clamp is installed around the end of the hose near the fitting. It is attached by cable to an eyelet on an adjacent wall or other nearby rigid surface.

As long as the pressure line remains attached at the fitting, the clamp exerts essentially no force on the hose. If the fitting fails, however, the force of the fluid leaving the free end of the hose causes the cam on the clamp to compress the hose with a positive locking action. The clamp and cable thus prevent the hose from whipping violently and possibly injuring workers or damaging objects.

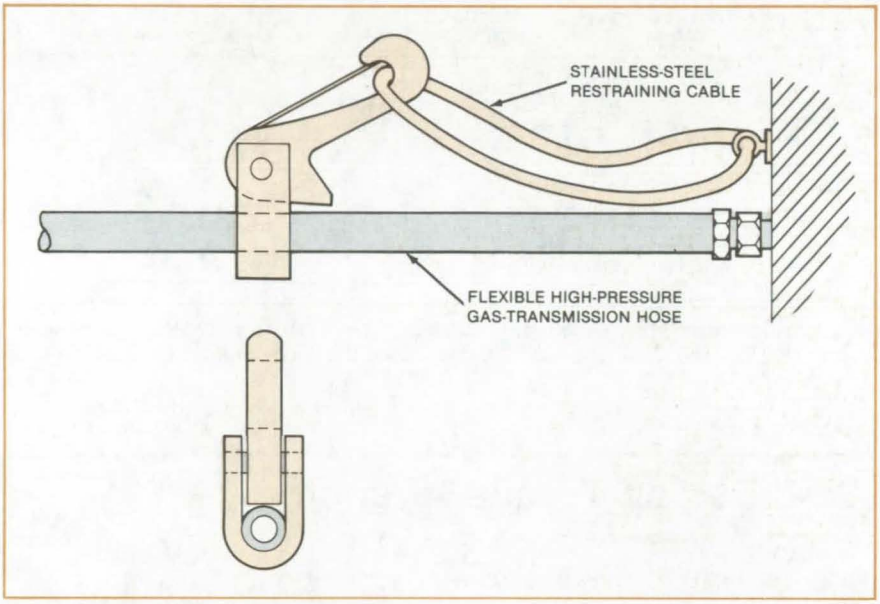


**Safety Restraint for Transmission Hose** applies a positive grip if the coupling fails while the hose is pressurized.

*This work was done by James A. Aliberti of* **Kennedy Space Center.** *No further documentation is available.*

*Inquiries concerning rights for the commercial use of this invention should be addressed to the Patent Counsel, Kennedy Space Center [see page A5]. Refer to KSC-11205.*

# Unidirectional Flexural Pivot

Durable pivot rotates in only one direction.

*Goddard Space Flight Center, Greenbelt, Maryland*

A new flexural pivot deflects in only one angular direction (either clockwise or counterclockwise) and has a longer operating life than many previous designs. (A flexural pivot is a frictionless bearing that is particularly suitable for small angular deflection; it is made with crossed spring elements and needs no lubrication.)

As the figure shows, the new pivot consists of two rings interconnected by three flat metal parallelograms (the springs) welded into grooves or slots in the inside diameters of the rings. The metal springs lie along chords of the inside diameter of the structure; that is, the spring that is welded in a slot at about 2 o'clock in ring A is welded into a slot at 6 o'clock in ring B.

The springs prevent the rings from moving axially either toward or away from each other. Moveover, they allow relative rotation of the two rings in only one direction. For the connections shown in the figure, ring A can rotate clockwise relative to ring B, because such rotation compresses or shortens the springs; the springs can do so by bowing outward (i.e., buckling) slightly. The rotation of ring A counterclockwise relative to ring B would require that the springs stretch or lengthen; they can not do so, and therefore the counterclockwise rotation is not possible. The direction of rotation is reversed simply by reversing the slants of the springs.

In previous flexural pivots, the springs were subjected to considerable tensile stress that tended to cause frac-

turing at their attachments to the outer rings. In the new pivots, the springs flex (that is, they elastically buckle) to relieve the compressive stress imparted by the angular rotation. There is no tensile stress at the joints: Fractures due to tensile stress are thereby eliminated, and the pivot lasts longer.

*This work was done by Hossein Bahiman of* **Goddard Space Flight Center.** *For further information, Circle 60 on the TSP Request Card.*

*This invention is owned by NASA, and a patent application has been filed. Inquiries concerning nonexclusive or exclusive license for its commercial development should be addressed to the Patent Counsel, Goddard Space Flight Center [see page A5]. Refer to GSC-12622.*

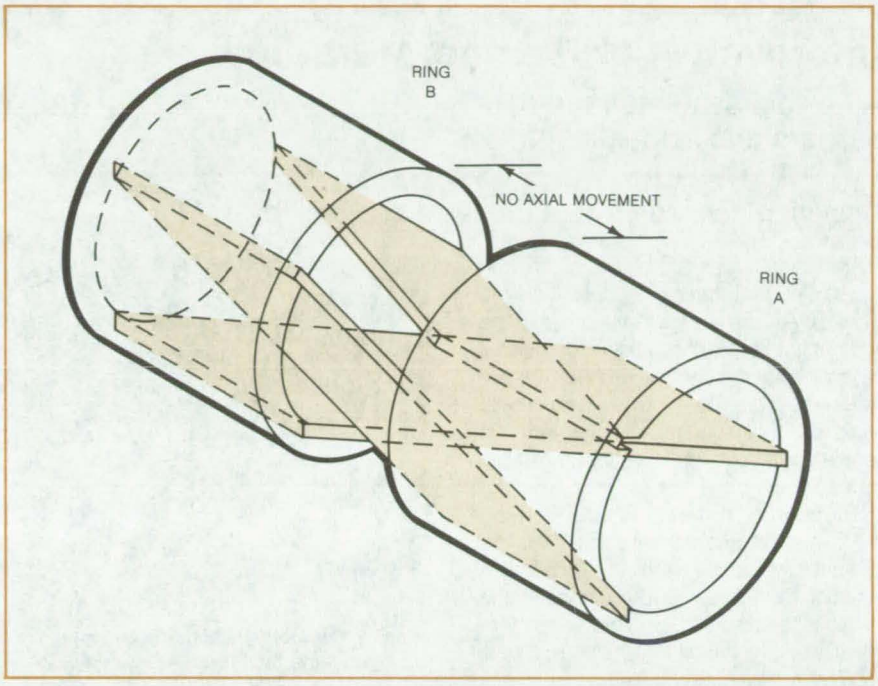


In this **Unidirectional Flexural Pivot,** two coaxial rings are fastened in a connection that is rigid for axial motion, is rigid for one direction of rotation, but permits flexure for the opposite direction of rotation.

# Technique for Machining Glass

A process for machining glass with conventional carbide tools

*Goddard Space Flight Center, Greenbelt, Maryland*

Small holes are machined in glass by ordinary carbide tools if the operation is done carefully and the right lubricant is used. The procedure is in use in the Optical Laboratory at Goddard Space Flight Center for such diverse applications as drilling mounting holes in curved mirror blanks, drilling feedthrough sensor holes in fiber-optic bundles, and milling grooves in crown glass.

A small quantity of a lubricant for aluminum such as Steco TAP MAGIC lubricating oil, or equivalent, is applied to the area of the glass to be machined; and a carbide tool — typically a tungsten carbide drill bit driven by a drill press at 1,800 revolutions per minute — is placed against the workpiece with light pressure (see figure). Periodically the tool is raised to clear the work of glass dust and particles. Additional lubricant is applied as lubricant is displaced. Milling is carried out in a series of 5- to 10-mil (0.1- to 0.2-mm) steps.

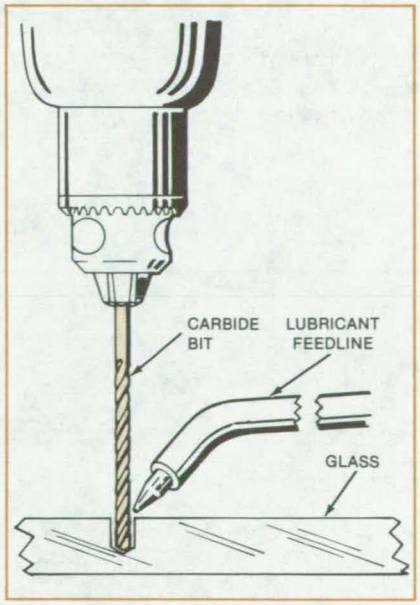


A **Precise Hole** is drilled in glass with a standard carbide bit ranging in diameter from 0.018 inch (0.5 mm) to 0.125 inch (3.2 mm).

The edges, rims, wall, and floor surfaces of machined areas appear smooth to visual inspection and to the touch.

*This work was done by Stephen H. Rice of* **Goddard Space Flight Center.** *For further information, Circle 61 on the TSP Request Card.*

*This invention is owned by NASA, and a patent application has been filed. Inquiries concerning nonexclusive or exclusive license for its commercial development should be addressed to the Patent Counsel, Goddard Space Flight Center [see page A5]. Refer to GSC-12636.*

# Improved High-Temperature Seal

A flexible seal has four barriers against leakage.

*Lyndon B. Johnson Space Center, Houston, Texas*

The high-temperature seals on the Space Shuttle orbiter elevons will be improved by a new design that increases the number of leak barriers, allows for thermal expansion, and cuts the weight by more than two-thirds. The improved seal should be useful in other applications where it is necessary to seal gaps between moving surfaces.

The main components of the seal, seen in Figure 1, are constructed from Inconel (or equivalent alloy) metal foil. An outer foil wrapper maintains contact between the surfaces to be sealed, which are the cylindrical tube and the baseplate in this mockup. The foil wrapper is formed into telescoping sections, allowing for length adjustment to compensate for temperature changes. There is a double thickness of foil wrapper over most of the length.

A secondary seal, which is enclosed within the outer seal, consists of a ceramic cloth sleeve wrapped around a foil tube containing an alumina mat filler. As shown in Figure 2, the seal presents four barriers to airflow. The previous design, described in "Improved Wrapped-Curtain Seal" on page 435 of *NASA Tech Briefs,* Vol. 4, No. 3, had only two flow barriers. A weight reduction of the Space Shuttle orbiter elevon seals from 138 to 32 lb (63 to 20 kg) is expected.

*This work was done by Kenneth E. Wood, Paul P. Zebus, and Alan R. Olson of Rockwell International Corp. for* **Johnson Space Center.** *No further documentation is available.*
*MSC-18790*

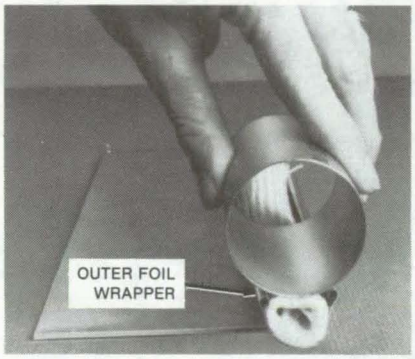


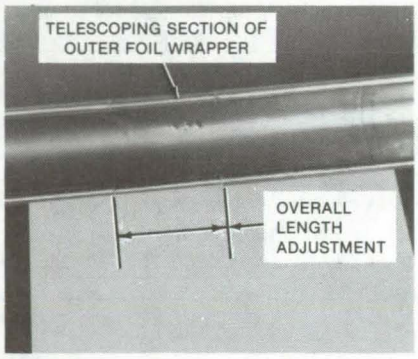


Figure 1. **Components of the Telescoping Elevon Seal** are shown in a mockup. Here, the cylindrical tube and the baseplate represent the surfaces to be sealed.

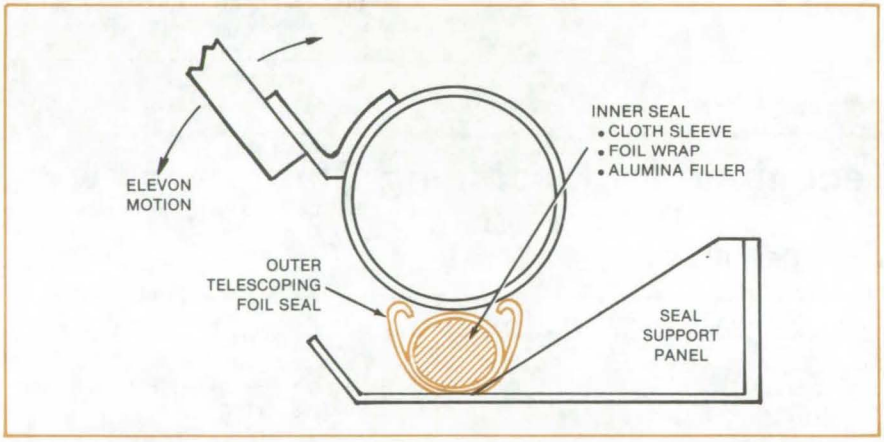


Figure 2. The **Improved Seal** presents four barriers to airflow, instead of only two as in the previous design.

# Compact Liquid Deaerator

Gas escapes quickly from thin liquid films sprayed in vacuum.

*Lyndon B. Johnson Space Center, Houston, Texas*

Gases are removed from liquids by a new deaerator that takes up only 5 inches (12.7 cm) at the top of a medium-sized storage tank. It has a multiple cascading header that exposes more fluid at lower pressures than typical commercial deaerators.

The deaerator was originally developed for a potable-water tank aboard the Space Shuttle, but it can be used in other fluid systems where gas-free liquids are essential. Potential applications are in hydraulic systems for aircraft and heavy machinery, in cooling systems where maximum heat transfer is needed, and in pumping systems where deaerated liquid is needed to prevent cavitation of the pump. It can also maintain a uniform mixture in liquids that stratify or settle.

Forced into the deaerator by an external pump, the liquid discharges through

an annulus chamber and sets of headers having adjustable gaps. The gaps expel the liquid as thin films that are exposed to a partial vacuum (see figure). The gaps are adjusted for uniform and smooth flow without ripples and turbulence.

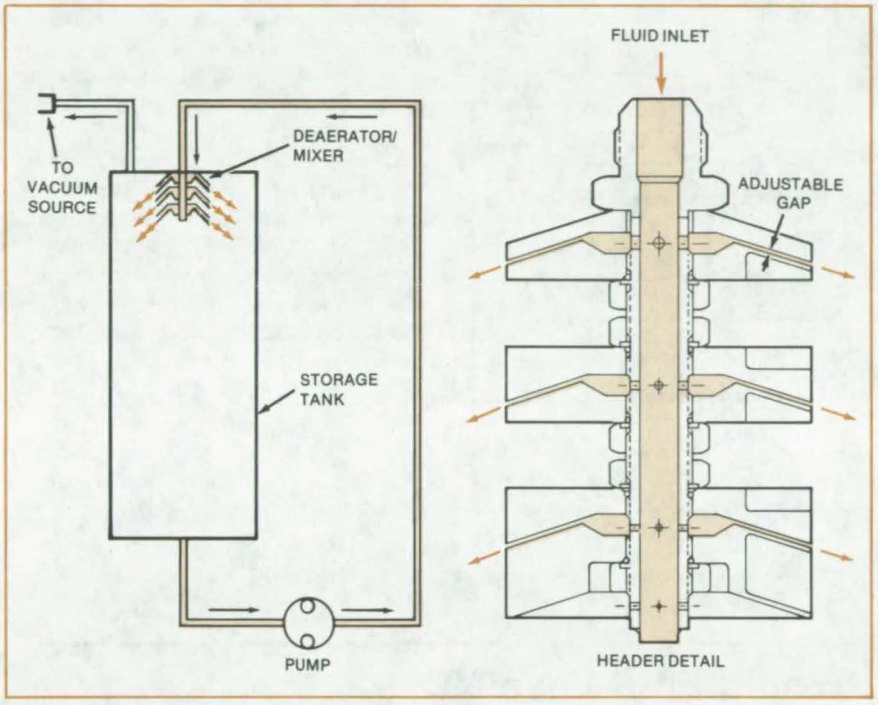


**Deaerator/Mixer Spills Smooth Cascades** of liquid through a vacuum, into which dissolved gases evaporate. The liquid-discharge gap — and the thickness of the cascade film — can be adjusted according to the liquid-discharge and storage-tank pressures to ensure most efficient gas removal.

The thinner the liquid film, the faster the rate of outdiffusion of gases; and the greater the film area, the greater the rate of deaeration. In its present form, the deaerator furnishes up to 1,050 in.$^2$ (6,774 cm$^2$) of liquid area in a tank 29 inches (74 cm) in diameter. In a larger tank, it would spray the liquid over an even larger area. The nominal operating pressure is 2.5 to 7.5 psig (17 to 51 kN/m$^2$). At higher pressures, the exposure area can be doubled. Since the fluid is sprayed circumferentially, local stratification is prevented, and mixing is assisted.

The pressure level of the partial vacuum should be kept above the vapor pressure of the fluid to prevent loss of the fluid by evaporation in the vacuum. If a vacuum below the fluid vapor pressure is needed, chilling the fluid will help to reduce loss.

*This work was done by Samuel T. Yamauchi of Rockwell International Corp. for* **Johnson Space Center.** *No further documentation is available.*

*Inquiries concerning rights for the commercial use of this invention should be addressed to the Patent Counsel, Johnson Space Center [see page A5]. Refer to MSC-18936.*

# Touch Sensor Responds to Contact Pressure

Measurement of contact pressure improves the sensitivity of robot manipulators.

*NASA's Jet Propulsion Laboratory, Pasadena, California*

A new pressure sensor for a mechanical hand gives better feedback of the gripping force and more-sensitive indication of when the hand contacts an object. Optical fibers bring light into cells on the gripping surface. Light is reflected from a flexible covering into other fibers leading to detectors. Distortion due to tactile pressure changes the amount of reflected light.

The new device is superior to previous sensors. For example, television or other direct-viewing systems are not sensitive to contact pressure, and the contact area is often hidden from view. Electrical sensors are subject to electrical noise, especially at the low signal levels associated with low contact pressure. Optical sensors have been used to detect proximity [see "Fiber-Optic Proximity Sensor" (NPO-14653) on page 408 of *NASA Tech Briefs,* Vol. 4, No. 3] or contact but not contact pressure.

The new optical sensor is illustrated in the figure. The sensing surface of the hand is divided into cells by opaque partitions. An optical fiber brings light into each cell from a lamp, light-emitting diode, or other source. Another fiber carries light from the cell to a detector; for example, a photodiode or phototransistor. The cells are covered by an elastic material with a reflective interior surface. The rest of the cell is coated with a nonreflective material.

As shown in the figure, pressure against a cell cover causes a distortion, which changes the internal reflection of light. The change is sensed by the detector, and the output signal informs the operator of contact. The greater the pressure and distortion, the greater is the change in light reflection. Thus, grip pressure can be sensed using analog circuitry.

If only a touch indication is desired, a threshold detector can be included in the electronics. In an automatic manipulator, the detector signal could control the manipulator movements.

The cells can be arranged such that those in each row share one light source, while those in each column

(continued on next page)

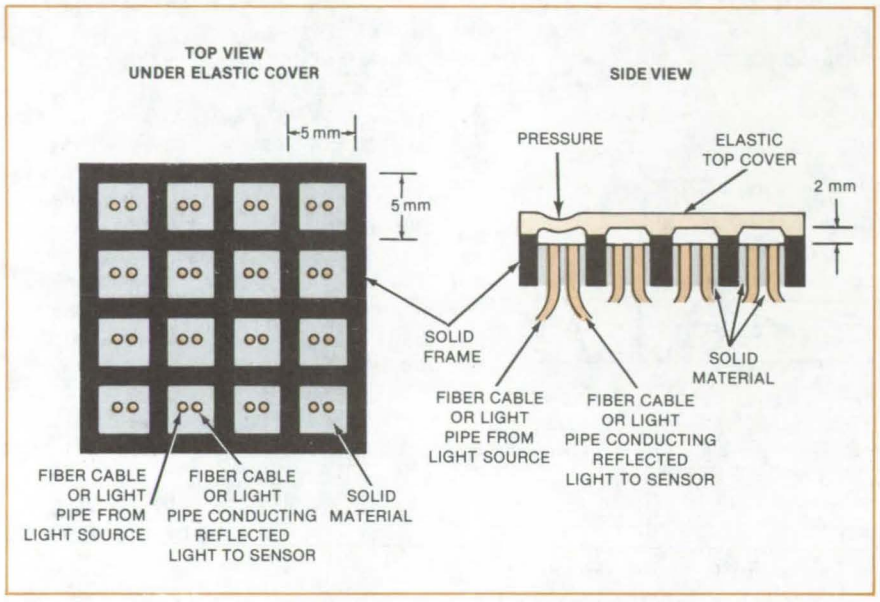


An **Optical Tactile Sensor** for mechanical hands senses contact pressure via the change in light reflected from an elastic covering.

share one detector. This reduces the number of sources and detectors and facilitates scanning. For example, a 10-by-10 matrix would have 100 sensing points while requiring only 10 sources and 10 detectors. The array can be scanned by sequentially pulsing sources and detectors.

*This work was done by Antal K. Bejczy of Caltech for* **NASA's Jet Propulsion Laboratory.** *For further information, Circle 62 on the TSP Request Card.*

*Inquiries concerning rights for the commercial use of this invention should be addressed to the Patent Counsel, NASA Resident Legal Office-JPL [see page A5]. Refer to NPO-15375.*

# Staged Turbojet Engine Would Emit Less NO

## A proposed combustor is simpler than previous multiple-stage designs.

*Ames Research Center, Moffett Field, California*

A new turbojet-engine concept could reduce nitric oxide emissions to a level from one-fifteenth to as little as one three-hundredth that of conventional units. The new multiple-stage combustor could overcome the flame-instability problems associated with previous low-flame-temperature systems. Furthermore, it operates in a relatively-simple adiabatic mode, without elaborate fuel-flow and air-circulation patterns.

In turbojet combustors, three main reactions give rise to nitric oxide:

$$O_2 + N \longrightarrow NO + O \quad (1)$$
$$N_2 + O \longrightarrow NO + N \quad (2)$$
$$OH + N \longrightarrow NO + H \quad (3)$$

The nitric oxide forms at the completion of the combustion process and proceeds at a rate determined by the flame temperature and by $\phi$, the molecular ratio of fuel to air ($\phi = 1.0$ represents a stoichiometric mixture). Under rich and stoichiometric ($\phi \geq 1.0$) conditions, reactions (2) and (3) predominate. Under lean ($\phi < 1.0$) conditions, all three reactions occur at a significant rate, provided that the temperature remains above 2,200 K.

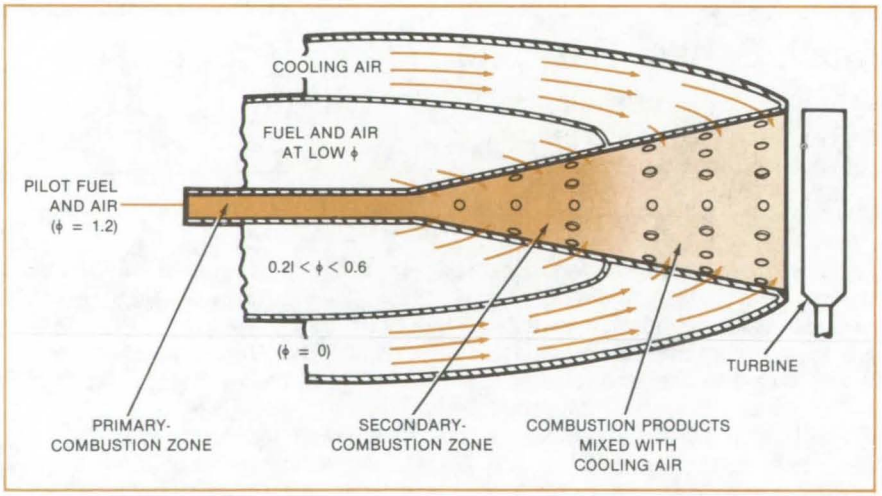


The **Staged-Combustion System** for turbojet engines has three main zones. A rich mixture burns in the primary-combustion zone, igniting a lean mixture in the secondary-combustion zone. Cooling air is added to the combustion products after the secondary-combustion zone. The parameter $\phi$ is the molecular ratio of fuel to air, with $\phi = 1$ representing a stoichiometric mixture.

When the gas temperature decreases below 2,200 K, the rates of formation of nitric oxide become insignificant. Consequently, NO emissions can be reduced if most of the fuel is burned below this temperature. Previously, this was done by elaborate injection and mixing systems, which introduced cooling air into rich-burning com-

bustors, or by lean-burning combustors that were vulnerable to flameout.

An example of the new combustor concept is shown in the figure. A small amount of fuel and air in a rich ($\phi$ = 1.2) mixture is injected into the pilot tube and ignited. The rich mixture assures a hot, stable flame in the primary-combustion zone. This flame produces free radicals that serve as ignition sources for the very-lean secondary-combustion zone. Thus, it acts as a pilot flame to sustain combustion under leaner conditions than would ordinarily support a flame.

Most of the fuel and air are injected into the conical secondary-combustion zone as a lean ($\phi$ = 0.21 to 0.6) mixture. As $\phi$ decreases, so do the flame temperature and the NO emissions. (At adiabatic flame temperatures less than 1,630 K, the flame is calculated to become unstable. This results in a lean-burning limit of $\phi$ = 0.21.) Cooling air is added to the stream after the secondary-combustion zone.

*This work was done by Roger A. Craig of* **Ames Research Center** *and Huw O. Pritchard of the Centre for Research in Experimental Space Science, York University. For further information, Circle 63 on the TSP Request Card.*

*Inquiries concerning rights for the commercial use of this invention should be addressed to the Patent Counsel, Ames Research Center (see page A5). Refer to ARC-10814.*

# Improved Cable Grip Reduces Wear

Rolling contact reduces wear of cable and grip.

*Ames Research Center, Moffett Field, California*

An improved cable grip reduces wear due to sliding friction between the cable and the gripping surfaces. Drive wheels are grooved with a helical pattern that meshes with the lay of the cable, analogous to a worm gear. The cable is gripped between the drive wheels and guide rollers, and the cable pull is exerted on the grip when the drive wheels are slowed by hydraulic clutches.

A moving cable is conventionally gripped by forcing two metal plates or dies against opposite sides of the cable. Friction between the cable and dies produces high temperatures and rapid wear. The dies, made of softer material than the cable, wear out rapidly, and the cable also suffers appreciable wear.

In the new system (see figure), the drive wheel maintains rolling contact with the cable without slipping. The meshing of the drive wheel and the cable reduces the clamping force required to maintain the grip on the cable. Without the helical grooves, the clamping force required to prevent slippage between the drive wheel and cable is so great that cold rolling of the cable occurs.

Two hydraulic wet clutches brake each drive wheel. Fluid shear brakes the drive wheels as the clutch plates are forced together. Metal-to-metal contact of the plates occurs only when the drive wheels are locked.

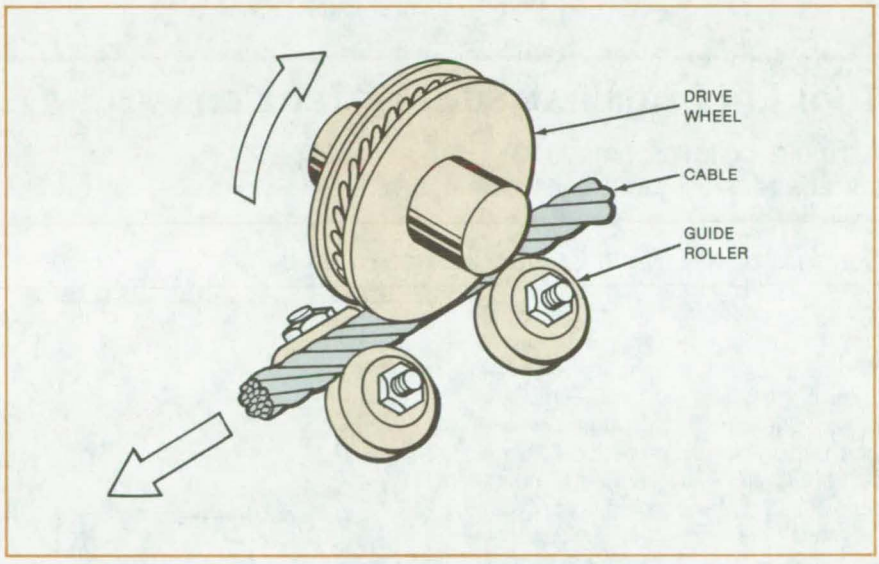


The **Cable Grip** includes a drive wheel with a helical pattern and guide rollers. The drive-wheel rotation is stopped by a hydraulically operated clutch. The guide rollers can be rotated away to release the cable. In the final design, the grip will have four drive wheels of the kind shown here.

A test of a prototype grip with a single drive wheel utilized a six-strand cable 0.75 inch (1.91 cm) in diameter and a load of 1,800 lb (8,000 N). No sliding between the cable and drive wheel was detected during the test, which indicates cable and grip wear will be minimal.

This helical cable grip was originally developed for San Francisco cable cars. However, it is also applicable to other cable-operated systems, such as ore trams in mines, overhead cable cars, and ski lifts.

*This work was done by Richard J. Peyran of* **Ames Research Center.** *For further information, Circle 64 on the TSP Request Card.*
*ARC-11318*

# Vacuum Head Removes Sanding Dust

Tool removes dust as it sands.

*Lyndon B. Johnson Space Center, Houston, Texas*

A modified sanding block scoops up the dust it creates and delivers it to a vacuum exhaust tube. The block sands, shapes, or polishes without introducing contaminating particles into the air. It is useful, for example, where dust presents a health hazard, interferes with such processes as semiconductor manufacture, or could destroy wet paint or varnish finishes. It could be used to sand such toxic materials as lead paint.

The block is fitted with a plenum around its periphery (see figure). The plenum connects to the hose of a commercial vacuum cleaner, which draws off dust particles around the block as fast as they are produced.

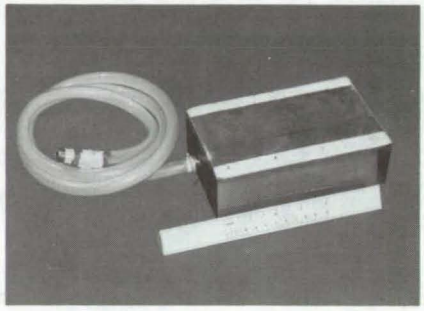

**The Vacuum Sander,** shown as a prototype, prevents sanding dust from entering a work area, since dust particles are drawn off as quickly as they are produced.

The vacuum sander was originally developed for hand sanding of the fused-silica tiles that insulate the exterior of the Space Shuttle. It prevents silica dust from entering the work area.

*This work was done by Clarence G. Bengel and Jack W. Holt of Rockwell International Corp. for* **Johnson Space Center**. *For further information, Circle 65 on the TSP Request Card.*
*MSC-19526*

# Tool Lifts Against Surface Tension

A simple tool overcomes
surface tension gently but firmly.

*Goddard Space Flight Center, Greenbelt, Maryland*

When surface tension makes it difficult to remove an object from a mounting plate, a simple tool can release the object with little effort and without damage. Developed for removing a battery from a greased cold plate, the tool is just one example of how a specialized piece of simple hardware can save time and labor, particularly in a task that is to be repeated many times.

The thermally-conductive grease coating between the battery case and the cold plate ensures effective heat transfer, but considerable force is required to break the surface tension created by the grease. The larger and heavier the battery, the more difficult it is to remove.

The tool is made from two steel angles with welded gussets on their sides (see figure). The angles are attached to opposite sides of the battery case by a nut and bolt. On each angle, a long fine-thread bolt is inserted in a nut that has been welded in place. The bolt passes through a hole

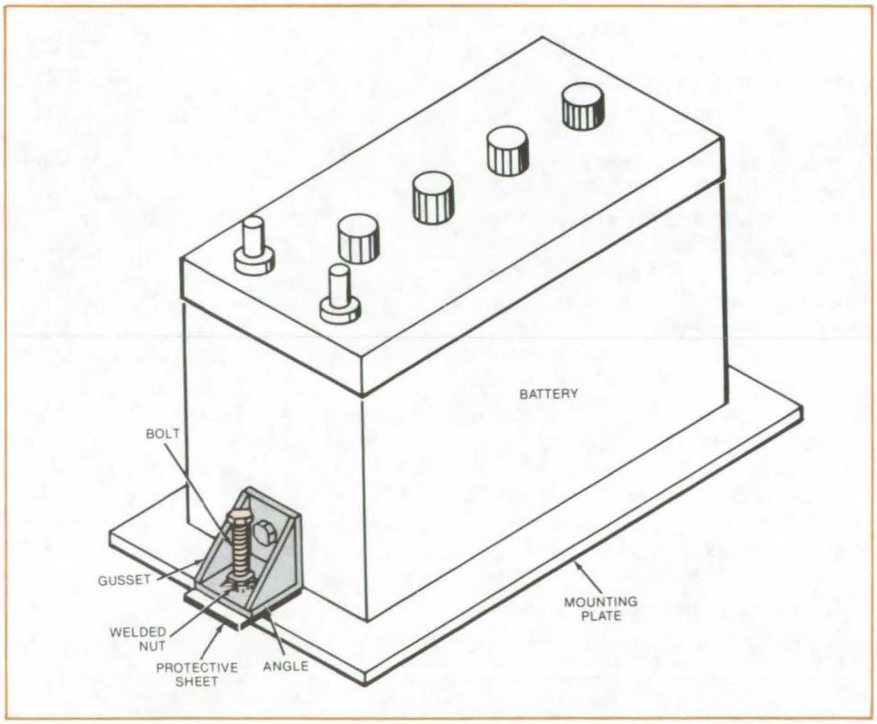


**A Bolt Is Tightened** in a steel angle, as is another bolt (not shown) on the opposite side of the battery. As the bolts press against protective sheets of metal on the mounting plate, they lift the battery, overcoming the surface tension of grease on the mounting plate.

in the angle, so that the tip of the bolt butts against the mounting plate.

To remove the battery, each bolt is tightened half a turn so that the angles and the battery are forced away from the mounting plate until the surface tension is broken. Sheets of metal 1/16 inch (1.6 mm) thick inserted under the angle bases are bearing surfaces for the bolts so that the mounting plate is not damaged.

*This work was done by Paul Miller, Steven McCormick, Edward Muegge, and Paul Devereaux of McDonnell Douglas Corp. for* **Goddard Space Flight Center**. *No further documentation is available.*
*GSC-12672*

# Four-Degree-of-Freedom Platform

A compact motion-control system consists of three hydraulic actuators and a carriage.

*Ames Research Center, Moffett Field, California*

Hydraulic actuators make a new motion control system more compact and more efficient than previous designs that use gimbals. The system moves a platform in four degrees of freedom — simultaneous pitch, roll, yaw, and displacement. Developed for flight simulators, the kinematic concept may also be useful in stabilizing platforms for shipboard equipment, material-handling machinery, and construction equipment. A scale-model platform has been built.

Conventional flight simulators employ three gimbals and a carriage for simultaneous pitch, roll, yaw, and displacement. Because the new platform has less dead mass than gimbaled simulators, it requires less energy and can respond more rapidly.

The new system uses three hydraulic actuators to generate pitch, roll, and yaw and a carriage to generate displacement (see figure). Since the three actuators produce only angular, rather than translational, motion, their stroke is kept to a reasonable length. A fixed center post restrains the platform from translational motion, except that created by the carriage. If the carriage were eliminated and the actuators were to translate the platform, the system would be slightly more efficient, but the actuator strokes would be longer.

According to calculations, a 5-ft (1.52-m) actuator stroke combined with carriage translation is adequate for a helicopter and fixed-wing aircraft simulator developed for Ames Research Center. The total weight of a full-scale system is expected to be less than 26,000 lb (11,800 kg). It could be built at relatively low cost with readily available components.

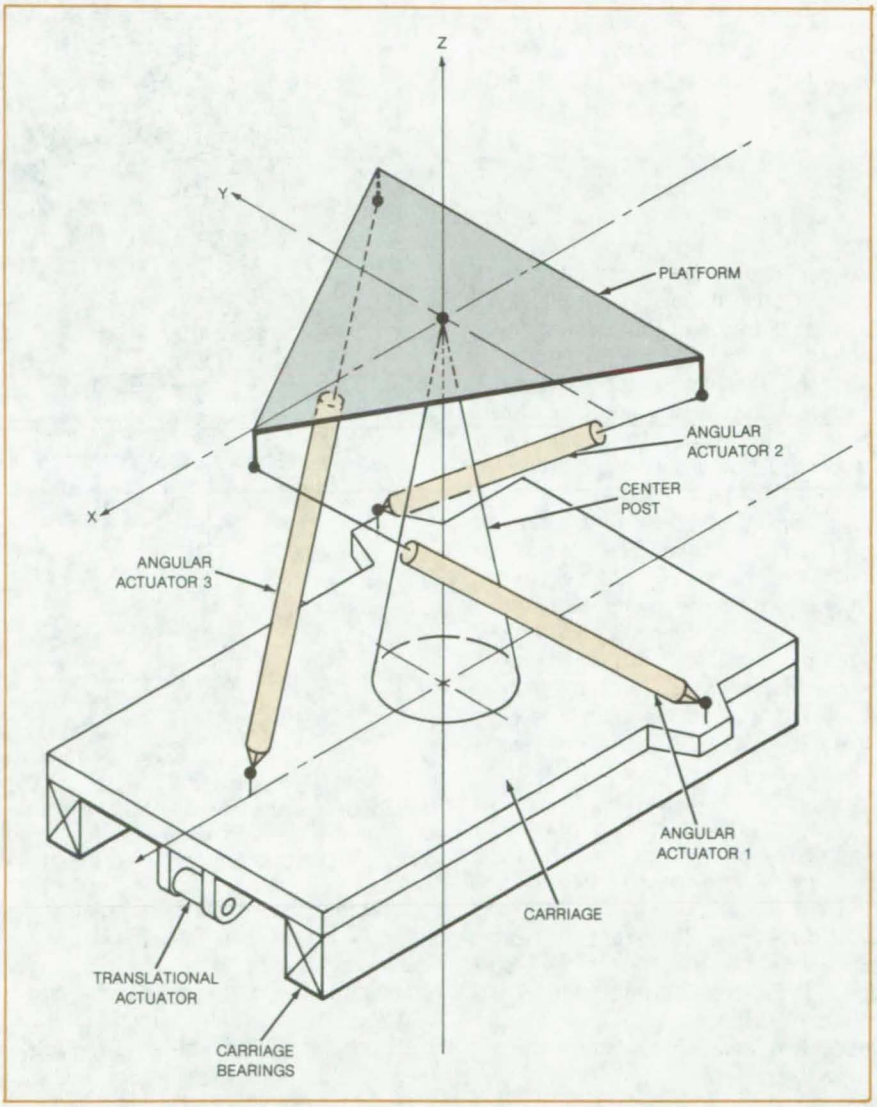


**Three Canted Hydraulic Actuators** transmit angular motion, while a carriage transmits translational motion to a movable platform. There is no kinematic coupling between translational and angular motions. Mechanical stops prevent overtravel.

*This work was done by Richard C. Chou of the Franklin Institute for* **Ames Research Center**. *For further information, Circle 66 on the TSP Request Card.*
*ARC-11286*

# Explosive Separation of Electrical Connectors

Proposed remote-disconnection device for unthreaded connectors would not release combustion products.

*Lyndon B. Johnson Space Center, Houston, Texas*

A concept proposed for separating the electrical cable that connects the Space Shuttle to deployable payloads could be used to sever electrical connections in other inaccessible environments. Among suggested applications are undersea exploration, chemical processing, and areas with high levels of radiation. Although triggered explosively, the connector would not release combustion products that could damage sensitive electronics.

The cable would be connected by a standard friction (nonthreaded) plug and receptacle. A special piston attached to the plug would fit into a mating cylinder attached to the receptacle. To push the piston out and thus push the plug out of the receptacle, a pyrotechnic charge in the cylinder would be fired by an operator at a remote location. Retaining pins would prevent the escape of the piston and the combustion products produced by the firing.

As the figure shows, the device includes an annular cylinder with a mating annular piston. The cylinder is attached to the receptacle half of the connector, while the piston is attached to the plug half. Within the cylinder is another piston, which butts against the piston attached to the plug. The plug piston is slotted in several places to bypass entrapment pins that restrain the cylinder piston.

When the device is triggered, pyrotechnically-generated high-pressure gas is ported to a plenum chamber behind the trapped piston. As the pressure increases, the trapped piston pushes on the plug piston with sufficient force to fracture three retaining shearpins. The trapped piston continues to stroke, thus separating two connector halves. At that point the trapped piston contacts the entrapment pins in the annular cylinder. The combined shear strength of these pins is greater than the force acting on the trapped piston. Thus, all the products of combustion are retained within the annular cylinder by the trapped piston.

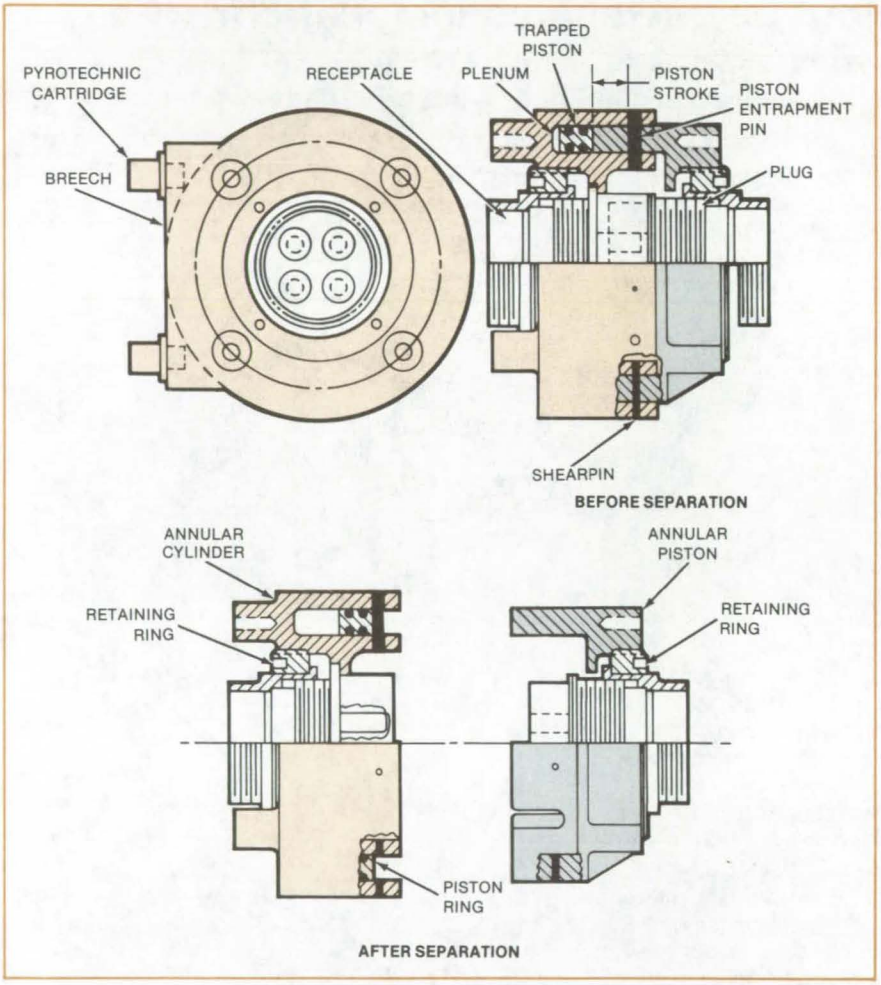


The **Cable Separator** is attached to the plug and receptacle of a standard friction (unthreaded) electrical connector. The locking collar or flange of a conventional connector is removed first to make room for the added hardware. The cylinder and pistons are cylindrical rings that completely encircle the plug and receptacle.

*This work was done by Richard T. Barbour of Rockwell International Corp. for* **Johnson Space Center.** *No further documentation is available.*
*MSC-18828*

# Reliable "Unlatch"

Unique geometry
assures release.

*NASA's Jet Propulsion Laboratory, Pasadena, California*

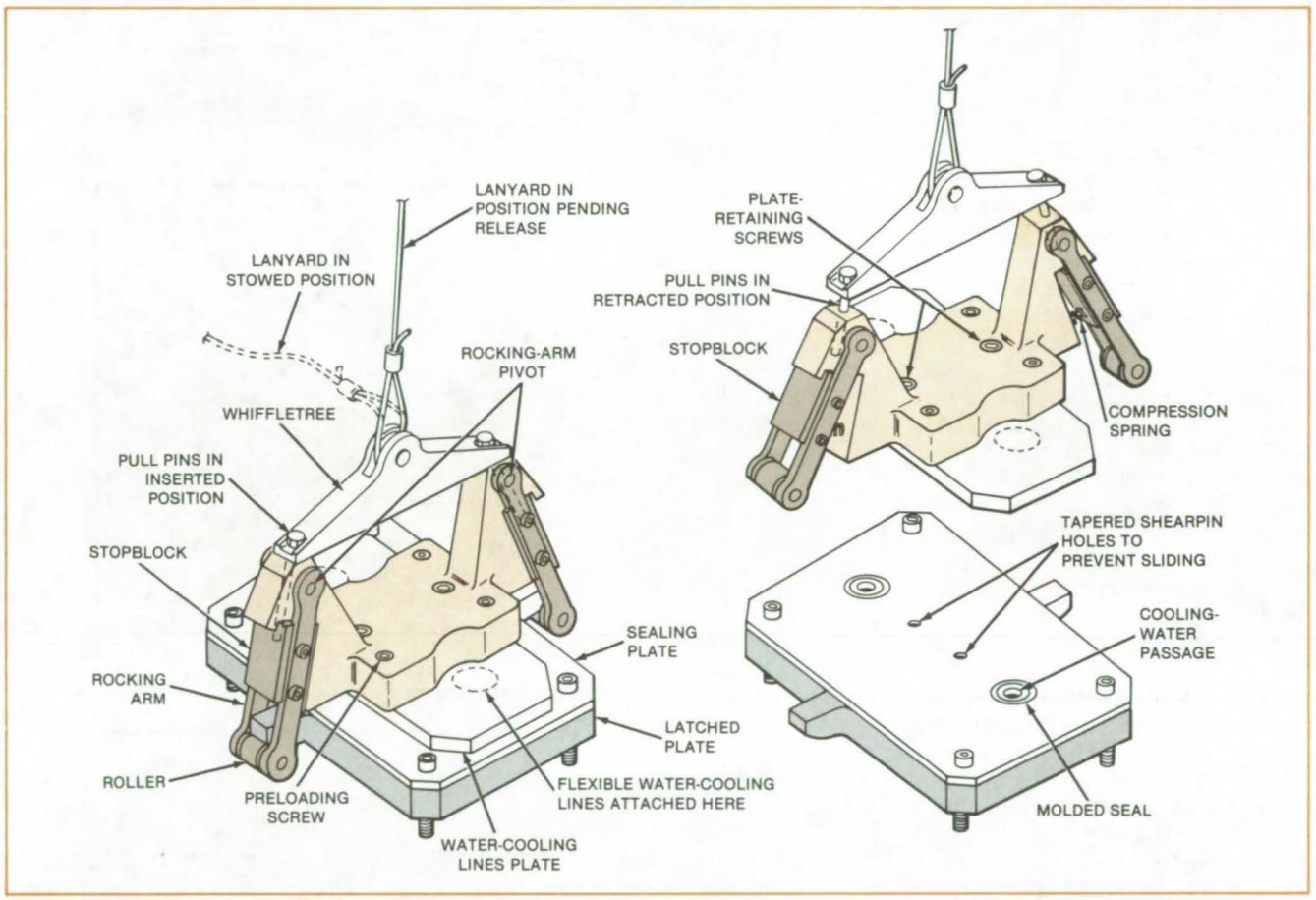


The **Reliable Unlatching Mechanism** utilizes preloading, a favorable geometric arrangement of mating surfaces, and redundancy to assure release. Even if only one rocking arm initially releases, the entire assembly will rotate or rock sideways to complete the unlatching.

A preloaded "unlatch" employs rocking hooks on each side of a yoke. The preloading and geometrical arrangement produce an outward kick that assures disconnection even when only one of the hooks disengages. The device was originally designed to hold cooling-water lines in place on the Galileo spacecraft and to release them just prior to launch from the Space Shuttle orbiter. It would be useful in other applications requiring reliable remote disconnection of cables or pipes.

In the latched position, as shown in the left portion of the figure, the rollers are in contact with the catching surfaces. The pull pins have been pushed into mating holes in the yoke and in the stopblocks, so that the rocking arms cannot rotate outward. Loading screws, which are tightened during the mounting procedure, clamp the water seals together.

Unlatching is initiated when the pull pins are pulled out by the lanyard acting on the whiffle tree. Because the pivot of each rocking arm lies toward the outside from the center of curvature of its catching surface, the preloading force kicks the roller toward the outside. The slope and the radius of the catching surface can be designed for more or less outward kick; consequently, allowance can be made for sufficient force to overcome such effects as freezing of the rollers. Additional outward force is supplied by a compression spring between each rocking arm and the yoke. This force is primarily for convenience of latch assembly.

If only one rocking arm releases, unlatching still occurs. Releases on one arm relieve the preload and allow the assembly to pivot about the contact point of the latched roller. The latched arm, free of its loading force, is then pushed outward by its compression spring to complete the release, or else the entire device rocks and shifts sideways until the latched roller leaves its catching surface.

*This work was done by Thomas O. Killgrove of Caltech for* **NASA's Jet Propulsion Laboratory.** *For further information, Circle 67 on the TSP Request Card.*
*NPO-15438*

# Latch With Single-Motion Release

Latch is secure,
yet easy to release.

*Lyndon B. Johnson Space Center, Houston, Texas*

An improved latching and locking mechanism cannot be loosened by vibration, yet can be released by one hand turning a lever. The latch is intended to hold an object such as a battery securely and to allow the object to be removed easily when necessary. The mechanism was originally proposed for retaining a battery in the backpack of an astronaut's space suit for extravehicular activity. It would allow the astronaut to change life-support batteries quickly with just one hand.

A key component of the device is a spring-loaded sliding latch plate. When the operator pushes a fresh battery (or other object) into the latch (see figure), an engagement pin on the battery contacts a beveled surface on the latch plate and pushes the plate up. As the pin moves past the bevel, it crosses a groove that allows a spring to push the plate down over the battery. To ensure that the battery is not jarred loose by vibration, a spring holds the lock lever in place across the groove in which the battery pin is held.

To release the battery, the operator simply pushes the flat edge of the lock lever. The lock spring is weaker than the latch spring; therefore the push first pivots the lock and uncovers the battery pin. Then the latch spring begins to compress, and the latch plate starts to move away from the pin. The ramp surface of the lock pries the battery from the case as the lock is pushed farther.

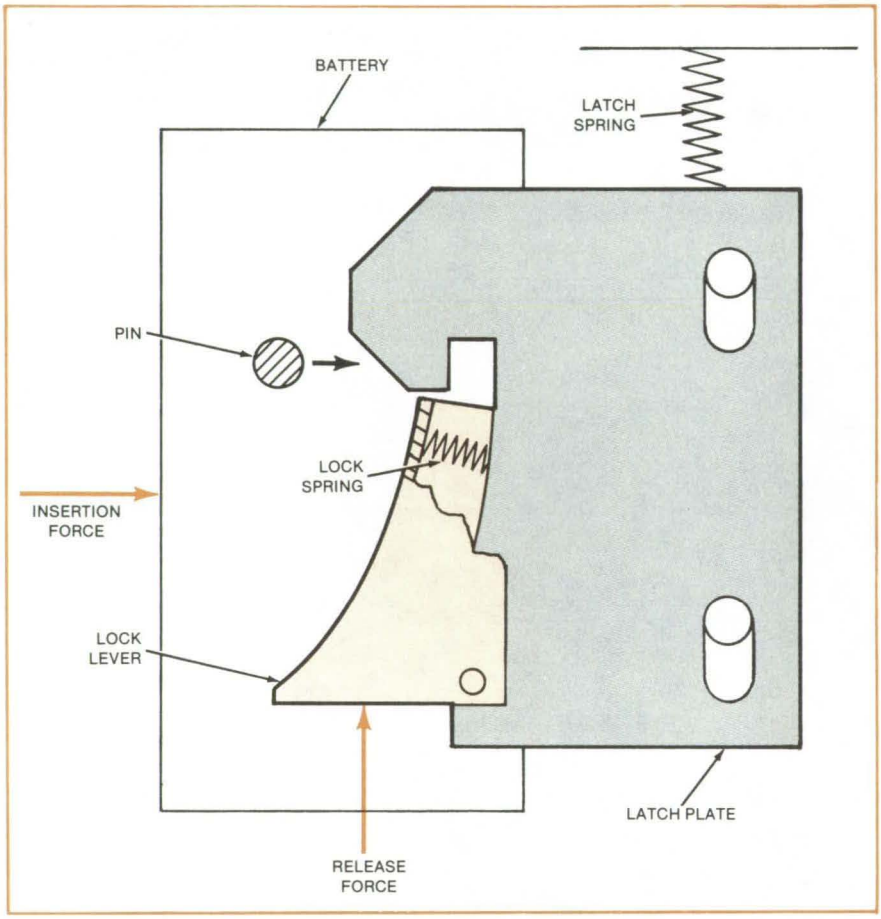


A **Quick-Load/Quick-Release Mechanism** allows an object such as a battery to be inserted with a single motion, locks and latches the object, and allows the object to be released with a single motion.

*This work was done by Drel N. Setzer and Sonne L. Hooper of Pan American World Airways, Inc., for* **Johnson Space Center.** *No further documentation is available.*
*MSC-18923*

# Fabrication Technology

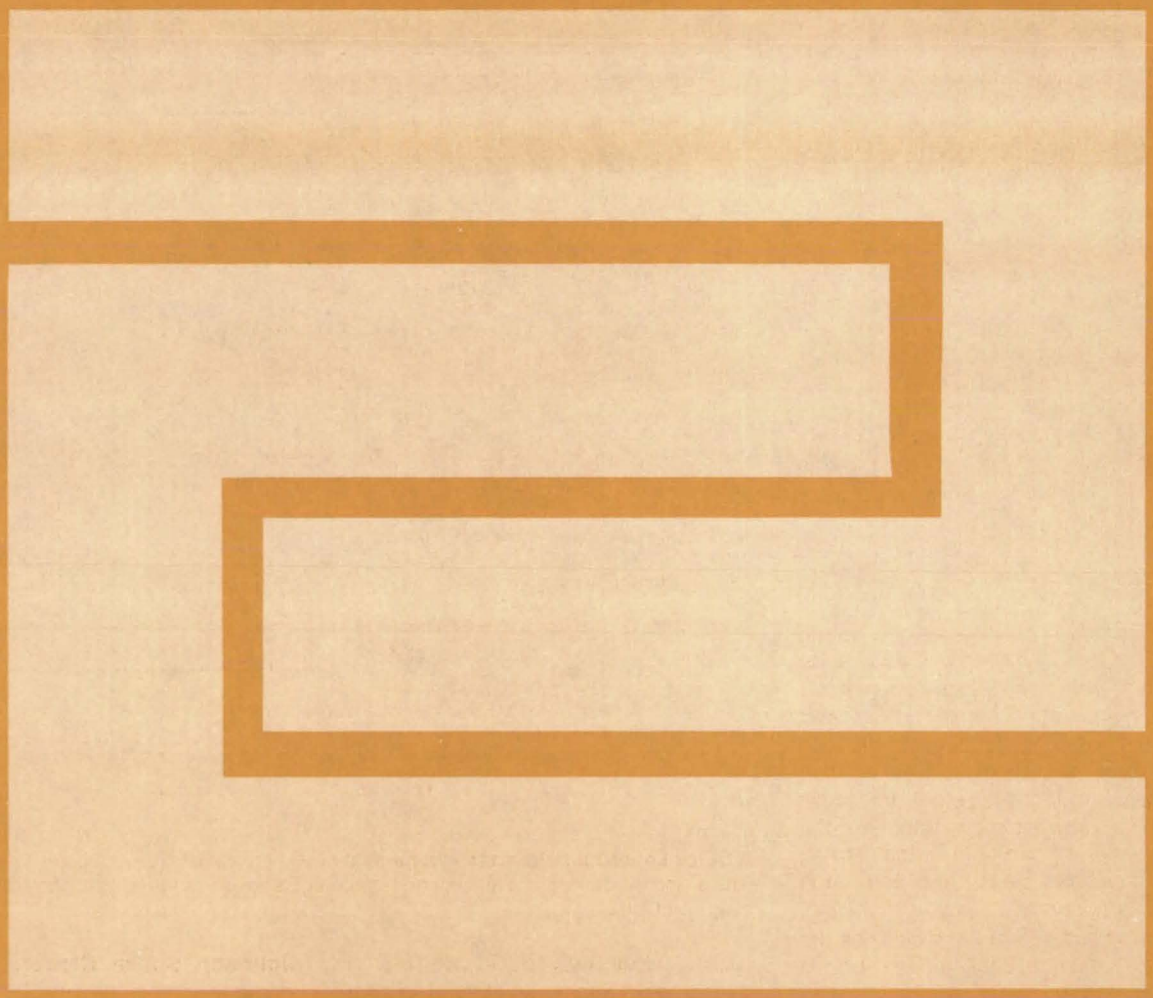

## Hardware, Techniques, and Processes



## Books and Reports



## Computer Programs

# Sound Waves Levitate Substrates

## Acoustic levitation permits contactless manipulation and processing of small articles.

*NASA's Jet Propulsion Laboratory, Pasadena, California*

A system recently tested at NASA's Jet Propulsion Laboratory uses acoustic waves to levitate liquid drops, millimeter-sized glass microballoons, and other objects for coating by vapor deposition or capillary attraction. Sound waves from a focusing radiator are reflected from a concave reflector. The field of the resulting standing acoustic wave contains a force-free volume under the reflector, and movement of the captured article out of that region is resisted by the field. Suggested applications for the facility include the manufacture of laminated or highly accurate spheres such as nuclear fuel pellets, coating objects with precious metals, and applying pharmaceutical coatings.

For the tests, a spherical focusing radiator was used. However, for full-scale operation, the cylindrical focusing radiator shown in the figure is preferred. Ceramic piezoelectric transducers generate the acoustic energy, which is then transmitted to the cylindrical aluminum shell. For maximum energy transfer to the air, the transducers must be closely coupled to the shell, and their resonant frequencies must be the same. Cooling of the radiator may be required, to reduce thermal side effects, such as internal polarization of the piezoelectric and the generation of a temperature gradient in the acoustic field.

The trough-shaped radiator focuses the acoustic energy to a line. An article to be processed would be captured under a reflector and moved along the line from one work station to the next. Typical processing steps at the work stations might include coating, heating, cooling, drying, or inspecting.

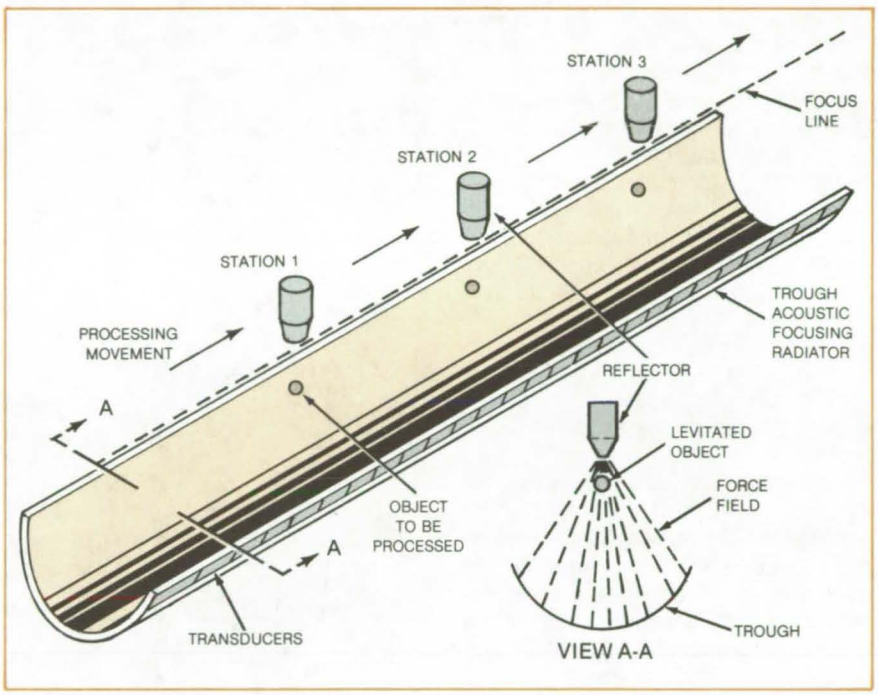


A **Cylindrical Contactless Coating/Handling Facility** employs a cylindrical acoustic focusing radiator and a tapered reflector to generate a specially-shaped standing-wave pattern. The article to be procesed is captured by the acoustic force field under the reflector and moves as the reflector is moved to different work stations.

The system was developed to fabricate laminated fusion-target pellets. Contactless levitation applies precise, even coatings to spherical substrates by vapor deposition or capillary dispersion. Coating mists or fluids are directed toward the particle by the levitating field. While the coatings can also be applied by electrostatic levitation, a vacuum system would be required.

The suspended drop or other article can be rotated and moved vertically and horizontally by frequency and amplitude modulation of the sound field. The control of the field; the reflector movement; the heating, cooling, coating, and inspecting; and the injection of the article into the force field can be done automatically by computer control.

*This work was done by Mark C. Lee and Taylor G. Wang of Caltech for* **NASA's Jet Propulsion Laboratory.** *For further information, Circle 68 on the TSP Request Card.*
*NPO-15435*

# Protective Garment Ensemble

A totally enclosed garment protects against toxic substances.

*John F. Kennedy Space Center, Florida*

A proposed protective ensemble for toxic environments would consist of a fully enclosed garment, complete with breathing air, air-conditioning, and emergency air. It would be suitable for a 2-hour continuous mission.

Toxic propellants are usually handled by an operator wearing a totally-enclosed protective garment. The garments in use at Kennedy Space Center were developed nearly 20 years ago. Increasingly strict standards prohibiting the exposure of workers to propellants and the requirement to use protective garments in other restrictive locations stimulated the need for a new protective garment.

In the configuration depicted (see figure), an environmental-control unit is attached to the user's back. In alternative modes, the unit is in a remote case and is hand-carried, or a pressurized air line is used instead of the unit. The environmental-control unit uses liquid air that is vaporized to provide both breathing air and cooling.

The garment contains a flow-diverter valve that can be activated to isolate the environmental-control-unit recirculation system and direct breathing air to the head area. The valve may be activated manually if the coverall becomes torn or is penetrated in a toxic environment, protecting the operator as he egresses from a contaminated area. The valve vent on the environmental-control unit has been altered to minimize reverse migration of contaminants and to prevent penetration by an impinging toxic fluid stream.

Other improvements over existing protective garments include:

- lighter weight;
- a "low-level" alarm in the environmental-control unit;
- the ability to work in a vertical or horizontal attitude;
- a redundant seal on the entry closure;
- integration of the emergency breathing-air supply into the ensemble; and
- a propellant-resistant, lighter weight helmet.

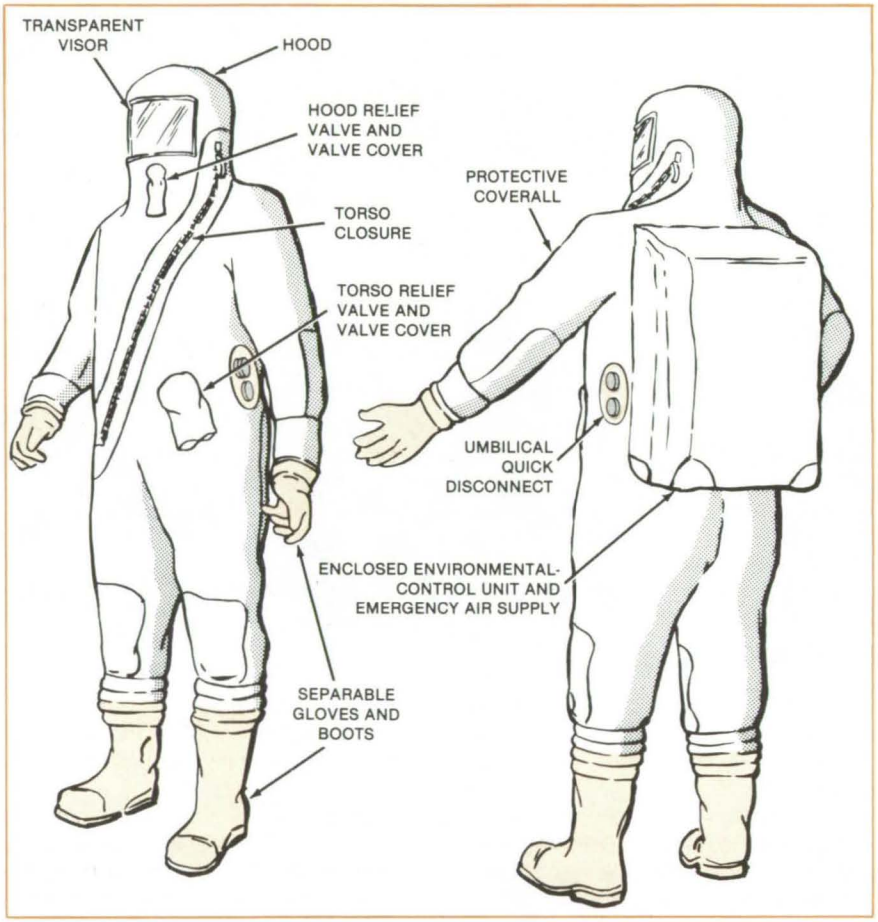


**Protective Garment Ensemble** with an internally-mounted environmental-control unit contains its own air supply. Alternatively, a remote-environmental control unit or an air line is attached at the umbilical quick disconnect.

*This work was done by Michael E. Wakefield of Martin Marietta Aerospace for* **Kennedy Space Center.** *For further information, Circle 69 on the TSP Request Card.*
*KSC-11203*

# Thermally Insulated Glove With Good Tactility

Elastomeric pins would insulate without impairing flexibility.

*Lyndon B. Johnson Space Center, Houston, Texas*

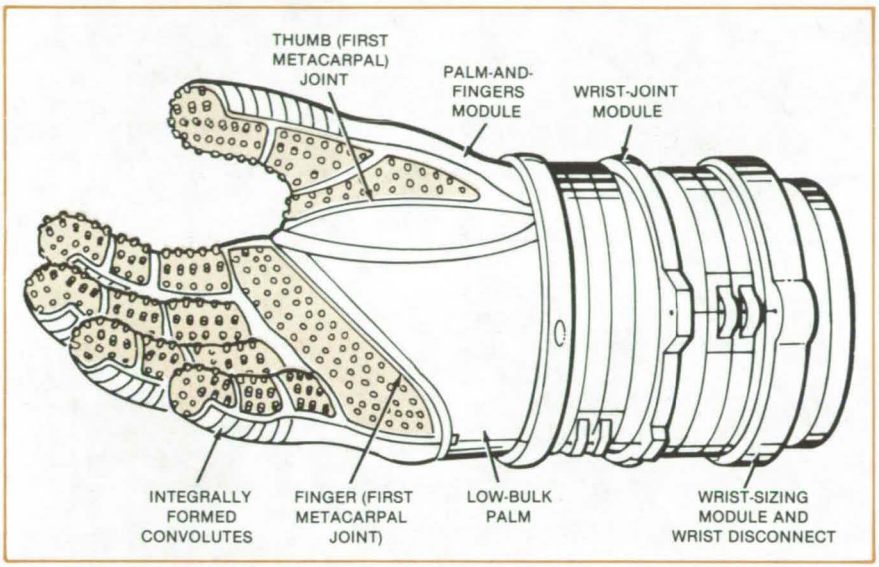


Figure 1. **Thermally Insulated Glove** contains short, closely-spaced elastomeric pins that insulate without impairing flexibility.

A proposed glove would provide good thermal insulation while allowing more flexibility and tactility than previous designs. The glove was originally intended for astronaut's use at temperatures of 200° F (93° C), which are routinely encountered in extravehicular activity; however, it could be used for handling hot or cold objects in other applications as well.

As shown in Figure 1, many short, stiff elastomeric pins molded in the outer layer of the glove form a heat-insulating surface barrier. By confining the pins to the interjoint areas of the palm, fingers, and the back of the hand, joint mobility is retained; and, because the pins move independently, they do not impair the flexibility of the underlying laminated surface. Each pin is relatively incompressible and thus transmits applied forces with little attenuation. This would preserve the wearer's sense of touch.

Previous gloves used many insulating layers to block heat transfer. However, they reduce the wearer's "feel" by absorbing motions and masking local contact forces and surface textures. Such gloves may also be too bulky to conform to the sharp bends required of the fingers. In contrast, the elastomeric pins would be flexible and yet would have little compressibility.

The length, diameter, and spacing of the pins determine their insulating qualities (Figure 2). Because heat conduction through the pins must be minimized, it follows from Figure 2 that for closer pin spacing, each pin must be longer or more slender, or both.

To satisfy grip and tactility requirements, pin spacing should be fairly close, perhaps 5 to 8 pins per inch (2 to 3 pins per centimeter). The closest pin spacing required for tactility should be about 8 pins per inch (3 pins per centimeter), which coincides with the

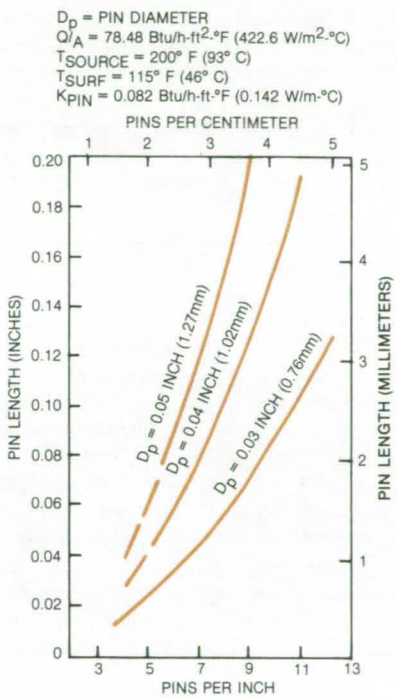


Figure 2. **Glove Thermal-Insulation Requirements** dictate the relationships among pin length, pin diameter, and number of pins per unit surface length. The characteristics shown are for a heat flux of 78.48 Btu/h-ft$^2$.

spacing of pressure sensation receptors in the skin of the fingers. However, although pins placed close together may enhance tactile resolution, they may have to be so thin that they bend, resulting in a "spongy" feel and a "squirmy" grip. Overall tactility is expected to be enhanced by reducing the sponginess, even at some loss of tactile resolution.

*This work was done by Robert Balinskas of United Technologies Corp. for* **Johnson Space Center.** *No further documentation is available.*
*MSC-18926*

# Lightweight Face Mask

High-impact face-protection mask has many possible applications.

*Langley Research Center, Hampton, Virginia*

A high-impact face mask originally designed for medical patients promises to have many other possible applications. The mask (shown in photograph) was intended to protect the faces of epileptic and cerebral palsy patients during seizures. Configurations could be designed for other users, such as muscular dystrophy patients, football linesmen and riot-control police.

The basic mask is fabricated of fiberglass, Kevlar® aramid fiber, and thermosetting epoxy resin. Two layers of 0.0085-inch (0.022-centimeter) fiberglass cloth, with seven layers of 0.0085-inch Kevlar between them, are vacuum-molded using Epon 815® epoxy resin with 25 percent curing Agent U® Curing time is 6 to 8 hours at room temperature. The resin is mixed with 5 percent white pigment.

This **Lightweight Face Mask** originally developed to protect epileptic patients during seizures could have many other medical and nonmedical applications.

Polyvinyl alcohol is the release agent.

After vacuum molding and curing, excess material is trimmed with a saw, and the eye and mouth openings are cut out with a carbide dental burr. The mask is then primed inside and out with gray primer, sanded, and coated with white lacquer. The masks are extremely lightweight, the lightest of the configurations (the cerebral palsy model) weighing only 136 grams.

(Kevlar® is a registered trademark of E. I. du Pont de Nemours & Co., Inc.; Epon 815® and Agent U® are registered trademarks of Shell Chemical Company.)

*This work was done by Wade E. Cason III, Robert M. Baucom, and Robert C. Evans of* **Langley Research Center.** *No further documentation is available.*
*LAR-12803*

# Contamination Control During Weld Repairs

Internal pressure keeps chips and shavings from pipe interiors.

*Marshall Space Flight Center, Alabama*

By using internal pressure, weld defects in pipes or tanks are repaired without contaminating interiors that cannot be protected or recleaned. A multistep procedure was developed for contamination-free repairs of weld defects in the Space Shuttle orbiter main engine. The contamination could be caused by chips milled or routed from the repaired area or by abrasive particles eroded from the cutting tool.

In routing the defect area, the method of initial breakthrough is important. To control the spread of large chips, the defect is first routed to a thin wall. The pipe is filled with an inert gas at 3-psi ($2 \times 10^4$ $N/m^2$) positive pressure to prevent oxidation, and heat is applied to weaken the thin area. The weakened, thinned area deforms, blisters, and breaks, dispelling particles outward. A small hole, about 1/8 in. (3 mm) in diameter resulted when the thinned area was heated on part of the orbiter main engine.

The next step enlarges the hole and further removes metal defects. Using ordinary shop air, at an internal pressure of 15 psi ($1 \times 10^5$ $N/m^2$), the hole is enlarged, and metal defects are removed. A rotary file at a rotation rate of 1,800 rpm is used. When the size of the opening exceeds 3/8 in. (9.5 mm), much of it is covered with tape, except for 1/8 in., to maintain airflow; and the pressure is constantly adjusted to maintain 15 psi.

The procedure can be used with pipes or tubing that is attached to components with critical internal clearances. The method has also been successfully used to cut completely through a pipe with a handsaw.

*This work was done by M. L. Cassidenti and R. K. Burley of Rockwell International Corp. for* **Marshall Space Flight Center.** *No further documentation is available.*
*MFS-19652*

# Technique Lowers Weld Power Requirements

A spacer and smaller welds replace a single deep weld.

*Marshall Space Flight Center, Alabama*

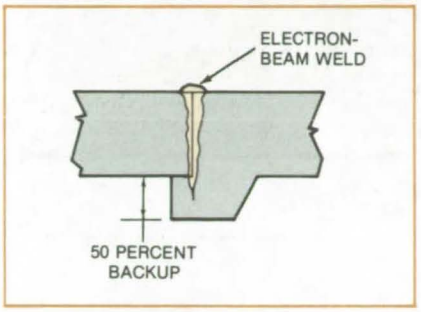


Figure 1. A **Deep Weld** is conventionally used to join heavy sections.

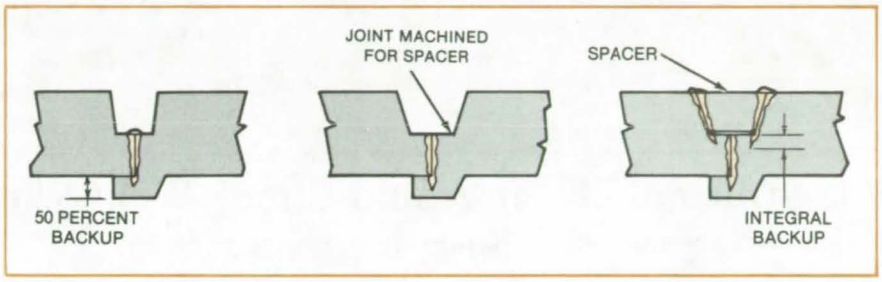


Figure 2. **Three Electron-Beam Welds** and a spacer are used to replace a single deep electron-beam weld. The projections of the last two welds beyond the spacer add an integral backup.

To join heavy sections, a machined spacer and three short electron-beam welds could be used in place of a single deep electron-beam weld. This technique would reduce the power required for welding, making it possible to use low-power sources. It also could be used in place of deep welds where the sections are of unequal depth and one section has limited backup (see Figure 1).

The heavy sections to be welded would be prepared as shown in Figure 2. By removing material from both pieces to be welded, the depth of the weld is reduced. The first short electron-beam weld is then made. Next, the joint is machined to accept a spacer. When the spacer is installed, it is welded in place with two short electron-beam welds, completing the joint.

*This work was done by Richard Pessin of Rockwell International Corp. for* **Marshall Space Flight Center.** *No further documentation is available. MFS-19655*

# Weld-Wire Monitor

An impedance bridge determines whether weld-wire composition and diameter are within specifications.

*Marshall Space Flight Center, Alabama*

Changes in the size or composition of weld wire being fed to an automatic welding machine are detected by an impedance-monitoring instrument. The instrument triggers an alarm if the changes could affect weld quality or cause weld failure. It could find applications in the construction of pipelines or nuclear powerplants.

As it is fed to a weld joint, the wire passes through a sensing coil that is part of a Maxwell electrical-impedance bridge. The bridge is balanced for the particular weld-wire alloy and diameter. A null detector with a preset threshold senses an unbalance, whether caused by a change in wire diameter or by a change in alloy composition, such as might result from placing the wrong wire type on the feed roll. The null detector activates an alarm

(continued on next page)

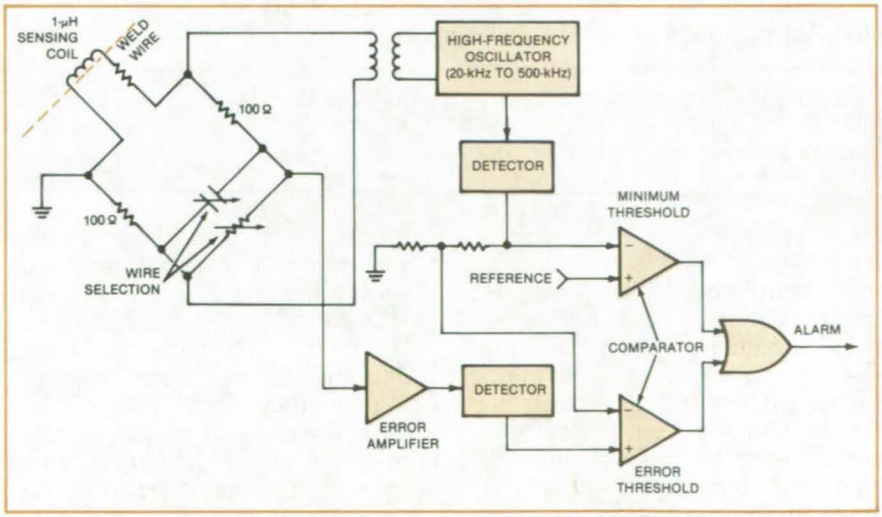


**Weld Wire Passes Through a Sensing Coil** composed of 20 turns of wire and having an inductance of about 20 μH. With a high-frequency oscillator providing a reference signal, the Maxwell bridge currents become unbalanced if the wire composition or diameter — and therefore the wire impedance — changes significantly.

or stops the wire-feed mechanism. An operator selects the bridge-balancing components with a switch so that different wire alloys and dimensions can be accommodated.

The Maxwell bridge in the figure uses a 20-turn sensing coil. Detection circuitry converts the ac error signal from the bridge to a dc error signal, which is supplied to a comparator/threshold detector. The high-frequency signal generator that excites the bridge also provides the reference signal for the threshold detector. Although the generator output amplitude is not critical, an alarm informs the operator of a signal-generator failure so that a null equivalent will not be maintained with an incorrect wire.

In laboratory tests with an oscilloscope as the null detector, the following wire alloys could be distinguished from each other: Hastelloy C, Hastelloy W, Inconel 718, Inconel 82, stainless 316, and Inconel 625. In addition, Inconel X and Inconel A No. 92 could be distinguished from the other alloys, although they could not be distinguished from each other.

*This work was done by R. Olson and J. R. Hall of Rockwell International Corp. for* **Marshall Space Flight Center.** *No further documentation is available.*

*Inquiries concerning rights for the commercial use of this invention should be addressed to the Patent Councel, Marshall Space Flight Center (see page A5). Refer to MFS-19603.*

## Eddy-Current Meter Would Check Weld Wire Online

A simple technique would detect unauthorized wire before it is used.

*Lyndon B. Johnson Space Center, Houston, Texas*

An eddy-current meter would monitor weld filler wire before it is used, in a new proposal for eliminating time-consuming weld inspections and repairs. Originally proposed for spacecraft assembly, the technique would improve welding operations in other applications by identifying unauthorized or contaminated filler wire.

The eddy-current meter could be incorporated into hardware placed over the wire along the path from the supply spool to the welder or takeup spool (see figure). Eddy-current sensors are sensitive to wire properties and can differentiate between alloys.

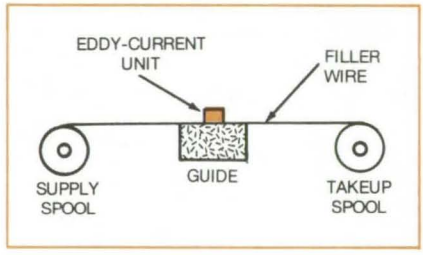


An **Eddy-Current Meter** samples an entire spool of welding wire to test for contaminated or unauthorized filler wire.

Since the unit monitors the entire length of wire used in welding, the completed welds need not be inspected individually. This technique would save time, avoiding human interface and production delays.

*This work was done by George R. Bailey of General Dynamics Corp. for* **Johnson Space Center.** *No further documentation is available.*
*MSC-18891*

## "Ruggedized" Microcomputer Bus

A standard microcomputer bus is improved to withstand shock, temperature, and vacuum.

*Goddard Space Flight Center, Greenbelt, Maryland*

A "ruggedized" version of the STD microcomputer bus withstands the rigors of spaceflight. It could be used as a basis for microcomputers in other hazardous environments, including those at high and low temperatures, those in vacuum, or those subject to extreme shock and vibration. A prescription for converting commercial STD-compatible printed-circuit cards to ruggedized versions can be obtained by requesting the Technical Support Package referenced at the end of this article.

Among the modifications that make the bus rugged are:

- Upgrading the electronic parts to MIL-SPEC and extended-temperature-range components;
- Improving the heat-transfer design for a vacuum environment;
- Using low-outgassing materials;
- Changing to more-durable connectors; and
- Strengthening the bus to withstand shock, vibration, and acoustic effects.

Aluminum-core circuit boards and heat-conducting card guides are used for good thermal dissipation. To reduce outgassing and improve reliability, the conventional edge-of-card contacts and input/output connectors are altered to circumferential contacts. Also, the crystal oscillator on the central-processing-unit card is changed to improve the temperature range and shock/vibration tolerance.

*This work was done by Thomas J. Budney and Robert W. Stone, Jr., of* **Goddard Space Flight Center.** *For further information, Circle 70 on the TSP Request Card.*
*GSC-12691*

# Boron/Aluminum-Titanium Hat-Section Stiffener

Advanced composite structural element combines stiffness, light weight, and durability.

*Lyndon B. Johnson Space Center, Houston, Texas*

Laminated boron/aluminum structural elements enhanced by a titanium metal facing are proposed for applications requiring strength, stiffness, and durability. The new "hat" section elements (see figure) have been suggested as replacements for machined aluminum alloy panels in the wing of the Space Shuttle orbiter, with significant savings in weight expected. Although sections of boron/aluminum are already used in many structures, the added durability offered by the protective titanium overlay could open up new applications for these versatile materials.

The stiffened-skin structure is made from three to six layers of boron/aluminum tape 0.007 in. (0.18 mm) thick, diffusion-bonded between titanium sheets 0.005 in. (0.127 mm) thick. Loads are transferred at the ends of the panel through machined aluminum fittings. In the areas of these attachments, additional titanium facings ("titanium end doublers") enhance shear and bearing strength.

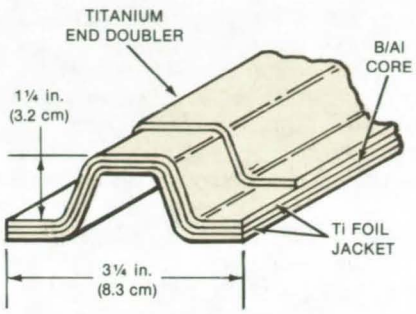


The **B/Ai-Ti Hat-Section Stiffener** is formed from laminated boron/aluminum and titanium foils. Double layers of titanium at the end of a section offer additional strength and protection.

In a typical fabrication sequence, the laminar sheets are cleaned to remove oxides and hydrocarbons, then laid up on a forming die. Conforming stainless-steel covers are placed above and below, and end caps are welded on to form a stainless-steel envelope. The envelope is evacuated and sealed. Diffusion bonding (in which aluminum is the diffusing metal) occurs when the package is subjected to high pressures and temperatures in an autoclave. After bonding, the steel covering is cut away, and the section is machined and finished as required.

Tests suggest ultimate tension/compression capability of 115 to 130 ksi ($795 \times 10^6$ to $895 \times 10^6$ N/m$^2$) for the section. This results in a high strength-to-weight ratio. The weight can be reduced further by tailoring the local section thickness to the loading requirements, even to the extent fo stepping the plies within an element.

*This work was done by Charles R. Maikish and Ronald R. Eckberg of General Dynamics Corp. for* **Johnson Space Center.** *For further information, including procedures for fabricating hat-section stiffeners, Circle 71 on the TSP Request Card.*
*MSC-18895*

# Prolonging the Life of Refractory Fillers

A silicon carbide coating prevents embrittlement at high temperatures.

*Lyndon B. Johnson Space Center, Houston, Texas*

The useful life of a refractory glass-cloth gap filler is increased by coating it with a suspension of silicon carbide in butanol and polyethylene. The silicon carbide increases the emittance of the cloth from the 0.3-to-0.4 range to the 0.7-to-0.8 range. The coated material thus maintains a much lower temperature. For example, a cloth filler that normally operates at 2,300° F (1,260° C) operates at only 1,900° F (1,030° C) after it has been coated.

The coating is applied to the refractory-fiber cloth filler that seals the gaps between insulating tiles on the Space Shuttle orbiter. Tests showed that the cloth fibers would be embrittled by the extreme temperatures encountered on reentry into Earth's atmosphere and that only 25 percent of the thousands of fillers would be reusable after a mission. With the coating, however, 85 percent of the fillers would be reusable.

The silicon carbide/butanol/polyethylene suspension is sprayed or brushed on. The polyethylene in the butanol carrier gives the suspension sufficiently low viscosity that the silicon carbide can penetrate the cloth fibers. The butanol evaporates after it is applied, and the polyethylene burns off when its temperature reaches approximately 1,000°F (538° C).

Many emittance-control agents and suspension agents were tried. However, only the combination of silicon carbide, butanol, and polyethylene has the required temperature resistance and flexibility.

*This work was done by Calvin Schomburg and Robert L. Dotts of* **Johnson Space Center.** *No further documentation is available.*

*Inquiries concerning rights for the commercial use of this invention should be addressed to the Patent Counsel, Johnson Space Center [see page A5]. Refer to MSC-18832.*

# New Method For Joining Stainless Steel to Titanium

A quasi-metallurgical bond is formed by a modified welding process.

*Lyndon B. Johnson Space Center, Houston, Texas*

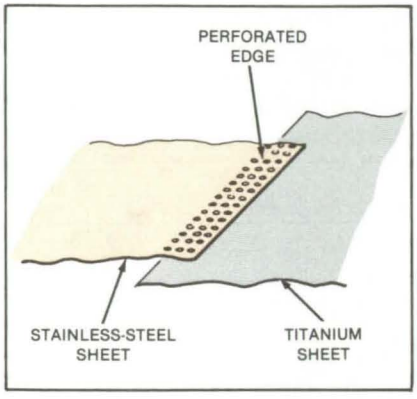


After the **Edge of the Stainless-Steel Sheet Is Perforated,** it is joined to the titanium by resistance seam welding. Titanium flows into the perforations, forming a strong interlocking joint.

A combination of techniques bonds stainless steel to titanium with good reliability. Since it is very difficult to weld these materials to each other, they are usually joined by mechanical fasteners or by diffusion bonding. The new technique would be less expensive than either of these methods and would be faster in mass production.

In the new process the edge of the stainless-steel sheet is perforated with an array of holes, typically 0.008 inch (0.2 mm) in diameter, to create approximately 40 percent open area in the perforation region. The holes are produced by photoprocessing followed by chemical etching. The perforated edge is then placed over the edge of the titanium sheet (see figure) and the two are resistance seam-welded together. The flow of molten titanium into the holes of the stainless-steel sheet results in a joint with high shear and peel strengths.

The new process creates a quasi-metallurgical bond between the thin sheets of stainless steel and titanium. The bond strength is as high as that of the annealed stainless steel and titanium. Other metals for which no reliable method of welding exists could possibly be bonded this way, although they would have to be tested on a case-by-case basis.

*This work was done by William H. Emanuel of McDonnell Douglas Corp. for* **Johnson Space Center.** *No further documentation is available.*
*MSC-18820*

# Orientation Insensitivity for Electrochemical Sensor

A polypropylene wick makes a hydrazine sensor independent of orientation and vibrations.

*John F. Kennedy Space Center, Florida*

By using a wettable polypropylene wick, the performance of an electrochemical hydrazine sensor is made independent of its orientation. The wick keeps all the electrodes in constant contact with the electrolyte solution so that one or more of the electrodes do not become isolated from the electrolyte if the sensor is tilted or vibrated. (Electrode isolation causes surges in the sensor response.) Other electrochemical sensors, particularly those that use alkaline electrolytes, could also use the polypropylene wicks.

The wick for the hydrazine sensor consists of a thin sheet [0.005 inch (0.13 mm) thick] or several thin sheets [with a combined thickness of 0.150 inch (3.81 mm)] of wettable polypropylene material in contact with all of the sensor electrodes. A possible wick material is RAI Research Corp. Product A-1260, or equivalent. To make the material wettable, either woven or nonwoven polypropylene is grafted with polar groups. Attempts to use glass-fiber or glass-wool wicks as the absorbent material were unsuccessful because the alkaline electrolyte attacked the glass.

Tests of a portable toxic-level hydrazine analyzer using the new wick show that the instrument output varies by no more than 5 parts per billion in any attitude or during any attitude change. The analyzer was rested on all six surfaces while sampling 280 parts per billion of monomethylhydrazine.

*This work was done by Raymond B. Cromer of Becton-Dickinson and Co. for* **Kennedy Space Center.** *No further documentation is available.*

*Title to this invention has been waived under the provisions of the National Aeronautics and Space Act [42 U.S.C. 2457(f)] to the Energetics Science Division of Becton-Dickinson and Co., 85 Executive Boulevard, Elmsford, New York 10523.*
*KSC-11176*

# Improved Air-Treatment Canister

A proposed integrated water evaporator would avoid undesirable condensate.

*Lyndon B. Johnson Space Center, Houston, Texas*

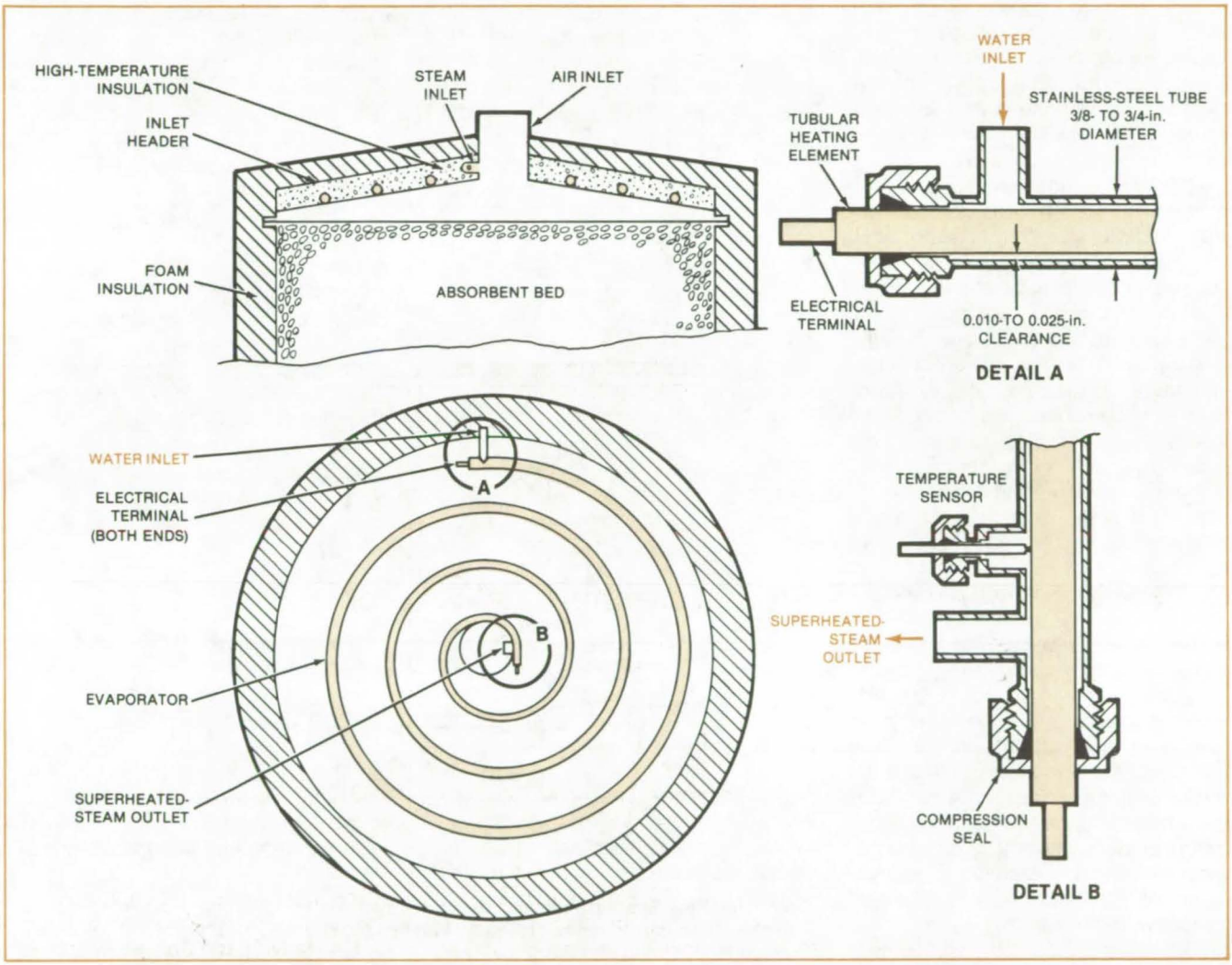


In an **Improved Air-Treatment Canister,** the heater-in-tube preheats the canister header, thus preventing condensate from entering the absorbent bed. It would deliver 2.7 pounds (1.2 kg) of steam per hour at 15 psi (100 kN/m$^2$) while consuming about 1,750 watts of electrical power.

A proposed air-treatment canister integrates a heater-in-tube water evaporator into the canister header. This improved design prevents water from condensing and contaminating the chemicals that regenerate the air.

Air-treatment devices in recirculating systems use absorption materials (such as solid amines) to remove $CO_2$. The bed of absorption material is packaged between screens inside an insulated metal canister. The material is reactivated by passing superheated steam through it.

The canisters work most efficiently when both air and steam enter a header on top of the bed, flow down through the bed, and exit at the bottom. However, in this arrangement, water condenses on the inlet header and migrates into the bed of absorbent.

As shown in the figure, the water evaporator in the improved canister consists of a tubular heating element inside a slightly-wider metal tube. The length may vary from 100 to 200 inches (250 to 500 cm) with an outside diameter of three-eighths to three-fourths of an inch (9 to 19 mm). Once assembled, the heater may be bent into any desired shape. In the proposed canister, the heater is evenly spiraled about the inlet header. The evaporator is brazed to the header.

*This work was done by Albert M. Boehm of United Technologies Corp. for* **Johnson Space Center.** *No further documentation is available.*
*MSC-18942*

# Easily Assembled Reflector for Solar Concentrators

Mirror segments do not need individual alinement.

*NASA's Jet Propulsion Laboratory, Pasadena, California*

Reflectors for concentrating solar collectors are assembled quickly and inexpensively by a method that employs precontoured supports, plastic film, and adhesive to form a segmented glass mirror. The new method is self-focusing. It does not require skilled labor at any stage.

Although glass mirrors are the most efficient reflectors, they have not been cost-competitive with polished metal reflectors. Grinding glass stock to a concave reflecting contour is too expensive for low-cost solar energy, and efforts to assemble concave reflectors as a mosaic of mirror segments have been hampered by the necessity for focusing each segment individually as it is mounted. Focusing is time consuming and expensive for reflectors larger than 3 ft (1 m) in diameter.

A series of curved ribs, which form the framework of the reflector and are curved to the requisite reflector shape, is set in place (see figure). A sheet of strong but flexible plastic, such as polyolefin or polyvinyl chloride, is attached to the ribs with an adhesive, such as butyl rubber. The flat mirror segments are bonded to the sheet with an adhesive. A segment assumes the general orientation of the sheet area to which it is bonded. In combination, the segments closely approximate a parabolic or spherical curved surface.

Segments up to 12 inches (30 cm) long can be supported entirely by the sheet, without a backup rib, provided that alternate rows of segments are rib supported. The rib structure is therefore simplified, and weight is reduced.

Although the method was developed primarily for the erection of reflectors in the field, it is also adaptable to the factory. The segments can be bonded to the sheet at the mirror fabrication plant. The rolled stock of mirror and sheet is then transported to the field site, where the sheet is bonded to the rib structure.

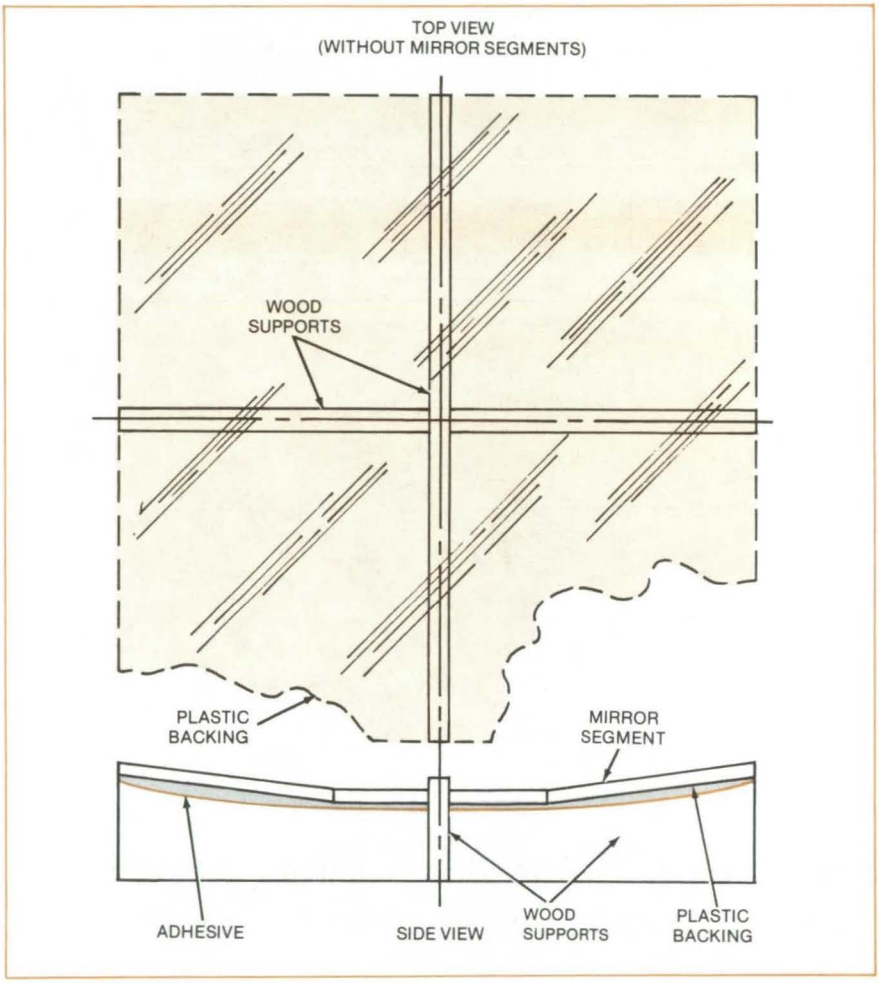


**Contoured Ribs Support Film and Mirror Segments** in this drawing of an experimental reflector. Nine mirror segments, each 4 inches (10 cm) long, are bonded to the sheet. The combined mirror surface closely approximates a spherical surface with a radius of curvature of 36 inches (0.91 m). In tests, the prototype produced nine overlapping focused images of the Sun.

The method is especially suitable for developing countries, since it can be used to set up small high-concentration solar-energy units. The units could be used for generating heat for industrial processes, such as metal processing. Larger units could be assembled with ribs made of local hardwoods.

Off-the-shelf commercial mirror stock is used. Commercial silvered glass can easily be cut into square or rectangular segments with a glasscutter. If a mirror segment is damaged, it can be repaired at low cost. For instance, if a windblown rock cracks a segment, it can be removed with a solvent and replaced.

*This work was done by Frank L. Bouquet and Takashi Hasegawa of Caltech for* **NASA's Jet Propulsion Laboratory.** *For further information, Circle 72 on the TSP Request Card.*
*NPO-15518*

# Integrated Solid-Electrolyte Construction

Porous wire-screen electrodes would improve cell performance.

*NASA's Jet Propulsion Laboratory, Pasadena, California*

A proposed construction method for electrolytic cells would integrate porous surface electrodes into a block of solid electrolyte. The porous electrodes would facilitate unrestricted gas flow thereby improving cell performance.

Among applications for solid-electrolyte cells are oxygen production from carbon dioxide, the extraction of oxygen from air, sewage treatment, and fuel cells. To allow gas flow through the cell, the electrodes and the electrolyte must be porous perpendicular to the surfaces. Furthermore, the electrodes must be highly conductive electrically along the surfaces.

In previous cells, a platinum paste or ink was applied to the electrolyte surface and then fired. To be porous, the paste film had to be thin; but this is contrary to the requirement of high electrical conductance.

In the new technique, the electrodes would be platinum wire screens embedded in the electrolyte surface. The electrolyte is formed from stabilized zirconia, doped alumina, or other ion-conducting material by pressing the powder of the material in a die or by slip casting followed by sintering at high temperature. Before inserting the electrolyte material in the die, the walls would be lined with the electrode screen material. The cell structure is shown in the figure.

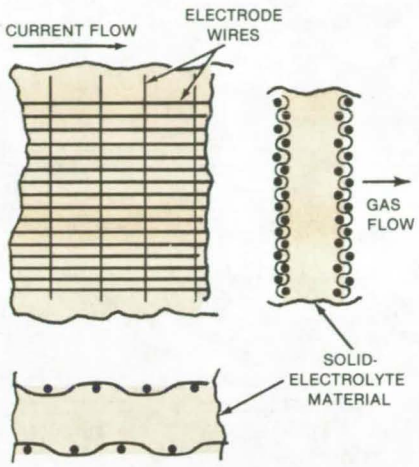


**Electrode Wire Mesh Is Embedded** at the surface of the solid electrolyte. This construction would assure high electrode conductance and low resistance to gas flow.

While the surface area of the wire-screen electrodes is less than the deposited-film electrodes, the smaller area should not limit performance. Experiments have shown that the most detrimental effect of thick-film platinum electrodes is their resistance to gas flow, which results in a large pressure drop, causing in turn an effective voltage drop. The electrode area is not the limiting parameter.

With the wire screen even partially embedded, sufficient platinum is exposed to facilitate the ionization and deionization of the oxygen conducted through the electrolyte. The pressure-drop voltage loss of the solid electrodes is considerably larger than the polarization loss caused by the decrease in platinum area.

*This work was done by Robert Richter of Caltech for* **NASA's Jet Propulsion Laboratory.** *For further information, Circle 73 on the TSP Request Card.*
*NPO-15471*

# Assembling Multicolor Printing Plates

Wave soldering joins plates without clogging ink channels.

*Lewis Research Center, Cleveland, Ohio*

A method has been devised that simplifies plate assemblies used in multicolor, single-step printing processing. Multicolor commercial printing utilizes two copper plates to direct ink flow. These are joined together with an adhesive interface material. This standard joining operation utilizes thermosetting plastic sheets as the adhesive. During the pressure/heat process cycle, the plastic material flows and clogs up small holes and flow passages. This clogging results in imperfect color printing and necessitates extensive hand reworking.

The improved joining method uses wave-soldering techniques developed for integrated-circuit-board assemblies. Thermosetting plastic is replaced by wave soldering, which applies a thin even coat of solder to the mating copper surfaces. This is done after ink holes and channels have been protected by water-soluble, high-temperature solder mask.

Solder mask prevents the solder from wetting and clogging the ink holes and channels. Soldered surfaces of the copper plates are positioned and heated under a low pressure to form an integral two-plate part. Hot water is then flushed through the ink feed holes to remove the solder mask from ink-flow channels. This technique produces a trouble-free composite multicolor printing plate.

*This work was done by William J. Waters of* **Lewis Research Center.** *No further documentation is available.*

*Inquiries concerning rights for the commercial use of this invention should be addressed to the Patent Counsel, Lewis Research Center [see page A5]. Refer to LEW-13598.*

# Selective Etching of Semiconductor Glassivation

An open-circuited stripe can be repaired without destroying the entire passivation layer.

*Goddard Space Flight Center, Greenbelt, Maryland*

A selective etching technique removes portions of the glassivation on a semiconductor die for failure analysis or for repairs. This is not possible with the standard technique, in which an etching solution is applied to the entire die surface.

As shown, a periodontal needle attached to a plastic syringe is moved by a microprobe. The syringe is filled with glass etch. First, a drop of hexane and vacuum pump oil is placed on the microcircuit die, and the hexane is allowed to evaporate. This leaves a thin film of oil. Then, the microprobe brings the needle into contact with the area of the die to be etched.

Capillary action causes a small droplet of etch to flow onto the die. The oil film sufficiently increases surface tension to keep the glass etch concentrated in the specific area of application. The etch is washed off, and the microcircuit is ultrasonically cleaned of the oil film in a beaker of acetone.

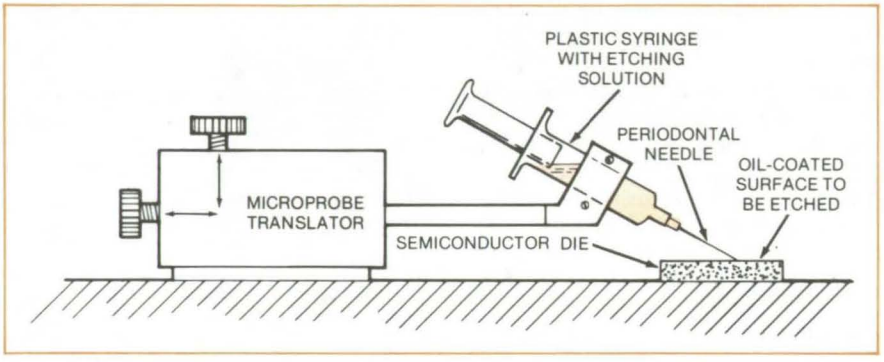


The **Device for Selective Etching** contains a syringe filled with a glass-etching solution that is applied by a periodontal needle. The glass etchant is $H_2O$:$CH_3COOH$:$NH_4F$:HF in the ratio 12:11:8:2 by weight. Glassivation approximately 0.65 to 1.0 micron in thickness has been removed.

Using this technique, it is possible to etch an area 0.23 mm in diameter. The technique can be applied to any glassivated die. An open-circuited stripe can be repaired without destroying the entire passivation layer. The technique makes it economical to fix a manufacturing defect on the die of an expensive or scarce device.

*This work was done by Nelda Casper of Sperry Corp. for* **Goddard Space Flight Center.** *No further documentation is available.*
*GSC-12667*

# Indium Second-Surface Mirrors

Corrosion-resistant mirrors may be used in solar-energy concentrators.

*NASA's Jet Propulsion Laboratory, Pasadena, California*

Corrosion-resistant second-surface mirrors are constructed from indium metal vapor-deposited on glass. Preliminary tests show them to be comparable in reflectance to silvered or aluminized mirrors.

Conventional silvered-glass mirrors rapidly degrade when exposed to atmospheric contaminants and Sunlight. Polished aluminum is also attacked by a combination of heat, Sunlight, and atmospheric contamination. Thus, a longer-lived, reflective material was sought for solar concentrators. Indium was selected because it is resistant to corrosion in air at room temperature. It also resists attack by organic acids.

Indium has relatively low melting and boiling temperatures (157° and 2,075° C, respectively) and wets smooth, clean glass. Consequently, it is well suited to vacuum vapor deposition onto glass. A typical mirror would resemble an ordinary second-surface silvered mirror with metal deposited on the rear surface of the glass and a protective paint or other coating (see figure).

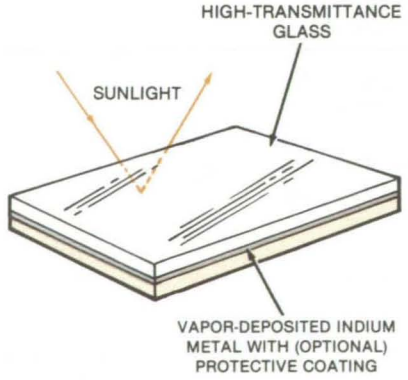


**Second-Surface Mirrors** are formed by vapor deposition of indium onto glass. The mirrors have reflectances comparable to those of ordinary silver or aluminized mirrors and are expected to show superior corrosion resistance.

The initial reflectance tests were done on 2- and 4-inch (5- and 10-centimeter) glass squares of thickness 0.058 inch (1.47 millimeters) with indium directly vapor-deposited onto one glass surface. Environmental tests have not yet been done.

*This work was done by Frank L. Bouquet and Takashi Hasegawa of Caltech for* **NASA's Jet Propulsion Laboratory.** *For further information, Circle 74 on the TSP Request Card.*
*NPO-15085*

# Matching Dissimilar Graphical Scales

A composite of two engineering drawings is created by projecting an enlargement of one on the other.

*Lyndon B. Johnson Space Center, Houston, Texas*

When parts of an assembly are shown on separate drawings with different scales, it may be difficult to visualize the relative sizes of the parts and their relationships to one another when in use. To show the parts at a common scale, one or more drawings are often replotted, using proportional dividers or the superposition of a fine grid to facilitate freehand copying onto a scaled grid. However, these methods are time-consuming and error prone.

An alternative technique permits rapid scale matching for two drawings and easy tracing of a composite image. The technique uses a standard overhead projector and a transparency of one drawing to project an enlarged image, the scale of which matches the scale of the second drawing (see figure). The image may then be traced directly onto the copy of the second drawing.

If the scales of the two original drawings are not very different, the focus range of a standard overhead projector may not be sufficient to permit the scale adjustment. In this case, one of the drawings can be reduced, and the reduced image then can be made into a transparency and projected.

In one-to-one tracing, there is less chance of making an error than in replotting. Moreover, if a permanent copy of the composite drawing is not required, measurements can be made directly on the composite image, thus eliminating entirely the need for any expensive drafting effort.

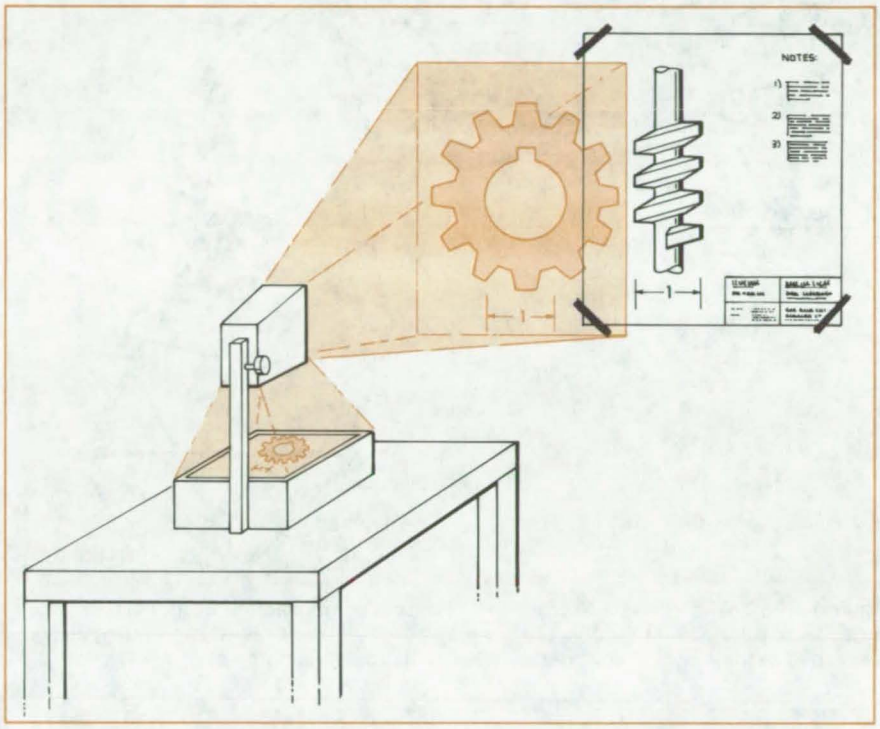


The **Projection of One Drawing on Another,** with the projected image adjusted to have the same scale as the other drawing, permits quick comparisons of such features as the relative sizes of parts and clearances or interferences in assemblies.

*This work was done by Robert H. French of The Magnavox Co. for* **Johnson Space Center.** *No further documentation is available.*
*MSC-14864*

# Dish Antenna Would Deploy From a Canister

Portable paraboloidal dish would be assembled onsite.

*NASA's Jet Propulsion Laboratory, Pasadena, California*

A proposed microwave antenna would be stored compactly in a canister and deployed onsite. When assembled, the antenna (see Figure 1) would consist of 37 hexagonal tiles supported by a truss.

The proposed reflector is built up from modules like the one shown in the detail in Figure 1. The struts at the corners of the triangular frames are hinged so that each module is stored and deployed by a simple rotary motion of the frames. Adjacent modules are hinged to each other in a pattern that progresses across the antenna, alternately connecting the upper (paneled) and lower frames.

(continued on next page)

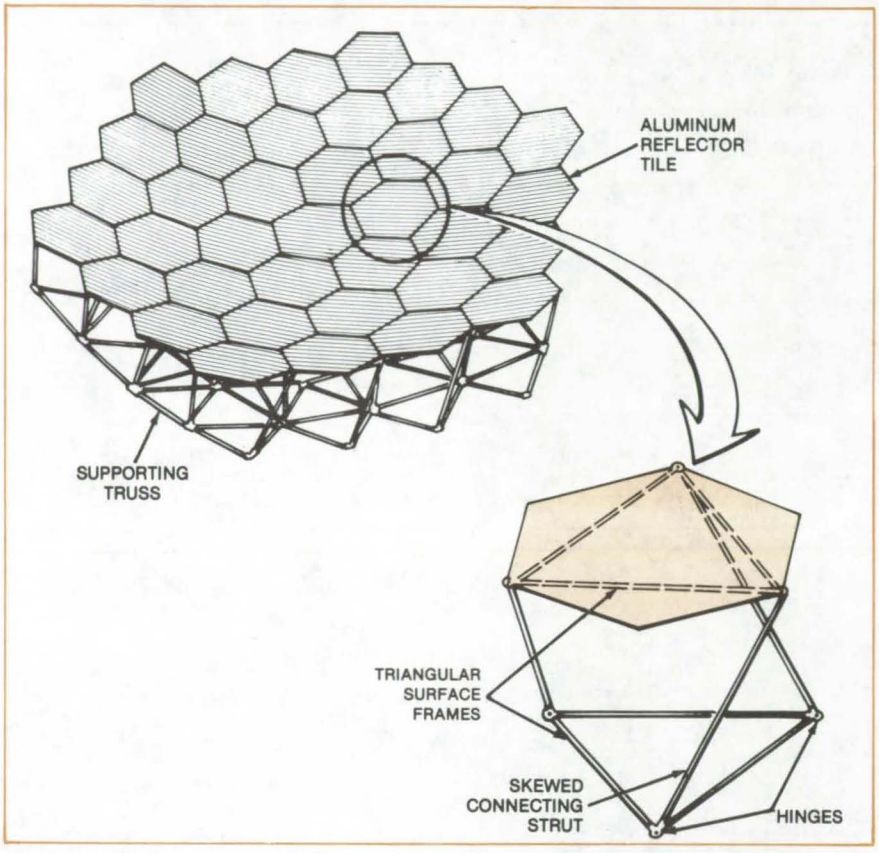


Figure 1. The **37-Tile Portable Microwave Antenna** is composed of hexagonal tiles supported by a truss. A truss module is shown in the detail. The skewed connecting struts are hinged at their ends. They are rotated during storage and deployment.

The entire assembly is stored in a canister that contains the mechanisms to extend each module, rotate it to the proper position, and secure the joints to the mating modules. A deployment sequence is shown in Figure 2.

Each hexagonal tile, consisting of an aluminum honeycomb sandwich, is attached to the supporting structure at three points. During fabrication, the honeycomb cores are machined to shape while mounted on the support. The aluminum facesheets are bonded to the cores to complete the tiles. The reflecting surfaces are ground, and the mounts are adjusted for final accuracy. In the portable system, the antenna would be retracted into the canister for deployment in the field.

*This work was done by Laurence A. Finley and John A. Hedgepeth of Astro Research Corp. for* **NASA's Jet Propulsion Laboratory.** *For further information, Circle 75 on the TSP Request Card.*
*NPO-15448*

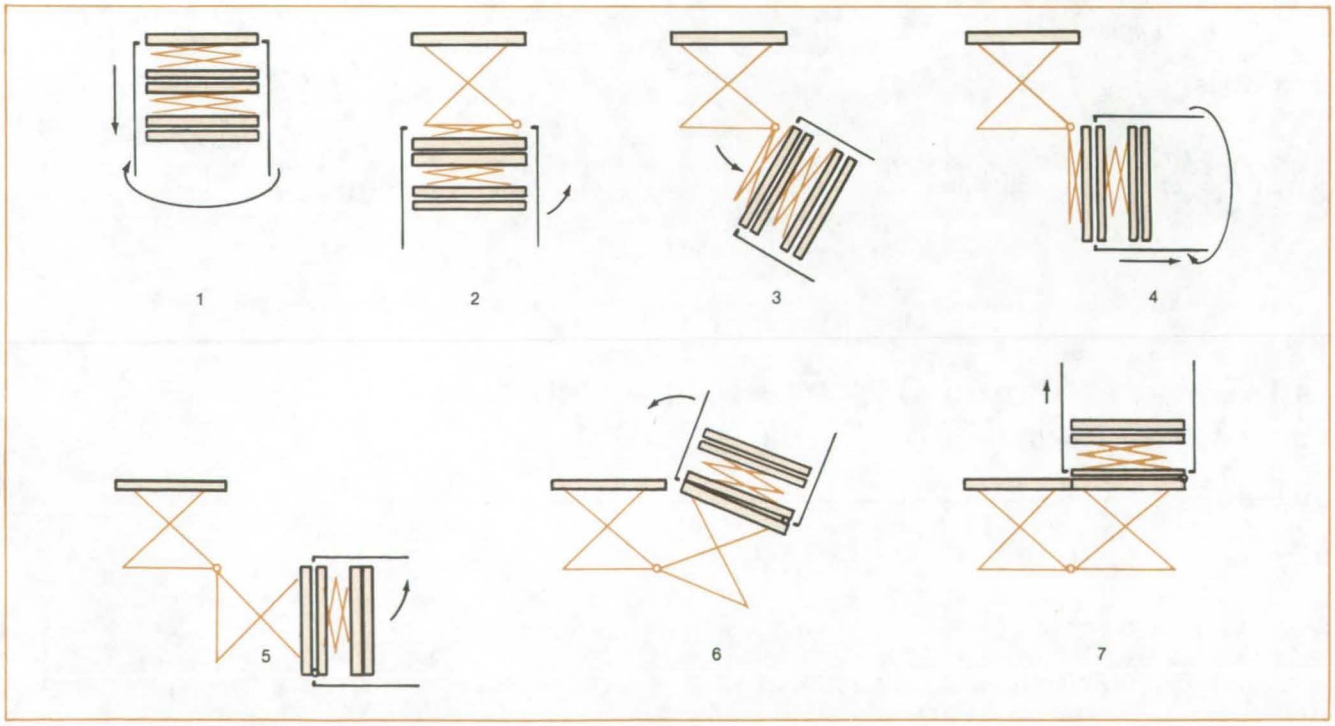


Figure 2. **During a Deployment Sequence,** the stored truss modules are unfolded by rotating as they emerge from the canister. They are then rotated into position and fastened to the mating modules.

# Air Bag Applies Uniform Bonding Pressure

Compliant bag in a box holds parts in place while adhesive cures.

*John F. Kennedy Space Center, Florida*

An air-bag box applies constant uniform pressure to tiles and other objects undergoing adhesive bonding. The box is basically a compliant clamp with adjustable force and position. It can be used on irregular surfaces as well as on flat ones.

The box is open on one side and contains an inflatable bag. Both the box and bag are made of clear plastics. The open side of the box is placed over the work (which may be, for example, a refractory tile to be bonded by glue or epoxy to a surface). After the box is adjusted, it is held firmly by a bolt or threaded rod attached to a floor stand or jack. Foam pads on the edges of the box prevent it from damaging delicate surfaces (see figure).

Pressurized air is fed to the bag through a tube so that it expands, filling the box and pressing against the work. Air is allowed to bleed from the bag via another tube. Control valves on both tubes allow the bag pressure to be adjusted. A recording device attached to a sensor on the bag air inlet monitors the bag pressure during the curing period.

*This work was done by Charles A. Gillespie of Rockwell International Corp. for* **Kennedy Space Center.** *No further documentation is available. KSC-11182*

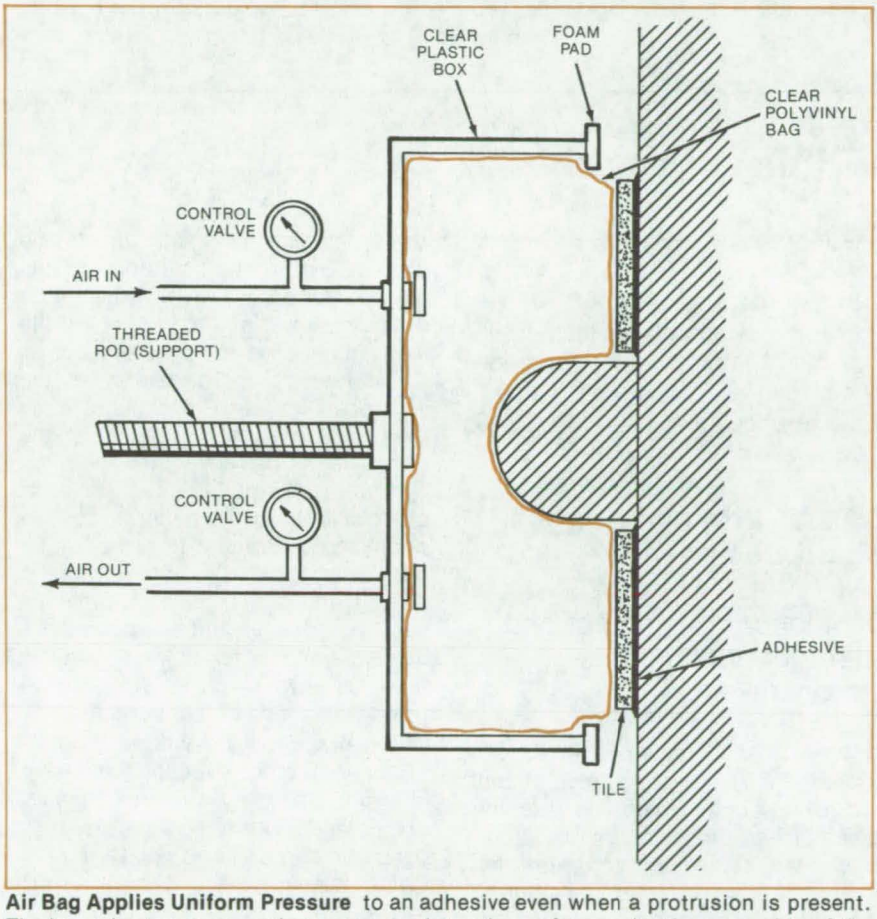


**Air Bag Applies Uniform Pressure** to an adhesive even when a protrusion is present. The bag adopts a contour that accommodates the surface under the open side of the box.

# Books and Reports

These reports, studies, and handbooks are available from NASA as Technical Support Packages (TSP's) when a Request Card number is cited; otherwise they are available from the National Technical Information Service.

## Glasses for Solar-Cell Arrays

Properties and processes for encapsulants are detailed

Glass is critical in solar-cell arrays, since it protects cells from the environment while allowing light to reach the surfaces of the cells. A new report presents data on glass for the encapsulation of solar-cell arrays, with special emphasis on materials and processes for automated high-volume production of low-cost arrays.

The report provides extensive data on the physical properties of glasses suitable for photovoltaic applications (that is, glasses having low distortion and low solar absorptance). Curves and tables give information on such properties as solar transmittance, chemical durability, thermal expansion, dimensional stability, thermal conductivity, density, and viscosity. Soda-lime-silica glasses, borosilicate glasses, and a variety of special and developmental glasses are covered.

Commercial suppliers of glass are listed. Factors that affect the cost of glass are examined: type (sheet, float, or plate), formulation, and energy consumed in manufacturing.

(continued on next page)

Several methods of improving glass properties are suggested. It is important, for example, that iron content be reduced during processing, since iron absorbs light at the same wavelengths as silicon solar cells. Tempering by chemical diffusion is recommended for making glass 10 times stronger. Treatments for reducing reflection losses at the front and back surfaces are suggested.

The effects of in-service conditions are considered. Dust and dirt, for instance, can accumulate on a glass cover and reduce solar-cell efficiency. Hail damage is a problem only for very large hailstones — greater than 1.5 in. (3.8 cm) for tempered glass 0.19 in. (0.5 cm) thick. Abrasion by sand can cause a small loss in transmissivity, particularly in desert areas.

*This work was done by Frank L. Bouquet of Caltech for* **NASA's Jet Propulsion Laboratory.** *To obtain a copy of the report, "Glass for Low-Cost Photovoltaic Solar Arrays," Circle 76 on the TSP Request Card.*
*NPO-15528*

# Computer Programs

These programs may be obtained at very reasonable cost from COSMIC, a facility sponsored by NASA to make new programs available to the public. For information on program price, size, and availability, circle the reference letter on the COSMIC Request Card in this issue.

## CADAT Printed-Wiring-Board Designer

Component placement and interconnection paths are optimized.

The CADAT printed-wiring-board system (PWB) designs printed-circuit and hybrid-circuit boards. It is comprised of four programs: the preprocessor, the placement program, the organizer program, and the router. The preprocessor combines user-supplied data and library data to produce input for the placement program. The user-supplied data consist of a list of components, a list of the connections between components, and board identification information. The library data specify the physical size and pin placement for each component and describe the board area and pin logic. From these data, the preprocessor prepares the Placement Input File (PIF).

The placement program utilizes the PIF to assign components to specific areas of the board. This program optimizes the placement solution in terms of the interconnections between components. A Pin Connection File (PCF) is generated and passed to the organizer program. The organizer converts the PCF data into a list of pin pairs and determines the board layer on which the pin pair should be placed. The program also determines the optimal order in which the router program should attempt to lay out the paths connecting the pin pairs.

The router program determines the wire paths that are to connect each pin pair. It obtains information on the pin pairs to be connected and the available wire-path area on each board layer from files generated by the organizer program. Once the router has determined a viable layout, a printed image of the wire paths on each board layer and an artwork file are generated. An optional artwork tape for hybrid dielectric isolation boards may also be generated.

The programs are written in FORTRAN IV for batch execution and have been implemented on a Xerox Sigma V computer. The PWB system was developed in 1973. (Related articles on the CADAT system are found on pages 394 through 396 of *NASA Tech Briefs,* Vol. 5, No. 3, and on pages 507 and 508 of Vol. 5, No. 4.)

*This program was written by C. D. Brinkerhoff of M&S Computing, Inc., for* **Marshall Space Flight Center.** *For further information, Circle H on the COSMIC Request Card.*
*MFS-25464*

## Composite-Material Point-Stress Analysis

Outputs include laminate elastic and thermal properties and allowable load levels.

PSANAL computes composite-laminate elastic and thermal properties and the allowable load levels for any combination of applied membrane and bending loads occurring at a point. Basic linear orthotropic stress/strain relationships and standard composite-laminate theory formulas are utilized.

Mechanically applied loads may consist of three stress resultants and three stress couples, which are assumed to be acting in constant ratio and may be applied in any combination. A constant temperature is assumed through each laminate thickness. Individual lamina thermal loads are computed and included in the allowable-load analysis. No restrictions are placed on laminate balance or symmetry. Unidirectional "unwoven" tape and pseudounidirectional bidirectional "woven" fabric prepregs are accommodated.

Inputs to PSANAL include lamina properties, allowable strengths and strains, safety factor, laminate description, and applied loads. The failure criteria are that no lamina matrix failure is permitted at limit load and that no fiber failure is allowed at ultimate load. The lamina failure criteria include maximum-stress and maximum-strain criteria.

PSANAL handles up to 10 different prepreg materials and 50 plies per laminate. Its outputs include laminate elastic properties, laminate thermal properties, and allowable load levels.

PSANAL is written in FORTRAN IV for batch execution and has been implemented on an IBM 370 computer with a central memory requirement of approximately 100K of 8-bit bytes. The program was developed in 1975.

*This program was written by Francis S. Spears of Rockwell International Corp. for* **Johnson Space Center.** *For further information, Circle J on the COSMIC Request Card.*
*MSC-18978*

# Mathematics and Information Sciences

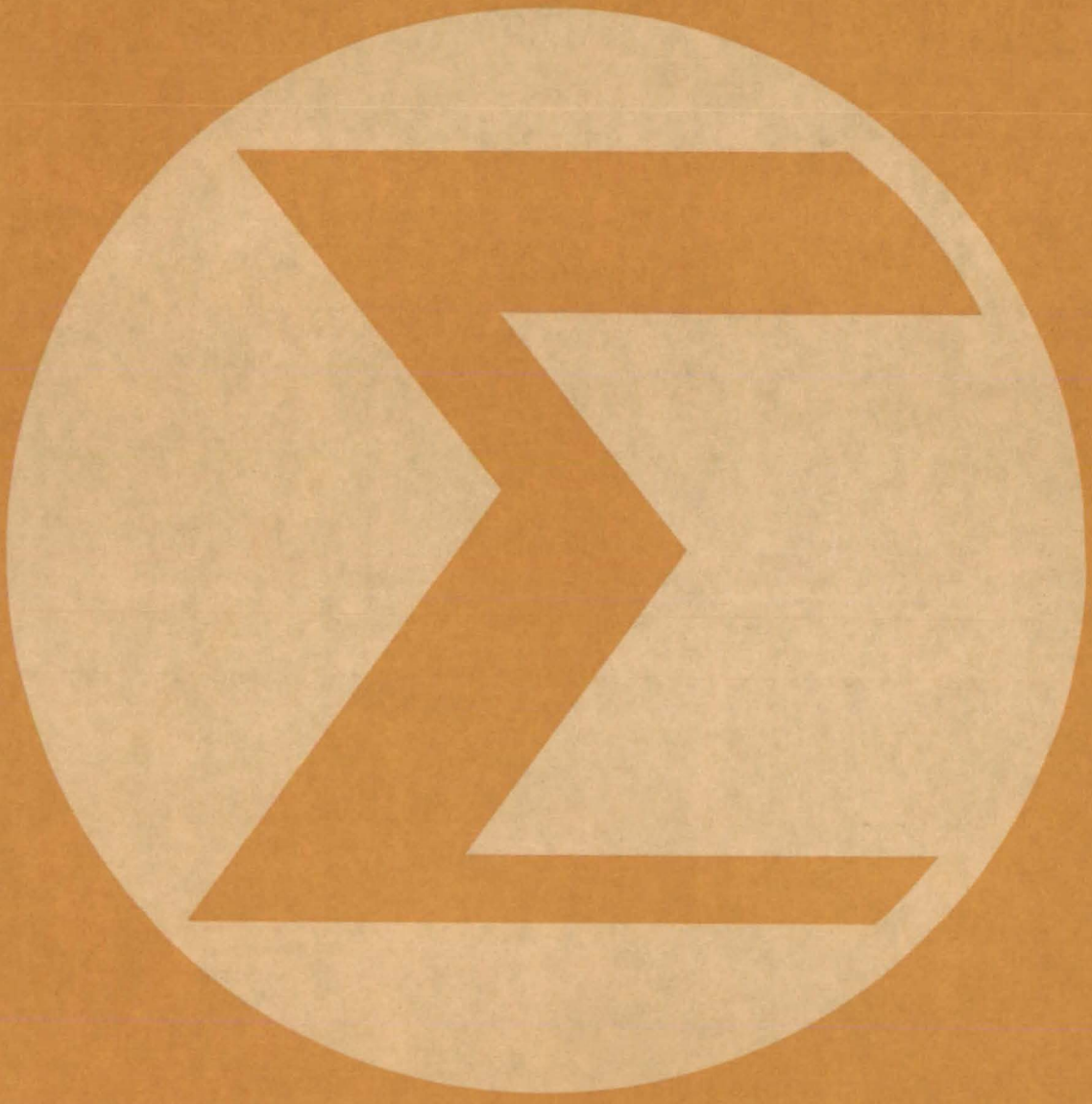

## Hardware, Techniques, and Processes

# Calculating the Performance of a Solar Reflector

Nomograms show the efficiency of thermal-energy collection and the useful heat collected.

*NASA's Jet Propulsion Laboratory, Pasadena, California*

A new method calculates the efficiency and useful heat of a parabolic solar concentrator. The method uses a three-part nomogram, consisting of a main chart and two other components.

The main chart solves the equation shown in Figure 1, which has the simplified form:

$$\eta_C = C_1 - C_2 \frac{\Delta T}{I_b}$$

where $C_1$ is the net absorptance (optical efficiency) and $C_2$ is the heat-loss coefficient. The useful heat $Q_u$ is the product of the dish efficiency $\eta_C$ and the insolation intensity $I_b$.

The user enters the components of the nomogram knowing the diameters of the paraboloid, of the paraboloid aperture, and of the receiver; the focal length of the dish; its reflectance; the ratio of the reflective area to the aperture area; the air velocity and temperature; the receiver temperature; and the day and hour. The user then proceeds to plot lines to intercepts on the nomogram to find the results.

Figure 2 illustrates the computation that solves for $C_2$. It shows four of the boxes and part of the procedure that finds the coefficient for heat losses through radiation, convection, and conduction.

*This work was done by Mehmet K. Selcuk of Caltech for* **NASA's Jet Propulsion Laboratory**. *For further information, including the complete nomogram, Circle 77 on the TSP Request Card.*
*NPO-15314*

$$\eta_C = \Phi \bullet G \bullet \varrho \bullet \alpha_{eff} - \left[ \frac{\varepsilon h_r + h_C + \frac{A_W}{A_a} h_k}{CR} \right] \frac{\Delta T}{I_b}$$

WHERE:

| | | | |
|---|---|---|---|
| $\eta_C$ | = Efficiency of Thermal-Energy Collection | $\varepsilon$ | = Effective Emittance of Receiver Aperture |
| $\Phi$ | = Intercept Factor | $h_r$ | = Equivalent Radiative Heat-Transfer Coefficient |
| G | = Geometric Shadowing | $h_C$ | = Convective Loss Coefficient |
| $\varrho$ | = Reflectance | $A_W$ | = Receiver-Cavity Wall Area |
| $\alpha_{eff}$ | = Effective Absorptance | $A_a$ | = Aperture Area |
| a | = $\eta_{Optical}$ | $h_k$ | = Equivalent Conduction-Loss Coefficient |
| CR | = Concentration Ratio | $\Delta T$ | = $T_{Receiver} - T_{Ambient}$ |
| | | $I_b$ | = Beam Insolation Intensity |

Figure 1. The **Equation Solved** by the parabolic-dish nomogram gives the concentrator efficiency $\eta_C$.

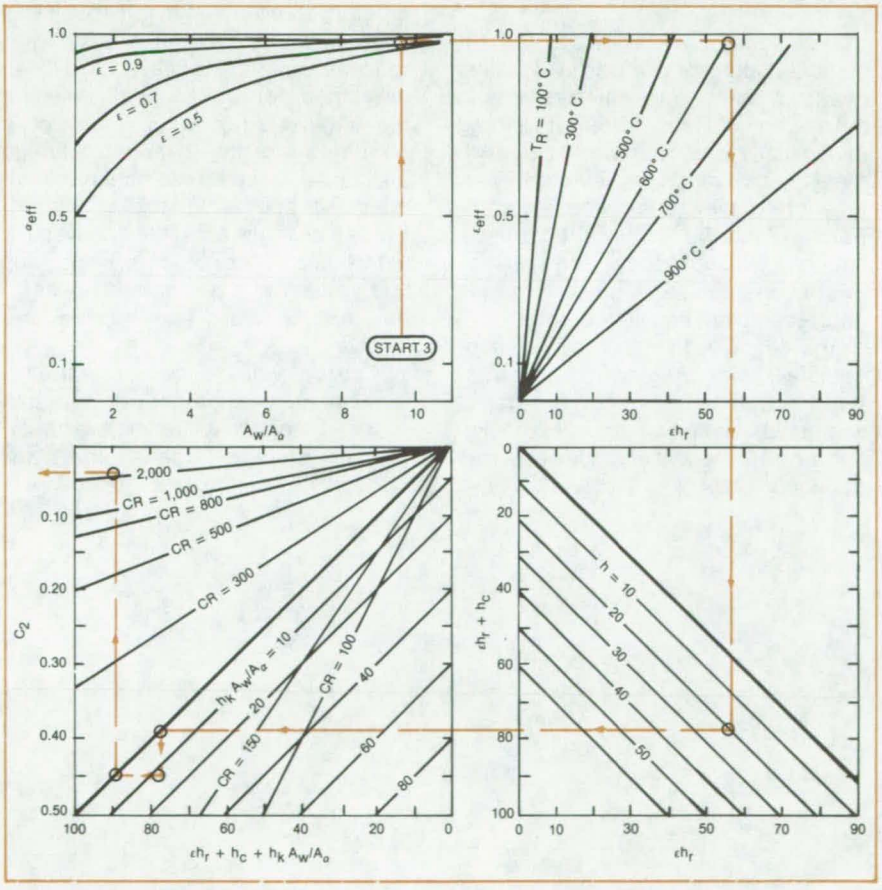


Figure 2. This **Portion of the Nomogram** is part of the computation to determine the heat-loss coefficient.

# Program Structure Combines Segmentation and Dynamic Storage

A single program is used for both batch and interactive modes.

*Langley Research Center, Hampton, Virginia*

Novel programing techniques incorporate the advantages of overlaying into segmented loads while retaining all the dynamic load advantages of segmentation, employing those capabilities that best suit the mode of operation, whether batch or interactive. The user is allowed to load a program automatically in a variable manner, based solely on a single data input to the program, to maintain minimal field lengths for interactive use, thereby improving overall turnaround time and program interaction, or to maintain minimal input/output for batch runs, thereby reducing job costs.

The overlay loader allows a program to be structured into portions called overlays, only one of which resides in core at any one time. Data are stored dynamically in core at the end of each overlay, but must be restored each time a new overlay is called into core. Furthermore, the overlay structuring is set up in program code, and changes in structure require changes in code and recompilation of the program.

The segment loader allows a relocatable binary program to be structured at load time into portions called segments. Recoding and recompilation are not necessary. However, all data, normally stored dynamically in blank common, reside in core at a level below the longest possible branch of loaded segments. Thus, segmentation eliminates the necessity to restore data when new segments are called into core, reducing input/output costs; however, it increases the overall field length of the executing program, which is a major disadvantage in interactive runs.

The conflict could be resolved by maintaining two versions of the same program, each with a different code for input/output and different segment-loading directives. However, maintaining two versions of the same program presents difficulties and is time consuming and error-prone.

Three programing steps have been developed for automatically varying the segmented load structure of a program and the dynamic storage allocation to suit best the mode of operation desired: batch or interactive. All changes are based on a single data input to the program, and only one version of the program needs to be maintained. The techniques involve:

1. Coding within the program to suppress scratch-pad input/output for a batch run or translating the in-core storage area from blank common to the end-of-code +1 address of a particular segment for an interactive run;
2. Automatic altering of the segment load directives prior to loading, based on data input to the program, to vary the structure of the load for interactive and batch runs; and
3. Automatic editing of the load map to determine the initial addresses for in-core data storage for an interactive run.

Using these methods, the programer incorporates all the advantages of overlay structure into segmented loads while retaining all the dynamic load advantages of segmentation. All of these steps, accomplished by the programer in prewritten code and small files of editing commands, are automatically performed in the job stream with no action required by the user except to change one data card.

*This work was done by Sherwood H. Tiffany of Kentron International, Inc., for* **Langley Research Center.** *Further information may be found in NASA CR-3315 [N80-31071/NSP], "Segmentation, Dynamic Storage, and Variable Loading on CDC Equipment" [$8]. A copy may be purchased [prepayment required] from the National Technical Information Service, Springfield, Virginia 22161.*

*LAR-12830*

# SUBJECT INDEX

National Aeronautics and
Space Administration

Washington, D.C.
20546



SPECIAL FOURTH-CLASS RATE
BOOK

FOURTH-CLASS MAIL
POSTAGE & FEES PAID
NASA
WASHINGTON, D.C.
PERMIT No. G 27

NASA

*This portable radiometer for monitoring crop growth is a terrestrial adaptation of NASA satellite remote-sensing techniques. Either hand held or mounted on a pole above the growth area, the radiometer indicates crop health, yield, and other characteristics.* [*See the bottom of page A1.*]